

Project Number: YXM-0701

## **Design of a Dual Heart Rate Variability Monitor**

A Major Qualifying Project Report:  
Submitted to the Faculty  
of the

WORCESTER POLYTECHNIC INSTITUTE

In partial fulfillment of the requirements for the  
Degree of Bachelor of Science  
By

---

Boyla O Mainsah

---

Thomas R Wester

October 26<sup>th</sup>, 2007

Approved:

---

Prof. Yitzhak Mendelson, Major Advisor

---

Suresh Atapattu, Co-Advisor

# Table of Contents

Authorship.....	v
Acknowledgements.....	vii
Abstract.....	viii
Abbreviations.....	ix
Table of Figures.....	x
Table of Tables.....	xiv
1. Executive Summary.....	1
2. Literature Review.....	3
2.1 Heart Rate Variability.....	3
2.2 Medical Significance.....	5
2.2.1 Diagnostic Capabilities.....	5
2.3 Current Methods and Practices.....	6
2.3.1 Electrocardiography.....	6
2.3.1.1 Principle.....	7
2.3.1.2 Methods for Acquisition.....	8
2.3.1.3 Limitations of Electrocardiography.....	9
2.3.2 Photoplethysmography.....	10
2.3.2.1 Principle.....	10
2.3.2.2 Sensor Probes.....	12
2.3.2.3 Methods for Light Detection.....	12
2.4 Electrocardiography versus Photoplethysmography.....	14
2.5 Mathematical Models.....	16
2.5.1 Signal Conditioning.....	16
2.5.2 Time Domain Analysis.....	17
2.5.2.1 Statistical Methods.....	18
2.5.2.2 Geometrical Methods.....	20
2.5.3 Frequency Domain Analysis.....	24
2.6 Current Devices.....	25
2.7 Future Developments.....	26
3. Project Approach.....	28
3.1 Hypothesis.....	28
3.1.1 Dry Electrodes.....	28
3.1.2 PPG Signal Alternative.....	28
3.2 Specific Aims.....	28
3.2.1 Photoplethysmography Acquisition.....	29
3.2.2 Electrocardiogram Acquisition.....	29
3.2.2.1 Comparison of Dry Electrodes with Gel Electrodes.....	29
3.2.3 Correlation of ECG and PPG signals.....	30
4. Analysis of Needs and Specifications.....	31
4.1 Initial Client Statement.....	31
4.2 User Requirements.....	31
4.3 Objectives.....	32
4.4 Constraints.....	35
4.5 Revised Client Statement.....	35
4.6 Functions.....	36

4.6.1	System Inputs.....	37
4.6.2	Signal Amplification and Filtering .....	37
4.6.3	Signal Digitization .....	38
4.6.4	Signal Storage .....	38
4.6.5	Interbeat Interval Detection .....	38
4.6.6	Signal Artifact Detection .....	38
4.6.7	Rate and Rate Variability Algorithms.....	39
4.6.8	Heart Beat Beep and Alarm Controls .....	39
4.7	Initial Design Specifications.....	41
4.7.1	Physical Dimensions.....	41
4.7.2	Example Industry Specifications .....	41
4.7.2.1	PPG .....	41
4.7.2.2	ECG.....	41
5.	Alternative Designs.....	42
5.1	PPG .....	42
5.1.1	Sensor Wavelength .....	42
5.1.2	Sensor Mode .....	43
5.1.3	Sensor Location .....	44
5.1.4	Sensor Architecture.....	49
5.1.5	Filters .....	50
5.2	ECG.....	54
5.2.1	ECG Electrodes.....	54
5.2.2	ECG Electrode Location.....	57
5.2.3	Filters .....	59
5.3	Software Algorithms.....	60
5.3.1	R-R Interval Detection.....	60
5.3.1.1	Peak Time Location .....	61
5.3.1.2	Elapsed Time .....	61
5.3.2	Heart / Pulse Rate Calculation .....	62
5.3.2.1	Rate Averaging .....	62
5.3.2.2	Frequency Analysis.....	63
5.4	User Interface.....	64
5.4.1	Layout .....	64
6.	Methods.....	66
6.1	PPG .....	66
6.1.1	Photodetection Unit .....	66
6.1.2	Filter Design.....	68
6.1.3	Power Optimization .....	70
6.2	ECG.....	73
6.2.1	Electrodes.....	73
6.2.2	Filter Design.....	73
6.3	Software .....	74
6.3.1	Signal Acquisition.....	76
6.3.2	Signal Filtering.....	76
6.3.3	Peak Detection .....	79
6.3.3.1	Threshold Adjustment.....	80

6.3.4	Peak-to-Peak Interval Calculation .....	81
6.3.5	Time Interval Error Correction .....	82
6.3.6	Rate and Variability Calculations .....	82
6.3.7	Audible and Visual Alerts and Alarms .....	85
6.3.7.1	Heart and Pulse Rate Alarm .....	85
6.3.7.2	System Fault Alarm .....	86
6.3.7.3	Heart Beat Alert .....	86
6.3.8	Signal Storage .....	86
6.4	Final Design .....	88
6.4.1	ECG Electrodes .....	89
6.4.2	PPG Sensor Probe .....	89
6.4.3	Device Hardware .....	91
6.4.4	Software .....	94
6.4.5	User Interface .....	95
7.	Results .....	97
7.1	PPG .....	97
7.1.1	Sensor Probe .....	97
7.1.2	Power Optimization .....	98
7.1.2.1	Current Amplitude .....	98
7.1.2.2	Current Duty cycle .....	99
7.2	ECG .....	100
7.2.1	Electrodes .....	101
7.3	Software Evaluation and Testing .....	102
7.3.1	Signal Acquisition .....	104
7.3.2	Peak Detection .....	105
7.3.3	ECG and PPG Data Comparison .....	107
7.3.4	Motion Artifact .....	111
7.3.5	Comparative Software Validation .....	115
7.3.5.1	ECG .....	115
7.3.5.2	PPG .....	116
7.3.6	Manual Software Validation .....	117
7.3.7	Valsalva Maneuvers .....	121
7.4	FDA Regulations .....	122
8.	Analysis and Discussion .....	124
8.1	PPG .....	124
8.2	ECG .....	125
8.3	Software .....	130
9.	Conclusion .....	132
10.	Recommendations .....	133
10.1	PPG .....	133
10.1.1	PPG Circuit .....	133
10.1.2	Device Battery life .....	133
10.1.3	Motion Artifact Reduction .....	133
10.1.4	Sensor Platform .....	135
10.2	Device Testing .....	136
10.3	ECG .....	136

10.3.1	Adaptive Filtering (Active EMG).....	136
10.4	Software.....	137
10.4.1	Signal Discrimination.....	137
10.4.2	Threshold Reset Control.....	138
10.4.3	Microcontroller Development.....	139
References	.....	140
Glossary	.....	143
Appendix A.	LabVIEW Files.....	145
Appendix B.	Device Drawings.....	163
Appendix C.	Bill of Materials.....	171
Appendix D.	Component Specifications.....	173
Appendix E.	User's Manual.....	175
Appendix F.	Test Results.....	186
Appendix G.	Industry Product Specifications.....	191
Appendix H.	Physiological Information.....	195

## Authorship

Abstract	Boyla/Thomas
1. Executive Summary	Boyla/Thomas
2. Literature Review	
2.1 Heart Rate Variability	Thomas
2.2 Medical Significance	Thomas
2.3 Current Methods and Practices	
2.3.1 Electrocardiography	Thomas
2.3.2 Photoplethysmography	Boyla
2.4 Electrocardiography versus Photoplethysmography	Boyla
2.5 Mathematical Models	Boyla
2.6 Current Devices	Boyla
2.7 Future Developments	Thomas
3. Project Approach	
3.1 Hypothesis	Boyla/Thomas
3.1.1 Dry Electrodes	Thomas
3.1.2 PPG Signal Alternative	Boyla
3.2 Specific Aims	Boyla/Thomas
3.2.1 Photoplethysmography Acquisition	Boyla
3.2.2 Electrocardiogram Acquisition	Thomas
3.2.3 Correlation of ECG and PPG signals	Boyla
4. Analysis of Needs and Specifications	
4.1 Initial Client Statement	Boyla/Thomas
4.2 User Requirements	Boyla
4.3 Objectives	Boyla
4.4 Constraints	Boyla
4.5 Revised Client Statement	Boyla/Thomas
4.6 Functions	Boyla
4.7 Initial Design Specifications	
4.7.1 Physical Dimensions	Thomas
4.7.2 Example Industry Specifications	Boyla/Thomas
5. Alternative Designs	
5.1 PPG	Boyla
5.2 ECG	Thomas
5.3 Software Algorithms	Thomas
5.4 User Interface	Boyla
6. Methods	
6.1 PPG	Boyla
6.2 ECG	Thomas
6.3 Software	Thomas
6.4 Final Design	Boyla/Thomas
7. Results	
7.1 PPG	Boyla
7.2 ECG	Thomas
7.3 Software Evaluation and Testing	Boyla

7.4	FDA Regulations .....	Boyla
8.	Analysis and Discussion	
8.1	PPG.....	Boyla
8.2	ECG.....	Thomas
8.3	Software.....	Boyla/Thomas
9.	Conclusion.....	Boyla/Thomas
10.	Recommendations.....	Boyla/Thomas
Appendix A.	LabVIEW Files.....	Thomas
Appendix B.	Device Drawings.....	Boyla/Thomas
Appendix C.	Bill of Materials.....	Boyla/Thomas
Appendix D.	Component Specifications.....	Thomas
Appendix E.	User's Manual.....	Boyla
Appendix F.	Test Results.....	Boyla/Thomas
Appendix G.	Industry Product Specifications.....	Boyla
Appendix H.	Physiological Information.....	Boyla/Thomas

## **Acknowledgements**

We would like to thank all persons who assisted with the completion of this Major Qualifying Project. These people include:

Professor Mendelson for his assistance and guidance throughout the progress of the project, serving as project advisor.

Suresh Atapattu for all assistance with development of the LabVIEW aspect, and serving as co-advisor for the project.

Lisa Wall for assistance with locating device components and providing access to all necessary lab facilities.

Christian Wester for assistance with production of the prototypes.

Piyush Ramuka for assistance with PR validations.

## **Abstract**

Decreased heart rate variability (HRV) seems to predict increased risks of sudden cardiac death. Thus HRV monitoring may provide additional information that could help in the risk stratification of patients. We designed a dual-channel personal computer based monitor to calculate HR and HRV indices, from electrocardiogram (ECG) and photoplethysmogram (PPG) signals. Preliminary tests showed that the PPG signal can be used as an alternative to obtain accurate HRV values from resting subjects.

## **Abbreviations**

**ANS:** Autonomic Nervous System

**ASTM:** American Society for Testing and Materials

**BPF:** Band-pass filter

**CA:** Cardiac Arrest

**CHF:** Congestive Heart Failure

**CAD:** Coronary Artery Disease

**ECG:** Electrocardiogram

**EEG:** Electroencephalogram

**EMG:** Electromyogram

**FDA:** United States Food and Drug Administration

**Hb:** Hemoglobin

**HPF:** High-pass filter

**HR:** Heart rate

**HRV:** Heart rate variability

**LPF:** Low-pass filter

**NI:** National Instruments

**NN:** Normal-to-normal

**PCC:** Pairwise comparison chart

**PPG:** Photoplethysmogram

**PNS:** Parasympathetic Nervous System

**PR:** Pulse rate

**PRV:** Pulse rate variability

**PVC:** Premature Ventricular Contraction

**R:** Correlation coefficient

**rMSSD:** Root mean square of the successive differences

**SEE:** Standard error of estimate

**SDNN:** Standard deviation of NN intervals

**SNR:** Signal-to-noise ratio

**SNS:** Sympathetic Nervous System

## Table of Figures

Figure 2.1: Comparison of the SNS and PNS on heart activity [3].	4
Figure 2.2: Affects of CAD presence on HRV [6]	6
Figure 2.3: Einthoven's triangle [9]	8
Figure 2.4: Sample electrical signal for single heart beat indicating ECG electrical components	8
Figure 2.5: Frequency spectrum of bioelectric events [12]	10
Figure 2.6: Arteries acting as pressure reservoirs by varying cross-sectional area [16]	11
Figure 2.7: Light absorption through tissue as a function of pulsatile blood flow [17]	11
Figure 2.8: Transmittance (a) and reflectance (b) PPG probes [14]	13
Figure 2.9: Illustration of beat-to-beat intervals within ECG and PPG signals [3]	15
Figure 2.10: Flow chart summarizing steps for ECG HRV analysis [7]	16
Figure 2.11: Irregular heart rhythm shown as PVC [3]	17
Figure 2.12: Interval tachogram from Mini Logger® monitor during various activities; redrawn from [33]	20
Figure 2.13: N-N interval histogram to compute HRV triangular index [34]	21
Figure 2.14: HRV analysis using Poincaré Plot [37]	22
Figure 2.15: Examples of Poincaré plot patterns with different HRV values [38]	23
Figure 2.16: Frequency power spectrum of HRV [40]	24
Figure 4.1: Weighted objectives tree	35
Figure 4.2: Design black box with inputs and outputs	36
Figure 4.3: Physiological signal processing using sensors, signal processing, and outputs [56]	37
Figure 4.4: Developed transparent box of device design with inputs and outputs	40
Figure 5.1: Absorption spectra of oxygenated and deoxygenated Hb [15]	43
Figure 5.2: PPG Sensor location alternatives [28], [46]-[47]	47
Figure 5.3: Design alternatives for PPG sensor architecture	49
Figure 5.4: PPG signal obtained after LabVIEW software filtering	53
Figure 5.5: Clean PPG signal after pre-hardware filtering	54
Figure 5.6: Wet (a) and dry (b) ECG electrodes	55
Figure 5.7: Chest versus extremity electrode placement	58
Figure 5.8: Time peak locations	61
Figure 5.9: Peak detection via timer	61
Figure 5.10: HR averaging	63
Figure 5.11: PR by frequency analysis	63
Figure 5.12: Sample industry monitor by Mindray PM 7000 [54]	65
Figure 6.1: Light emission and detection circuit	66
Figure 6.2: Differential transimpedance amplifier	67
Figure 6.3: Single op-amp transimpedance amplifier	67
Figure 6.4: Quad op-amp pin specification	68
Figure 6.5: Fourier analysis of a PPG waveform	68
Figure 6.6: PPG band-pass filter	69
Figure 6.7: LM 555 timer circuit outputting 5V pulsatile	70
Figure 6.8: PPG circuit to investigate current amplitude	72
Figure 6.9: ECG high-pass filter design	73

Figure 6.10: Software flow chart .....	74
Figure 6.11: LabVIEW program block diagram .....	75
Figure 6.12: Signal acquisition and A/D conversion .....	76
Figure 6.13: ECG (top) and PPG (bottom) software filter settings .....	77
Figure 6.14: Signal filtering and gain .....	78
Figure 6.15: Sample PPG signal (a) and respective derivative (b) .....	78
Figure 6.16: Signal peak detection .....	79
Figure 6.17: ECG threshold adjust .....	80
Figure 6.18: PPG threshold adjust .....	81
Figure 6.19: Peak-to-peak timer .....	81
Figure 6.20: Example signal error elimination block diagram .....	82
Figure 6.21: HR and HRV calculations .....	84
Figure 6.22: High/Low HR and PR alarm .....	85
Figure 6.23: Signal fault detection .....	86
Figure 6.24: ECG audible peak indicator .....	86
Figure 6.25: Waveform file name window .....	87
Figure 6.26: Raw signal down-sampling and storage .....	87
Figure 6.27: Sample recorded data .....	88
Figure 6.28: Final ECG electrode .....	89
Figure 6.29: ECG electrode leads .....	89
Figure 6.30: Reflectance forehead sensor probe .....	90
Figure 6.31: Sensor photodetection unit .....	90
Figure 6.32: PPG sensor DB9 input connector .....	91
Figure 6.33: Hardware printed circuit board .....	91
Figure 6.34: Final device hardware case .....	92
Figure 6.35: Device hardware inputs .....	93
Figure 6.36: Device hardware output connections .....	93
Figure 6.37: Final hardware device assembly .....	93
Figure 6.38: Final block diagram .....	94
Figure 6.39: Front panel with labels .....	96
Figure 7.1: PPG signals from prototype and commercial sensors .....	97
Figure 7.2: Plot of relative signal amplitude against current (mA) .....	99
Figure 7.3: Detected signals from different LED current duty cycles .....	100
Figure 7.4: Initial ECG hardware implementation tests .....	100
Figure 7.5: Full ECG hardware filtration results .....	101
Figure 7.6: ECG electrode test results of industry, gel, and dry electrodes .....	102
Figure 7.7: Experimental setup for data recording .....	103
Figure 7.8: Typical ECG and PPG during rest .....	105
Figure 7.9: Signal peak detection for ECG (a) and PPG signals (b) .....	106
Figure 7.10: Simultaneously recorded HR and PR .....	107
Figure 7.11: PPG signal (a) and corresponding derivative (b) .....	108
Figure 7.12: Beat-to-beat interval double count due to missed beat .....	109
Figure 7.13: Beat-to-beat double count rejection .....	109
Figure 7.14: Corrected HR and PR from resting subject .....	110
Figure 7.15: Comparison of between instantaneous HR and PR .....	110
Figure 7.16: Comparison of SDNN (a) and rMSSD (b) variability indices .....	111

Figure 7.17: Comparison of HR and PR values during low (a) and high (b) activity ....	113
Figure 7.18: Comparison of HR (a) and PR (b) during moderate intensity movement..	114
Figure 7.19: Comparison of HR (a) and PR (b) during moderate intensity movement..	115
Figure 7.20: PR comparison between prototype and commercial PPG devices.....	116
Figure 7.21: R-R Interval comparison between manual and software calculations revealing inaccuracies in software algorithm .....	117
Figure 7.22: R-R Interval comparison between manual and updated software calculations for ECG.....	118
Figure 7.23: Manual and Software IHR (top) and IPR (bottom) Correlation.....	120
Figure 7.24 Comparison of between IHR and IPR with updated software .....	121
Figure 7.25: IHR (a) and R-R Intervals (b) changes during a Valsalva maneuver.....	122
Figure 8.1: ECG circuit Revision B .....	127
Figure 8.2: Industry dry electrode suite .....	129
Figure 10.1: Adaptive noise cancellation for motion artifacts reduction in PPG signal.	134
Figure A.1: LabVIEW front panel .....	146
Figure A.2: LabVIEW block diagram .....	147
Figure A.3: ECG threshold adjust control front panel.....	150
Figure A.4: ECG threshold adjust control block diagram .....	150
Figure A.5: PPG threshold adjust control front panel.....	151
Figure A.6: PPG threshold adjust control block diagram .....	151
Figure A.7: ECG signal conditioning front panel .....	152
Figure A.8: ECG signal conditioning block diagram .....	152
Figure A.9: PPG signal conditioning front panel.....	153
Figure A.10: PPG signal conditioning block diagram .....	153
Figure A.11: ECG signal analysis front panel .....	154
Figure A.12: ECG signal analysis block diagram with 8-beat HR average.....	155
Figure A.13: ECG 5-beat HR average .....	156
Figure A.14: ECG instantaneous HR.....	156
Figure A.15: PPG signal analysis front panel .....	156
Figure A.16: PPG signal analysis with 8-beat PR average.....	157
Figure A.17: PPG with 5-beat PR average .....	158
Figure A.18: PPG instantaneous PR .....	158
Figure A.19: ECG audible beep front panel .....	158
Figure A.20: ECG audible beep block diagram.....	158
Figure A.21: Signal fault analysis front panel .....	159
Figure A.22: Signal fault analysis block diagram.....	159
Figure A.23: Signal recording front panel .....	160
Figure A.24: Signal recording block diagram.....	161
Figure A.25: Alarm control front panel .....	162
Figure A.26: Alarm control block diagram showing dual analysis .....	162
Figure A.27: Alarm control for HR analysis .....	162
Figure A.28: Alarm control for PR analysis .....	162
Figure B.1: ECG Circuit Revision A .....	164
Figure B.2: ECG Circuit Revision B .....	164
Figure B.3: ECG Circuit Revision C .....	164
Figure B.4: Simple transimpedance amplifier .....	165

Figure B.5: Differential transimpedance amplifier .....	165
Figure B.6: PPG circuit schematic .....	166
Figure B.7: Printed circuit board schematic .....	167
Figure B.8: Hardware case specifications .....	168
Figure B.9: Printed circuit board images .....	169
Figure B.10: Hardware assembly images .....	169
Figure B.11: Exterior hardware views .....	170
Figure E.1: PPG sensor suite .....	177
Figure E.2: ECG electrode leads .....	177
Figure E.3: Hardware suite with labels .....	178
Figure E.4: Software front panel with labels .....	179
Figure F.1: PPG circuit test points .....	187
Figure F.2: ECG/PPG elapsed time error analysis .....	188
Figure F.3: Stainless steel electrodes .....	189
Figure F.4: Ag/AgCl electrode without adhesive .....	190
Figure F.5: Ag/AgCl electrode with adhesive .....	190
Figure G.1: Industry forehead PPG sensor .....	193
Figure G.2: Marquette Medical Systems holter monitor .....	194
Figure G.3: Internal view of Marquette holter monitor .....	194
Figure H.1: Anatomic references of perfusion measurements .....	196
Figure H.2: Ranking of perfusion measurements .....	196
Figure H.3: Einthoven's triangle [9] .....	197
Figure H.4: ECG Electrode placements [12] .....	197

## Table of Tables

Table 2.1: Statistical HRV Measures.....	19
Table 2.2: Frequency Domain HRV measures .....	24
Table 4.1: Pairwise Comparison Chart for Design Objectives .....	33
Table 5.1: Comparison of Transmittance and Reflectance PPG Probes.....	44
Table 5.2: Pairwise Comparison Chart for PPG Sensor Location Objectives.....	45
Table 5.3: Numerical Evaluation Matrix for PPG Sensor Locations.....	47
Table 5.4: Pairwise Comparison Chart for PPG Filter .....	51
Table 5.5: Numerical Evaluation Matrix for PPG Filter Design .....	52
Table 5.6: Pairwise Comparison Chart for ECG Electrode Type.....	56
Table 5.7: Numerical Evaluation Matrix for ECG Electrode Type.....	56
Table 5.8: Pairwise Comparison Chart for ECG Sensor Placement.....	57
Table 5.9: Numerical Evaluation Matrix for ECG Sensor Placement.....	58
Table 5.10: Pairwise Comparison Chart for ECG Filter Design .....	59
Table 5.11: Numerical Evaluation Matrix for ECG Filter Design.....	60
Table 6.1: PPG Filter Characteristics.....	70
Table 6.2: ECG Filter Characteristics.....	74
Table 7.1: Measurements for Calibrated Threshold .....	107
Table 7.2: Time duration for motion activities .....	112
Table 7.3: Activity level statistical data.....	113
Table 7.4: ECG Validation Results.....	116
Table 7.5: HRV Measures from 3 subjects.....	119
Table 8.1: Comparison of estimated battery life for different LED currents.....	125
Table C.1: Bill of Materials .....	172
Table D.1: Component Value Listing.....	174
Table F.1: ECG elapsed time error analysis .....	188
Table F.2: PPG elapsed time error analysis .....	188
Table F.3: Signal comparison with motion artifact .....	189
Table G.1: Dual channel ECG/PPG monitor .....	192
Table G.2: Portable pulse oximeter sensor battery life.....	192
Table G.3: Marquette Medical Systems Holter Monitor .....	194

## **1. Executive Summary**

Sudden Cardiac Death (SCD) is responsible 400,000 to 460,000 deaths per year in the United States [1]. Prior studies have shown that heart rate variability (HRV) analysis can predict mortality in recent cardiac episode survivors. This is because of the reduction in the body's ability to regulate the heart rate (HR) through the autonomic nervous system. Patients will present with increased HR and reduced abilities of the HR to adapt to changing conditions. Patient cardiac health monitoring following a severe cardiac episode could be beneficial as a reduced HRV, may help to risk stratify patients. HRV data is typically obtained through the electrocardiogram (ECG) via gel-based electrodes. However, this approach is problematic when used in a dynamic environment where subjects may be active, due to problems associated with motion artifacts. Motion artifacts may be especially problematic when due to signal corruption from electromyogram (EMG) signals. Alternatively, HRV data may be obtained from a photoplethysmogram (PPG) signal. The PPG signal represents varying levels of light absorption due to pulsations of the arteries and arterioles caused by blood pressure changes during the heart cycle.

The goals of the project are to obtain both ECG and PPG signals for HRV calculations and to compensate for the problems associated with each signal analysis. For the PPG signal, this involves a reduction in motion artifacts as well as optimizing device battery life. For the ECG signal, dry electrodes must be shown to work as effectively as gel-based electrodes in a dynamic environment. Data obtained from ECG and PPG signals must be closely correlated to show the PPG signal as an effective alternative to help prevent problems associated with ECG signal acquisition.

Optimizing battery life of the PPG unit was done by reducing the power requirements of the PPG photodetection unit. To minimize the affects of motion artifacts within the PPG signal, areas of the body were analyzed to determine the portion least susceptible to motion artifacts. Problems associated with gel-based ECG electrodes were attenuated through implementation of dry electrodes. Signals obtained via dry electrodes were used to determine whether dry electrodes offer an effective alternative to gel-based electrodes.

ECG and PPG signals were recorded and analyzed simultaneously under rest and motion artifacts conditions. Correlation values close to 1 would indicate a strong relationship between signals. Ability to accurately display desired outputs will be vital for device use in long term patient monitoring.

## **2. Literature Review**

### ***2.1 Heart Rate Variability***

HRV is often used as an indicator of the health of a patient's autonomic nervous system (ANS) [2]. The heart acts as a pump circulating the appropriate amount of blood throughout the body through rhythmic contraction and relaxations. HR contraction is triggered by the sino-atrial (SA) node, which consists of a group of specialized nerve cells that generate the necessary electrical impulse to initiate heart muscle contraction. Impulses are usually generated at a rate of 100-120 times per minute during rest [3].

However, HR in healthy individuals typically ranges between 60-80 beats per minute (bpm) during rest and varies depending on body activity e.g. variations of the HR are most noticeable to an average person during times of increased physical stress. This is because HR is continuously controlled by the ANS whose net regulatory effect dictates HR. The ANS is the portion of the nervous system that controls involuntary functions in the body [3]. From its central nuclei located in the brain stem, activities are coordinated and controlled through afferent and efferent fibers of the peripheral nervous system. There are two branches of the ANS, the sympathetic (SNS) and parasympathetic nervous systems (PNS) that always work in an antagonistic manner to control organ function (see Figure 2.1). In the heart, stimulation by the SNS increases heart function such as HR, stroke volume etc. with a response time of about 5 seconds. In contrast, the PNS stimulation causes a decrease in HR, with an almost instantaneous response time. At rest, both SNS and PNS actively regulate HR with parasympathetic dominance. However, the balance between each system activity changes constantly based on a feedback mechanism to adapt instantaneous HR based on internal and external environmental conditions.

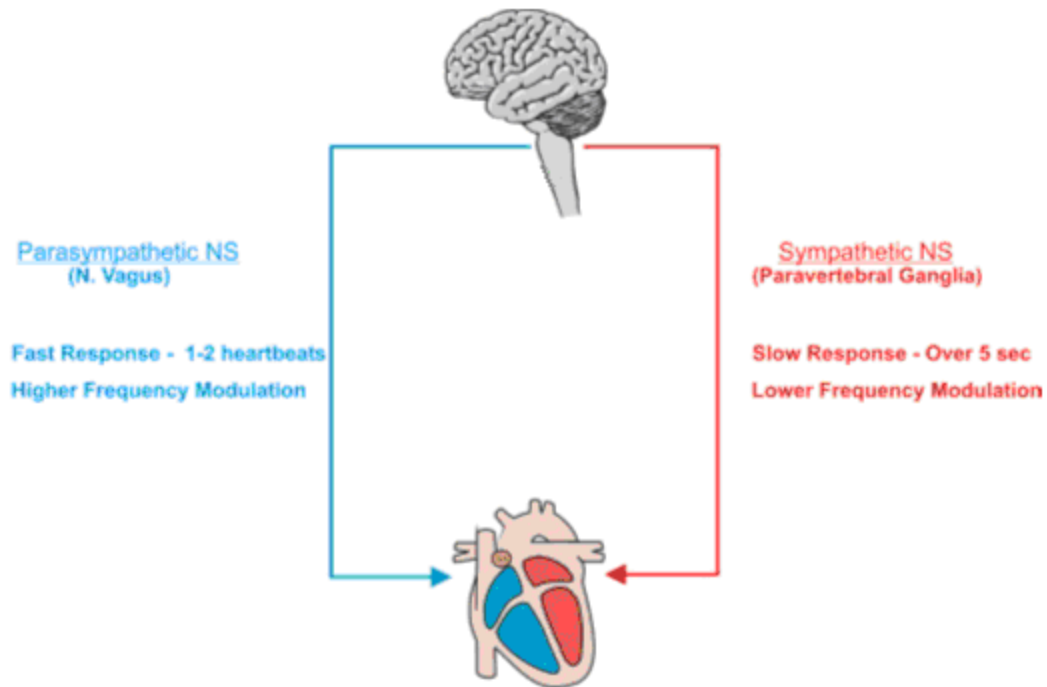


**Figure 2.1: Comparison of the SNS and PNS on heart activity [3].**

Variability is controlled through the withdrawal or expressions of the two systems [4]. During rest, the ECG of healthy individuals exhibits rhythmic variation in R-R intervals, a phenomenon, known as respiratory sinus arrhythmia (RSA). RSA fluctuates at the phase of respiration; cardio-acceleration during inspiration, and cardio-deceleration during expiration. During exercises, HR increases as the parasympathetic system response is attenuated, creating a greater response due to the sympathetic nervous system [4]. The inability of the body to maintain self-regulation has associated itself in many common cardiac conditions. Most of these are caused by poor response of either the sympathetic or parasympathetic nervous systems, resulting in an abnormally high or low HR and an inability to adequately regulate the HR. This is subsequently represented as a poor HRV value, or a low standard deviation of the differences between normal-to-normal beats. Problems relating to unbalanced SNS or PNS activity can be deduced from HRV analysis [5].

## ***2.2 Medical Significance***

In addition to blood pressure, HR, and the ECG recordings, HRV is a significant diagnostic tool used to assess cardiovascular function during cardiopathophysiology. Recent studies have observed a significant relationship between the autonomic nervous system and cardiovascular mortality, linking HRV with major cardiac ailments such as coronary artery disease (CAD) and SCD, or cardiac arrest (CA). The changes are usually manifested as abnormalities with the sympathetic and parasympathetic nervous system activities. As seen with CAD, activity within the PNS is attenuated while the response due to the SNS is accentuated, resulting in a perceivable increase in the HR and a reduction in HRV [6].

### **2.2.1 Diagnostic Capabilities**

The major reason for the interest in measuring HRV stems from its possible ability to predict survival after heart attack. Several studies have related HRV changes to estimate the mortality rate of patients with specific cardiac problems. Significant indicators of potential problems have been associated with hypertension (HTN), congestive heart failure (CHF), CAD, and SCD [6]-[7]. Shown in Figure 2.2, are examples of the affects of CAD on HRV. Within the figure, it can be seen that all of the variability indices decrease with the presence of CAD. CHF patients have been shown to have a generalized decrease of all frequencies of variability. In addition, CHF patients also exhibited a decrease in the PNS functionality with a further decrease of the high frequency variability components such as respiration. SCD or CA in patients has been shown to have a direct relation to the power spectrum of HRV. Examples of this are through variations within the HRV indices and depressions of the HRV indices themselves [7]. CAD has been shown to be manifested as an attenuation of the PNS and an accentuation of the SNS [6].

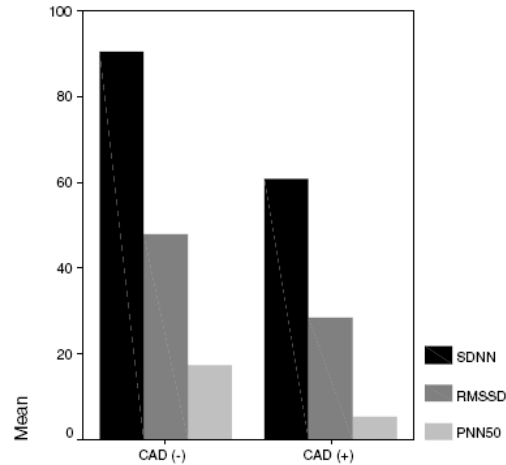


Figure 2.2: Affects of CAD presence on HRV [6]

### 2.3 Current Methods and Practices

Currently there are two major methods of analysis for HRV. While the formulas for HRV indices remain the same, the methods of signal acquisition differ. These two methods respectively are through ECG and PPG signals. Each of these two methods is used to acquire the normal beat-to-beat intervals of the heart rhythm.

#### 2.3.1 Electrocardiography

The ECG is used to detect the electrical signature of the heart [8]. This is an important tool for determining the rate and rhythm of the heart. The ECG of the body is generated from the nerve impulses propagating within the heart. These are due to the depolarization and subsequent repolarization of the atria and ventricles of the heart muscles.

A variety of methods are available for detection of the QRS complex of the normal heart beat. The most common method is through determination of the QRS peak by analysis of threshold values. By scrutinizing the signal amplitudes, it is possible to determine whether the signal has crossed over a specified threshold value. Analysis of the time between peaks can be used to determine the HR and HRV indices. A second method is through isolation of the QRS complex by way of limiting the signal frequencies to only the high frequency components of the QRS. Threshold detectors based on frequency

content can then be employed to detect the QRS complex, eliminating the remainder of the signal and noise while retaining a good trigger point for the cardiac cycle and subsequently for finding the instantaneous HR or time between beats.

### **2.3.1.1 Principle**

The ECG is used to detect and monitor the electrical signals of the heart. This is done by determining the voltage potential across the heart, using two bi-polar leads placed on either side of the heart. When analyzing the ECG signal, there are multiple techniques for acquiring the signal from the body, these being dependent on the placement of the electrodes. Relative placement of the electrodes determines the area of the heart the ECG signal will be acquired from. As the electrical signals propagate through the heart, it is possible to view the ECG. Electrical propagations running perpendicular to the placement of the electrodes will not result in a visible potential change, while potential changes along the axis between the two electrodes will be recorded. An example of the possible placements for the electrodes is shown in Figure 2.3. The top row within the figure gives the general electrode placements for use with Einthoven's Triangle. These placements are Leads I, II, and III, respectively, where when the Lead I and III electrodes are placed perpendicular to one and other, the sum of the two resulting signals will provide the Lead II signal.

Electrical signals obtained through the ECG indicate various portions of the hearts contraction cycle [10]. A sample of a single heart beat is shown in Figure 2.4, where the peaks of the various individual portions of the signal are noted. The initial small wave, labeled as the P wave, corresponds to the depolarization of the atria. The following QRS complex represents the depolarization of the ventricles as well as the repolarization of the atria. Finally, the T wave represents the end of the heart cycle with the repolarization of the ventricles. With the cycle concluded, the heart is then ready for the next beat.

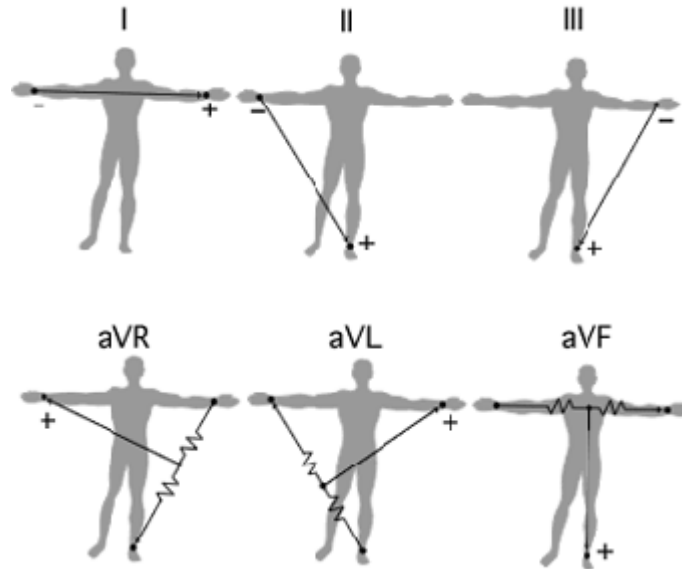


Figure 2.3: Einthoven's triangle [9]

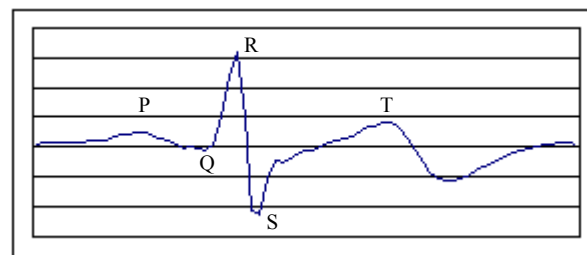


Figure 2.4: Sample electrical signal for single heart beat indicating ECG electrical components

The above signal of the ECG can be used to determine the heart function. As the QRS complex is representative of the beat of the heart, an analysis of the QRS complexes within a signal sample can allow for analysis of the heart function. Determining the number of QRS occurrences in a minute provides the number of beats per minute. Furthermore, an analysis of the time between QRS peaks will allow for a further analysis of the functions of the heart, with specific relation to the HRV.

### 2.3.1.2 Methods for Acquisition

For the majority of applications for ECG signals, the signals are acquired through gel-based electrodes. These are used to reduce the effective resistance between the skin and electrode surface contact. However, problems can exist with this method. Since the gels used by these electrodes are water based, over time the gels can dry, causing an increase

in the resistance between the skin and electrode contact surface. Other problems can exist from skin irritation caused by extended contact of the gel with the patient's skin [11].

Dry ECG electrodes have been employed in an attempt to alleviate the problems associated with gel-based electrodes [11]. By employing a dry electrode, it is possible for the patient to wear the electrode continuously without experiencing any adverse effects. Furthermore, with the elimination of electrode contact gel, resistance changes over time can be eliminated. For this to be an effective alternative to gel-based electrodes, the signal quality and reliability of the electrodes must be comparable. The final hypothesis was that dry ECG electrodes could be used as an effective alternative to gel-based electrodes in acquiring ECG signals and measuring accurate HRV values while preventing problems associated with long-term ECG gel use.

### **2.3.1.3 Limitations of Electrocardiography**

Current methods for the determination of the ECG involve the detection of electrical potentials between two points using a reference ground. Potential problems with this are due to the necessity of requiring lead connections from the two points to determine the electrical potential across. Further problems that may be experienced with the ECG are that the ECG signals are not the sole electrical signals present within the body. All nerve impulses within the body can be represented as electrical signals of varying amplitudes and frequencies, see Figure 2.5. As such, signals with frequency ranges that overlap the frequency range of the ECG signal cannot be removed based on simple frequency range based filtration. Noted within the figure are the frequency cutoffs, shown as time period. From this, the ECG signal is seen as containing frequencies between 0.5 to 50 Hz. Overlapping the ECG are signals from the EMG and the electroencephalogram (EEG).

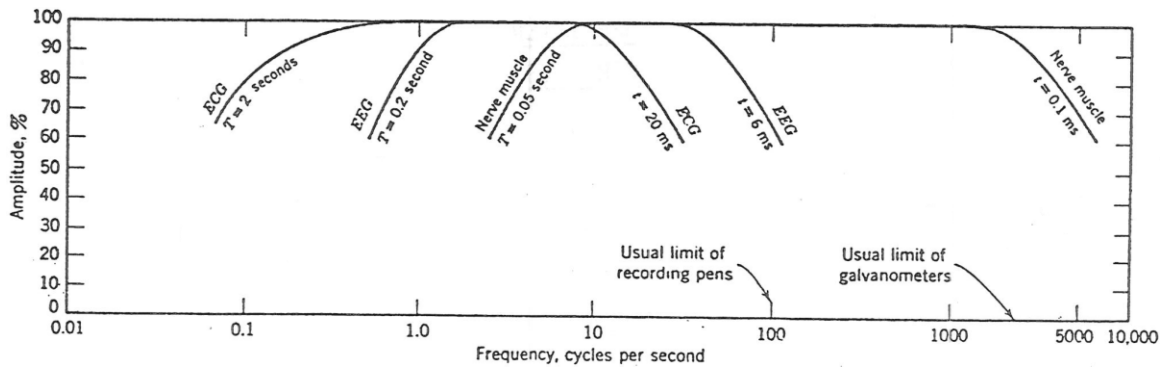


**Figure 2.5: Frequency spectrum of bioelectric events [12]**

From Figure 2.5, it can be seen how it is possible for signal artifacts to enter into the ECG signal. Due to the location of the ECG electrode placements on the chest, there remains a significant chance for EMG signals to be recorded along with the ECG. Depending on the degree of muscle activity, there will be varying degrees of corruption due to EMG noise. Should muscle activity be high enough, this may cause the ECG signal to not be easily distinguishable, and thus preventing analysis of the signal.

## 2.3.2 Photoplethysmography

### 2.3.2.1 Principle

Photoplethysmography is based on the differences in light absorbance due to changes in arterial configuration during the various stages of the cardiac cycle. During the cardiac cycle, the heart undergoes rhythmic contractions (systole) and relaxations (diastole) creating pressure changes in blood vessels. No blood is pumped out when the heart is relaxing and refilling. To ensure continuous blood flow in the capillaries, arteries are functionally specialized to serve as pressure reservoirs [16]. Elastin fibers present in arterial walls enable them to stretch and accommodate the extra blood volume during systole. Arteries therefore behave as balloons, changing their diameters during the different phases of the cardiac cycle (see Figure 2.6).

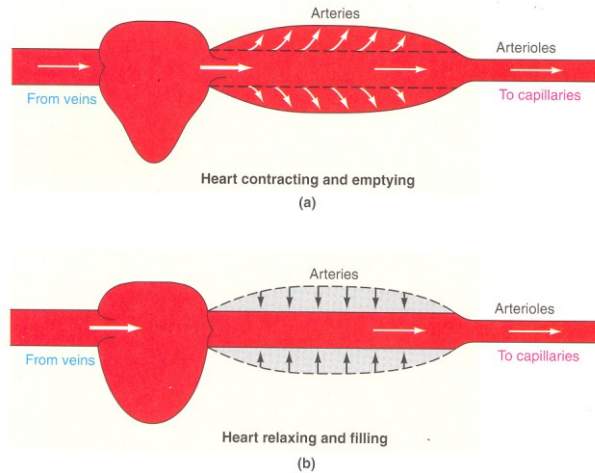


**Figure 2.6: Arteries acting as pressure reservoirs by varying cross-sectional area [16]**

During systole, there is more blood volume in the arteries resulting in an increase in arterial diameter. The optical path length of light increases, hence more light is absorbed by blood. This causes a decrease in the amount of transmitted light, and so the PPG waveform reaches a minimum peak. The opposite is true during diastole and the PPG waveform reaches a maximum peak (see Figure 2.7). The PPG waveform thus consists of a distinguishable AC component due to pulsatile arterial blood flow. The DC component represents the composite absorbances of the non pulsatile portion of arterial blood, as well as of other tissue types such as veins, bone, muscles, etc.

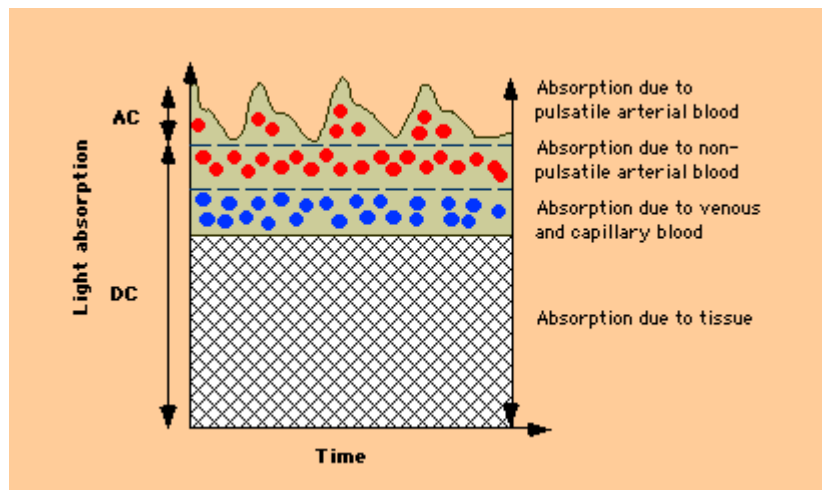


**Figure 2.7: Light absorption through tissue as a function of pulsatile blood flow [17]**

Changes in arterial blood volume during heart activity are thus reflected as pulsations in arterial blood flow. Signal processing algorithms can thus be applied to compute pulse rate (PR), and pulse rate variability (PRV), and thus HR and HRV.

### **2.3.2.2 Sensor Probes**

The PPG sensor probe consists of a light emitting source and a photodetector. The amount of light that is transmitted from the light source is detected by the photodetector as a current. This current, proportional to the amount of transmitted light, is converted to a voltage by a trans-impedance amplifier. The detected signal undergoes further conditioning such as filtering and signal amplification to extract the PPG waveform.

### **2.3.2.3 Methods for Light Detection**

PPG sensors can be classified into two types based on the relative position of the LED with respect to the photodetector, namely transmittance and reflectance mode sensors [14].

#### ***Transmittance mode***

Signal detection via transmittance mode is dependent on light being transmitted through tissue. It thus requires soft tissue and minimal bone tissue (that significantly reflects light) to allow maximal transmittance of light. The LED and photodetector are placed on opposite sides of tissue thus requiring a small tissue length (see Figure 2.8a). As a result transmittance sensors are limited to peripheral locations of the body such as the earlobe, fingers, nasal septum, toes etc.

#### ***Reflectance mode***

Reflectance photoplethysmography is dependent on light being reflected from tissue and light reflection is usually facilitated by the presence of bone tissue. LED's and photodetectors are placed adjacent to each other in the sensor (see Figure 2.8b). As a result of this architecture, reflectance sensors can be placed at various locations in the body.

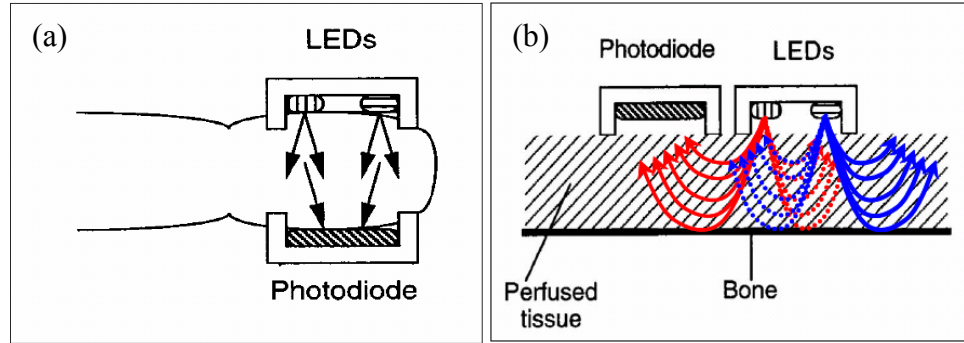


Figure 2.8: Transmittance (a) and reflectance (b) PPG probes [14]

### ***Transmittance versus Reflectance***

The main advantage of transmittance sensors is that most light is transmitted through soft tissue. Finger sensors are the most popular commercial probes used in clinical settings for patient monitoring. However as transmittance probes are limited to peripheral locations, sensors are easily susceptible to inaccuracies due to environmental conditions such as vasoconstriction. Reflectance photoplethysmography is often facilitated by the presence of bone tissue, with higher amplitude being obtained from regions such as the forehead and chest [18]. Reflectance probes can be used both invasively and non-invasively in many areas in the body, especially those that cannot be accessible by transmittance probes. Wouda et al utilized a tampon-like vaginal reflectance PPG sensor to demonstrate differences in vaginal vasocongestion in women with and without dyspareunia during sexual arousal [19]. Sometimes, reflectance probes are most applicable when monitoring HR during conditions of compromised peripheral blood flow [20].

Motion artifacts adversely affect the accuracy of PPG measurements. Peripheral sensors such as the finger and toe are easily susceptible to artifact due to movement of limbs, limiting patient activity during recordings. Johnston et al demonstrated reduced motion artifacts in reflectance sensors, obtaining greatest signal stability from forehead sensors during motion [21]. However, motion artifacts reduction is still one of the many challenges in designing long term wearable health monitors where high specificity is desired [22]. Several approaches like motion artifacts removal or correlation such as in simple analog filtering and software adaptive filtering have been developed to attenuate the problems due to this limitation.

Power consumption is also an important criterion in LED selection. To guarantee a good PPG signal, the intensity of light transmitted or reflected must be strong enough to be detected by the photodetector. The intensity of incident light is directly proportional to the LED drive current. LED's are usually 2-10% efficient, thus most of its energy is dissipated as heat [14]. While power consumption may not be a problem with AC powered PR monitors, it is the main limitation when designing battery operated and portable units as most of the power is consumed by the LED e.g. in a microcontroller PPG unit, 70% of the power is consumed by LED's and RF transmitter [18]. Savage et al demonstrated the preference of a reflectance sensor with a large photodetection area as the estimated battery life was 18 times higher than transmission mode sensor, due to the lesser current requirements for reflectance sensors (1.9-3 mA) compared to transmittance sensors (19.6- 46mA) [23].

#### ***2.4 Electrocardiography versus Photoplethysmography***

HRV is a measure of changes in instantaneous HR. It is easily calculated by analyzing time series of beat-to-beat intervals from ECG tracings from its distinguishable QRS complex. Although the P wave serves as a reference point for onset of cardiac events, the R wave is generally preferred in HR measurements due to higher signal to noise ratio (SNR) [24]. However, the ECG signal is susceptible to baseline drift, power line noise, motion artifacts due to electrode movement as well as electrical muscle activity interference [25]. ECG signals are also traditionally acquired via gel electrodes, to maintain good surface contact. However, gel electrodes are usually uncomfortable for patients especially in long term recordings because of potential skin irritation, as well as drying [11].

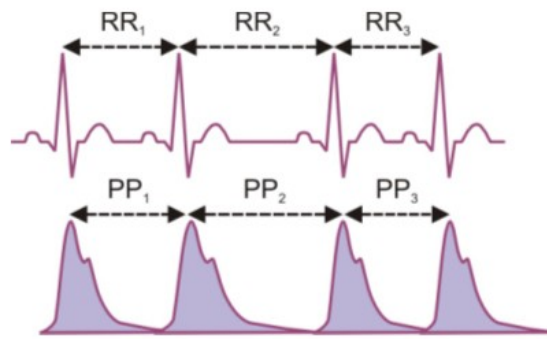


**Figure 2.9: Illustration of beat-to-beat intervals within ECG and PPG signals [3]**

Alternatively, HRV data can be extracted from the PPG as the heart cycle is reflected via pulsations in arterial blood flow (see Figure 2.9). Comparative studies have shown correlation between HRV measurements obtained from ECG and PPG signals [26]. Mendelson et al compared HR and HRV data obtained from simultaneous ECG and reflectance mode PPG recordings [27]. Correlations coefficients of 0.9 and 0.91 were observed for HR/ PR and HRV/PRV values, respectively. Bolanos et al. also observed similar correlation using a PDA-based system, with sophisticated HRV analysis such as autoregressive modeling, Poincaré plots, standard deviation etc. to better demonstrate correlation between the two signals [25].

PPG sensor systems are more compact and convenient for patient use. The PPG signal is detected optically, making it less susceptible to electric interference. The PPG signal requires only one wire for signal acquisition as opposed to three for the ECG. This reduction in wire content is thus desirable, especially during ambulatory conditions [25]. PPG signals also offer the versatile advantage of obtaining other vital physiologic signals like breathing rate and area perfusion, hence offering a better range of clinical applicability. PPG monitors can also be incorporated in non medical instruments, increasing their versatility. Kim et al. developed an armband sports MP3 player incorporating a HR monitoring unit via reflectance photoplethysmography [28]. Comparison with a professional medical sensor demonstrated an effectiveness of calculating PR within an error of <3% from 20 subjects.

## 2.5 Mathematical Models

In 1996, a Task Force of the European Society of Cardiology and North American Society of Pacing and Electrophysiology set standards for calculating HRV, to harmonize HRV measures. These measures involve time domain and frequency domain analysis [7]. Both methods utilize the same data set, using mathematical interpolations such as Fourier transforms to move between domains. The flow chart in Figure 2.10 outlines the necessary steps taken to process signals for HRV analysis. HRV can thus be expressed under different parameters and models, and the choice of methods depends primarily on the application and length of data recording.

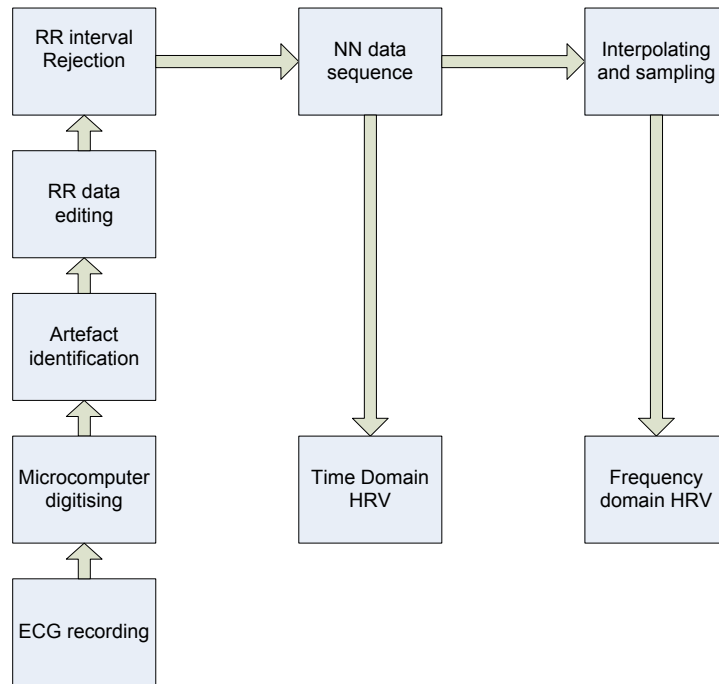


Figure 2.10: Flow chart summarizing steps for ECG HRV analysis [7]

### 2.5.1 Signal Conditioning

A sequence of beat-to-beat intervals can be obtained from ECG signals using appropriate software/hardware algorithms. Atapattu et al developed a simple computer algorithm for HRV acquisition and analysis [24]. They described a sequence of discrete normal to normal (NN) intervals as a grossly approximated impulse train of unit impulses that temporally locate peak occurrences. This can mathematically be described as an infinite series set of spaced impulses,  $\delta$  (see Equation 1).

$$P(t) = \sum_i^n \delta(t - t_i) \quad (1)$$

The time interval between consecutive impulses located at times  $s(t)$  and  $s(t+1)$ , for  $t=0, 1, 2, \dots, n$  can be described as a series  $x(t)$ , representing the normal to normal (NN) time interval series (see Equation 2).

$$x(t) = s(t) - s(t + 1) \quad (2)$$

The analysis of HRV assumes NN intervals are obtained from normal heart beats [29]. Figure 2.11 shows an irregular heart beat due to premature ventricular contraction. This leads to the absence of the P wave as a result of the lack of atrial contraction.

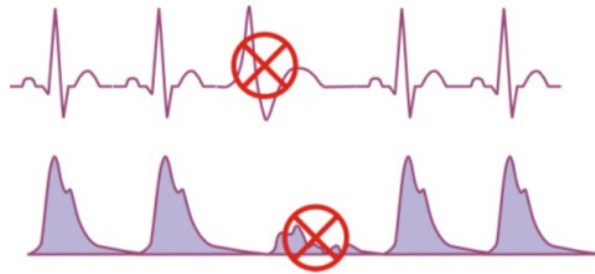


**Figure 2.11: Irregular heart rhythm shown as PVC [3]**

The PPG waveform is diminished due to decrease in heart stroke volume. The consequent R-R interval is thus significantly larger than adjacent intervals. Such increased R-R intervals are typically rejected from the HRV processing algorithm. This is because their irregularity can introduce erroneous deviations in HRV and cause misinterpretation of results. For this reason data after R-R editing is termed normal to normal or NN intervals (see Figure 2.10).

### **2.5.2 Time Domain Analysis**

Time domain methods for HRV analysis are derived by evaluating the HR or the intervals between successive beat-to-beat or normal-to-normal (NN) intervals. Simple time domain variables include the mean NN interval, the mean HR, the difference between night and day HR etc. Variations in NN intervals can also be observed to evaluate changes in instantaneous HR secondary to respiration, tilt, drug intake, exercise etc.

### 2.5.2.1 Statistical Methods

Several statistical indices have been developed to quantify HRV, and these indices are usually chosen based on length of time of ECG recordings. A typical manipulation involves calculating the mean and standard deviation of HR. The simplest and most commonly used index is the standard deviation of the NN (SDNN) interval (unit=ms) [29].

$$SDNN = \sqrt{\frac{1}{n} \sum_{i=1}^n (NN_i - m)^2} \quad (3)$$

Where:  $NN_i$  = duration of the i-th NN interval in the analyzed ECG (ms)

$n$  = number of all NN intervals

$m$  = mean duration

However, for large values of  $n$ , with the assumption that the mean of differences between neighboring intervals is negligible, the formula can be approximated into another HRV index, the root mean square of successive differences, rMSSD (unit: ms).

$$rMSSD = \sqrt{\frac{1}{n-1} \sum_{i=1}^{n-1} (NN_{i+1} - NN_i)^2} \quad (4)$$

The SDNN and rMSSD indices are preferentially used for short term, steady state analysis because vital information can be omitted in longer recordings as signals are averaged out. This problem can be resolved by adapting the formula for shorter time segments to take into account variations in longer recordings. Other indices to quantify HRV are listed in Table 2.1 below.

**Table 2.1: Statistical HRV Measures**

Measure	Unit	Description
SDNN index	ms	Mean of the standard deviations of all NN intervals for all 5 minute segments in the entire recording
SDANN	ms	Standard deviation of the averages of the NN interval in all 5 minute segments of the entire recording
NN50	ms	The number of interval differences of successive NN intervals greater than 50 ms
pNN50	ms	The proportion derived by dividing NN50 by the total number of NN interval

There exist no standard prognostic values for rMSSD and SDNN indices, although some studies have tried to establish some ranges. This is because identical statistical measures can result due to entirely different causalities. Patients are generally monitored over time, and from various studies with cardiac patients, the general pattern observed was the inference of better survival from increased HRV indices. In a study by Bilchick et al., 179 patients with CHF were treated either with doses of amiodarone (medication used for irregular heart beat) or a placebo and monitored over about a 4 year period [30]. Among 127 patients, an  $SDNN < 65.3ms$  ( $p=0.0001$ ) was a predictive value in worse survival, with an increase of 10ms of SDNN resulting in 20% decreased mortality risk. A study by UK-Heart of 433 CHF patients monitored over  $482 \pm 161$  days, indicated annual mortality rates for SDNN at 5.5% for  $>100$  ms, 12.7% for 50 to 100 ms, and 51.4% for  $<50$  ms [31].

One limitation of statistical methods is that their accuracy depends on the quality of the R-R data obtained. This is sometimes difficult in long term recordings (e.g. 24 hrs), as it requires careful maintenance of recording equipment, lead stability as well as patient cooperation [29]. The possibility of introducing artifact errors is likely if abnormal R-R intervals are not rejected. To ameliorate this problem, Kleiger et al proposed that the durations of neighboring R-R intervals of sinus rhythm usually do not differ by more than 20%, and thus only the set which satisfies this requirement be included in the respective calculations [32]. However, this approach may not always be successful in properly rejecting abnormal intervals. For long term recordings, statistical measures should be used when the quality of NN interval data is guaranteed. For 5 minute periods it is

believed that these measures quantify the slow components of heart although there is a lack of physiological understanding for this phenomenon [29].

### 2.5.2.2 Geometrical Methods

Geometrical methods provide visual representations of HRV data by converting the series of NN intervals into a geometric pattern. This is usually done using three approaches (a) converting a geometric pattern into an HRV measure, (b) obtaining parameters by interpolating the geometric pattern to a mathematically defined shape and (c) classifying geometric shapes into several pattern-based categories representing different HRV classes [7].

#### *Interval Tachogram*

A simple graphic representation is plotting NN interval duration against time, an interval tachogram. However, given the long and repetitive nature of the heart cycle, the tachogram is often cumbersome to analyze and thus preferentially mapped to the frequency domain for analysis. It is usually suitable when analyzing HR trends during specific activities. Figure 2.12 shows an interval tachogram recorded from a patient using Mini Logger® monitor, with a strapped chest electrode. As observed, interbeat interval decreases with increases in body stress (e.g. walking, jogging) due to increased HR [33].

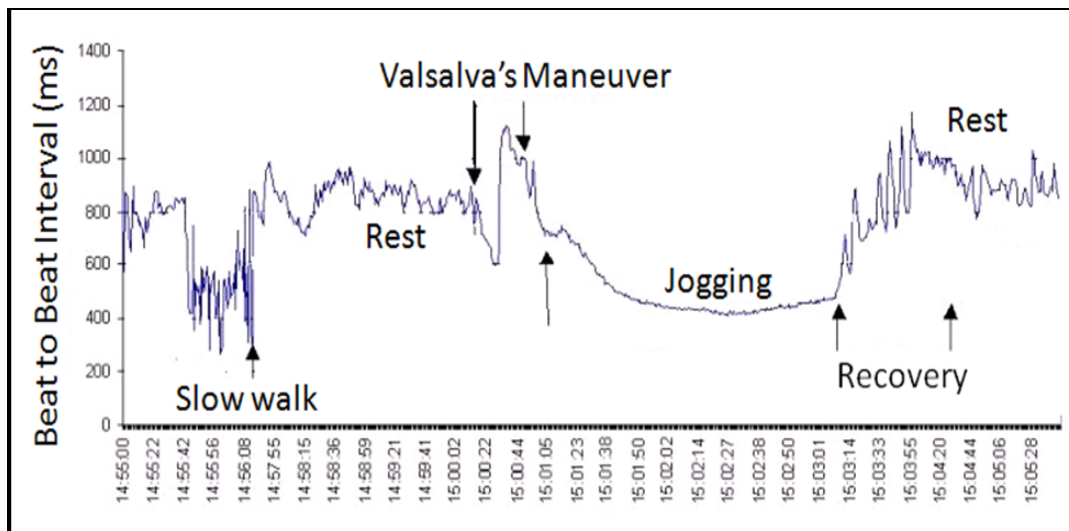
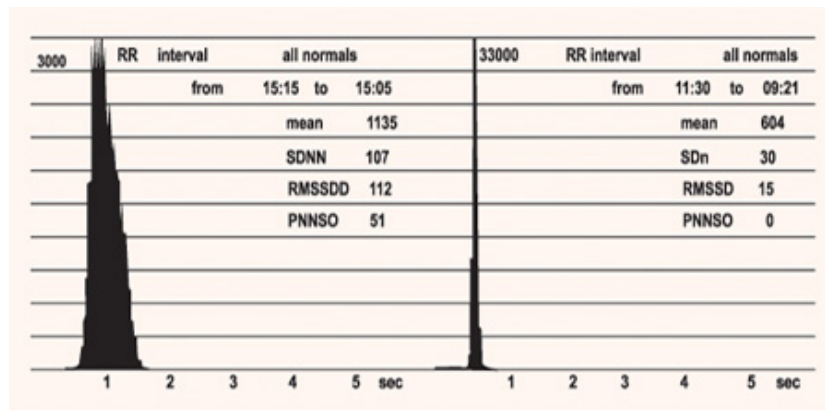


Figure 2.12: Interval tachogram from Mini Logger® monitor during various activities; redrawn from [33]

### ***HRV Triangular Index***

Another method involves calculating HRV triangular index from a sample density histogram of NN intervals. This method is most suited in histograms that have a dominant peak, where the histogram assumes a triangular shape whose height corresponds to the number of R-R intervals with modal duration (H), and area of the histogram corresponds to number of all NN intervals used to construct the histogram, A [34]. The baseline width i.e. HRV index is then computed by the fraction  $A/H$ . Based on the spread of the histogram, individuals with defective heart rate variability can easily be discerned, as can be seen in Figure 2.13. A decrease in histogram spread indicates a low HRV triangular index. Also observe the reduction in modal R-R intervals, compared to that of a normal person.



**Figure 2.13: N-N interval histogram to compute HRV triangular index [34]**

In a study of 385 survivors of acute myocardial infarction, Odemuyiwa et al demonstrated that HRV triangular index of  $< 20U$  had a sensitivity of 75% and specificity of 76% in the prediction of arrhythmic events, 40% and 83% respectively in the prediction of sudden deaths, respectively [35].

### ***Poincaré Plots***

HRV data can also be analyzed using a Poincaré plot, where each NN interval is plotted as a function of the previous interval (see Figure 2.14). The data can be interpreted visually or quantitatively, and one advantage is that abnormal beats are usually observed

as outliers on the plot. The Poincaré plot typically appears as an elongated cloud of points oriented along a line-of-identity. The dispersion of points perpendicular to the line-of-identity reflects the level of short-term variability ( $\Delta R-R_t$ ), while the dispersion of points along the line-of-identity is thought to indicate the level of long-term variability ( $\Delta R-R_t$ ) [36].

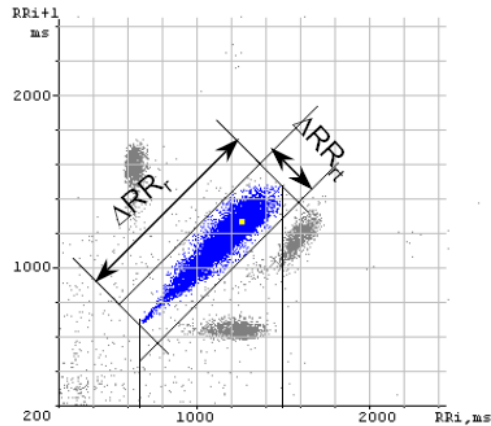


**Figure 2.14: HRV analysis using Poincaré Plot [37]**

Some studies have classified Poincaré plots based on their relative patterns such as torpedo or comet shape, which indicate various ranges of HRV (see Figure 2.15, A and B).

Contreras et al. observed that lagged Poincaré widths and spectral indices might be a useful tool to distinguish normal from pathological HRV, recommending additional tests for validations [39]. Paškevičiūtė et al demonstrated Poincaré plots constructed from long-term ECG recordings of R-R intervals might be potential tool in diagnostics of atrial fibrillation, atrial flutter and other supraventricular dysrhythmias (see Figure 2.15 C) [38]. This was as a result of observed characteristic plot shapes in patients after long term ECG recordings of 43 patients suffering with respective conditions.

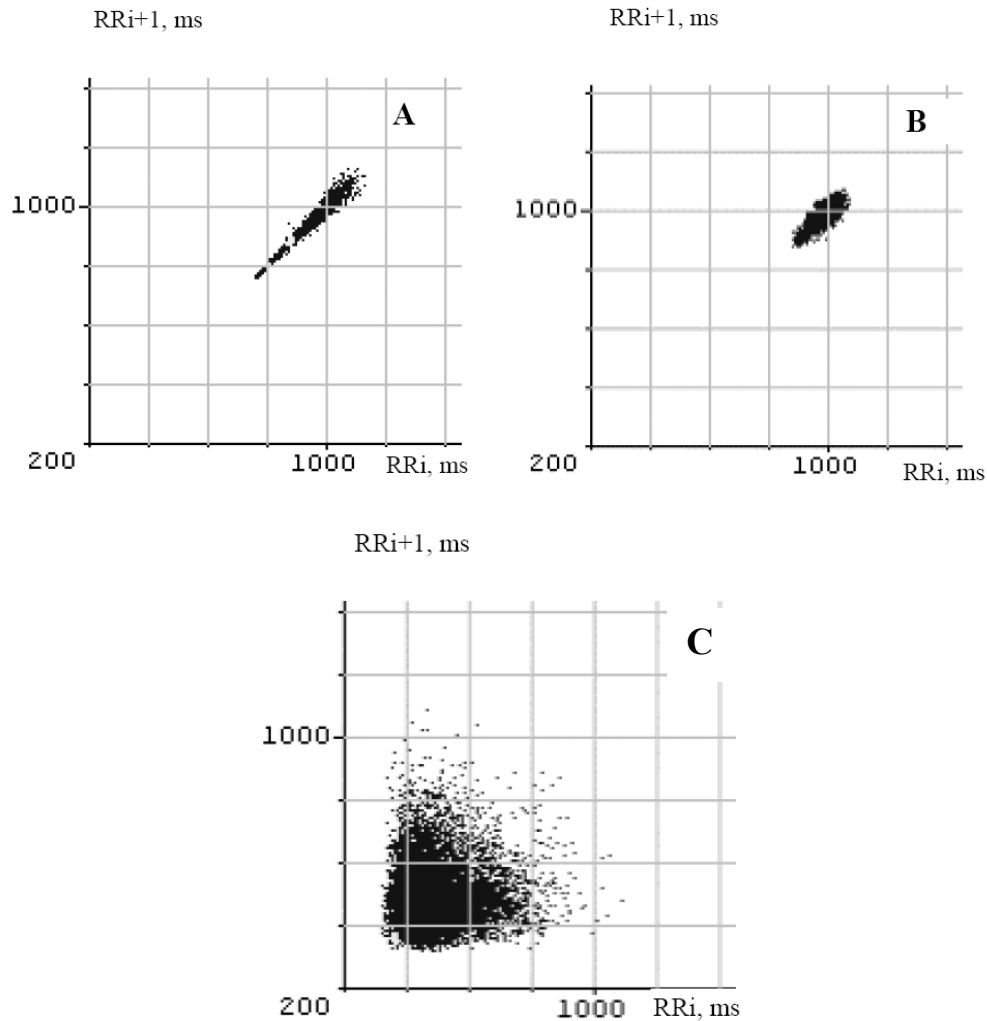


**Figure 2.15: Examples of Poincaré plot patterns with different HRV values [38]**

The weakness of using Poincaré plot analysis lies in the subjective interpretation and classification of plot patterns, hence no precise definition for the conditions for which they represent. The studies above assessed their results by comparing Poincaré between normal and cardiac patients, and assessing the change in the plot geometry in patients monitored over time. Nonetheless, geometric methods can often provide a reasonable assessment of HRV when the quality of R-R interval does not permit the use of statistical methods. Another important factor to note is that these methods can only be valid from data generated from a substantial number of data points and the longer the recordings being more effective [29].

### 2.5.3 Frequency Domain Analysis

With additional resampling and Fourier transforms, the interval tachogram can be analyzed to obtain its frequency components. The HRV spectrum, usually obtained from short term recordings of 2 to 5 minutes, contains three main characteristic components. These frequency components give an insight on the influence of central nervous activity on the respiratory cycle (see Figure 2.16).

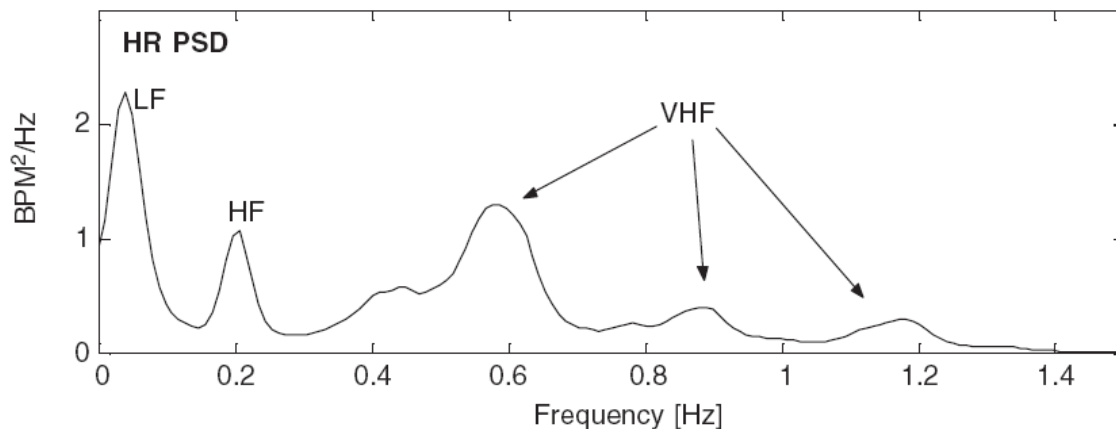


Figure 2.16: Frequency power spectrum of HRV [40]

Table 2.2: Frequency Domain HRV measures

Measure	Unit	Description
High Frequency (HF)	ms <sup>2</sup>	Total power from 0.15 to 0.4 Hz
Low Frequency (LF)	ms <sup>2</sup>	Total power from 0.04 to 0.15Hz
Very Low Frequency (VLF)	ms <sup>2</sup>	Total power from < .04Hz
LF/HF ratio	none	Ratio of high frequency to low frequency component
Total power	ms <sup>2</sup>	The variance of NN intervals over the temporal segment usually $\leq 0.4$ Hz

The HF component reflects parasympathetic tone and fluctuations caused by respiratory sinus arrhythmia. The LF component reflects of both parasympathetic and sympathetic tone. Frequencies in the very low ranges (VLF) are typically not good diagnostic indicators and do not have a well defined physiological explanation. The LF/HF gives the balance between parasympathetic and sympathetic activity on HR. Spectral recordings over longer recordings of a 24-hour period usually include an Ultra Low frequency

(ULF) component, from  $\leq 0.003\text{Hz}$  [7]. Depending on the level of body metabolism, the distribution of frequency contents changes depending on to HR [4]. Bigger Jr. et al studied 715 patients, 2 weeks after myocardial infarction to establish the relationship between frequency domain measures of HRV and mortality during 4 years of follow-up [43]. They demonstrated strong association between total ULF and VLF power components in predicting arrhythmic deaths.

## ***2.6 Current Devices***

Several ECG HRV measuring systems that utilize different algorithms processing methods have been developed. The Mini Logger Series 2000 is a commercial portable system that measures interbeat HR (IBI) intervals by a polar chest belt electrode system [33]. A pulse is transmitted each time an ECG “R” wave is detected to a hardware sensor suite. This unit can be programmed via software to record data at user selected intervals. The software also allows for setting parameters for data collection, downloading and charting results. Figure 2.12 shows a sample tachogram obtained from the device. US Patent 20060287605 developed by Lin et al describes a versatile portable HRV monitor with a built in central processing unit to perform time and frequency HRV analysis [44]. ECG signals are obtained via two electrodes. The systems algorithms allow for the elimination of irregular R-R intervals. HRV measures obtained from the device include time domain analysis measures such as mean NN interval; mean HR, standard deviation, rMSSD indices as well as frequency domain analysis of HF, LF, HF/LF components. The device also includes a data storage unit and data module that can transmit data via a USB interface. Data can also be wirelessly transmitted via Bluetooth to a personal computer, cell phone, database etc.

The existence of modern wireless technology has enabled the flexibility of patient monitoring options via wireless wearable sensors, for hospital environment, home use as well as outdoors. The convenience, portability and versatility of the Personal Digital Assistant (PDA) devices in health care management, has made them a popular choice for monitoring devices. Wearable sensors usually possess a Bluetooth radio to transmit acquired signals to a PDA unit. This data can be analyzed within the PDA using software, or uploaded to a web-server. This versatile platform allows for the easy transmission of

patient data, facilitating and accelerating patient care. PDA based systems developed by Mendelson et al and Bolanos et al compared and correlated HRV data obtained from PPG and PPG systems. Karlsson et al developed a similar PDA based system for house nursing; however their device assessed HRV via real time analysis of Poincaré plots [45]. They selected Poincaré plots as the preferred method of visualization because the overall geometrical pattern is less sensitive to error, as measurement errors such as detection errors and artifact can often be discerned as outliers. They stipulated that patients with atrial fibrillation would benefit from this device, due to the irregular and chaotic nature of their plots, providing an easy way even for patients to discern recurrence of atrial fibrillation. Further developments for their device included developing a smaller data acquisition module with improved battery life.

## ***2.7 Future Developments***

Future developments in the field are mainly focused on attaining a better signal while reducing general signal noise due to motion artifacts. Each of the methods of signal acquisition is being further adapted for incorporation into real-time monitoring systems. Such systems will allow for the user to gain more mobility, which can be especially beneficial for reducing overall healthcare costs [41]. Further benefits of increased mobility are allowing for long-term signal acquisition and analysis. This is especially important for the detection of rare signal anomalies or arrhythmias.

The ECG electrode design, with the development of dry ECG electrodes, is being applied to applications requiring continuous monitoring [41]. Problems associated with HRV can indicate increased risks of SCD [7]. Due to this it may be sometimes necessary to delay patient discharges. Developments of comfortable electrode systems designed for long-term monitoring will allow patients to be safely discharged with mobile monitoring systems [41]. Further advances include the development of wireless ECG monitoring systems. Such a device may allow for the patient to have further increased mobility while also allowing for transmission of ECG telemetry [42]. Other developments with the ECG signal are with the further understanding of the specific segments of the ECG signal. Specifically this applies to the P-P and P-R intervals [7]. Each of these features within the

signal can provide important information regarding the cardiac health of a patient. Future developments along these lines will provide for better detection of the P waves within the ECG signal. These methods for the ECG are being used to help facilitate long term monitoring of patients outside of the hospital environment.

PPG sensor developments are focused on the development of wireless transmission technology. This will help to eliminate potential problems with motion artifacts in addition to allowing for a more flexible sensor platform [23]. These developments will allow for the subject to have an increased range of mobility, allowing for earlier patient discharges while utilizing patient telemetry transmission for remote monitoring.

Further developments for HRV monitoring include improvements in the mathematical models used, and correlations between the HRV indices and other physiological functions [7]. Current methods for HRV analysis do not provide a wide spectrum of analysis methods, especially under changing environmental conditions. Signal correlations can be used to determine the affects of HRV on various physiological signals. This is especially important in determining how HRV is manifested throughout the body and in determining alternative methods for determining the HRV indices. An example of this can be shown within this report in the correlation of ECG and PPG signals.

## **3. Project Approach**

### ***3.1 Hypothesis***

HRV has been shown to have certain predictive values for patients who are likely to suffer from SCD. To date, cumbersome methods have prevented the use of HRV as an effective tool. Although the human ECG is easy to acquire, utilizing gel-based electrodes makes it impractical for use in a dynamic setting where subjects remain active. Alternatively, HR information can also be obtained non-invasively from the PPG signal. However, correlation between HRV derived from the ECG or a PPG signal need to be established. This project is based on two hypotheses.

#### **3.1.1 Dry Electrodes**

Gel-based electrodes can cause skin irritation during extended use and signal quality may degrade over time due to electrode drying. Use of dry electrodes can alleviate the problems associated with gel-based electrodes while still maintaining an adequately good signal quality for analysis. This will allow for more effective long term patient monitoring.

#### **3.1.2 PPG Signal Alternative**

Heart electrical activity is reflected in pulsatile arterial blood flow, so PPG signals can be used as a reliable non-invasive alternative to obtain HRV data. This avoids the problems that arise with difficulties in acquiring ECG such as baseline drift, EMG interference and utilizing gel based electrodes in active subjects.

### ***3.2 Specific Aims***

The overall goal of the project is to acquire ECG and PPG signals simultaneously, and calculate HR and PR, as well as respective variability indices (SDNN and rMSSD indices). Waveforms and computed indices should be displayed. The design should also have set of controls for user to change certain parameters.

### **3.2.1 Photoplethysmography Acquisition**

The two major aims addressed in designing the PPG unit of the device include optimizing power consumption as well as minimizing motion artifacts to prevent PPG system inaccuracies. Optimizing power consumption assumes most of the power in the device circuit will be used to drive the LED in the PPG circuit. It was assumed that the dominant power consumption was due to the LED. Other factors that may also affect the power requirement include LED emission wavelength and PPG sensor mode. The effects of varying LED drive current amplitude as well as current duty cycle will be investigated. It is also assumed that motion artifacts introduced in the device are due primarily to the location of the PPG sensor, as well as the relative motion of the sensor at the attachment site. Sensor locations will be evaluated to determine which is least susceptible to motion artifacts.

### **3.2.2 Electrocardiogram Acquisition**

The specific aim of the electrocardiogram portion of the system is to acquire the ECG signal through experimental dry electrodes. This should be done with a minimum of hardware components to decrease the possibilities of component failure and reduce overall device cost. Signals for the ECG system are to be examined based on the QRS complex locations. From this information, the time between peaks of the signal is to be determined. This will then be used to calculate the HR of the subject and from this to determine the HRV indices.

#### **3.2.2.1 Comparison of Dry Electrodes with Gel Electrodes**

The dry electrodes used for the system must be comparable in their functioning to gel-based electrodes. The immediate goal of the dry electrodes is to produce a signal with similar quality to gel-based electrodes. Furthermore, the dry electrodes must limit potential motion artifacts and additional noise contained within the system. During long-term use, the electrode system selected must prevent signal degradation due to electrode gel drying. Finally the electrodes chosen must provide for decreases in the potential for skin irritations caused by materials used in the electrode construction.

### **3.2.3 Correlation of ECG and PPG signals**

The final aim is to correlate HRV and PRV obtained from simultaneous ECG and PPG recordings, i.e. respective rate and variability indices. Algorithms should minimize standard error of estimate between PPG and ECG derived indices. A correlation coefficient close to 1 will also indicate a strong relationship between the two signals, demonstrating that the PPG can be used as an alternative for HRV calculations.

## **4. Analysis of Needs and Specifications**

The main objective of this MQP project is to design HRV monitor. Current methods utilize the ECG signal for HRV analysis, via time domain and frequency domain analysis. Alternatively, the PPG can be used for HRV data analysis since PPG waveforms are caused by pulsatile arterial blood flow during the various stages of the heart cycle.

### ***4.1 Initial Client Statement***

For this project, Professor Yitzhak Mendelson and Suresh Atapattu were considered the sole clients. They provided the MQP group with the following initial client statement, and a budget constraint of \$450.

*The correlation between HRV derived from the ECG or a PPG signal needs to be established. Since SCD occurs during normal daily function, it is imperative to have a reliable monitoring system that can function in normal life situations. The goal of this project is to design and construct a small microprocessor-based ECG/PPG recording device that will acquire the ECG and PPG signals of a moving person simultaneously using surface contact non-gel electrodes and optical PPG sensor.*

Given the brief nature of the initial client statement, the MQP group clarified clients' objectives through gathering more information through literature search, client interviews and brainstorming sessions, in order to develop a more detailed engineering statement expressing the clients' wants. The clients wanted a clinically acceptable device for HRV monitoring with the versatility of offering a wide variety of desirable outputs. Desired system outputs included signal waveform as well as HR/PR rate and respective variability indices. The clients also requested that rMSSD and SDNN variability indices be displayed in real time.

### ***4.2 User Requirements***

The MQP group identified two types of users for the device: patients and physicians. The device was going to be used for continuous HR monitoring by a patient at risk of SCD. To enable patient carry out some normal daily activities, design considerations for the

patient included ease of use, as well as patient comfort and convenience. The physician has to be able to make predictions and administer proper therapeutic or preventive action based on interpretation of patient data. This is especially critical given the importance that HRV data can sometimes predict mortality after a patient survives a cardiac episode. Therefore, the MQP group determined that the device outputs were to be accurately calculated and displayed in a clear manner. The outputs of interest to the physician include ECG and PPG signals, HR and PR, as well as computed HRV and PRV indices. The accompanying software also was going to be easy to use, with minimal technical knowledge. The MQP group determined that the device should allow for function controls, offering the flexibility of changing desired system outputs or modifying system parameters. The device was also to possess high and low alarm controls to monitor patient HR within a certain range as desired by the physician. The MQP group also determined that signal storage was important to allow retrieval of patient data to create patient records for better health care management. Desirable features in clinical monitoring devices, such as a QRS detection beep would also help to indicate each heart beat.

### ***4.3 Objectives***

Based on client interviews and user requirements, the MQP group developed a set of design objectives and sub-objectives and ranked them in a pairwise comparison chart (PCC) summarized in Table 4.1, to determine what area to focus most on during the design. Each element in a row was compared to a corresponding column element. Row elements were assigned a score of 1 if considered more important than column feature, 0 if considered less important and 0.5 if equally valued. An (x) is assigned for the same row and column entry (Note: this PCC model will be applicable throughout the whole design).

**Table 4.1: Pairwise Comparison Chart for Design Objectives**

	User Friendly	Reliable	Versatile	Safe	Total	Weight %
User Friendly	x	0	0	1	1(+1)=2	20%
Reliable	1	x	1	1	3(+1)=4	40%
Versatile	0	0	x	1	1(+1)=3	30%
Safe	0	0	0	x	0(+1)=1	10%
					Total	100%

- 1. The device should be reliable (40%)**
  - a. The device outputs should be accurate
  - b. The device should correlate data obtained from PPG and ECG
  - c. The device should have minimal parts to minimize device failure
  - d. The device should be durable to withstand extended patient use
- 2. The device should be versatile (30%)**
  - a. The device should provide visual and numeric outputs
  - b. The device should have dual ECG and PPG channels
  - c. The device should store data for further signal analysis
  - d. The device should be battery operated
    - i. The device battery should require minimal change
- 3. The device should be user friendly (20%)**
  - a. The device should display outputs in a clear manner
  - b. The device should allow for physician control of output parameters
  - c. The device should have easy user instructions and software interface
  - d. The device sensors should be comfortable to wear
  - e. The device hardware should be portable
    - i. Cell phone to PDA size range
- 4. The device should be safe (10%)**
  - a. The device hardware should have no sharp edges
  - b. The device should be electrically insulated

The MQP group ranked system reliability highest due to the critical nature of the device. Inability of the device to accurately calculate and display its values may have severe consequences if proper therapeutic action is not administered. It was also necessary to design a device that would be able to correlate data obtained from ECG and PPG systems in order to demonstrate that PPG signals can be used alternatively to calculate HRV. The MQP group determined that minimal design parts are desired to decrease the probability of device failure. It was also important to assure that device withstand extended patient use for long-term monitoring.

The MQP group ranked device versatility second to provide a wide range of options that the physician could use to facilitate diagnosis. These included ECG and PPG signal displays as well as HR, PR, HRV and PRV indices. The MQP also decided to design a dual channel, as opposed to two separate devices to facilitate simultaneous recording of ECG and PPG signals and make better signal comparison. Since both signals are processed differently due to their different characteristics, their systems can be made independent. Data storage was also necessary for further signal analysis and creation of a patient database. The MQP group decided that a battery operated device would also allow for easy patient transportation as well as operate during lack of electrical power.

The MQP group evaluated that user friendliness was a design consideration applicable to both patients and physicians. It is vital that system outputs be displayed in a clear manner in order to facilitate easy comprehension of displayed results. The MQP group determined that data interpretation is usually facilitated by its layout as well as aesthetics. It was also necessary to allow the physician a degree of control over certain parameters e.g. alarm controls, type of data displayed etc. so that the device could serve as a better tool for analysis. Device instructions had to be easy to interpret, anticipating potential problems that could arise during use. The device sensors had to be comfortable for long term patient use. The MQP group determined that the ideal device size was to be within a cell phone to PDA size range to facilitate device transportation. Overall, the duality of device user i.e. patient and physician was going to pose conflicting design considerations in achieving a balance between patient comfort and ease of use as well as clinical acceptability.

Although device safety is important, the MQP determined that that there was low risk of electrical shock due to the battery operated hardware and so this would not contribute a significant amount of difficulty in ensuring electrical safety. For an average adult, the amount of current necessary to trigger ventricular fibrillation is between 75 and 400mA [12]. The design of the device will have currents no more than 15mA to minimize risk of macro shock. An insulated device case with no sharp edges was to be used for the device hardware with RoHS compliant materials.

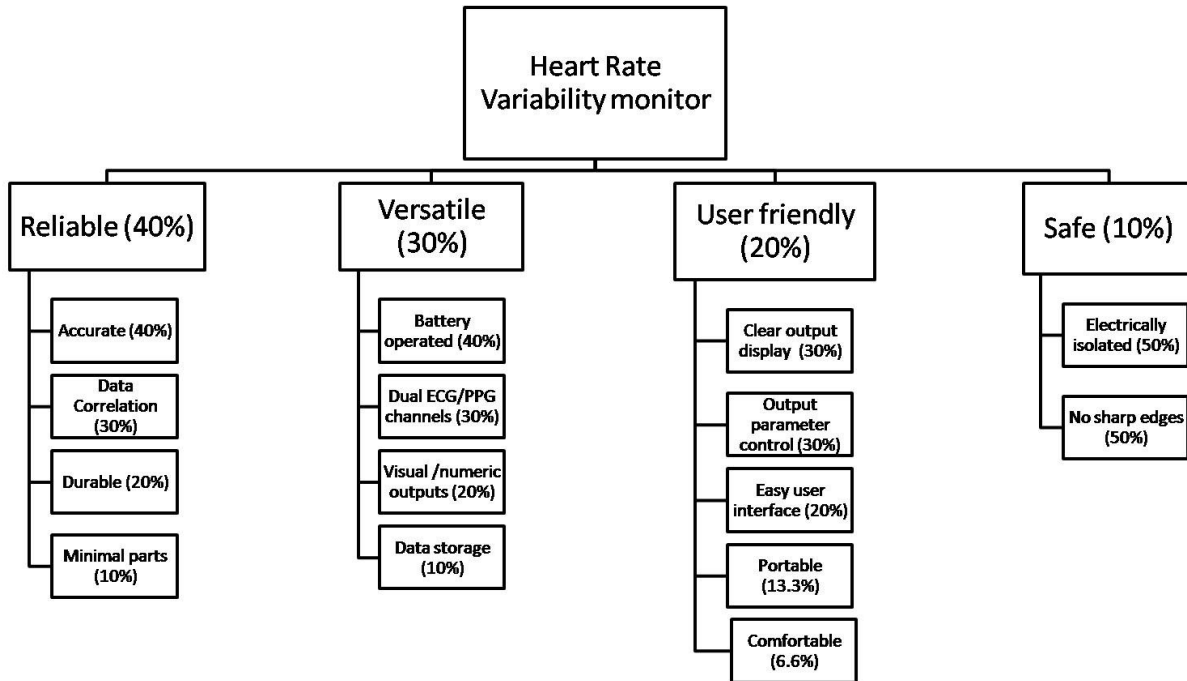


Figure 4.1: Weighted objectives tree

#### 4.4 Constraints

The MQP group identified the following design constraints that could limit the implementation of the design project:

- Budget: Funding for the device implementation was limited to \$450 from the WPI Biomedical Engineering Department
- Regulatory Requirements: The MQP group had to design a device in compliance with FDA regulations and ASTM standards to validate its use as a clinical device.

#### 4.5 Revised Client Statement

Based on the weighted objectives, the MQP group developed a revised client statement which was approved by the client. This was done in an effort to better define the final goals of the project. Due to limited knowledge of the MQP group, the microprocessor unit of the device was replaced by combinational hardware and software routines. Software processing for the signal was via LabVIEW software. The intended outcome

would be to develop algorithms that would be later used in a microprocessor based device. The following is the revised client statement:

*The goal of this project is to design and build a functional PC-based HRV monitor. The device will be a versatile dual-channel monitor capable of calculating HRV and PRV indices from electrocardiograph (ECG) and photoplethysmograph (PPG) signals, respectively. ECG signals will be collected via dry electrodes and PPG signals from a standard sensor interface. The device will include a hardware portion encasing the bio-amplifiers and filters for acquiring the ECG and PPG signals. Signals obtained will be filtered and processed by hardware and software using LabVIEW Software. Signals will be refreshed and updated at least every five seconds. Outputs of the system will include displays of the ECG and PPG signals as well as respective rate and variability indices. Raw waveforms will be stored for later access and analysis. The hardware will operate on battery power, continuously for more than twenty-four hours. The total budget of the design should not exceed \$450.*

#### **4.6 Functions**

The MQP group selected the black-box method (see Figure 4.2) as the most appropriate tool to determine device functions that would realize stated objectives by identifying system inputs and outputs.

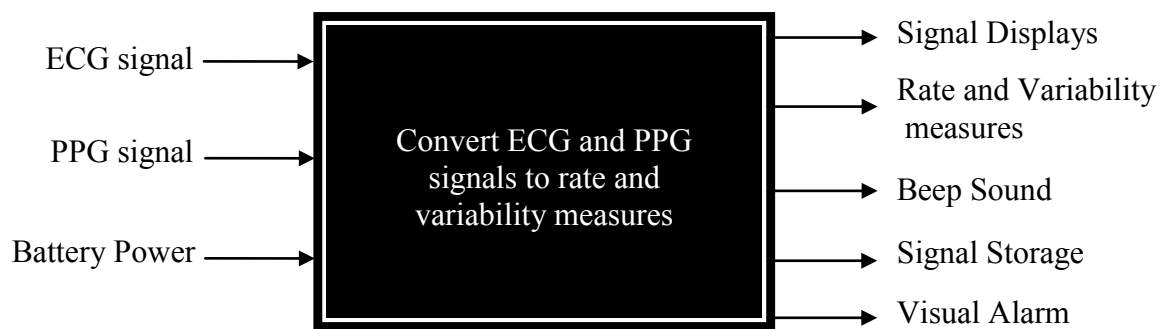


**Figure 4.2: Design black box with inputs and outputs**

This enabled the device sub-functions to be identified in a sequential flow of events by discerning how the system would process the signal to obtain the desired output. The MQP group developed a transparent box, shown in Figure 4.4, using considerations for

processing physiological signals (Figure 4.3) as well as the as HRV data (see Figure 2.10).

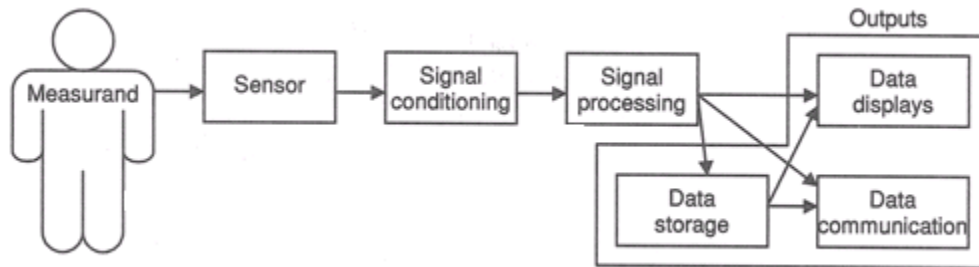


Figure 4.3: Physiological signal processing using sensors, signal processing, and outputs [56]

### 4.6.1 System Inputs

The MQP group had to design appropriate transducers that will be used to transform the signals of interest into electrical signals. These included electrodes for the ECG and a standard photodetection unit for the PPG signal. These transducers had to be appropriately packaged to guarantee good surface contact, and signal quality as well as be comfortable for the user to wear. Battery power was going to be used to power the device hardware. The MQP group identified EMG noise, optical interference and motion artifacts as primary sources of noise, and brainstormed several options to minimize their effect on system output accuracy.

### 4.6.2 Signal Amplification and Filtering

Physiological signals typically have low amplitudes and have to be amplified within the order of about 200-1000. These are effectuated by bio-instrumentation amplifiers for the ECG and a transimpedance amplifier for the PPG signal. There is also the presence of other physiological signals and high frequency noise which have to be removed. The MQP group considered filter characteristics that would satisfy the bandwidth requirements of our respective signals, as well minimize as the effect of signal noise.

### **4.6.3 Signal Digitization**

Software requires that signals be sample and digitized prior to processing. For LabVIEW, this would be implemented via National Instruments DAQ data acquisition hardware. It was vital to sample signals at a rate satisfying the Nyquist theorem of sampling signals with at least twice their maximum frequency content in order to guarantee signal reconstruction. It is recommended that signals used for HRV analysis be sampled at a frequency greater than 250Hz for proper peak detection [7].

### **4.6.4 Signal Storage**

Storage of ECG and PPG signals was important in order to allow creation of a database for further signal analysis.

### **4.6.5 Interbeat Interval Detection**

The raw data for calculating HRV are interbeat intervals obtained from either the ECG or PPG signals. This is usually determined from the ECG QRS complex which offers the advantage of having a high SNR, although artifact such as from noise or enhanced P or T waves can interfere with this peak detection. The MQP group anticipated the challenges with implementing a proper peak detection method for the PPG signal as it lacks a characteristic sharp peak. There is also the presence of a dicrotic notch that can introduce false peaks. The MQP group considered peak detection methods that would adapt itself for inherent differences in physiological signal amplitudes, through an adjustable threshold, calibrated based on incoming signal amplitudes.

### **4.6.6 Signal Artifact Detection**

HRV algorithms require the removal of abnormal beats for proper data interpretation, as their introduction could render the system results invalid. The MQP group investigated algorithms that would be used to minimize those introduced by motion artifacts as well as false peaks. The MQP group determined that these could be implemented either through amplitude or abnormal interbeat interval rejection.

#### **4.6.7 Rate and Rate Variability Algorithms**

The MQP identified that several processing algorithms would be implemented to calculate HR/PR. One method involved the direct averaging of interbeat intervals. Other methods include spectral analysis. HRV measures included rMSSD and SDNN indices through Equation 3 and Equation 4. Buffers are also necessary to store data values for these calculations.

#### **4.6.8 Heart Beat Beep and Alarm Controls**

The MQP group decided to implement audible QRS peak detection, to mimic a clinical device monitor. Also alarm controls were implemented to monitor patient HR within a certain acceptable range by using comparators.

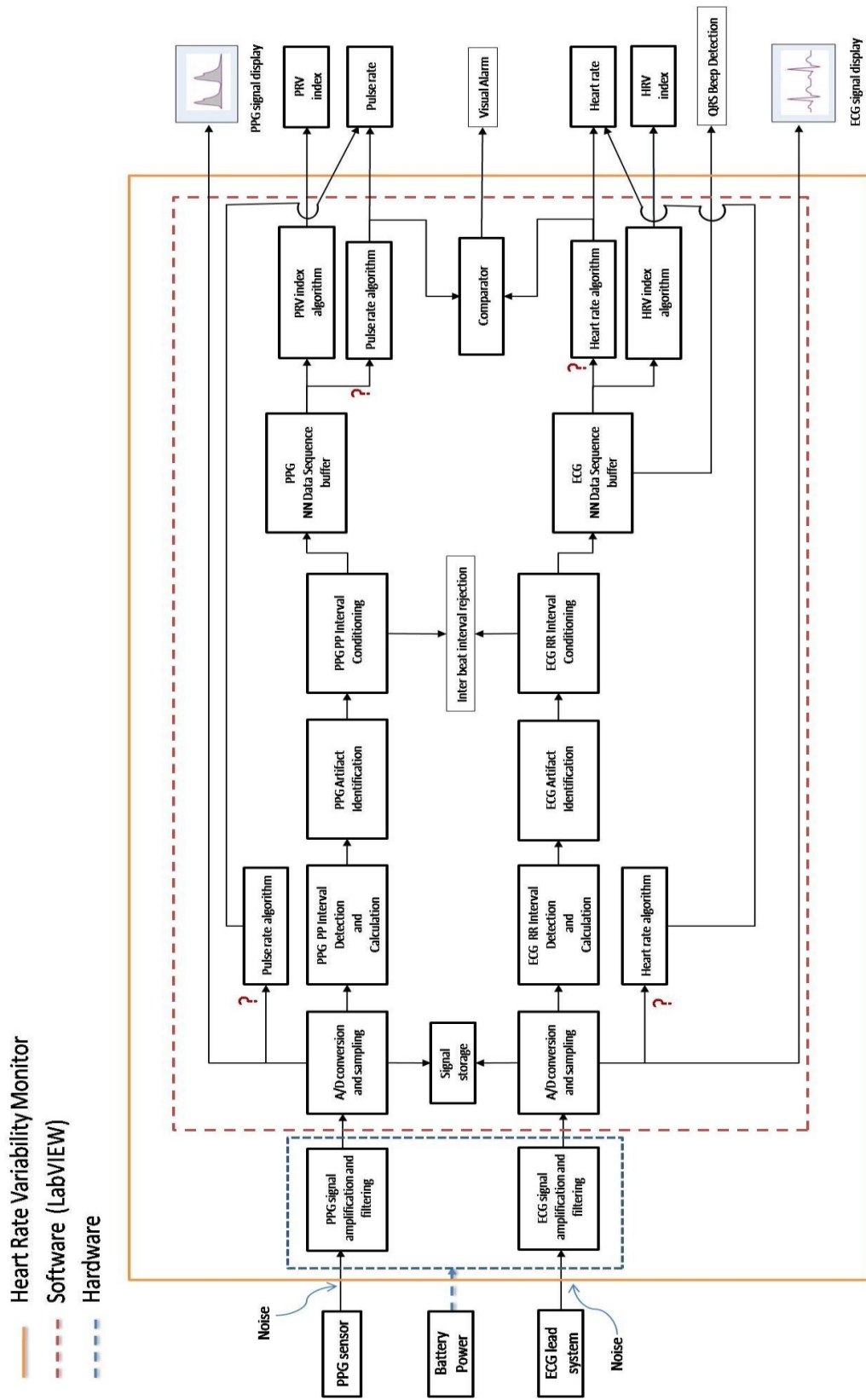


Figure 4.4: Developed transparent box of device design with inputs and outputs

## ***4.7 Initial Design Specifications***

The MQP group established initial device specifications to provide a basis for evaluating our final design. These specifications were primarily based on similar commercial devices, summarized in Appendix G.

### **4.7.1 Physical Dimensions**

The hardware portion of the device needed to be portable. In an effort to better describe the term ‘portable,’ the MQP group researched the characteristics of a few similar industry products for their size and weight. A range within cell phone to PDA size was considered to be ideal for our device. However, to allow for greater size, the maximal device size was set with regards to the Marquette Medical Systems Series 8500 Holter Monitor, an older version of portable heart monitoring device (see Appendix G). Physical dimensions of our device were capped at 6.00 x3.25 x1.125 inches and 10 oz weight.

### **4.7.2 Example Industry Specifications**

#### **4.7.2.1 PPG**

- PPG signal of at least 1V peak-to-peak amplitude
- Bandwidth between 0.5 – 20 Hz
- PR calculation range between 30-240 bpm
- PR accuracy of  $\pm 5$ bpm between 30-150 bpm
- Battery life greater than 6 days

#### **4.7.2.2 ECG**

- Standard ECG lead configuration
- Overall signal gain of one thousand
- HR detection range between 30-240 bpm
- Accurate to within  $\pm 5$ bpm

## **5. Alternative Designs**

The MQP group generated and evaluated the best possible alternative designs for implementation of the project. Design alternatives were weighted with reference to the design objectives, developed from the set objectives in section 4.3. The MQP group utilized a *divide and conquer* approach, by breaking down the device system into manageable sub entities that were easier to handle. Each of the sections below details the different design alternatives as well as their respective relative strengths and weaknesses.

### **5.1 PPG**

Functions of the PPG unit include extracting and conditioning PPG waveform appropriately prior to LabVIEW processing. It consists of a photodetection unit, bio-amplifiers and hardware filters. The photodetection unit consists of the LED, photodiode and transimpedance amplifier.

#### **5.1.1 Sensor Wavelength**

The MQP group evaluated wavelengths to determine the most suitable one for our design. This was determined by examining the absorption spectra of blood (see Figure 5.1). The main pigments responsible for light absorption in blood are hemoglobin (Hb), a metallo-protein and its oxygenated form HbO<sub>2</sub>. Red blood cells make up about half of blood composition and Hb within their cells is responsible for oxygen transportation [16]. The absorption coefficients of Hb and HbO<sub>2</sub> differ over the range 650nm-1000nm except at the isobetic wavelength of around 805nm. Wavelengths shorter than 600nm are typically not used for PPG applications because red skin pigmentation absorbs a great amount of light within this range [14]. Since arterial blood contains greater concentration of HbO<sub>2</sub>, it is necessary to select a wavelength greater than the isobetic length where the absorbance of HbO<sub>2</sub> is greater, to better capture the pulsatile PPG waveform.

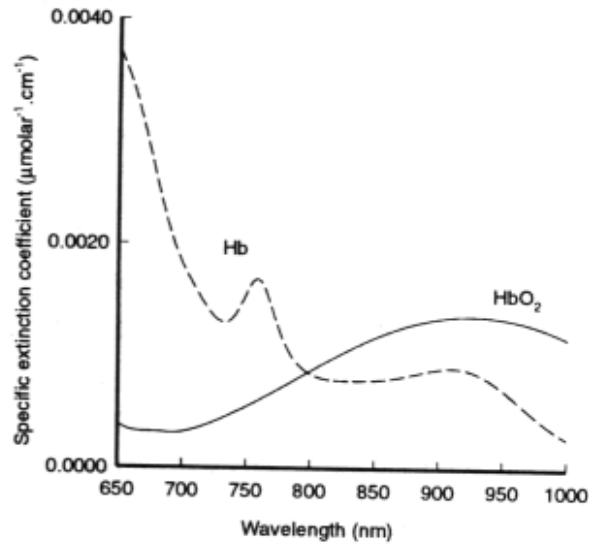


**Figure 5.1: Absorption spectra of oxygenated and deoxygenated Hb [15]**

Another criterion for wavelength selection is the relative flatness of the curve over the wavelength region. The peak emission spectra of LED's shift with temperature change. Theoretically, the peak wavelength of an LED is defined as the wavelength at which the radiated power is maximal, but usually the actual peak wavelength occurs over a bandwidth range [14]. Shifts in these peak emission spectra can pose problems in peak detection due to changing amplitudes resulting from different temperature conditions. The absorption spectra curve is relatively flat over the region of 900 to 950nm, and the bandwidth consideration is considered not important for accuracy due this flatness of the curve. An LED of peak emission wavelength of 940nm, with a low maximal power dissipation of 75mW (LTE-302-M) was thus selected.

### 5.1.2 Sensor Mode

PPG signals can be acquired by either transmittance or reflective mode. Table 5.1 summarizes difference between the two methods. The choice of transmittance or reflectance was going to be determined based on the selected sensor location.

**Table 5.1: Comparison of Transmittance and Reflectance PPG Probes**

Mode	Transmittance	Reflectance
Factor		
Principle	Dependent on light being transmitted through tissue, usually requires soft tissue to allow for maximal transmission	Dependent on light being reflected from tissue, and presence of bone tissue and thin skin layer facilitates light reflection
Sensor Placement	Sensor is limited to peripheral locations with small tissue size (e.g. ear, toe, nasal septum etc)	Sensor can be placed relatively anywhere in the body, both internally and externally
Blood Perfusion	Peripheral locations are subject to vasoconstriction	If location is close to body center, perfused region isn't too affected by vasoconstriction
Motion Artifact	Peripheral locations are susceptible to motion artifacts	Motion artifacts susceptibility depends on sensor location
Power Consumption	High; battery life approximately 4.8 hours[18]	Low; battery life approximately 73.3 hours[18]

### 5.1.3 Sensor Location

Sensor placement locations usually affect PPG signal quality, and site location also limits the mode of signal detection. In selecting the PPG sensor location, the MQP group considered the following factors:

1. Minimize power consumption: This is necessary to extend battery life. Batteries typically have a specified mAh (i.e. milliamp/hour) rating and thus lower current usage extends battery life. For example, for a 150 mAh battery, 0.5mA and 1mA current use will drain the battery in 300 and 150 hours, respectively. Power requirement also depends on sensor location, as well as mode of signal detection.
2. Area blood perfusion: System accuracy is dependent on the ability to obtain a high amplitude signal for processing. Highly perfused regions usually provide higher amplitude signal. In reflectance PPG, the presence of a bone beneath the perfused tissue also facilitates light reflection and thus better signal detection.
3. Minimize motion artifacts: Sensor location should be less susceptible to motion artifacts as the system is to be used for moderate daily activity. Motion artifacts can further be eliminated by filtering and software processing.
4. Stable sensor attachment: Sensor attachment should prevent dislocation of the sensor. This can be implemented by adhesives, bands or clips.
5. Sensor comfort: Sensor should be small in size, as well as be familiar to the person wearing the device.

The MQP group ranked evaluated and ranked these design factors in a PCC to determine the level of importance in sensor location consideration:

**Table 5.2: Pairwise Comparison Chart for PPG Sensor Location Objectives**

	Power Consumption	Blood perfusion	Sensor Stability	Motion Artifact	Sensor Size	Total Score	Normalized Fraction
Power Consumption	x	0	1	0	1	2(+1)	0.300
Blood perfusion	1	x	1	0.5	1	3.5(+1)	0.300
Sensor Stability	0	0	x	0	1	1(+1)	0.133
Motion Artifact	1	0.5	1	x	1	3.5(+1)	0.200
Sensor comfort	0	0	0	0	x	0(+1)	0.066

The MQP group ranked blood perfusion and motion equally highest because both affect signal quality as well as the accuracy and reliability of software algorithms. Signal integrity is a very critical factor in the technical design of wearable sensors. Therefore, signals with higher SNR are preferred. Minimizing motion artifacts is important considering that the patient is going to be using the device during normal daily activity.

Power consumption was ranked next among objectives because of the battery operated hardware. Hence, locations that minimize power requirement are preferred, as this will extend device battery life, reducing the problem of the user constantly changing batteries.

Sensor attachment should be stable to guarantee good skin contact during signal acquisition and prevent dislocation that can either result in false system alarms or introduce additional artifacts. This can be achieved either through adhesives, sensor clips, or bands. Adhesives pose the problem of dislocation due to wear of the glue material, as well as other factors such as sweat and skin oils. Clip sensors are more susceptible to signal motion artifacts [14]. Alternatively, sensors can be wrapped around measurement area using a band with adjustable straps, thus preventing the problem of dislocation.

The MQP group ranked sensor comfort lowest given the precedence of clinical considerations in the design. In addition, sensor probes can be made small enough due to the relative small sizes of LED's and photodiodes, although some locations may prove uncomfortable for the user.

Ranked objectives: Signal amplitude + motion artifacts > Power consumption > Sensor stability > Sensor comfort.

Transmittance probes have enabled the placement of PPG probes in virtually any part of the body. CJ Pujary identified at least 20 sensor locations that have been used in research [18]. Given the scope and time limitation of this project, it was necessary for the MQP group to narrow down sensor locations to at least a few sites to facilitate design alternative evaluation. Sensor locations were narrowed down based on clinical acceptability, sensor versatility, available research data as well as user familiarity and comfort. Some areas in the body can also utilize both transmittance and reflective modes e.g. cheek, finger, palm.

Four areas were primarily selected and these include: finger, ear, arm, and forehead (see Figure 5.2). These areas were ranked according to the five criteria developed above.

The following scale was used:

Motion Artifact:	most	1	...	4	least
Blood perfusion:	low	1	...	4	high
Power Consumption:	high	1	...	4	low
Sensor Stability:	unstable	1	...	4	stable
Sensor comfort:	uncomfortable	1	...	4	comfortable



Figure 5.2: PPG Sensor location alternatives [28], [46]-[47]

Table 5.3: Numerical Evaluation Matrix for PPG Sensor Locations

	Finger	Ear	Forehead	Arm
Motion artifacts	$0.300*1= 0.300$	$0.300*3= 0.900$	$0.300*3= 0.900$	$0.300*1= 0.300$
Blood perfusion	$0.300*3= 0.900$	$0.300*3= 0.900$	$0.300*4= 1.200$	$0.300*4= 1.200$
Power consumption	$0.200*2= 0.400$	$0.200*2= 0.4000$	$0.200*4= 0.800$	$0.200*3= 0.600$
Sensor stability	$0.133*3= 0.399$	$0.133*3= 0.399$	$0.133*3= 0.399$	$0.133*3= 0.399$
Sensor comfort	$0.066*2= 0.132$	$0.066*2= 0.132$	$0.066*3= 0.198$	$0.066*3= 0.198$
Total	2.131	2.731	3.497	2.697

Signal amplitude is generally evaluated by examining the blood perfusion (see Appendix H). Pujary ranked signal strength obtained from these areas as: finger base-high, ear-high, arm-medium and forehead-high [18]. However, Hummler et al examined the limitations of relying on perfusion index in selecting sensor location site, in cases with during poor peripheral perfusion such as during vasoconstriction or sepsis [48]. Using the perfusion index alone is thus not sufficient to evaluate signal accuracy. Peripheral locations are

most susceptible to vasoconstriction due to cold environmental conditions. The finger and the ear are mainly affected due to their smaller surface areas, hence ranked lower. Pálve assessed the performance of the transmittance and reflectance probes in compromised peripheral perfusion during cardiac surgery [49]. He concluded that even though the accuracy of pulse rate data was comparable, the reflectance sensor was more likely to obtain better readings under poorer peripheral circulation.

Transmittance sensors generally require a larger current than reflectance probes. Due to the large sizes of the forehead and arm, they are limited to reflectance probe sensors. The ear and finger can utilize both transmittance and reflectance modes [48], [51]. Savage et al were able to demonstrate that reflectance finger probes had a lower current requirement than transmittance probes, with battery life lasting 18 times longer than the latter [23]. Other means to extend battery life include achieving a balance between increasing the photo-detection surface area, reducing the amount of current and decreasing the duty cycle of the LED current source [52]. Increased photodetection area increases the amount of backscattered light detection. However, reducing current can adversely affect signal quality, because of the effective reduction in the intensity of the transmitted signal.

It was important for the MQP group to select a location that will be least susceptible to motion artifacts to minimize errors. Placing the sensor in limbs can limit patient mobility; hence the lower scores for finger and arm sensors. Fingers are even more susceptible due their smaller size. Johnston et al compared the effect of motion artifacts on measurement accuracy on forehead, jaw, chin and finger sensors [21]. Subjects were made to do a series of exercises such as talking, head movements and vertical motion. Signals recorded from the forehead demonstrated greater stability during all activities. Forehead sensors are also the preferred location of choice in military applications, to detect physiological parameters from moving soldiers [21]. By inference the ear sensor was also ranked like the forehead sensor.

Sensor attachment to measurement site should eliminate the possibility of dislocation under motion. The MQP ranked all sensors equally because of the possibility of using a variety of attachment options on the sites.

The MQP ranked sensor comfort lowest in finger due to decreased user mobility. The ear sensor can cause swelling due to soft tissue. Forehead and arm locations are considered to be familiar locations to the device user.

The MQP group thus selected the forehead sensor due to its low power requirement, least susceptibility to motion artifacts, higher signal amplitude and moderate sensor stability.

#### 5.1.4 Sensor Architecture

Since the MQP group selected a forehead sensor probe, it was limited to either adhesive or band type due to its size. Both attachment methods are used in clinical settings [47]. Since signals were going to be acquired from the same site, the MQP group considered long term sensor stability as the only factor for consideration. Two design architectures were considered for our design (see Figure 5.3).

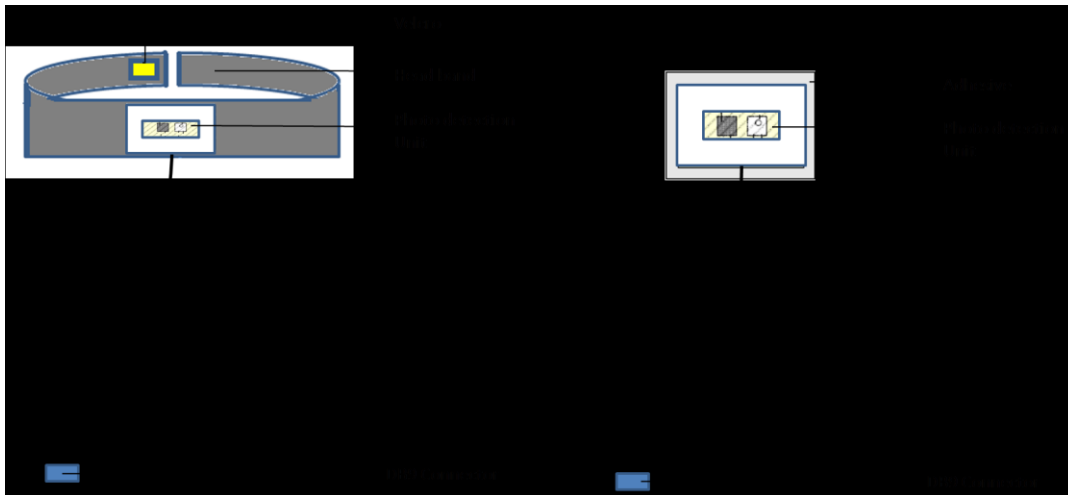


Figure 5.3: Design alternatives for PPG sensor architecture

### **Design A: Headband Sensor**

This design consists of an open end headband sensor with an attached photodetection unit. The photodetection unit was shielded with a pliable plastic, and surrounded by a padded cushion. The ends of the sensor band are attached with Velcro of varying lengths for user to adjust according to head circumference.

### **Design B: Adhesive Sensor**

This design consists of the photodiode arrangement mounted on a durable and pliable support. The photodetection unit was shielded with a pliable plastic, and surrounded by a padded cushion. Adhesives are attached to the backend of the diode support and changed as desired.

The MQP group used standard DB9 connectors as hardware inputs, to facilitate LED and photodiode arrangements. The MQP group used the same LED and photodiode specifications to better compare signals between both sensors. As expected, signals obtained from both sensors were comparable. However, the adhesive sensor was more susceptible to dislocation due to weakening of glue, which was facilitated by sweating as well as skin oils, thus requiring constant replacements. The MQP group determined that this might not be suitable for long term monitoring and constant adhesive replacement can also affect long term device cost. Drescher compared errors obtained from forehead sensors with elastic band, helmet and adhesive attachments under motion [53]. The tests confirmed a statistical difference in PR measurements between attachment methods, with band sensors offering lesser error than adhesive type sensors.

The MQP group selected the forehead band sensor due to its greater long term stability, guarantying good surface contact for signal acquisition.

### **5.1.5 Filters**

Filter functions include extracting and amplifying the AC component of the PPG signal, eliminating noise such DC component, baseline drift and 60 Hz noise. Filters have to fulfill the bandwidth requirement of the PPG waveform. The PPG signal is very similar

to that of blood pressure waveform, which can be reproduced with up to the tenth harmonic. The MQP group determined that filtering could either be implemented via hardware or software. In selecting filter type the following design factors were considered:

1. Minimize cost: Software filtering was readily available in the computer via LabVIEW. Reducing number of IC components in hardware will minimize mass production costs.
2. Flexibility: Filtering methods should be flexible to change characteristics like filter bandwidth, order, type etc.
3. Effectiveness: This is determined by its ability to meet its bandwidth specifications and eliminate noise.

The MQP group evaluated these factors in a PCC to determine their level of importance:

**Table 5.4: Pairwise Comparison Chart for PPG Filter**

	Cost	Flexibility	Effectiveness	Total score	Normalized fraction
Cost	x	0	0	0(+1)	0.167
Flexibility	1	x	0	1(+1)	0.333
Effectiveness	1	1	x	2(+1)	0.500

The MQP group ranked filter effectiveness highest because the ability to accurately determine PR is greatly dependent on the filter meeting its bandwidth requirement and eliminating the necessary noise. Flexibility to change filter parameters was considered for the design implementation to allow the testing of a variety of options design under minimal time. Device cost was ranked least because of the precedence of filter effectiveness on signal accuracy as well as the flexibility of the designer to change parameters during the design process under limited time. The MQP group evaluated both filtering methods in a numerical evaluation matrix, using the following nominal scale:

Effectiveness: High (1), Low (0)  
 Flexible: Yes (1), No (0)  
 Mass production cost: High (1), Low (0)

**Table 5.5: Numerical Evaluation Matrix for PPG Filter Design**

	Hardware	Software
Effectiveness	$0.500*0.0=0$	$0.500*1.0=0.500$
Flexible	$0.333*0.0=0$	$0.333*1.0=0.330$
Cost	$0.167*0.0=0$	$0.167*1.0=0.167$
Total	0	1

Software filtering utilizes digital filters which can be designed to fulfill its bandwidth requirements, with lesser degree of error hence ranked higher. The effectiveness of hardware filtering is greatly dependent on the tolerance values of filter components (resistors, capacitors, etc). These can be purchased in various tolerance ranges (1%, 5% 10%) with per unit cost increasing with decrease in tolerance values. However, active hardware filters can introduce additional noise like bias voltage as well as changing filter characteristics due to temperature. In addition, there is the likelihood of component failure.

Software filtering offers the advantage of being able to change filter parameters in a short time. LabVIEW software also has the option of changing filter type (Butterworth, Chebyshev etc). Software filtering is also programmable, can be designed, tested and implemented within a short time period, with greater versatility of implementing robust algorithms. Changing parameters in hardware requires physically changing components which can be time consuming. This can pose a problem especially in an already finished product should errors occur.

Although the initial cost of software is expensive, a one-time purchase can be downloadable to several units. However, it requires an analog to digital converter prior to signal processing. Mass production can reduce hardware component cost due to discounted low per unit cost, thus minimizing the number of components reduces overall device cost. However, cost can significantly be larger depending on the number of device units.

The MQP group implemented software filtering for PPG signal to satisfy the bandwidth requirement of the PPG signal. In general, the PPG waveform is similar to the blood pressure waveform which can be reproduced with as much as its 10<sup>th</sup> harmonic. For an average HR of 60bpm, i.e. 1Hz, the high cut off for this filter can be about 10Hz. To eliminate DC and baseline drift, the MQP group selected a low cut off of 0.5Hz. The MQP group selected a Butterworth filter because of its flat gain characteristics, and its steep roll off which could be achieved with higher filter order. However, an order of 3 was selected because greater filter settle time was observed in filters of higher order. The MQP group implemented a 3<sup>rd</sup> order Butterworth filter with bandwidth of 0.5-10Hz directly after the transimpedance amplifier stage. However, the resulting signal was very noisy (see Figure 5.4).

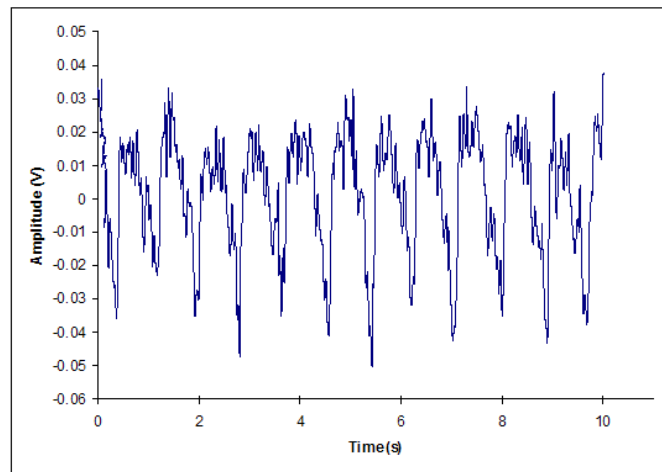


**Figure 5.4: PPG signal obtained after LabVIEW software filtering**

The MQP group explored several other options like increasing filter order, or changing filter type, and no change was observed in signal quality. Due to time limitation in exploring other software functions, the MQP group decided to pursue the option of implementing hardware filtering prior to LabVIEW, with additional filtering implemented via software. Signals pre-filtered with hardware were observed to be of better quality (see Figure 5.5). Initial testing for component values were implemented first on a breadboard until component values were finalized prior to soldering onto a printed circuit board.

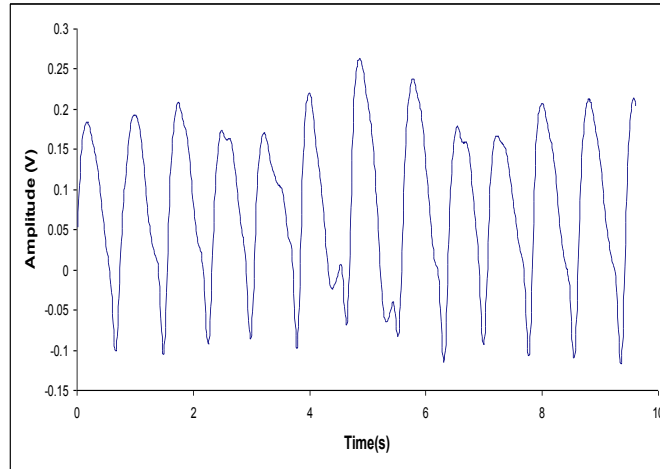


**Figure 5.5: Clean PPG signal after pre-hardware filtering**

## **5.2 ECG**

Objectives for the ECG portion of the project were to develop an effective method for acquiring the ECG signal, applying basic filtering, and sending the signal to the software for further analysis and display. This section of the project consists specifically of a standard instrumentation amplifier, connected to the body through experimental dry electrodes, and sent through to the software following basic analog hardware filtering.

### **5.2.1 ECG Electrodes**

The electrodes for the ECG system are a primary design consideration. The objective of the project was to develop and implement dry electrodes for the ECG monitor. This was done to allow for continuous use of the electrodes without the possibilities of electrode fouling due to drying of the electrode gel or skin irritation. With regards to the electrodes, three alternatives were tested for compliance with the design criteria. These alternatives were the use of stainless steel plates, silver/silver chloride contact, and silver/silver chloride contact with vinyl adhesive. The stainless steel plates were circular stainless steel metal contacts, approximately one inch in diameter. These plates were secured to the body via medical tape and connected into the circuit for analysis. Both of the silver/silver chloride electrodes were developed from standard gel-based electrodes. An example of the gel-based electrodes used is shown in Figure 5.6a, with an example of the dry electrode shown in Figure 5.6b. This design was divided into two parts, one retaining the

vinyl adhesive, the other with the adhesive removed to ensure that signal acquisition was done only through the metal contact surfaces, with the adhesive having no affect on the signal quality or strength.



**Figure 5.6: Wet (a) and dry (b) ECG electrodes**

Each design was capable of acquiring the signal to varying degrees. The results of testing for each of the electrodes can be found in Appendix F. Design evaluation criteria for the electrodes were as follows:

1. **Signal Quality:** depending on the chosen electrode type, there are degrees of baseline noise inherent to the electrode. The optimal design alternative should minimize this potential noise artifact.
2. **Electrode Motion Artifact:** depending on the electrode choice, there is the possibility for physical motion of the electrode. Should this occur, significant amounts of noise will enter the system due to the capacitive coupling between the skin and electrode surface [11].
3. **Ease of Use:** depending on the electrode alternative, varying degrees of attention is required for the use of the electrode. Should the electrode not in itself include a method for adhering to the body, additional methods for doing so would be required by the user.
4. **Reliability:** depending on the electrode alternative, the reliability of the chosen method can vary. This may be particularly evident with the stainless steel plates as variations between the sensors would prevent consistent data acquisition between tests.

**Table 5.6: Pairwise Comparison Chart for ECG Electrode Type**

	Signal Quality	Motion Artifact	Ease of Use	Reliability	Total Score	Normalized Fraction
Signal Quality	x	1	1	1	3(+1)	0.40
Motion Artifact	0	x	1	1	2(+1)	0.30
Ease of Use	0	0	x	1	1(+1)	0.20
Reliability	0	0	0	x	0(+1)	0.10

Of the given criteria, signal quality was the most important factor in determination of the appropriate electrode alternative. Without a sufficient signal quality, analysis of the signal is not possible. Should the quality be inherently poor with a certain design alternative, than that design would be an inappropriate choice. Each of the design alternatives was ranked to determine the overall effectiveness of each design. Rankings of the alternatives ranges from one to three, depending on how well the alternatives meet the criteria set forth.

**Table 5.7: Numerical Evaluation Matrix for ECG Electrode Type**

	Stainless Steel Plates	Ag/AgCl w/o Adhesive	Ag/AgCl w/ Adhesive
Signal quality	0.4*1	0.4*2	0.4*3
Motion Artifact	0.3*1	0.3*1	0.3*3
Ease of Use	0.2*1	0.2*1	0.2*3
Reliability	0.1*1	0.1*2	0.1*3
Total	1	1.5	3

For the tests performed on the different electrode alternatives, the silver/silver chloride electrodes with the surrounding adhesive performed the best. This greater performance than the other alternative designs allowed for a greater signal quality and most significantly a reduction in the possibility for electrode sensor movement due to the incorporation of the contact adhesive with the electrode sensor face. The results of the tests performed can be seen in Appendix F.

## 5.2.2 ECG Electrode Location

There were two primary alternative designs considerations for the ECG sensor location. Possible placements for electrodes were either on the extremities or on the chest. The following criteria were used to determine the relative effectiveness of each sensor location:

1. EMG Motion Artifact: Depending on the locations of the electrodes, greater or lesser degrees of motion artifacts may be present. This is primarily depending on the amount of muscles between the sensors, where greater amounts will have the ability to create a greater voltage potential.
2. Signal Strength: Depending on the proximity to the heart, the signals will have varying amplitudes. This is due to the differences in effective resistance that increasing degrees of tissue will cause.
3. Electrode Lead Length: Depending on the placement of the electrodes, greater or lesser degrees of wire is needed to make the connections between the electrodes and the hardware sensing suite.

**Table 5.8: Pairwise Comparison Chart for ECG Sensor Placement**

	Motion Artifact	Signal Strength	Lead Length	Total score	Normalized fraction
Motion Artifact	x	1	1	2(+1)	0.500
Signal Strength	0	x	1	1(+1)	0.333
Lead Length	0	0	x	0(+1)	0.167

From the criteria, it was determined that motion artifacts due to EMG signals were the most influential in determining the appropriate lead placement. This was determined since of the listed criteria, the motion artifacts were the only criterion that would prevent the signal from being properly analyzed. Signal strength could be compensated for by increasing the overall gain of the system, and lead length does not have a direct affect on the signal quality, only on the overall ease of use of the system. For ranking of the different alternatives, each was ranked in relation to the listed criteria. Values were given based on a scale of zero and one, where the design alternative that better attained the criteria was ranked higher. Equal attainment of a given criteria results in an equal ranking.

**Table 5.9: Numerical Evaluation Matrix for ECG Sensor Placement**

	Chest	Extremities
Motion Artifact	0.500*1	0.500*0
Signal Strength	0.333*1	0.333*0
Lead Length	0.167*1	0.167*0
Total	1	0

Following analysis of the two design alternatives, it was determined that the chest placement of the electrodes outperformed placement on the extremities. Placement on the chest allows for a reduction in the overall motion artifacts since there is a lesser degree of muscle activity occurring between the two electrodes. As such, the amplitude of EMG signals detected will be lesser. Furthermore, since the chest electrodes are anatomically closer to the heart, the overall strength of the signal is increased. Finally the lead length is reduced since there is a lesser amount of spacing between each of the three electrodes. This allows for the sensing hardware to be placed closer to each of the electrodes, reducing the necessary lead length. A comparison of the two signals can be seen in Figure 5.7, where the electrodes placed on the chest have greater overall amplitude and a slightly lower baseline noise.

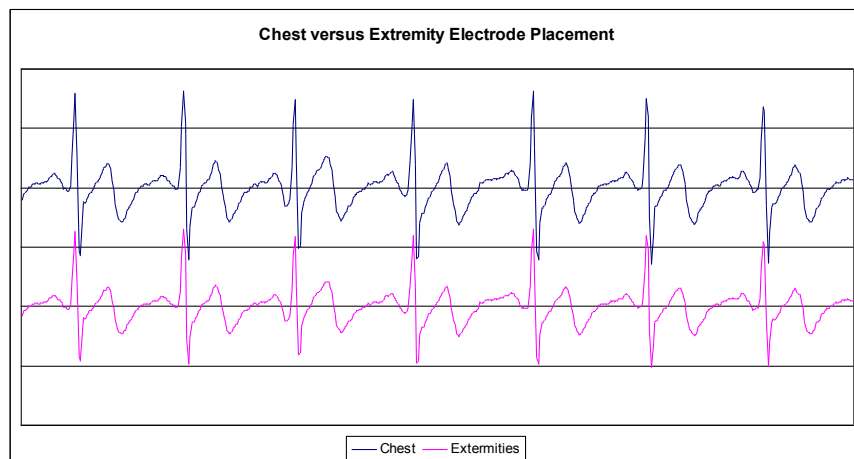


**Figure 5.7: Chest versus extremity electrode placement**

### 5.2.3 Filters

There were two main design alternatives considered for the filter portions of the ECG hardware. These alternatives were to condition the signal entirely with the use of analog hardware filters or to employ the use of software filters for the primary filtration of the signal. For this portion of the project, the two implementations of the design can be seen as Revision A and Revision C in Appendix B. Revision A is comprised of a single analog hardware filter. Its purpose is to prevent baseline drift of the signal, which is especially important for preventing signal saturation of the operational amplifiers. Revision C consists of full hardware filtration of the ECG signal. Design criteria established was used to evaluate the relative advantages and disadvantages of the filter alternatives. The following design criteria were used to evaluate the effectiveness of the ECG hardware filter alternatives:

1. Cost: Lowering the costs of the individual units will allow for greater production and lesser unit costs.
2. Reliability: Reductions in the total number of hardware components allows for increases in the overall reliability as there are fewer possible components that may fail during use.
3. Effectiveness: The filters must have sufficient effectiveness in order to provide the user with the expected signal outputs.

**Table 5.10: Pairwise Comparison Chart for ECG Filter Design**

	Cost	Reliability	Effectiveness	Total score	Normalized fraction
Cost	x	0	0	0(+1)	0.167
Reliability	1	x	0	1(+1)	0.333
Effectiveness	1	1	x	2(+1)	0.500

For the given criteria, the effectiveness of the design ranked highest. Without the ability to provide the user with the desired signal, the design would not be appropriate. Following this, the reliability of the device is ranked second with the overall device determined to have the least overall effect on the decision process. The ability of the two alternatives to meet the design criteria was determined based on a scale of zero to one.

The design alternative that better met the described criteria was ranked higher as one. The values from each were totaled then to determine the better alternative.

**Table 5.11: Numerical Evaluation Matrix for ECG Filter Design**

	Hardware	Software
Effectiveness	0.500*0	0.500*1
Reliability	0.333*0	0.333*1
Cost	0.167*0	0.167*1
Total	0	1

It was determined that the software filtering design was most capable of performing the requisite functions. Being that there were only a limited number of hardware components used to initially condition the signal, the reliability of the total design is increased due to lower possibilities for component failure. The effectiveness of the total design is furthermore increased primarily due to the ability to fine-tune the frequency ranges of the software. Utilizing a smaller bandwidth of frequencies, it is possible to disallow additional artifacts that would not be possible with the hardware filters. Finally the overall cost is reduced by limiting the necessary components of the design.

### **5.3 Software Algorithms**

One of the software functions is to implement algorithms for both rate and variability index calculations. Of interest are HR/PR as well as R-R time intervals. The algorithm choice was based on its effectiveness in implementing the desired function.

#### **5.3.1 R-R Interval Detection**

R-R time intervals were necessary for calculation of SDNN and rMSSD indices, by detecting peaks of ECG and PPG waveforms (see Equation 3 and Equation 4). Two methods were used to determine these intervals. Signal algorithms were investigated by inputting signals of known frequencies into the system, and comparing the observed time interval value with its ideal.

### 5.3.1.1 Peak Time Location

In this method, the R-R interval time between consecutive peaks is calculated by taking the time difference between peak occurrences. When peaks are detected, the locations are given with respect to the block of data being analyzed (see Figure 5.8). As such, raw location outputs are represented as a number between zero and one hundred. Time between peaks is determined by determining the peak locations with reference to the total acquisition and subtracting the previous location from the current. This total number is multiplied by the inverse of the sampling rate of the software to determine the overall time between peaks.

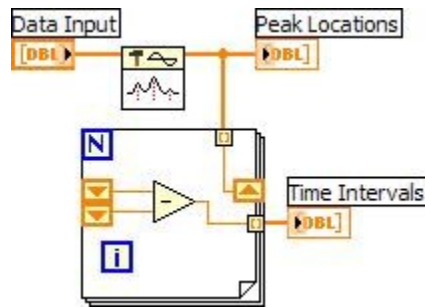


Figure 5.8: Time peak locations

### 5.3.1.2 Elapsed Time

In this method, the R-R interval time between consecutive peaks is calculated by initiating a timer each time a peak is detected. When a peak occurs, a binary 1 is displayed, and 0 if otherwise. The binary 1 initiates the timer to start measuring elapsed time. The timer is reset each time a new peak is detected, and the value of elapsed time stored in a buffer.

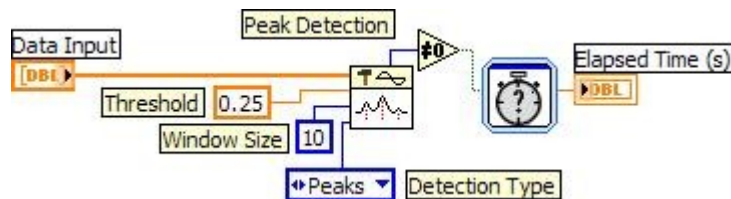


Figure 5.9: Peak detection via timer

Of the two design alternatives analyzed, it was determined that peak location was the better method. This was based on the fact that the program could not reliably detect the

location of the peak when used for timing between the peaks. This was due to the nature of the software and its method for analyzing data. The software portion of the program acquired data continuously at a 1000Hz sampling rate, and analyzed the data in blocks of 100 samples. Because of this, the elapsed timer was capable only of determining the locations of peaks to within a tenth of a second. This resolution would not have been capable of properly analyzing data.

### **5.3.2 Heart / Pulse Rate Calculation**

Two signal processing algorithms were investigated for measuring rates. These included rates calculated from a sequence of R-R intervals and via frequency analysis of the signal. Rate averaging was used for the ECG signal. Both methods were investigated in the PPG signal.

#### **5.3.2.1 Rate Averaging**

This algorithm was implemented by calculating the average value of a number of consecutive R-R time interval values. The R-R interval values are stored in a buffer as milliseconds between peaks. The inverse of this average was multiplied by 60,000 to obtain rate in beats per minute (see Figure 5.10).

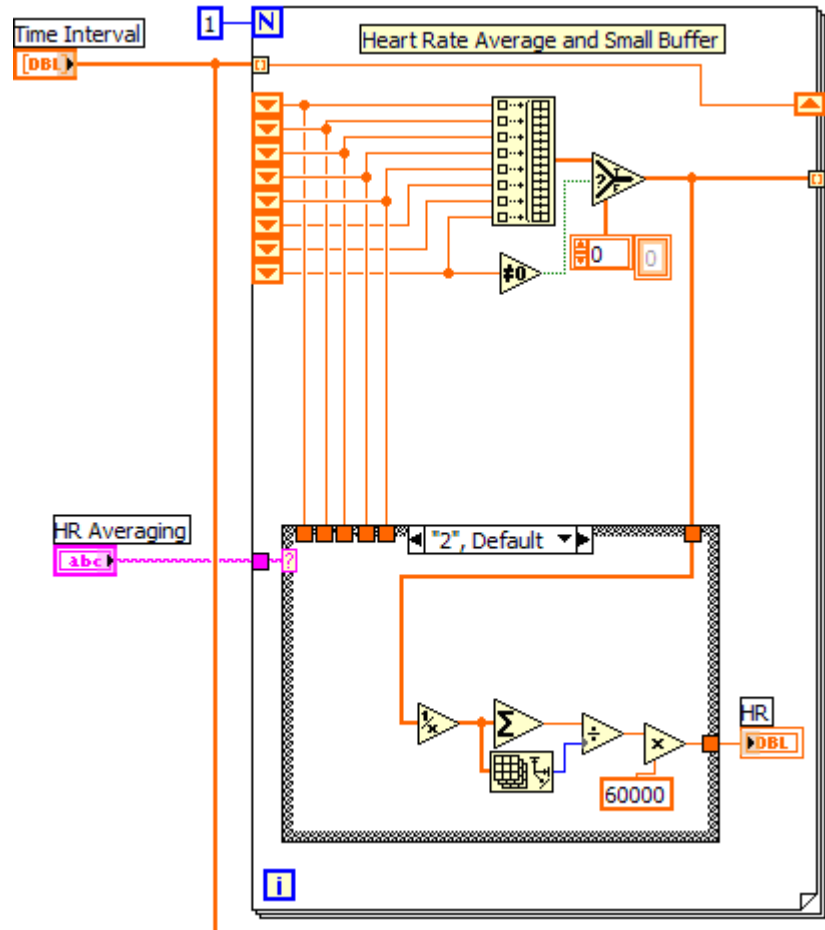


Figure 5.10: HR averaging

**5.3.2.2 Frequency Analysis**

This method calculated PR based on the spectral analysis of the blocks of the PPG signal. The largest amplitude frequency content corresponded to the fundamental frequency of the signal. This fundamental frequency was then multiplied by 60 to give PR.

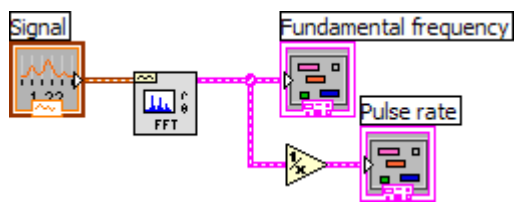


Figure 5.11: PR by frequency analysis

## **5.4 User Interface**

In designing the user interface, it is essential to meet user expectations by communicating the data accurately and clearly as well as meeting regulatory requirements for clinical acceptance. In particular, the US Food and Drug Administration Guidance for Pulse Oximeters and Diagnostic ECG as well as the *Standard Specifications for Pulse Oximeters, F1415-1992* from the American Society for Testing and Materials (ASTM) [14]. FDA standards include regulatory requirements as well as recommended device testing and documentation for submitting 510(k) for device approval in the US. ASTM standards are international specification and testing requirements that globally harmonize the quality of medical equipment. While data accuracy is addressed in the core aspect of the device design, clarity of data communication involves displaying the necessary information in a useful way to the device user. The desired outputs of the system include real time graphical displays of ECG and PPG physiological signals as well as computed HR/PR, rMSSD and SDNN HRV/PRV indices. Also necessary for this application are alarms that alert the user of specific activities e.g. acoustic alarms to indicate instances of heartbeat, or audio-visual alarms to indicate low or high heart rate. Function controls include the on and off switch, as well as alarm controls to indicate low and high heart rate. The ASTM standard requires that alarm controls be operator adjustable. Data storage and easy retrieval protocol is also useful a useful tool for further signal analysis, for better patient care.

### **5.4.1 Layout**

Several commercial heart/PR monitors were reviewed in designing a familiar user interface layout. In designing the layout, it is essential that the layout of the graphical displays, indicators and controls have a relationship. In most multi-signal monitors there are generally two types of relationships: vertical and horizontal. Horizontal relationships display data from obtained from the same physiological signal, while vertical relationships display similar data from different types of signals as can be seen in Figure 5.12. While the overall aesthetic between devices may be different, design outputs are generally displayed in a similar manner, for easy harmonization amongst healthcare

users. The user interface would thus implement the same basic layout for data communication.



Figure 5.12: Sample industry monitor by Mindray PM 7000 [54]

## 6. Methods

### 6.1 PPG

#### 6.1.1 Photodetection Unit

The photodetection unit consists of the standard photo-emitter photo diode circuit coupled with a transimpedance amplifier (see Figure 6.1). The MQP group selected an LED diode with a peak emission wavelength of 950nm (LTE), and also with a photodiode with a peak wavelength sensitivity of 940nm (QSB34ZR). The MQP group measured a 1.2V drop across the IR LED diode, to take into consideration when calculating our current values for the LED drive current.

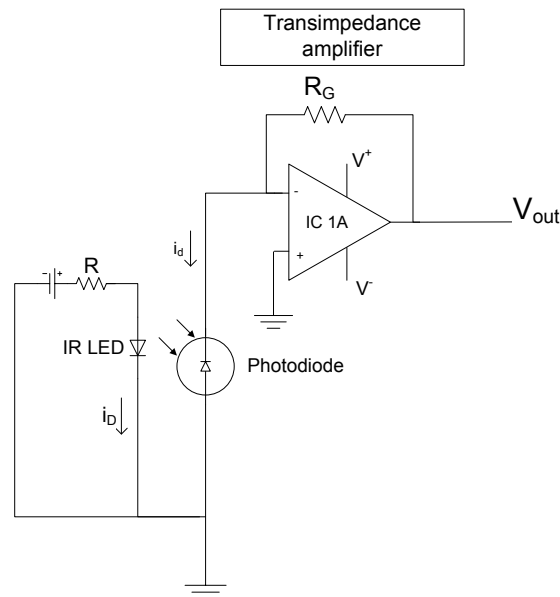
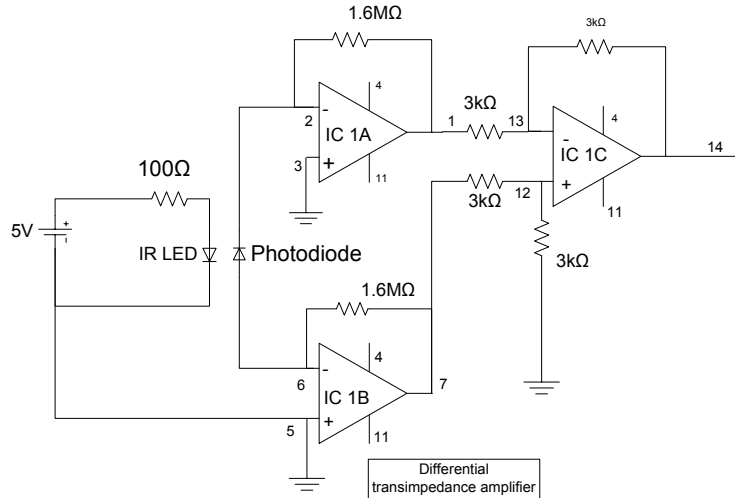


Figure 6.1: Light emission and detection circuit

The IR LED emits light with intensity proportional to the amount of current,  $i_D$ , through it. The photodiode generates an output current,  $i_d$ , proportional to the intensity of reflected light. The transimpedance amplifier converts the current to an output voltage, (see Equation 5). The generated current is usually very small, and so the gain resistor,  $R_G$ , is typically in the M $\Omega$  range.

$$V_{out} = i_d * R_G \quad (5)$$

Initially, the MQP project group thought that a differential transimpedance amplifier would more effective in collecting PPG signals, shown in Figure 6.2.



**Figure 6.2: Differential transimpedance amplifier**

However, there was the disadvantage of additional device components. A single transimpedance amplifier with increased feedback resistance proved as effective, and was thus selected, shown in Figure 6.3. For our initial tests, a current of value  $i_D$  was chosen at  $\approx 40\text{mA}$ , and a gain resistor of  $5\text{M}\Omega$  was chosen, though these were not the final values selected.

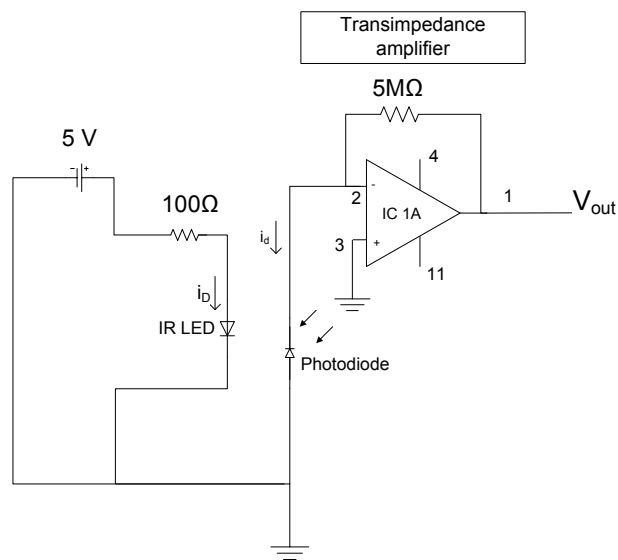


**Figure 6.3: Single op-amp transimpedance amplifier**

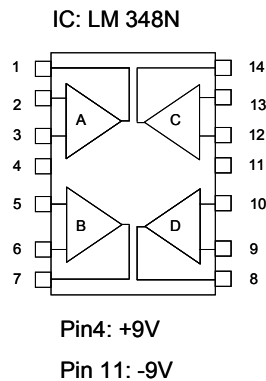


Figure 6.4: Quad op-amp pin specification

## 6.1.2 Filter Design

The MQP group designed filters to satisfy the bandwidth requirement of the PPG signal. The MQP group performed preliminary Fourier analysis of the PPG waveform, and realized it could be reproduced with as little as its third or fourth harmonic (see Figure 6.5). For an average HR of 60bpm, i.e. 1Hz, the bandwidth of the filter can be about 3Hz. A high cut of 10 Hz will thus be sufficient to accommodate HR up to about 240bpm To eliminate DC as well as baseline drift e.g due to breathing, a low cut off frequency of 0.5 Hz was selected.

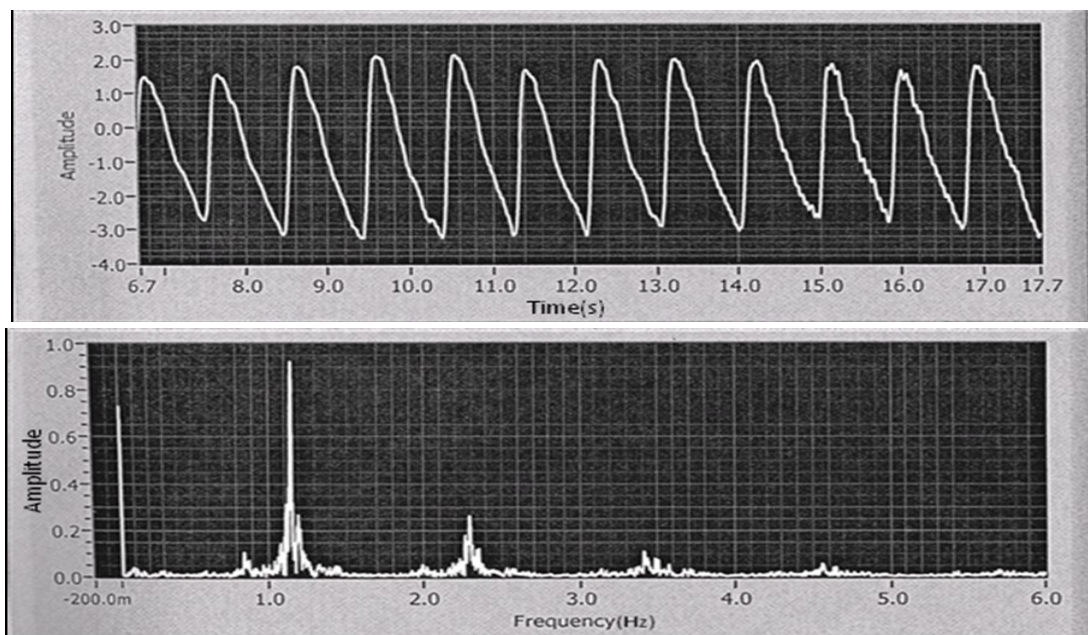


Figure 6.5: Fourier analysis of a PPG waveform

The MQP group thus constructed a hardware band-pass (BPF) filter (BW: 0.5 to 10Hz) with an overall gain of  $\approx 150$  by cascading high-pass (HPF) and low-pass (LPF) filters instead of a single op-amp BPF filter (see Figure 6.6). This was necessary to achieve a low gain in the high pass stage (gain = 4) to avoid saturating the op-amp with the high DC component from the photodiode. The MQP group calculated component values based on Equation 6, and selected the closest possible standard values. The MQP group implemented bias resistors,  $R_b$  in respective filter stages (i.e.  $R_b = \frac{R_f * R_i}{R_f + R_i}$ ) to minimize the effect of bias current of the filter.

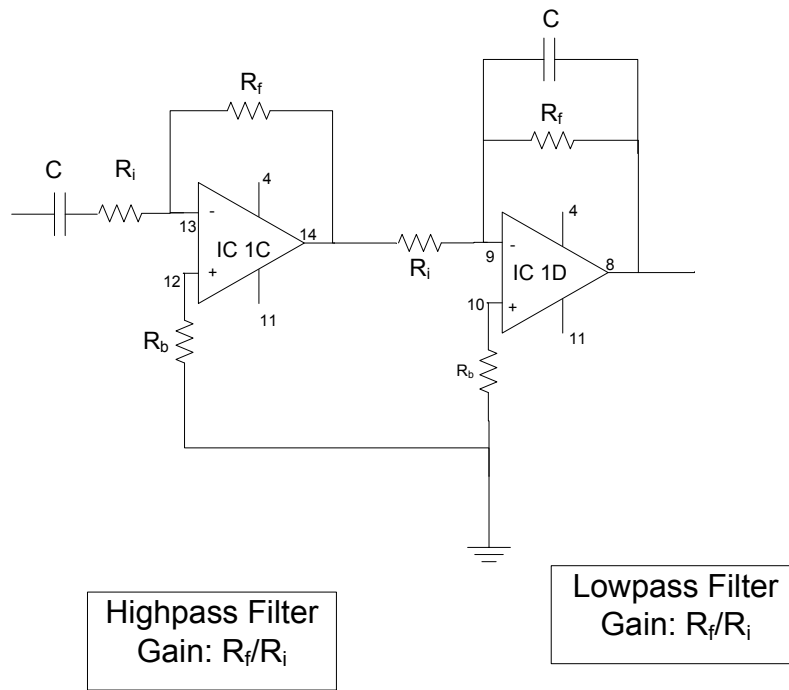


Figure 6.6: PPG band-pass filter

$$f = \frac{1}{2\pi * R * C} \quad (6)$$

Where:  $f$  = cut off frequency (Hertz: Hz)  
 $R$  = resistance (ohm:  $\Omega$ )  
 $C$  = capacitance (farad: F)

**Table 6.1: PPG Filter Characteristics**

	$f_c$	$R_i$	C	$R_f$	$R_{bias}$	Gain
<b>High-pass</b>	0.5 Hz	30k $\Omega$	10 $\mu$ F	120k $\Omega$	24k $\Omega$	4
<b>Low-pass</b>	10 Hz	3 k $\Omega$	0.1 $\mu$ F	160k $\Omega$	2.7k $\Omega$	37.2
Band-pass Filter bandwidth: 0.5-10Hz						148.8

### 6.1.3 Power Optimization

The MQP group explored options of minimizing power consumption via reduction of LED drive current and duty cycle. To obtain the minimum current requirement that could still produce an adequate waveform, the MQP group decreased the amount of circuit current and measured its effect on signal amplitude and quality.

The MQP group implemented a pulsatile current source using an LM555 timer (see Figure 6.7). The duty cycle ( $\delta$ ) of the power supply is dictated by  $R_A$  and  $R_B$  resistor values (see Equation 7).  $T_H$  represents the time when the voltage is at maximum, while  $T_L$ , the time when the voltage is at 0V. The MQP group made  $T_H$  and  $T_L$  values independent by putting a diode across  $R_B$ . The MQP group used a sample-hold IC after the transimpedance amplifier stage to keep voltage values constant during times when the LED is off.

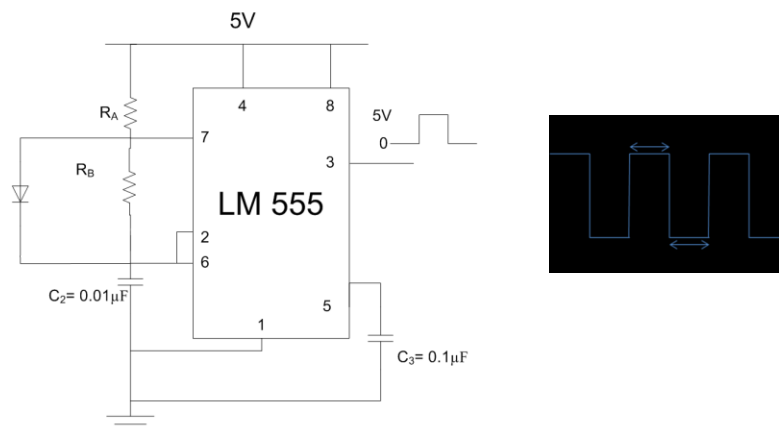


**Figure 6.7: LM 555 timer circuit outputting 5V pulsatile**

$$duty\_cycle = \frac{T_H}{T_H + T_L} * 100 \quad (7)$$

$$T_H = R_A * C_2 * \ln 2$$

$$T_H = R_L * C_2 * \ln 2$$

Due to increased noise as a result of signal sampling, the MQP group implemented an additional second order LPF stage. Signals at various test points in the circuit were observed to verify proper functioning of the PPG sample hold circuit (see Appendix F). To determine the duty cycle that would be optimal for our device, the MQP group observed the effect of various duty cycle percentages on signal quality. The average root mean square value of the current was approximated to 0.01  $\delta$ \*current at DC. This was done by using a pulsatile voltage from a power supply source.

Pin 4: +9V  
 Pin 11: -9V  
 IC: LM 348N

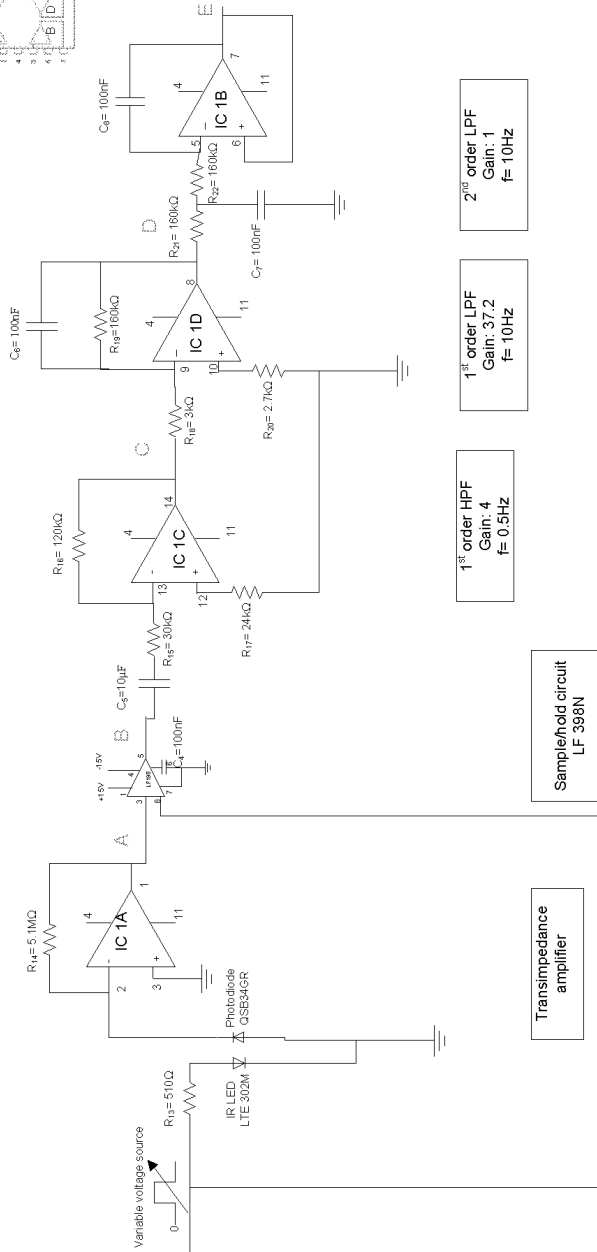
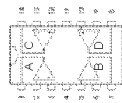


Figure 6.8: PPG circuit to investigate current amplitude

## 6.2 ECG

The final circuit design, shown in Appendix B as Revision A, consists of a standard instrumentation amplifier. Each of the two stages for this is set with a gain of 5. From that section, the signal filtered through the analog hardware filter described in 6.2.2, and has a gain of 5. The resulting total gain of the ECG hardware is 125.

### 6.2.1 Electrodes

The final design of the electrodes, shown in Figure 6.28, gives the design of the dry electrodes used for testing and experimentation. These electrodes are derived from VerMed's standard gel-based electrodes. Prior to use, the sponge and gel contained within were removed from the contact plate of the electrode. The contact plate was cleaned to ensure that there remained no residual gel. This allowed for the use of the metal contact plate with the surrounding adhesive to secure the electrode in place. By using this design, physical movement of the electrodes could be eliminated, providing a stable base for the contacts.

### 6.2.2 Filter Design

Hardware filtering was implemented through a HPF to remove baseline drift in order to avoid saturating the amplifier op-amps (see Figure 6.9). Removal of higher frequency components such as 60Hz electrical noise will be effectuated via software filtering. Component values were calculated based on Equation 6.

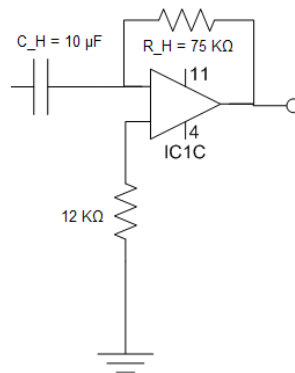


Figure 6.9: ECG high-pass filter design

**Table 6.2: ECG Filter Characteristics**

	$R_H$	$C_H$	$f_c$
High-Pass Filter	75 K $\Omega$	10 $\mu$ F	0.21 Hz

### 6.3 Software

Signals were sampled and digitized using LabVIEW DAQ Assistant, with analog inputs collected via a National Instrument's Data Acquisition Board with a sampling frequency of 100Hz. Functions of the software include additional signal filtering, peak detection, and signal conditioning to calculate HR/PR and respective SDNN and rMSSD indices. LabVIEW also has to display signal waveforms and their respective calculated measures, as well as effectuate device controls. Details of the sequence of software processes applicable to both signals are summarized in Figure 6.10.

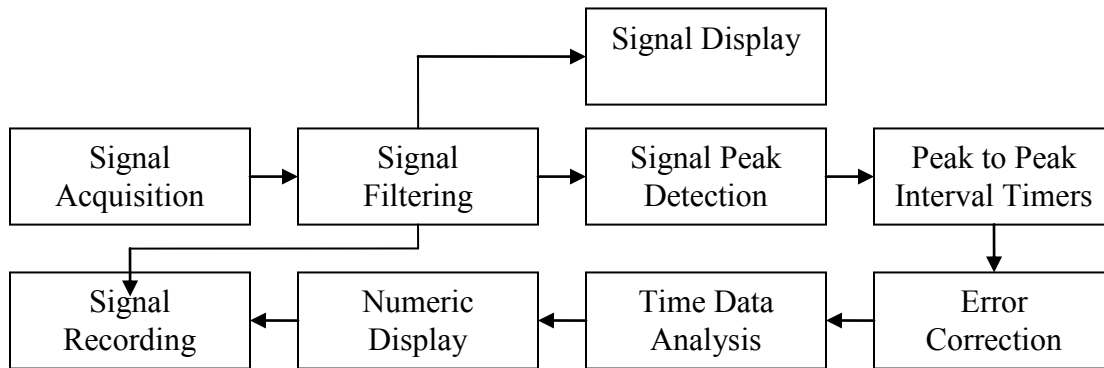


**Figure 6.10: Software flow chart**

The breakdown of each category will be further described in the following sections, via LabVIEW subVI programs.

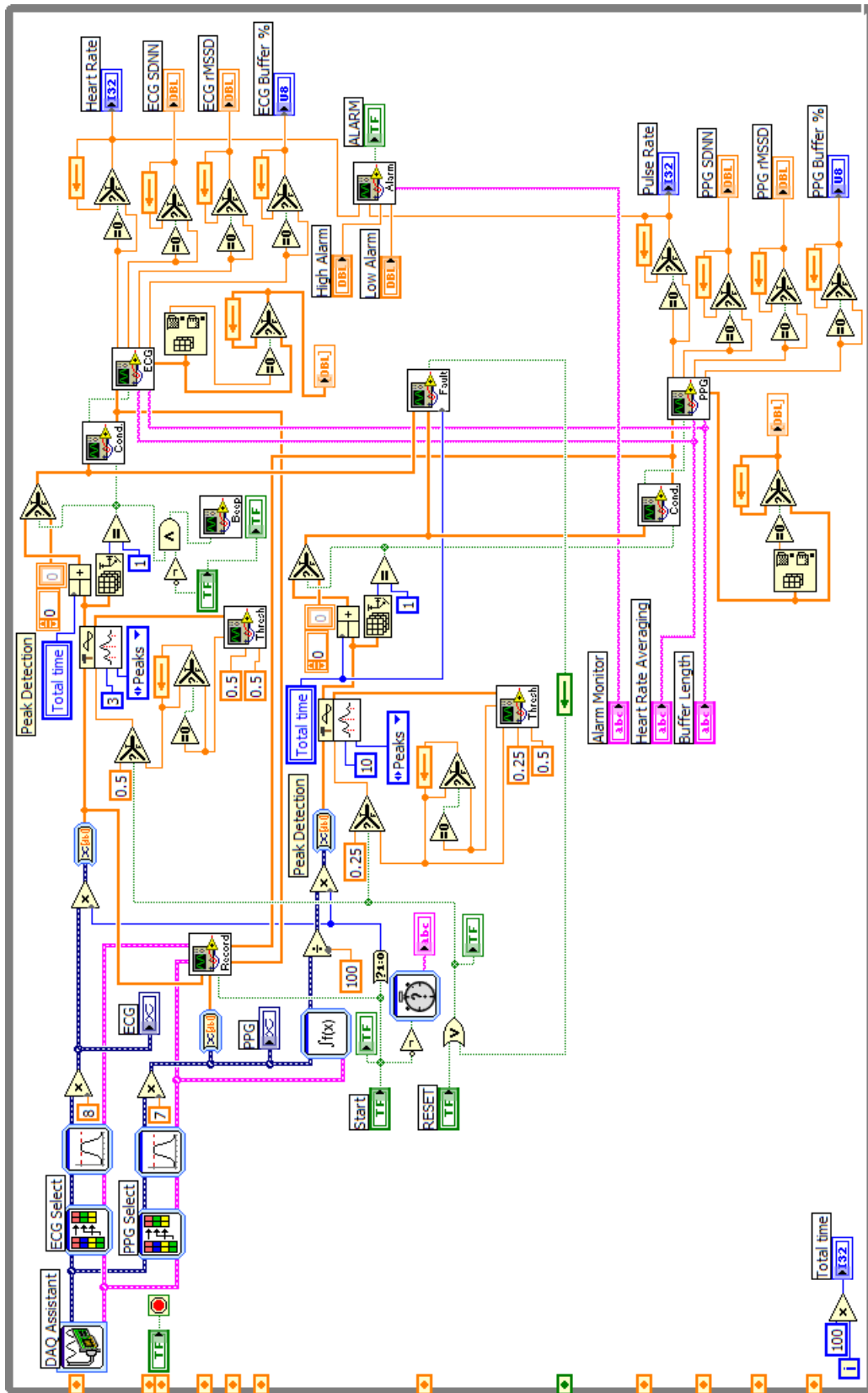


Figure 6.11: LabVIEW program block diagram

### 6.3.1 Signal Acquisition

Signal acquisition was done through the LabVIEW DAQ Assistant, with analog signals collected via NI DAQ board. Signal selectors were used to separate waveforms from their respective channels (see Figure 6.12). ECG and PPG signals were designated to channel 0 and channel 1 respectively in the DAQ Assistant since both signals were going to be processed differently.

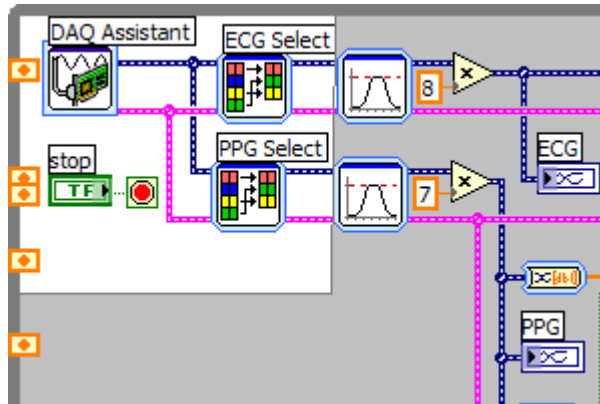


Figure 6.12: Signal acquisition and A/D conversion

### 6.3.2 Signal Filtering

Software filtering was implemented to remove residual signal noise, following hardware filtering. Shown in Figure 6.14 are filter VI locations for PPG and ECG signals. For the ECG, the filter bandwidth was set to 1Hz-35Hz to accommodate for the higher frequency components of the QRS complex. The signal was further amplified by a gain of 8 to achieve a total signal amplification of 1000 (125 from the hardware). The PPG signal bandwidth was set to 0.8Hz-8Hz. The signal was further amplified by a gain of seven to achieve a total signal amplification of approximately 1050 (148.8 from the hardware). Filter characteristics setting can be seen in Figure 6.13. Signals were displayed in the front panel after filtering.

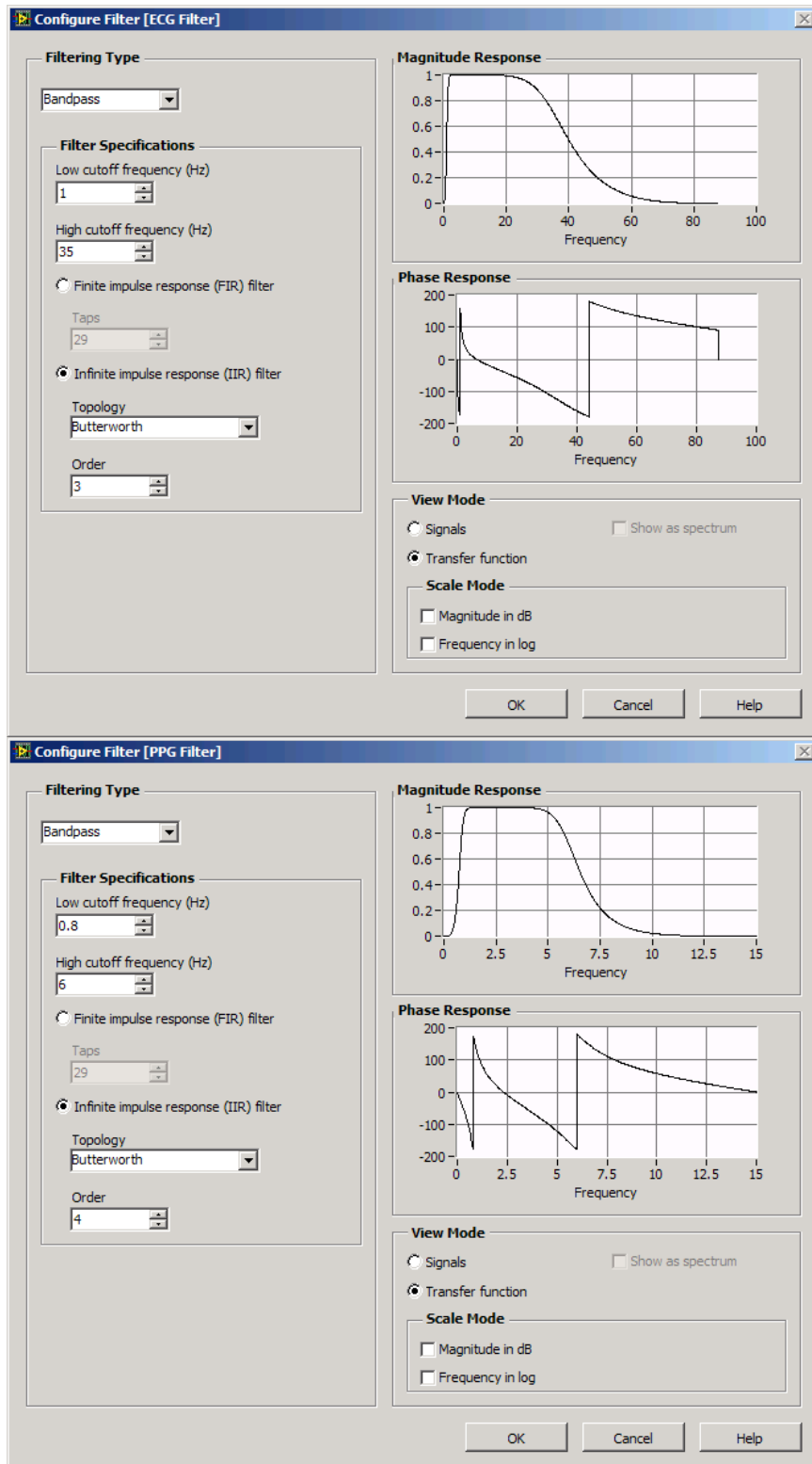


Figure 6.13: ECG (top) and PPG (bottom) software filter settings

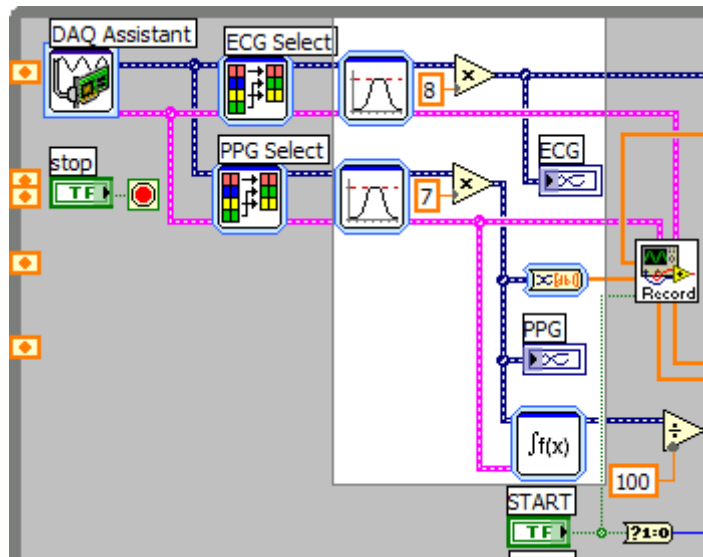


Figure 6.14: Signal filtering and gain

A further consideration for the PPG waveform is that it lacks the characteristic sharp demarcation in its waveform like that of the high amplitude QRS peak of the ECG waveform and so peak detection may not always be implemented effectively. The signal required a larger peak detection window. However, a dirotic notch can introduce an additional peak, causing the detection of multiple peaks. Since the PPG slope changes in polarity from peak-to-peak, a derivative filter was used to obtain a steeper signal peak and separate amplitudes due to the dirotic notch. This phase of the signal conditioning was done following the filtering of the signal and prior to the signal being sent through the remainder of the system to determine the signal peaks.

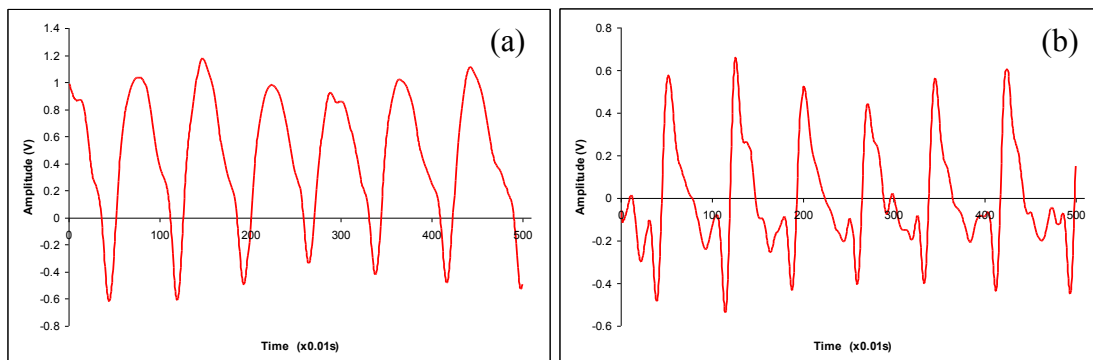


Figure 6.15: Sample PPG signal (a) and respective derivative (b)

### 6.3.3 Peak Detection

Peak detection was implemented to respective signals with an adjustable threshold detector. In real time, blocks of data were analyzed in a peak detection window to determine the maximum point greater than the threshold (see Figure 6.16). This allows the program to ignore erroneous artifacts present such as baseline noise or other peaks such as the P and T waves of the ECG signal. Each block of data consisted of 100 data points from the acquired signal. When a peak was detected, the location of the peak within the 100 samples was output. Following the determination of the point within the total, the total number of points input to the system was added to the peak location. The output of this addition gave the peak location with reference to the total signal acquired. Times between peaks were then calculated from this, as can be seen in Section 6.3.4.

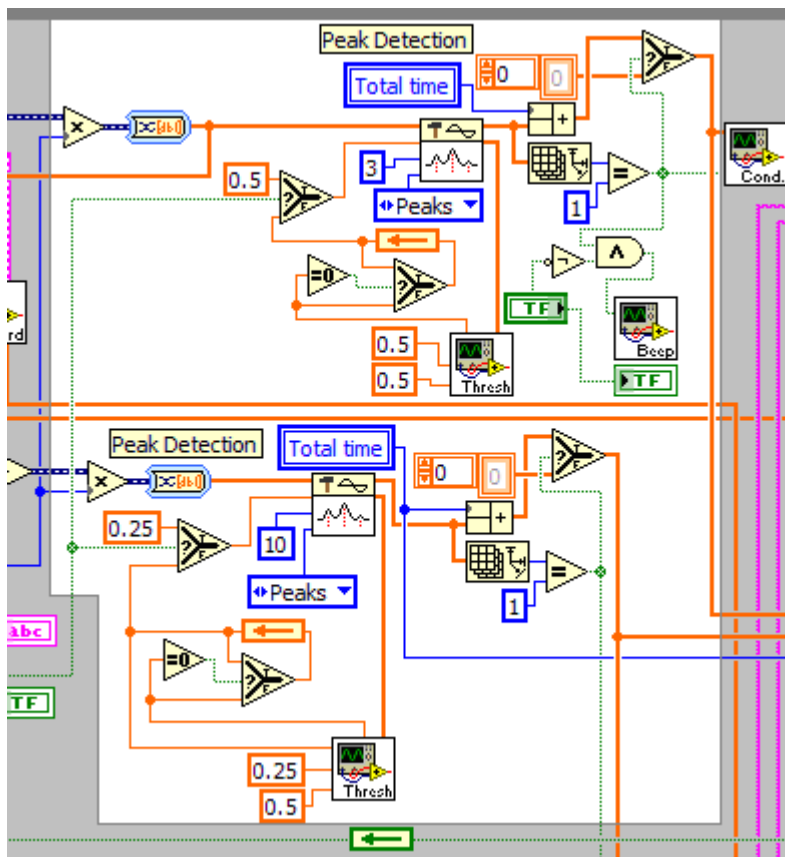


Figure 6.16: Signal peak detection

### 6.3.3.1 Threshold Adjustment

Adjustable threshold detection was necessary to account for the physiological variation of signal amplitude between individuals. Signals acquired from the same person can also vary depending on sensor placement. For the ECG, this was to account for factors such as skin resistance and electrode distance from the heart which can affect the overall peak amplitude. For the PPG, signal amplitude is affected by blood perfusion as well as bone density in signal reflection. Baseline drift due to breathing cycle also contributes to change in signal amplitude. Motion artifacts can also introduce additional peaks in the signal, resulting in abnormally high peak-to-peak time intervals. Both signals utilized similar methods for threshold calibration. When a peak is detected, its amplitude is recorded and sent to a 'for loop' for processing, and it re-executes each time a new value is received. This allows for the loop to act as a buffer to store a set of 5 consecutive peak amplitudes. Average amplitude of the 5 consecutive peaks is calculated and scaled to half its value and set as the new signal threshold.

Analysis of various ECG recordings from different individuals showed generally little change in ECG beat-to-beat amplitudes over time within the same individual. The above described method of 5 peak amplitude average was thus sufficient to implement the calibrated threshold (see Figure 6.17).

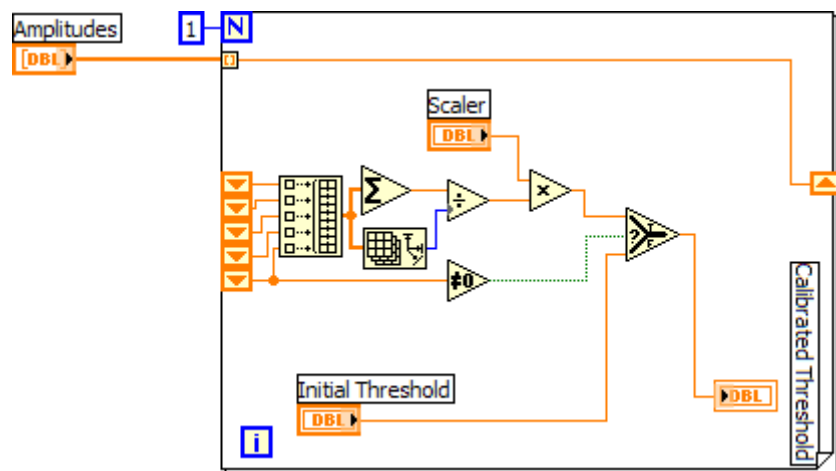


Figure 6.17: ECG threshold adjust

The PPG signal demonstrated greater peak-to-peak amplitude variability, especially due to possible baseline drift introduced from breathing as well as sensor movement. Erroneously high peak amplitudes introduced into the system can set the threshold average sufficiently high that detection of further peaks is not possible. To account for this error, a PPG threshold adjustment feedback was implemented by comparing newly calculated threshold value to previous values. The new threshold value would have to be within  $\pm 5\%$  of the previous value, or else it is rejected. As such, slow growths of the peak amplitude are acceptable, whereas sudden jumps in the peak values would be rejected (see Figure 6.18).

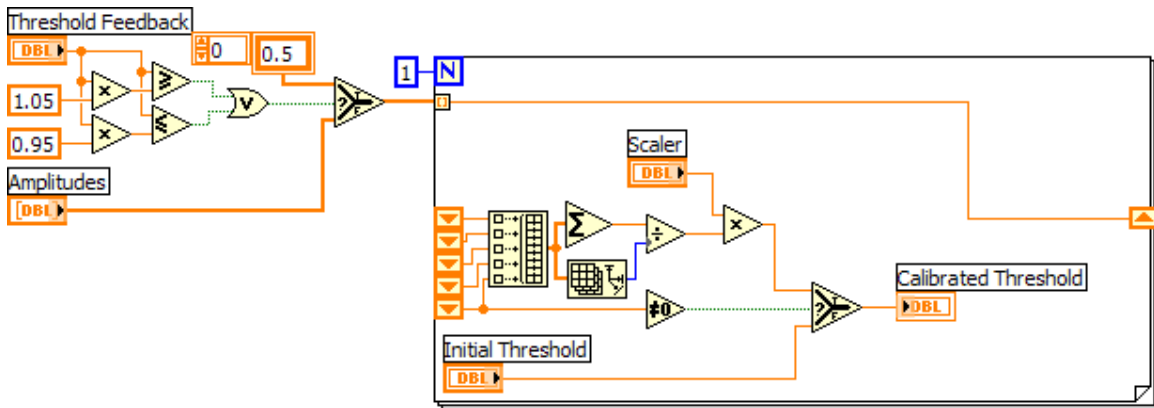


Figure 6.18: PPG threshold adjust

### 6.3.4 Peak-to-Peak Interval Calculation

As described in Section 6.3.3, peaks detected are output as their locations in milliseconds with respect to the total signal acquired. In order to determine the time between peaks, the previous peak time must be subtracted from the current. This was accomplished through utilizing shift registers to store the last data value and perform operations on the time locations (see Figure 6.19).

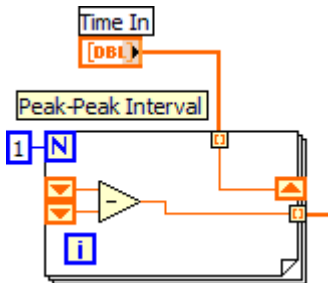


Figure 6.19: Peak-to-peak timer

### 6.3.5 Time Interval Error Correction

Following the determination of the time between peaks, it was necessary to analyze the times for possible anomalies. These included two possible problems; missing a beat and causing an abnormally high interval, or recording multiple false beats and causing an abnormally low interval. In order to prevent the propagation of incorrect values, comparators were used to correlate the present interval value with the previous. The current value had to be within 80% to 175% of the previous value. If not, this value was rejected and not propagated further into the system. Figure 6.20 shows an example of the signal error correction VI's used for both signals.

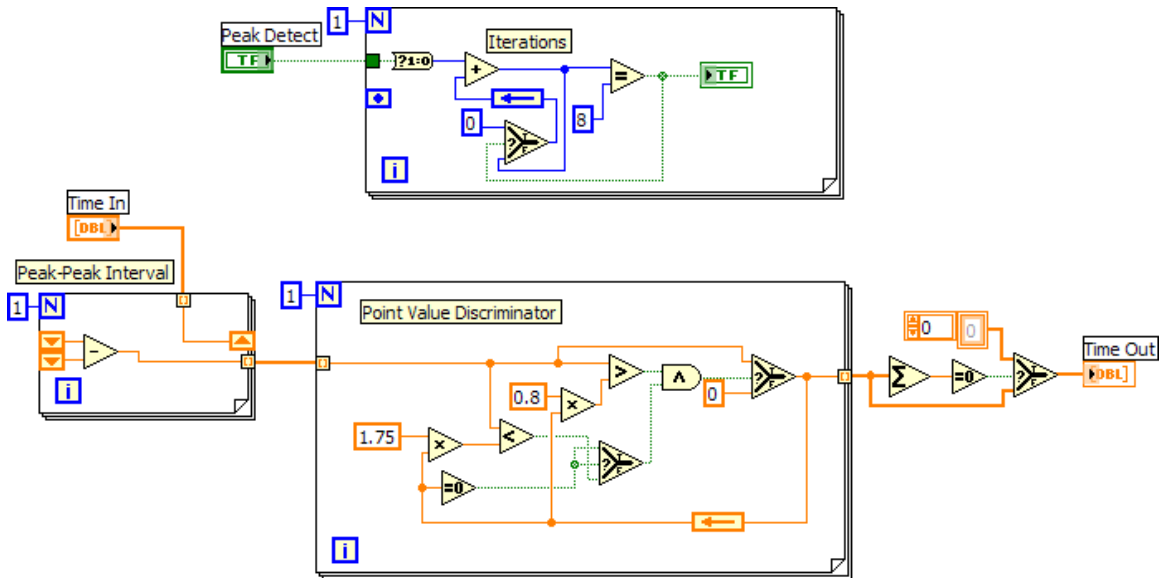


Figure 6.20: Example signal error elimination block diagram

A final component of the ECG and PPG conditioning subVIs are the iterations counters, which count the number of peaks detected. This portion of the subVI counts up to 8 as peaks are detected, and then generates Boolean true value on the 8<sup>th</sup> beat and resets. This signal indicator is used to update the subVIs that calculates respective rates and variability indices, as further detailed in Section 6.3.6.

### 6.3.6 Rate and Variability Calculations

The series of interbeat time intervals are used to calculate the numeric outputs; HR, PR, SDNN and rMSSD indices for the respective signals. This was achieved through different

‘for loops’ in the subVI, as can be seen in Figure 6.21. The algorithms are applicable for both ECG and PPG signals.

This first ‘for loop’, shown in Figure 6.21a, calculates HR. Three types of HRs can be determined by changing buffer sizes; instantaneous HR, a 5-beat average or an 8-beat average. These are some averaging methods used in various commercial devices (see Appendix G). The number of beat intervals averaged can be altered by selectively choosing the number of shift registers used to compute the average. The device user can thus control this through an averaging control in the front panel. The default setting is however set to an 8-beat average.

The second ‘for loop’, shown in Figure 6.21b, calculates the standard deviation between the normal-to-normal peaks (SDNN) index, calculated using Equation 3. Points were saved within a buffer, implemented via shift registers. The buffer was updated each time a set of 8 time intervals were obtained, to avoid overlapping, ensuring each data value within the buffer is a unique value. A secondary analysis implemented within this portion of the subVI is to determine HR trend. This was implemented by comparing the average from a current set of 8 time values to previous set. The difference between the values is then determined and displayed graphically to the user to indicate whether the HR is rising or falling.

The third and fourth ‘for loop’, shown in Figure 6.21c and Figure 6.21d, calculates the root mean squared of the successive differences (rMSSD) index using Equation 4. This was accomplished by using 2 sets of for loops. “For loop” c calculates the difference between interbeat time intervals. “For loop” d performs the rest of the mathematical computation using Equation 4.

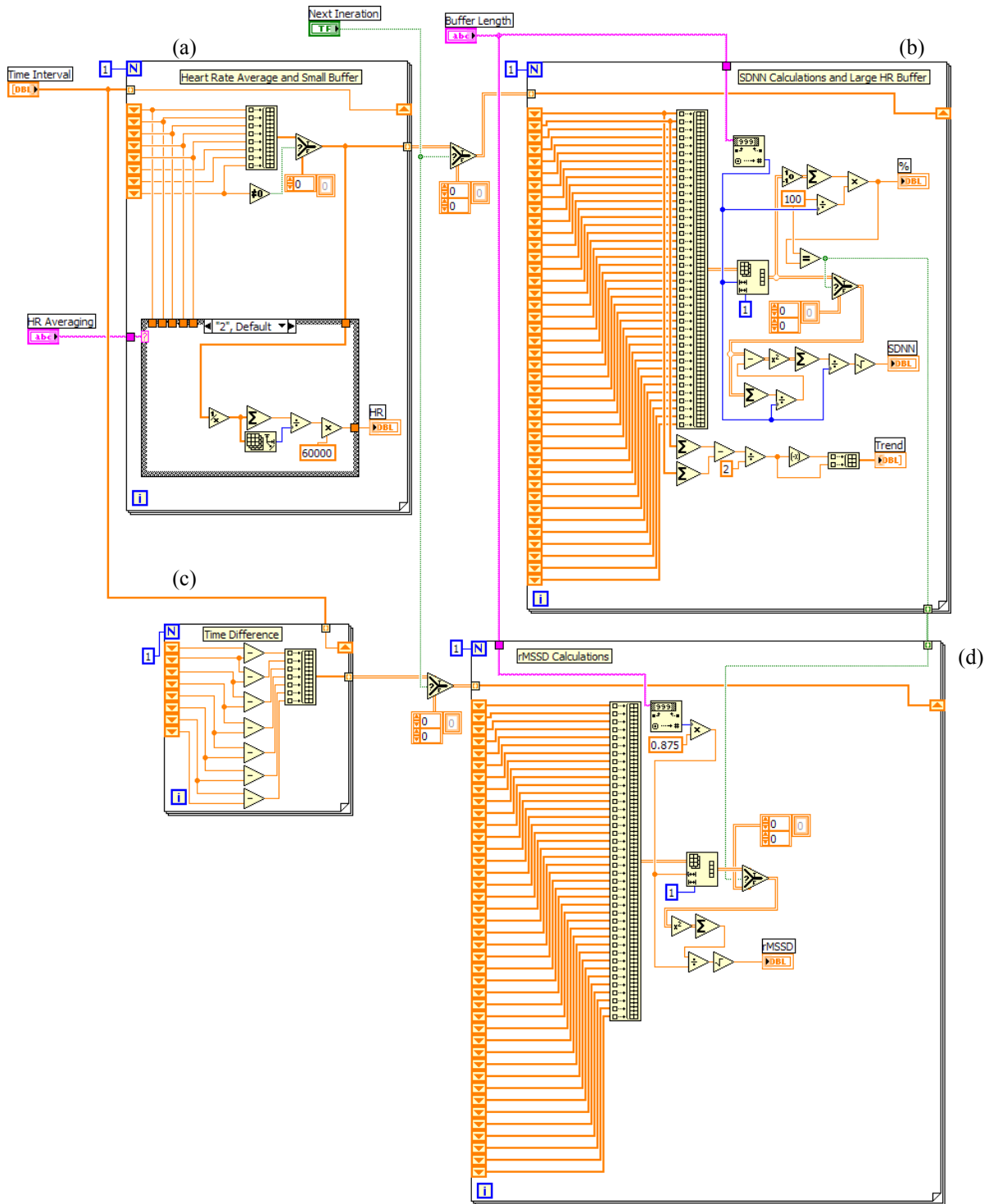


Figure 6.21: HR and HRV calculations

Usually, the SDNN and rMSSD indices are calculated for a period of five minutes. However, a varying window was implemented to allow for various lengths of time analysis. SDNN and rMSSD indices can be calculated for thirty seconds, one minute or

five minutes, depending on device user settings. This, like the system for determining the averaging length, was done by selectively choosing the number of shift registers used in calculation of the respective equations. Also, calculated indices do not display until their respective buffers are full. To avoid user impatience, buffer indicators were implemented to show the percentages with which respective buffers were full. This was necessary especially due to some level of impatience that can result for long wait times encountered with 5 minute calculations.

### 6.3.7 Audible and Visual Alerts and Alarms

Audible and visual cues were used to alert the device user of specific events or potential problems either physiological or software related. These may indicate situations that require user intervention.

#### 6.3.7.1 Heart and Pulse Rate Alarm

HR alarm controls are necessary to communicate critical information to the physician about the patient. Applicable for this system are high and low alarm controls. The ASTM Standard requires that all alarms be user adjustable, since these values may vary depending on individual patient [14]. HR and PR values are constantly compared to preset alarm thresholds. A condition loop is used to allow for monitoring of either both signals, or only one signal, as selected by the user. A PR or HR value not within preset range activates an alarm LED in the front panel.

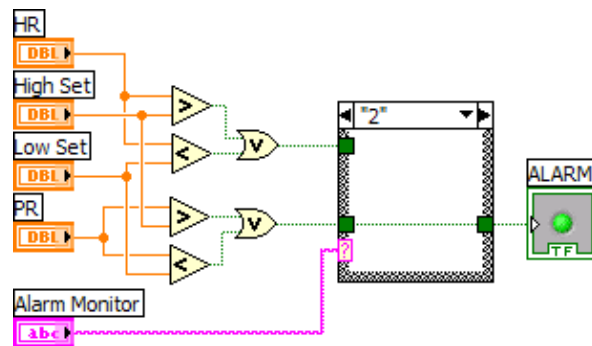


Figure 6.22: High/Low HR and PR alarm

### 6.3.7.2 System Fault Alarm

As indicated in Section 6.3.3.1 an adjustable threshold system was implemented. This section of the program determines whether a fault has occurred from not properly detecting the signal peaks. Inputs for this are the last peak locations of the ECG and PPG signals. Should the system time increase above 3 seconds since the last peak detected, the program determines that a fault has occurred. When detected, the program provides for visual cues to alert the user and attempts to automatically correct for the problem by fixing the detection threshold value.

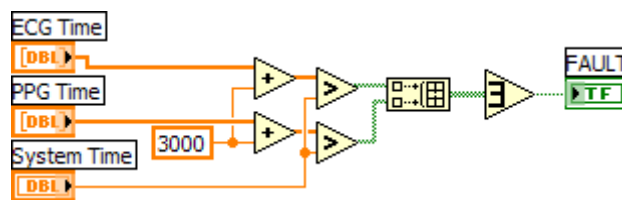


Figure 6.23: Signal fault detection

### 6.3.7.3 Heart Beat Alert

QRS detection beeps are also used in clinical monitoring devices to indicate heart beat occurrence. An audible indicator was used to indicate peak occurrences in the ECG signal. A mute button was implemented to turn the beep ON or OFF as desired by the user.

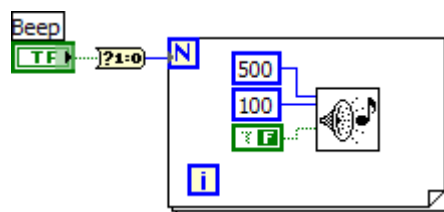


Figure 6.24: ECG audible peak indicator

### 6.3.8 Signal Storage

Data storage was also implemented for further signal analysis. These included ECG and PPG signal waveforms, as well as their respective interbeat interval time values. Each time that the program is run, a “Select a file to save” window was used to prompt the user to record a file name (see Figure 6.25). All files are by default to be saved to the computer desktop.

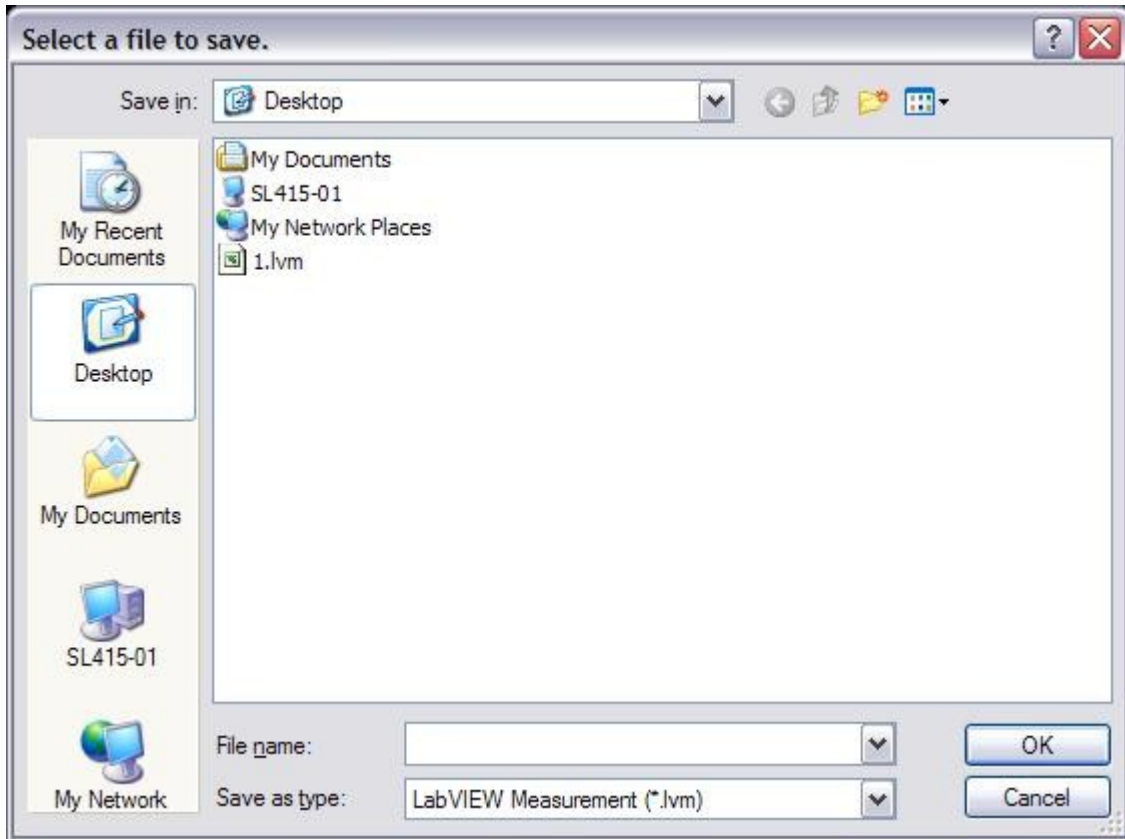


Figure 6.25: Waveform file name window

The data of interest is only recorded and compiled in a spreadsheet file only when the user initiates signal analysis. This is to allow the user to make any necessary sensor adjustments to obtain a proper signal prior to analysis and recording of the signal.

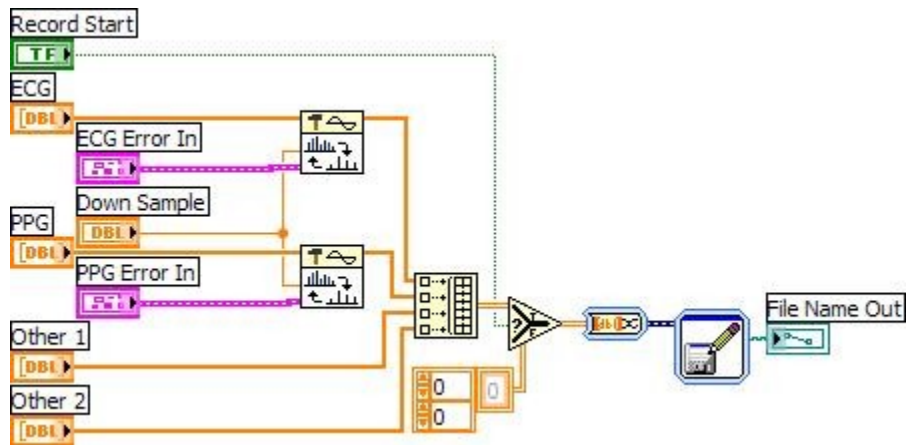


Figure 6.26: Raw signal down-sampling and storage

Data is saved in 4 columns in a text file with column-data designation as follows:

- Column 2: ECG signal
- Column 3: PPG signal
- Column 4: ECG NN intervals signal
- Column 5: PPG NN interval signal

Files are by default saved to the desktop in a text file and can be copied to MS Excel and plotted (see Figure 6.27). Values for columns 4 and 5 are by default given a zero value when no time interval is present. This is due to the method of saving the data, where a value for each point is required. As no values are propagated into the file when time intervals are not determined, null values are then represented as zero.

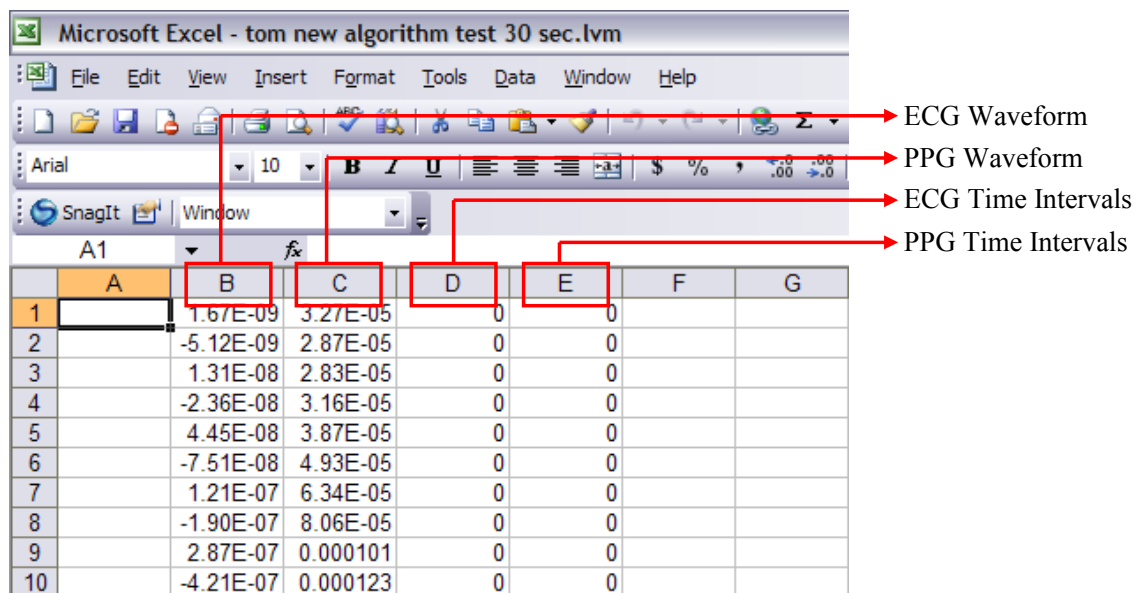


Figure 6.27: Sample recorded data

## 6.4 Final Design

The final design of the project utilized both a hardware sensor suite and software analysis to detect and display the physiological signals, determine the heart and PRs, and respective HRV indices.

### 6.4.1 ECG Electrodes

Experimental dry electrodes were implemented for the project. The electrodes used for the final design can be seen in Figure 6.28. These electrodes were connected into the hardware portion of the project through three ECG leads, utilizing standard electrode snap connections. Connections for the ECG electrodes were integrated into a single connection, which can be seen in Figure 6.29.



Figure 6.28: Final ECG electrode

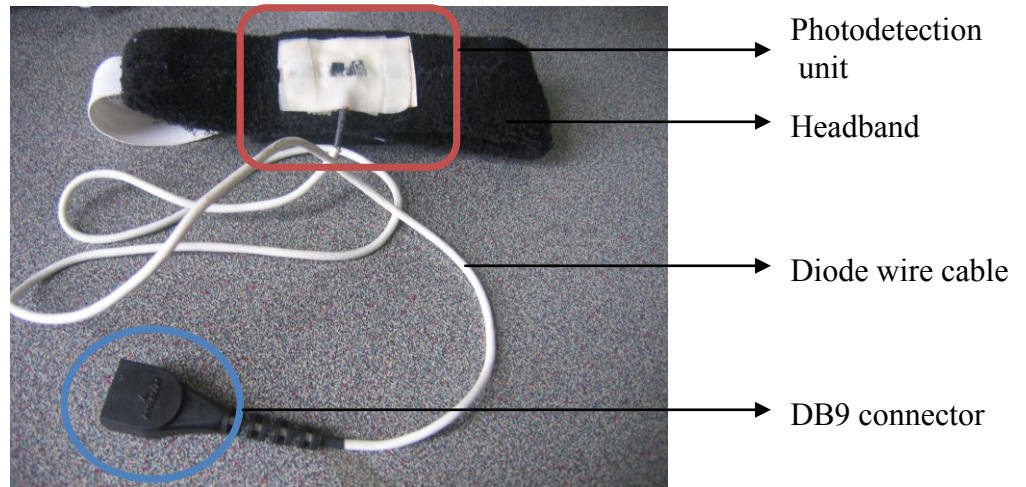


Figure 6.29: ECG electrode leads

### 6.4.2 PPG Sensor Probe

The MQP group designed a custom sensor probe, roughly modeled after the commercial reflectance Oximax MAX-FAST® sensor by Nellcor (see Appendix G). The LED and photodiode were mounted on an elastic band with adjustable straps. The MQP group used an elastic band due to better stability and previous studies indicated better signal accuracy when compared to adhesive tape [53]. The MQP group attached Velcro and elastic bands

of various lengths to account for variations in head circumference. The MQP group selected a dark headband color to limit optical interference. The photodetection was mounted unto the band, and covered with a plastic shield, surrounded by a cushioned cloth tape. The MQP group soldered diode wire connections unto a DB9 cable recycled from a commercial NONIN finger PPG sensor. The final design is seen in Figure 6.30.



**Figure 6.30: Reflectance forehead sensor probe**

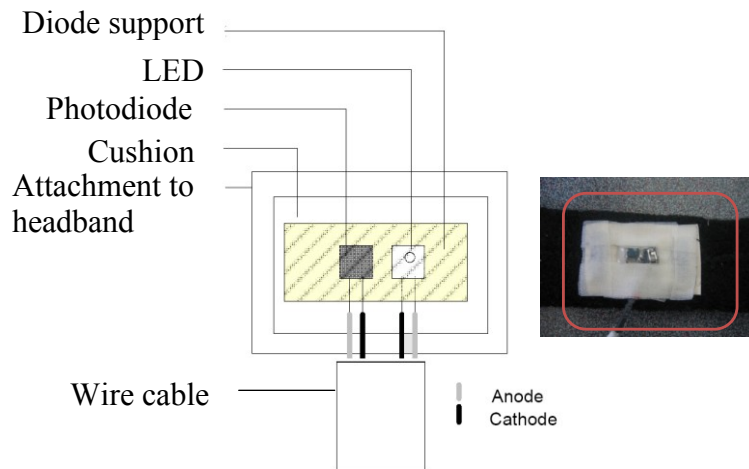


**Figure 6.31: Sensor photodetection unit**

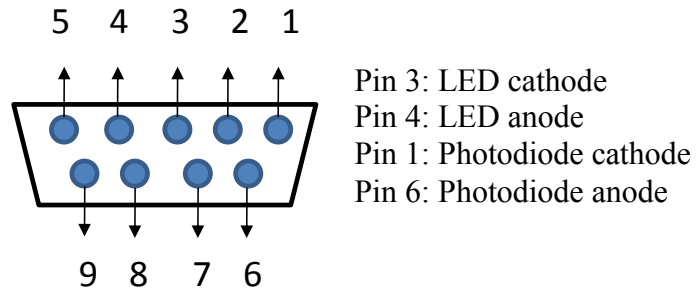


**Figure 6.32: PPG sensor DB9 input connector**

### 6.4.3 Device Hardware

The MQP group designed the hardware printed circuit board (PCB) using PCB123® software from Sunstone Circuits and ordered the PCBs from [www.pcb123.com](http://www.pcb123.com). This consisted of a 2 x 3 inch PCB board, with silk screen and corresponding components labeled to facilitate soldering. The MQP group soldered the respective components onto the PCB (see Figure 6.33). The final circuit drawing can be seen in Appendix B.

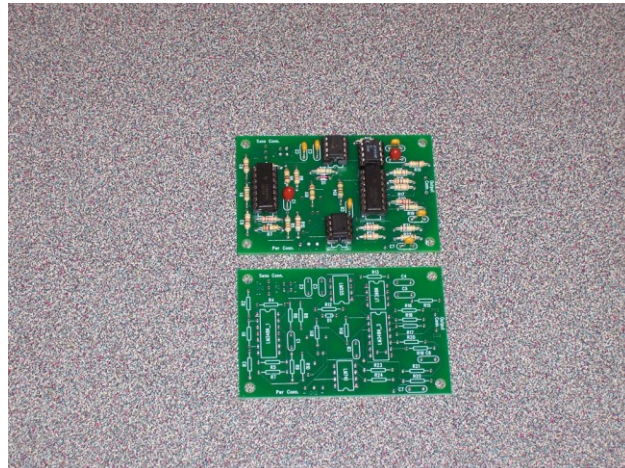


**Figure 6.33: Hardware printed circuit board**

Instead of designing and manufacturing a device hardware box, the MQP group purchased a readymade box, for better surface finishing. Dimensions of 4.31 x 3.06 x 1.37 inches were used to accommodate the size of the two 9V batteries. The MQP group selected a hardware case with round edges to avoid possibility of sharp edges. MQP group mounted and assembled the PCB and device battery inside the device case. Figure 6.34 shows an isometric view of the device hardware, with labeled device outputs and

switch. A switch was incorporated into the device box for turning the hardware ON and OFF.

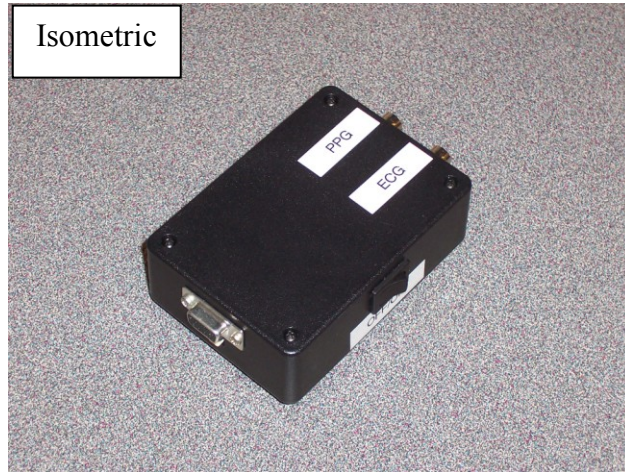


**Figure 6.34: Final device hardware case**

The MQP group localized device inputs and outputs at opposite sides to avoid confusion during connection. DB9 and 3-pin inputs were screwed unto one side of the case for the PPG sensor and ECG-lead systems (Figure 6.35). The MQP group used BNC cables as device output connectors, in order to be compatible with NI DAQ from National instruments (Figure 6.36). The MQP group labeled respective signal BNC connections to also avoid further confusion between signals as their labels corresponded to their software location processing. The MQP group inserted rubber feet on the device hardware floor for proper contact when placing on a surface, due to the probability of the device slipping when placed on smooth surfaces. The complete device assembly can be seen in Figure 6.37.



**Figure 6.35: Device hardware inputs**



**Figure 6.36: Device hardware output connections**

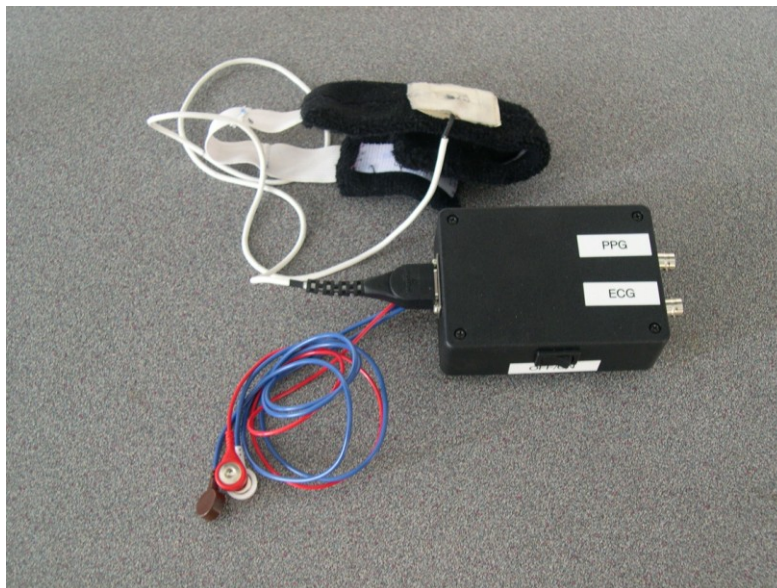


**Figure 6.37: Final hardware device assembly**

## 6.4.4 Software

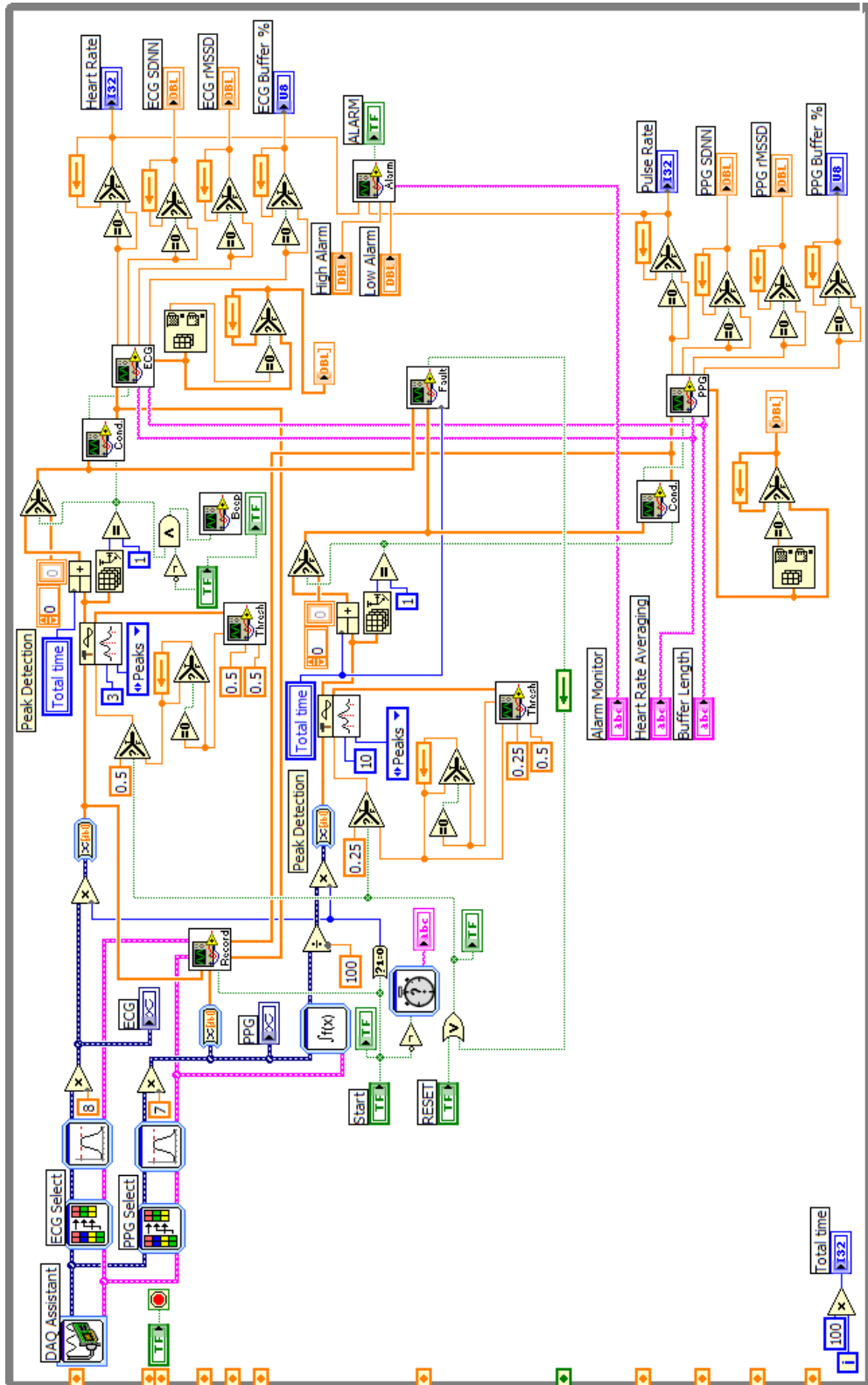


Figure 6.38: Final block diagram

## 6.4.5 User Interface

The device front panel consists of the following features:

- An arrow key button to start signal acquisition
- A Start button, to begin signal analysis
- ECG and PPG signal displays
- Numeric displays for HR, PR, SDNN and rMSSD for respective signals. These displays don't display any values till the Start button is activated
- Controls for HR/PR buffer size of IHR/IPR, 5-beat and 8-beat averages
- Controls for HRV/PRV buffer size of 30s, 1minute and 5minutes
- Indicators to alert user when SDNN and rMSSD buffers are full
- A Stop button to stop signal acquisition
- A visual alarm indicator and High and Low alarm controls.
- A reset button adjusting the threshold. The automatic reset takes 15s to effectuate. However, the threshold can be reset manually
- Trend Indicator for HR and PR

The complete front panel can be seen in Figure 6.39, and the labeling code is as indicated below:

A	Start Data Acquisition	L	PR display
B	ECG Signal display	M	PPG SDNN display
C	PPG Signal display	N	PPG rMSSD display
D	Stop button	O	PRV Buffer Indicator
E	High alarm control	P	Recording Time Elapsed
F	Low alarm control	Q	Manual Threshold Reset and LED indicator
G	Alarm LED	R	Start Data Analysis and LED indicator
H	HR display	S	Beep Mute Switch and indicator
I	ECG SDNN display	T	HR/PR averaging control
J	ECG rMSSD display	U	HRV/PRV Buffer Size control
K	HRV Buffer Indicator	V	Alarm setting control

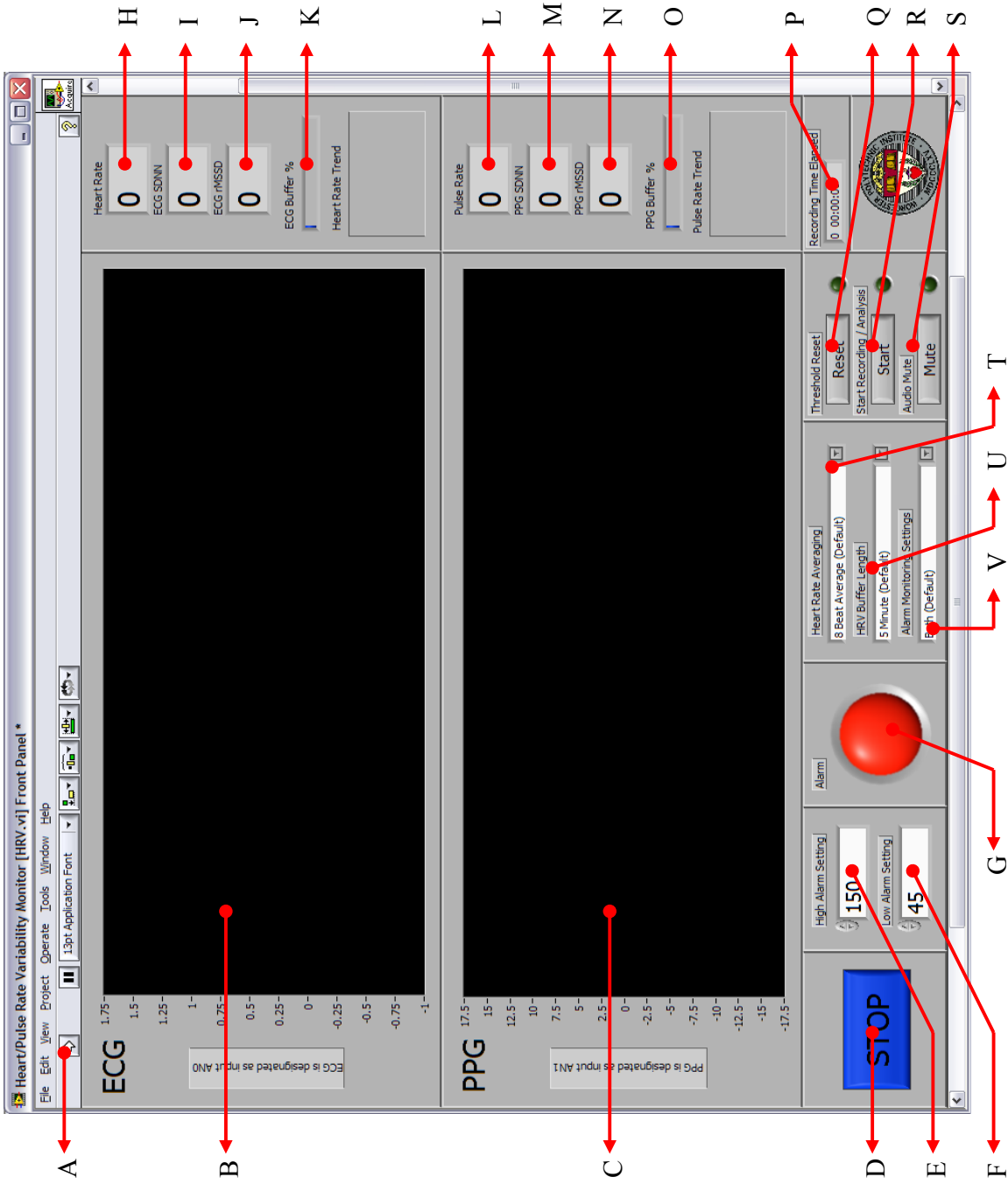


Figure 6.39: Front panel with labels

## 7. Results

The results for the project focused on three main parts; the PPG hardware, ECG hardware, and the software testing. Each of these three components of the project was tested individually to ensure functionality. After it has been confirmed that the hardware components of the project were functioning as expected, signals were then put through the software component of the project. For this portion, tests and experiments worked to confirm that the software was capable of accurately obtaining and analyzing the input signals. Errors present in the software portion of the project were also quantified to determine their cause and possible methods for attenuating the errors present.

### 7.1 PPG

#### 7.1.1 Sensor Probe

The MQP group designed a wearable forehead sensor for the PPG suite. To compare the quality of the sensor, signals obtained from the prototype and a commercial PPG sensor were compared. Given the popularity of finger sensors, a Nellcor finger PPG sensor was chosen for comparison. PPG signals obtained at 40mA LED drive current from the prototype and Nellcor were recorded simultaneously and compared. The 40mA was used as reference because typical PR monitors operate around current values of 40 mA or even higher e.g. Propaq® 100-50mA, Ohmeda ® -120mA [14]. Typical signals obtained from both probes are shown in Figure 7.1.

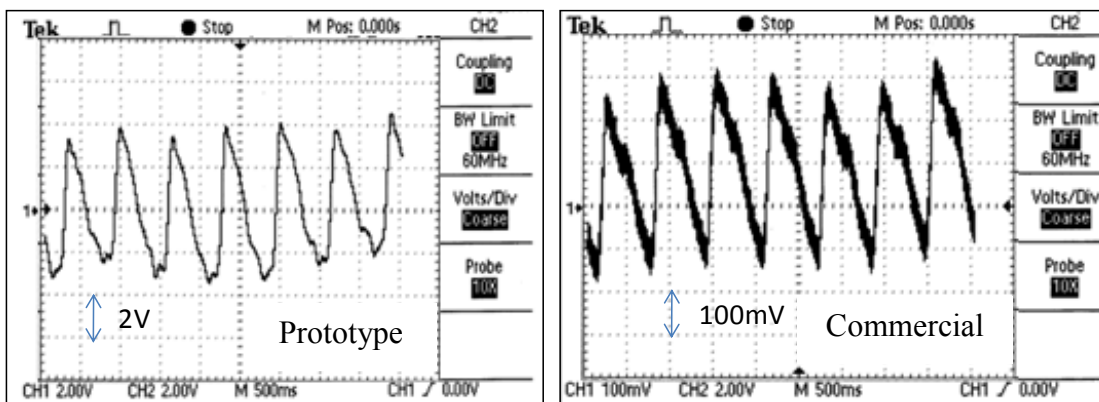


Figure 7.1: PPG signals from prototype and commercial sensors

The MQP group measured on average that signals obtained from the forehead sensor had 18 times higher amplitudes than that from the finger. Signals from the forehead had considerable improvements in SNR compared with the finger. This demonstrated that although the finger sensor is popularly used in monitoring systems, other sensor locations like the forehead provide better signal quality for data acquisition under motion conditions. With a peak-to-peak value of 6V at 40 mA current, this allowed for the reduction in current as it was only required that we have at least a 1V peak-to-peak signal displayed in the final device front panel. This allowed the possibility of reducing LED drive current, to optimize battery life.

## **7.1.2 Power Optimization**

### **7.1.2.1 Current Amplitude**

The measurement of high peak amplitudes in the forehead PPG sensor at 40mA allowed reduction in LED drive current. The MQP group also kept in consideration that the further current reduction decreases signal amplitude, which can affect system accuracy. LED currents were varied from 5, 8, 28, 38 and 48mA and their resulting amplitudes measured. This exercise was then repeated twice, and subsequent values recorded. Taking into account that signal amplitude is subject to variation during different applications, relative amplitudes were plotted against current. The relative amplitude was determined by taking the ratio of the signal amplitude to the highest measured amplitude of that trial. Figure 7.2 shows average values recorded, with standard deviations.

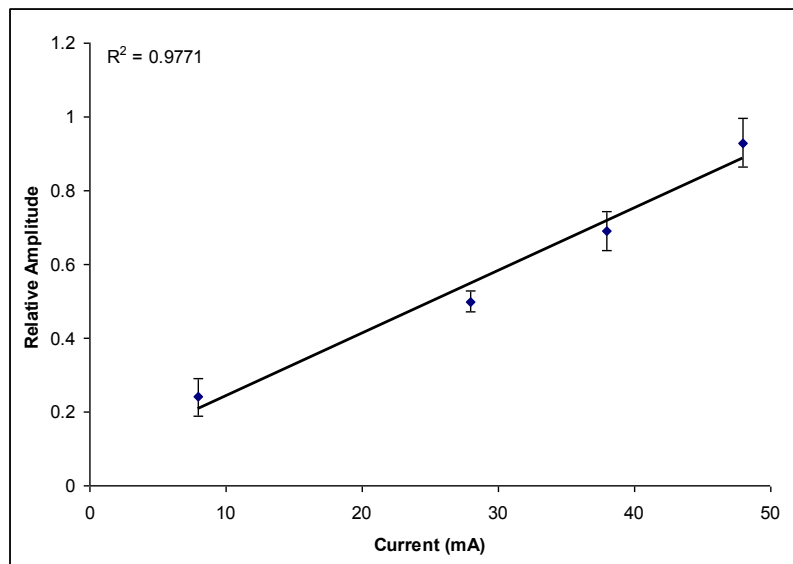


Figure 7.2: Plot of relative signal amplitude against current (mA)

### 7.1.2.2 Current Duty cycle

The MQP group determined that power can further be optimized by using a pulsatile current source to drive the LED. Using a pulsatile power source periodically switches the LED on and off, so the total effective time when the diode is off is reduced. A pulsatile current reduces the effective current of the LED, with a root mean square value of  $0.01 \cdot \delta \cdot \text{current}$ , where  $\delta$  is the current duty cycle. The MQP group evaluated the effect of LED current duty cycle on signal quality, to further reduce the power requirement of the LED driver circuit. Signals were measured at 20, 40, 60, and 80% duty cycle. Signals obtained from various test points of the circuit can be seen in Figure F.1. Figure 7.3 shows duty cycles measured at the 20 and 80% duty cycles. The MQP group observed no observable differences in signal quality measured at the respective duty cycle. As expected, signal magnification revealed the existence of small amplitude noise levels, which could easily be removed by software filtering. A duty cycle of 20% was selected, with approximately calculated values of  $R_A$  and  $R_B$  as 150 and 560k $\Omega$  for the device LM555 timer circuit.

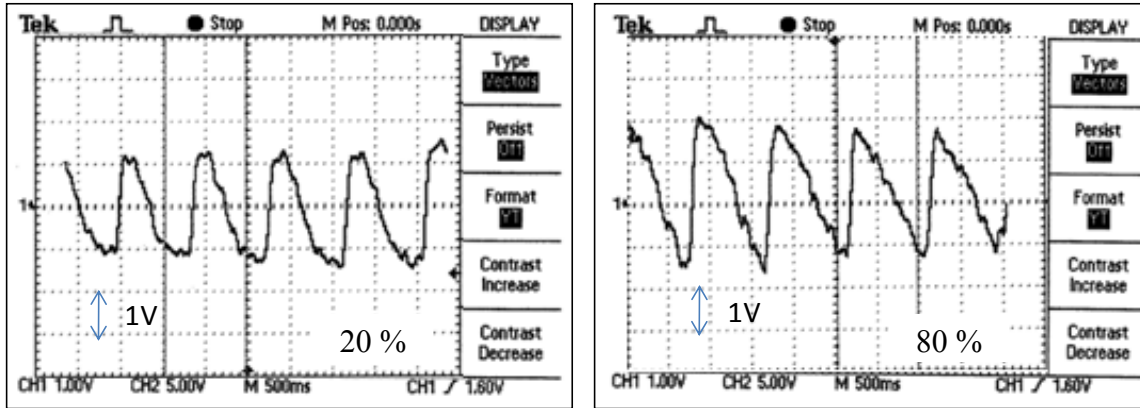


Figure 7.3: Detected signals from different LED current duty cycles

## 7.2 ECG

ECG hardware tests were conducted to analyze the performance of the hardware sensing circuit. The initial circuit design tested is shown in the schematic in Appendix B, Figure B.1. The primary goal of the initial circuit was to obtain the ECG with a minimal amount of filtering. The circuit shown in Figure B.1 gives the diagram for an instrumentation amplifier and HPF to prevent baseline drift. Following the HPF stage, no further filtering is done to the signal. The signal obtained, shown in Figure 7.4, contained significant 60Hz noise. Results for the second circuit design implemented, shown in Figure B.2, are similar to those shown in Figure 7.4. For this circuit design, a LPF was implemented, however this did not account for 60Hz noise present within the system.

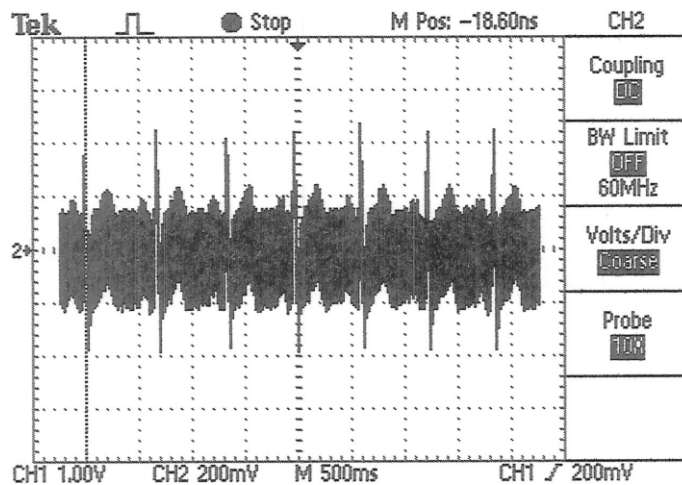
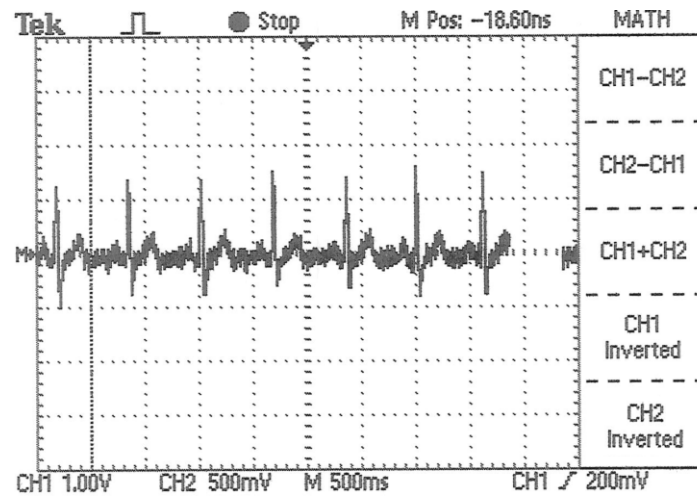


Figure 7.4: Initial ECG hardware implementation tests

After having confirmed the ability to collect the ECG signals, it was then attempted to filter the results via hardware based filters. Figure 7.5 shows a signal obtained after additional hardware filtering using a 60 Hz band-stop filter to remove signal noise (see circuit schematic in Appendix B, Figure B.3). The filter implemented followed the HPF and LPF. The band-stop filter worked by using a LPF and a HPF simultaneously with the frequency cutoffs set as the band-stop bandwidth. Following this, the signal was added together to reform the signal.



**Figure 7.5: Full ECG hardware filtration results**

### 7.2.1 Electrodes

Signals quality obtained from different ECG electrodes were assessed and compared. Figure 7.6 shows typical signals obtained from gel-electrodes, commercial dry electrodes and dry prototype electrode leads. Signals obtained from dry prototype and gel-electrodes were comparable. However, signals from the commercial dry electrode belt contained a significant amount of noise.

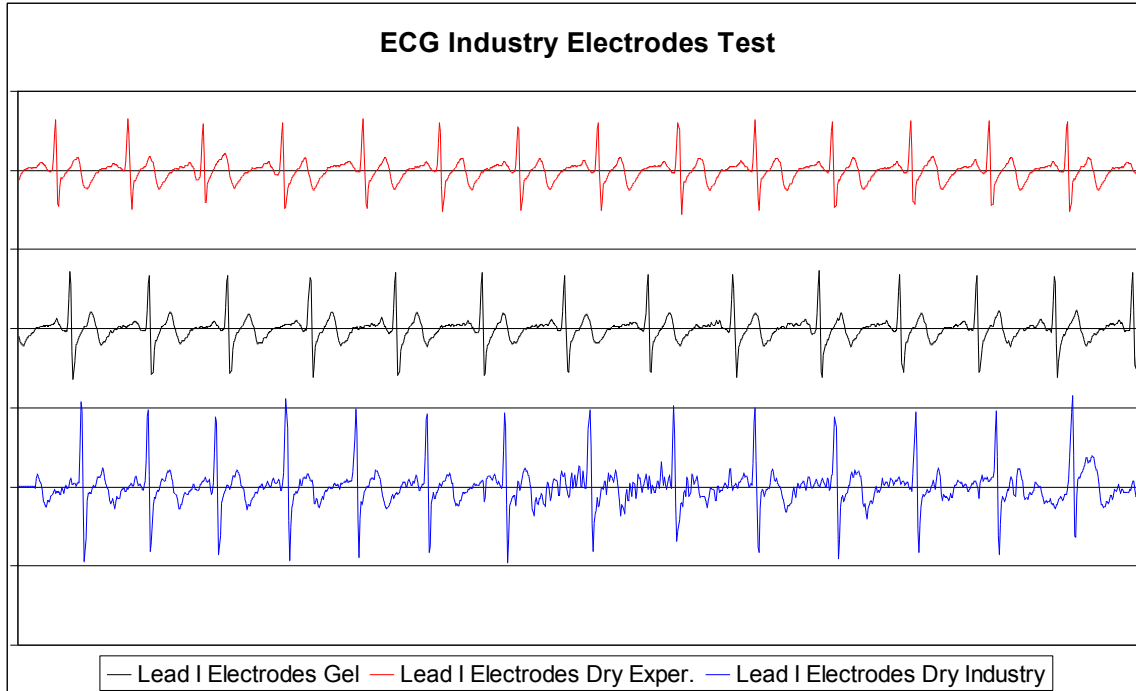


**Figure 7.6: ECG electrode test results of industry, gel, and dry electrodes**

From the results above, the dry electrodes were capable of providing the greatest signal amplitude. Of the gel and dry experimental electrodes, signal amplitudes for the gel-based electrodes were slightly higher. Baseline noise can be seen within each of the three electrode options used. Baseline noise is most significant within the commercially available dry electrodes. Baseline noise of the gel-based and experimental dry electrodes does not show a significant difference.

### ***7.3 Software Evaluation and Testing***

To investigate the effectiveness of our algorithms, we utilized testing protocols similar to that used by Bolanos et al and Johnston et al to compare HRV data obtained from the PPG and ECG signals [25], [27]. Both signals produce peaks due to ventricular depolarization and this forms the basis for comparison of ECG and PPG derived variability indices. The MQP group designed a dual channel monitor to facilitate simultaneous recording of both signals. We needed to demonstrate that our software was reliable in obtaining raw R-R intervals for HRV calculations as well as show that similar HRV data could be derived from ECG and PPG signals.

The designed ECG electrodes and PPG sensor were used to acquire signals simultaneously from three subjects. Signals were acquired from standard Lead II ECG configuration and forehead region, and processed in real time using LabVIEW. The experimental set up can be seen in Figure 7.7. All experiments were replicated twice in each individual.

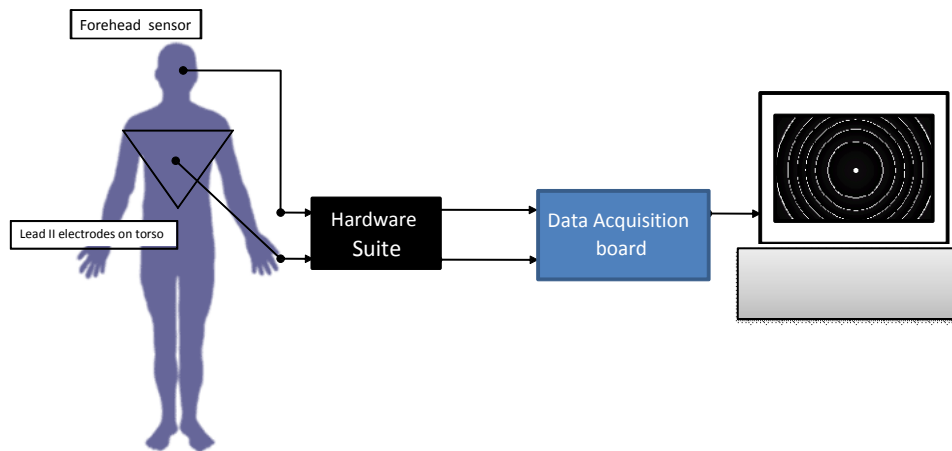


**Figure 7.7: Experimental setup for data recording**

*Test 1: Basal HR/PR*

Signals were recorded for 30seconds- 2 minutes, with subject at rest to obtain baseline HR and PR pulse rates.

*Test 3: Motion artifacts*

Subjects were asked to do a series of seven 15 second exercises, in the following order:

- No motion
- Upper extremity movement
- Lower extremity movement
- Lateral head movement
- Up-down head movement
- Fast Breathing
- Slow Breathing

### *Test 3: Valsalva maneuvers*

After obtaining baseline rates for 60s, subjects were asked to perform a Valsalva maneuvers i.e. forcibly exhaling against a closed mouth and nose.

The standard deviation, standard error of estimate (SEE) and correlation coefficient (R), were used for statistical analysis.

$$SEE = \sqrt{\frac{\sum (Y - Y_{est})^2}{N}} \quad (8)$$

Where Y is the expected value,  $Y_{est}$  is the estimated value, and N is the total number of points used for the analysis.

$$R = \frac{m \sum x_m y_m - \sum x_m \sum y_m}{\sqrt{[m \sum x_m^2 - (\sum x_m)^2] * [m \sum y_m^2 - (\sum y_m)^2]}} \quad (9)$$

Where, x and y represents the values being compared and m is the total number of points used for the analysis.

### **7.3.1 Signal Acquisition**

Figure 7.8 (a) and (b) show portions from typical ECG and PPG signals recorded during rest. On average, the ECG and PPG signal amplitudes were observed to be above the 1V peak-to-peak range, and signal quality was reproducible within all individuals. Both PPG and ECG signals exhibited changing amplitudes during rest due to breathing baseline drift, although this didn't contribute as a nuisance factor. The gradual change allowed for proper adaptive threshold peak detection. However, the MQP group observed the difficulty in sometimes obtaining the PPG signal as the headband had to be adjusted a couple of times for good surface contact. This resulted in tightening of the headband straps, which was uncomfortable for the subject. Sometimes this led to a reduction in signal amplitude, due to the compression of the artery.

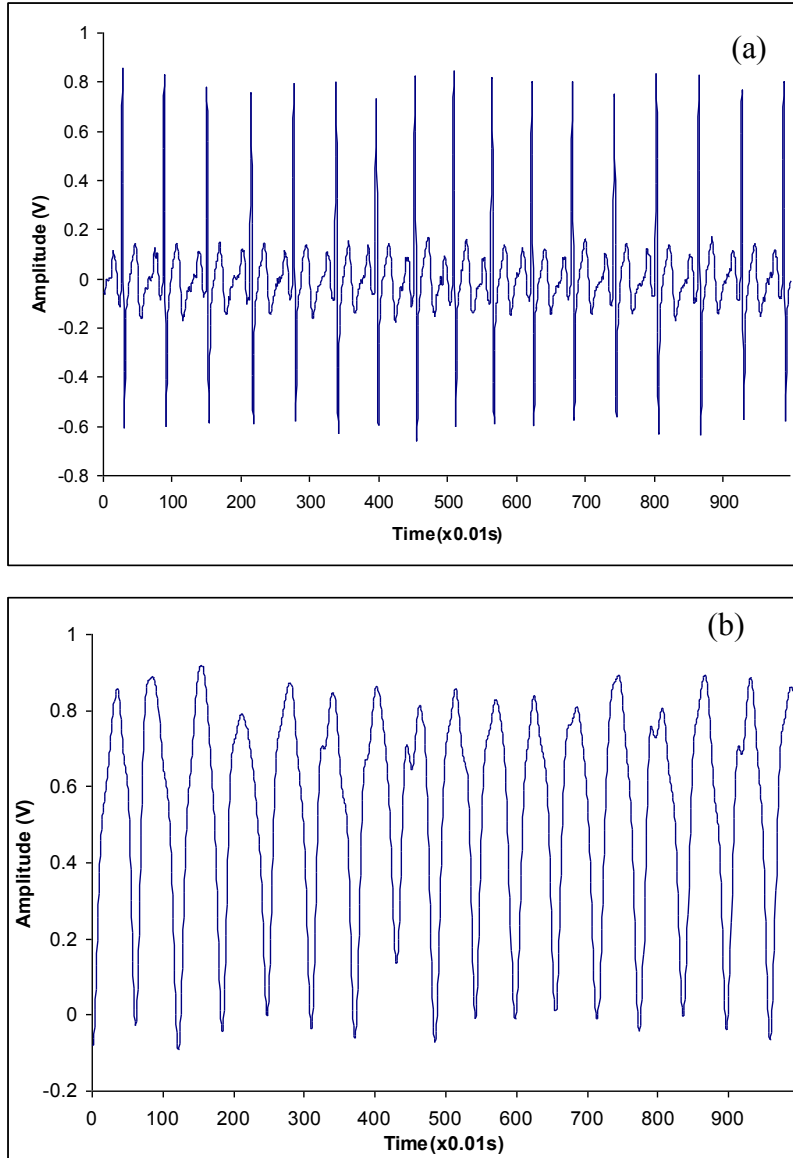


**Figure 7.8: Typical ECG and PPG during rest**

### 7.3.2 Peak Detection

The MQP group developed an adjustable threshold peak detection method to account for interbeat amplitude variations as well as differences in signal amplitudes between individuals. Figure 7.9 (a) and (b) shows the performance of our peak detection algorithms, with interbeat interval time calculated shortly after peak observance.

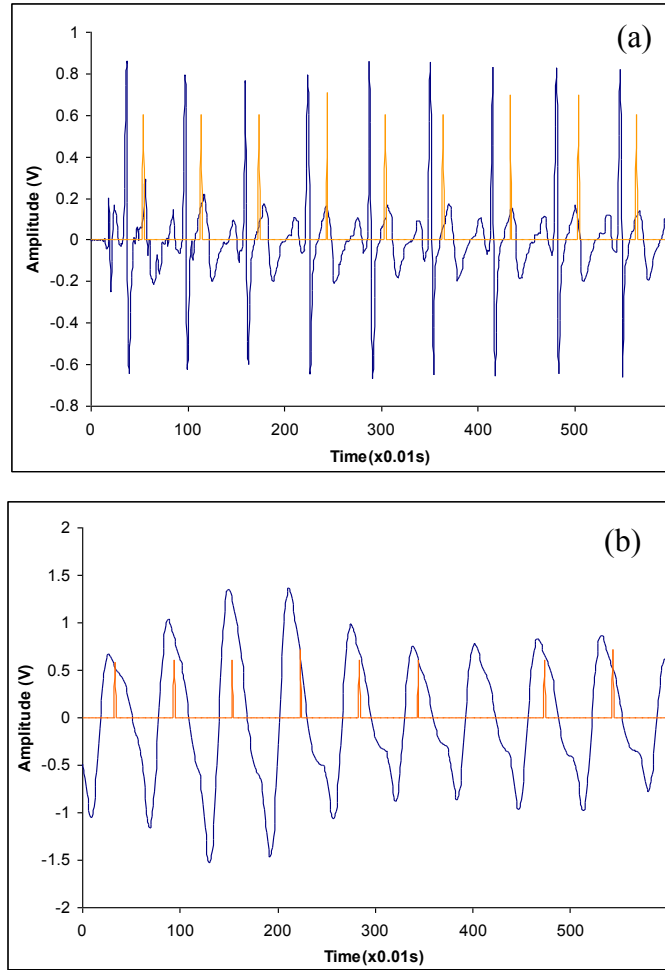


**Figure 7.9: Signal peak detection for ECG (a) and PPG signals (b)**

The MQP group determined the effectiveness of the adjustable threshold by using waveforms of known amplitudes from 0.5 to 2V. Triangular and sine waves from a power supply were used to simulate ECG and PPG signals, respectively. The MQP group set a threshold at a calibration scalar of 0.75 of the maximum amplitude and increased signal amplitude by slow increments of 0.5V, to observe changes in the threshold. The measured signal amplitude and calibrated threshold obtained by the peak detector were recorded. Table 7.1 summarizes sample results, which shows that the peak detection method properly detected maximum signal amplitude and implemented a scalar of 0.75. Similar results were also observed using pulse and ramp waveforms.

**Table 7.1: Measurements for Calibrated Threshold**

Wave amplitude	Measured amplitude by peak detector	Calibrated Threshold	Factor
2	1.99	1.498	0.753
1.5	1.49	1.12	0.751
1	0.98	0.748	0.757
0.5	0.498	0.374	0.785

### 7.3.3 ECG and PPG Data Comparison

ECG and PPG signals were recorded simultaneously for 2 minutes from subjects during rest, and their respective rates compared. Figure 7.10 shows sample results during one recording session using our initially developed algorithm.

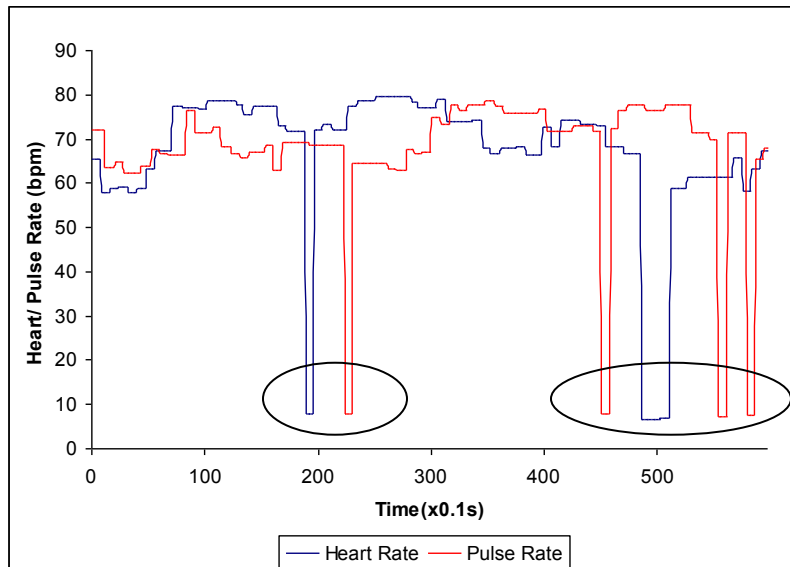


**Figure 7.10: Simultaneously recorded HR and PR**

The MQP project group observed that the PR deviated significantly from HR with a negative bias. The MQP group used statistical analysis to determine that the PR underestimated HR with a standard deviation of  $\pm 13$ bpm. It was determined that the main reason for this difference was the difficulty in determining peaks in the PPG waveform due to its rounded peak shape, as opposed to a sharp peak like that of the R wave in ECG waveform. There is also the presence of a dicrotic notch that can introduce false peaks. The MQP implemented a derivative method to obtain a waveform with a more distinct peak, and better separated the signal amplitude due to the dicrotic notch (see Figure 7.11).

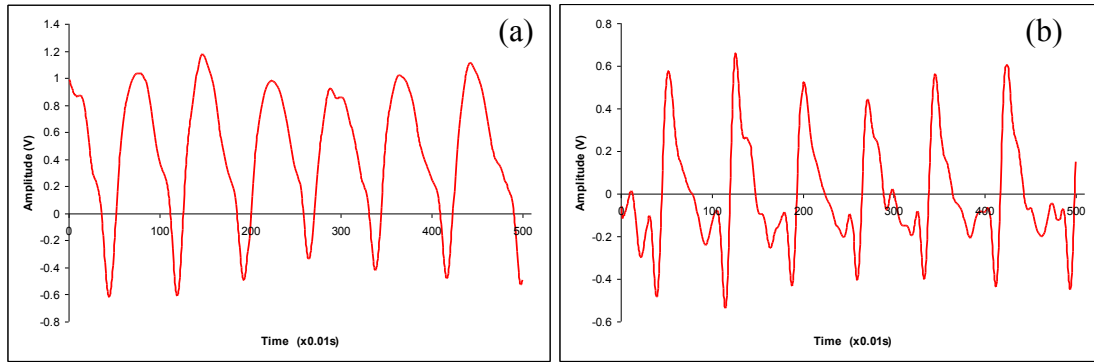


**Figure 7.11: PPG signal (a) and corresponding derivative (b)**

In addition to these deviations, the MQP group observed missed beats (about 2 for every 100 beats), highlighted as sharp drops in respective rates (see Figure 7.10), and this falsely activated the system alarm. The MQP group stipulated that the missed beats occurred due to the inability of the threshold detection window to adjust itself, especially if a peak was located just at its borderline. A default system value of around 8 bpm was thus output, hence the observance of the sharp drops. Due to time limitations, the MQP group could not implement an adjustable threshold detection window, and so developed an algorithm to omit these missed beats. Initially, when this was implemented it resulted in double values because time interval of the beat prior to a missed one was duplicated.

Figure 7.12 shows a plot of measured interbeat interval against time. The two abnormally high beats represent this phenomenon of time interval doubling. The MQP group implemented an algorithm to reject this abnormally high intervals, by comparing interbeat interval values with each other, and rejecting those that time intervals beyond 175% of their respective previous interval. Figure 7.13 shows the occurrence of a missed beat, but with no interval double count.

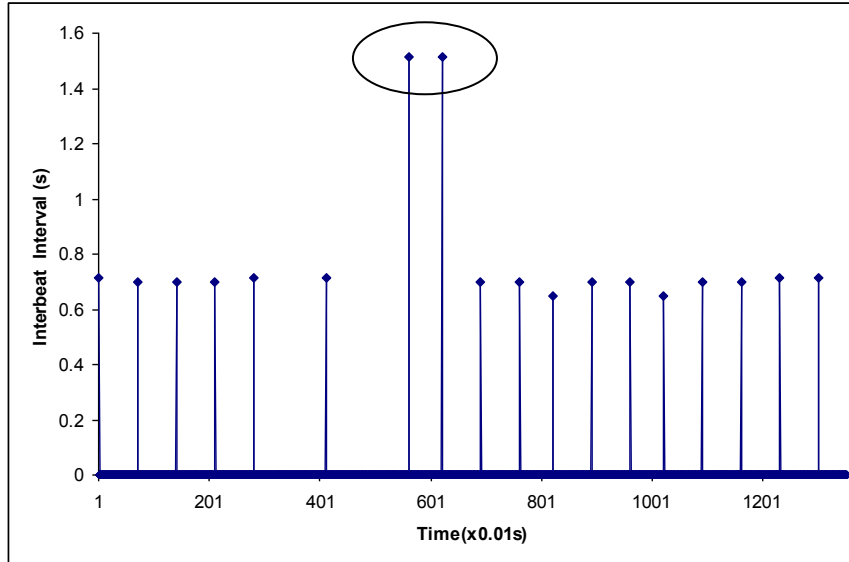


**Figure 7.12: Beat-to-beat interval double count due to missed beat**

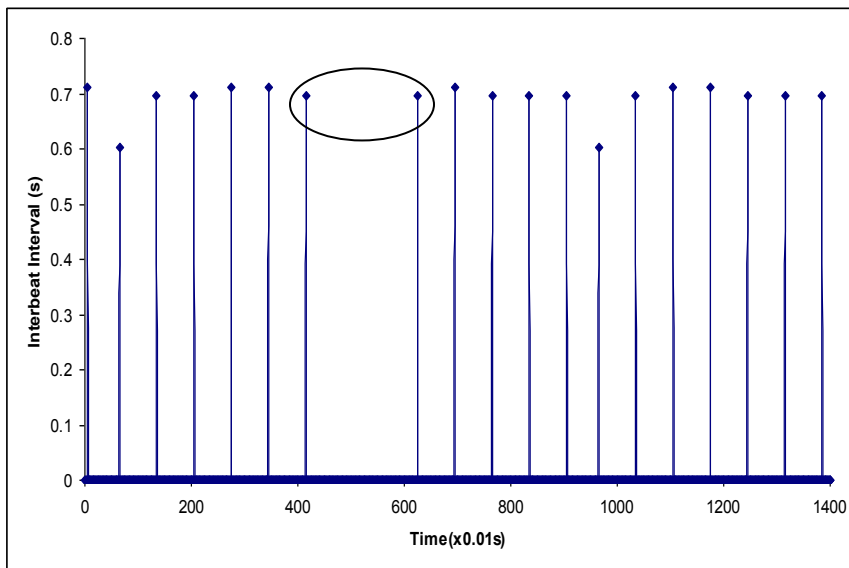


**Figure 7.13: Beat-to-beat double count rejection**

After optimizing our software we obtained a significant improvement in correlation between HR and PR. As observed in Figure 7.14, PR consistently followed HR, and we calculated that PR deviated from HR with a standard deviation of  $\pm 1.5\text{bpm}$ . Using MS Excel, we plotted a scatterplot of IHR and IPR to calculate correlation coefficient, R. Figure 7.15 shows a linear relationship between these two calculated rates with

$R = \sqrt{0.7866} = 0.89$ , a similar value to that obtained by Johnston et al ( $R=0.9$ ) with their algorithms to compare HRV data derived from PPG and ECG signals [27].

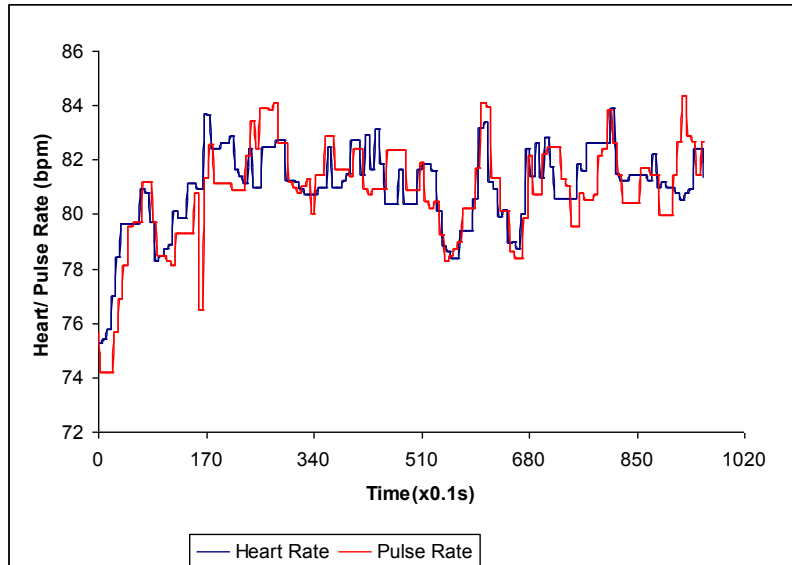


**Figure 7.14: Corrected HR and PR from resting subject**

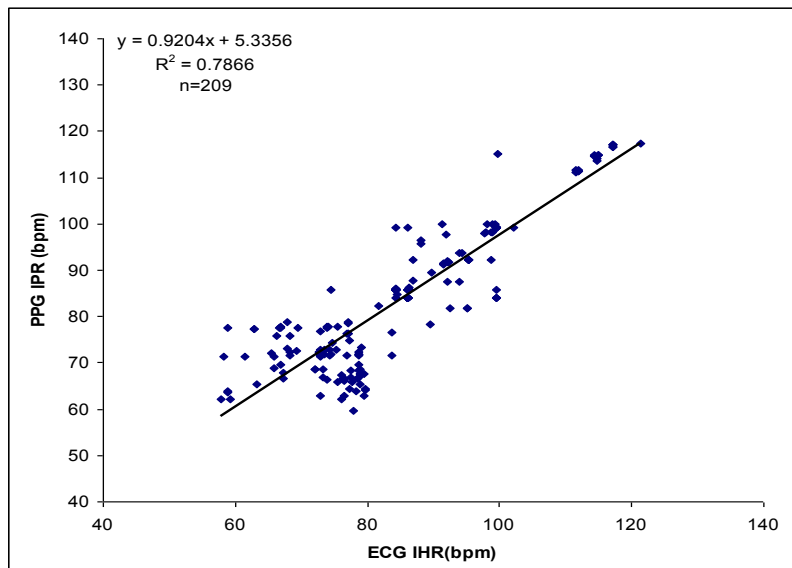


**Figure 7.15: Comparison of between instantaneous HR and PR**

SDNN and rMSSD indices obtained from simultaneous 2 minute recordings of both signals were compared. Comparison of inter-beat variability from data sets showed a close linear correlation between ECG and PPG indices, with a correlation coefficient of 0.88 and 0.94 for SDNN and rMSSD indices respectively.

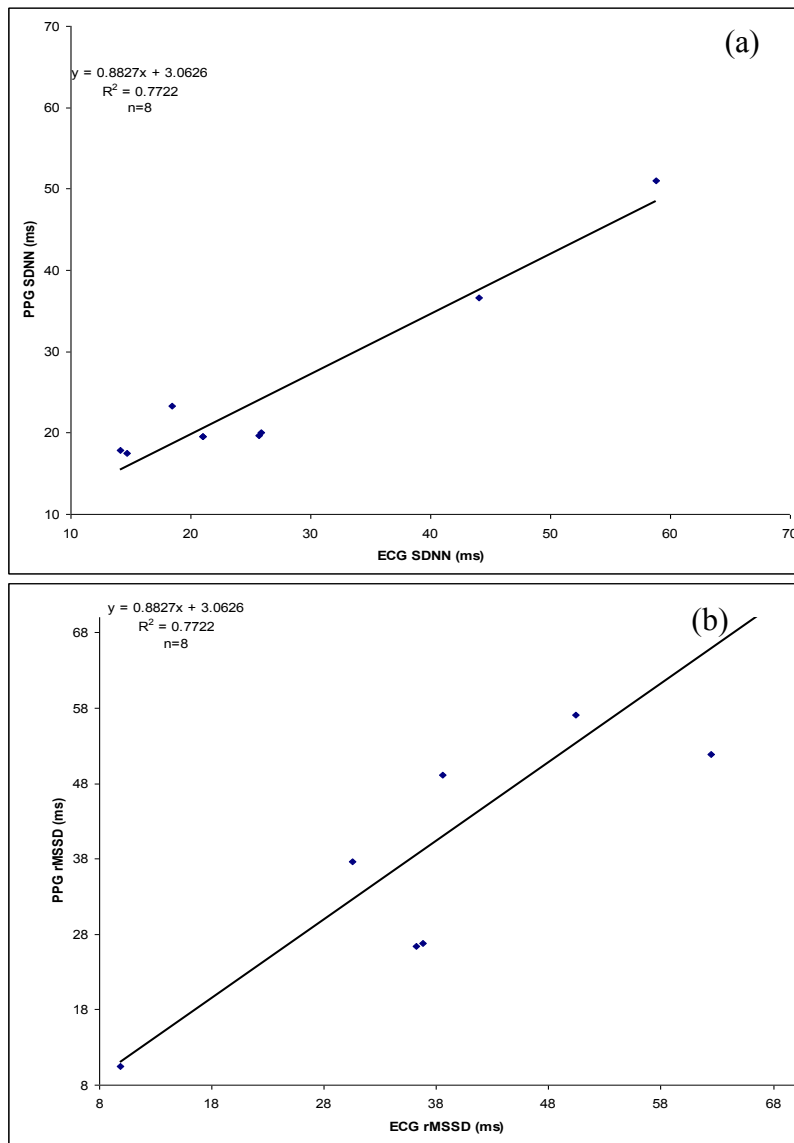


Figure 7.16: Comparison of SDNN (a) and rMSSD (b) variability indices

### 7.3.4 Motion Artifact

The MQP group was able to demonstrate good correlation between HRV measures obtained during rest. However, in order to determine if the developed algorithms could be efficient under motion, subjects were made to undergo a series seven continuous 15 second exercises, of moderate and high intensity. These exercises are summarized in Table 7.2.

**Table 7.2: Time duration for motion activities**

<b>Order</b>	<b>Activity</b>	<b>Time(ms)</b>
1	No motion	1-1500
2	Upper extremity movement	1501-3000
3	Lower extremity movement	3001-4500
4	Lateral head movement	4501-6000
5	Up down head movement	6001-7500
6	Fast breathing	7501-9001
7	Slow breathing	9001-10500

Figure 7.17 shows typical signal HR and PRs recorded from a subject under sequence of moderate (a) and high intensity (b) movement exercises. The MQP group determined the average HR and PR as well as standard deviations during these activities. Figure 7.18 (a-b) and Figure 7.19(a-b) summarizes the degree of variation during the motion exercises. The error bars represent the standard deviation or degree of rate variation during each exercise.

Similar rates and standard deviations were observed during moderate motion exercises. Overall, ECG signals demonstrated better signal stability during motion exercises, even though signals were more or less affected by limb movements. Increased signal noise was observed for the ECG, especially during upper body motion, due to additional noise introduced by the EMG signal. The PPG signals were most susceptible to increased distortion during head movements as well as high intensity exercises, leading to a greater degree of variance. This demonstrates the ever occurring challenge there is in designing wearable PPG sensors. While good signal correlation was observed during rest, better processing algorithms to eliminate motion artifacts need to be implemented to allow for long term patient monitoring of HRV using the PPG signals.

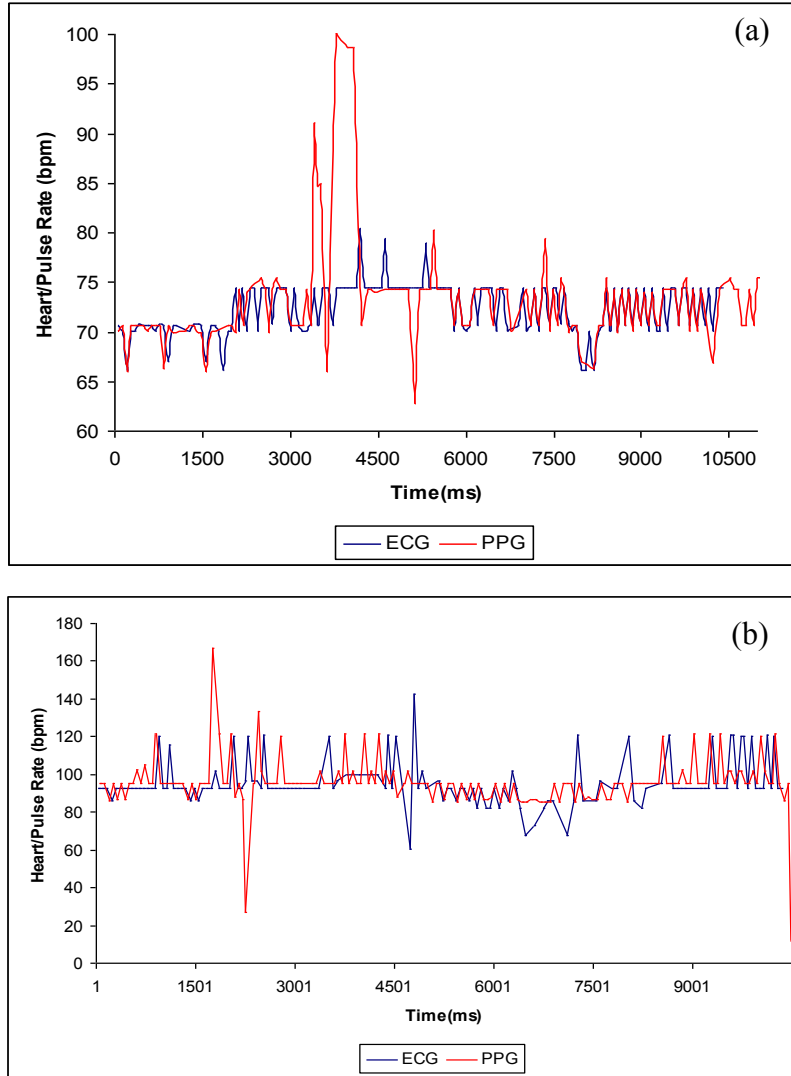


Figure 7.17: Comparison of HR and PR values during low (a) and high (b) activity

Table 7.3: Activity level statistical data

Activity	Low Intensity		High Intensity	
	ECG	PPG	ECG	PPG
Upper Body Motion	84± 4	83± 5	95± 7	94± 8
Upper Body Motion	88± 8	89± 8	101± 18	91± 2
Lower Body Motion	93± 7	92± 3	100± 9	100± 11
Lateral Head Motion	95± 6	93± 7	92± 5	91± 15
Up-Down Head Motion	90± 5	91± 8	89± 4	86± 13
Fast Breathing	85± 8	87± 7	94± 4	96± 12
Slow Breathing	90± 5	89± 7	101± 9	102± 14

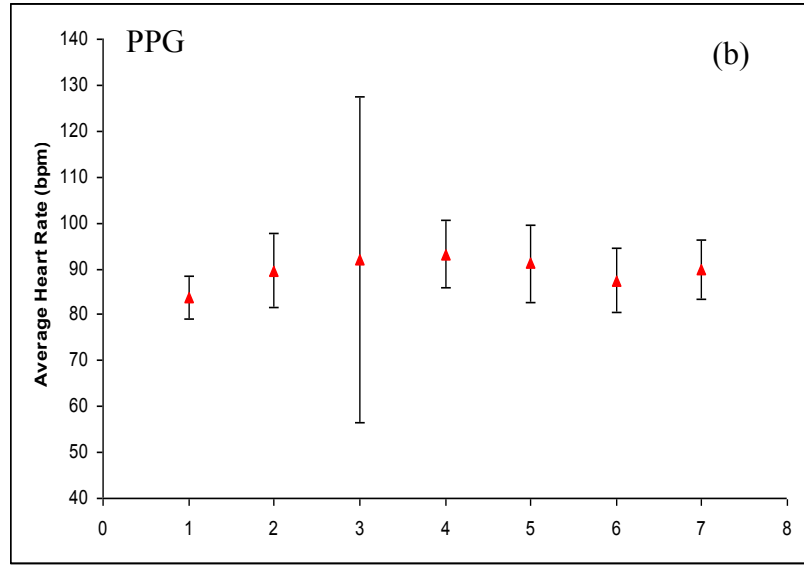
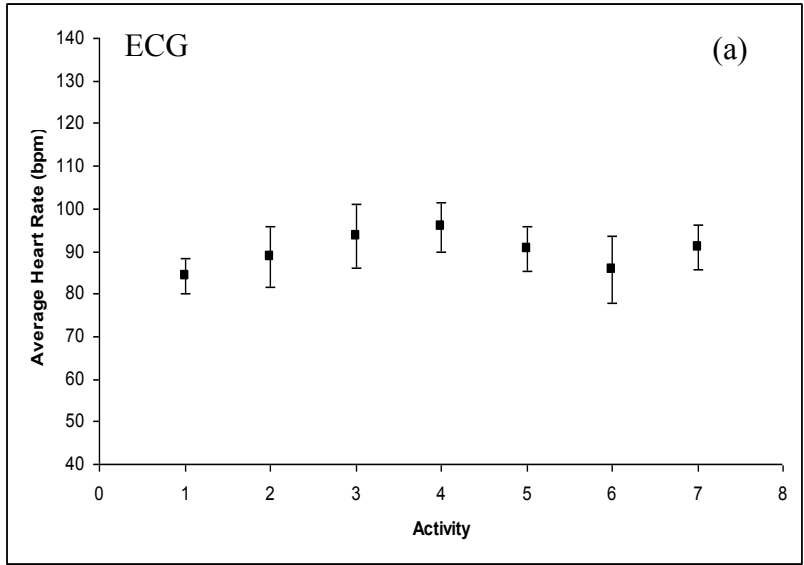


Figure 7.18: Comparison of HR (a) and PR (b) during moderate intensity movement

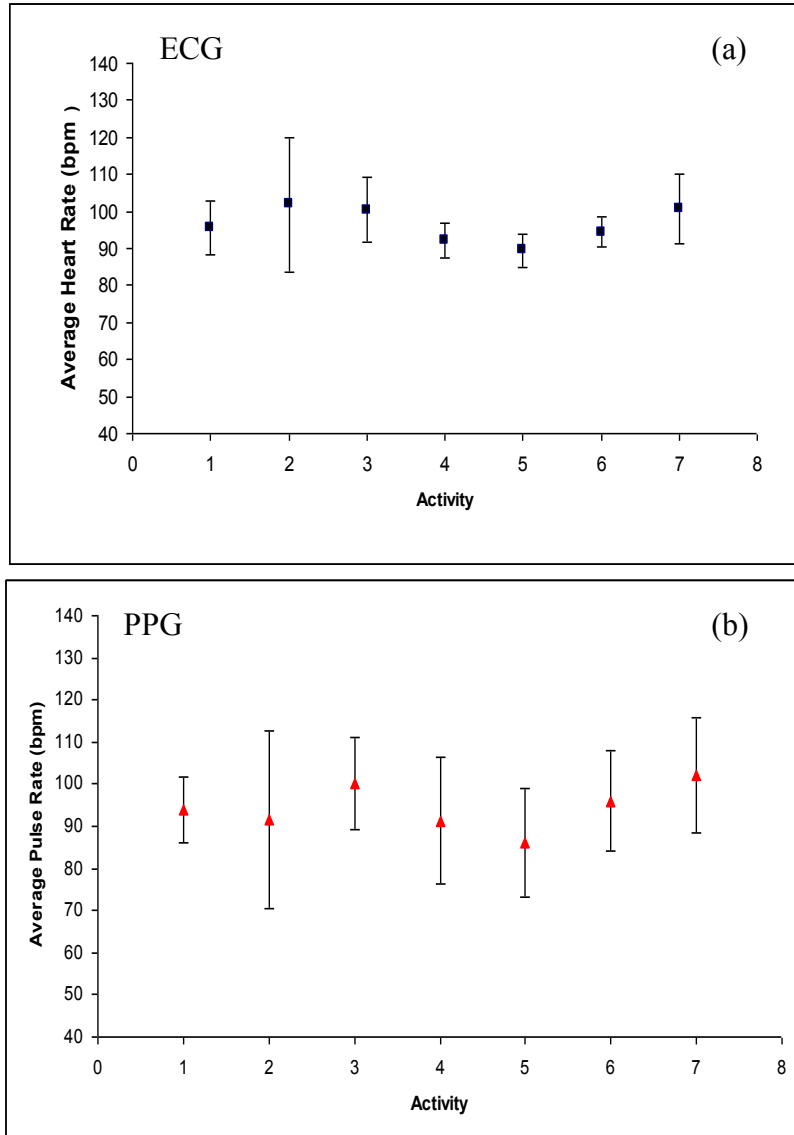


Figure 7.19: Comparison of HR (a) and PR (b) during moderate intensity movement

## 7.3.5 Comparative Software Validation

### 7.3.5.1 ECG

The ECG signal algorithms were validated against a simulated ECG signal of known frequency values at rates of 30, 60 and 120 beats per minute. This signal contained all of the major signal components for an ECG signal, including the P wave, QRS complex, and T wave. The expected time intervals were compared to averages interbeat time intervals obtained from the system. Each of the three signals was applied to the system over a period of time. Time periods from the start and end of the signal acquisition were

omitted to ensure that the simulated signal entering the system was at equilibrium, attenuating possible errors within the simulated signal itself.

**Table 7.4: ECG Validation Results**

Beats per Minute	Number of Peaks	Averaged Time Between Peaks	Expected Time Between Peaks	Percent Error
30	9	2.0036	2.00	-0.18 %
60	9	1.0044	1.00	-0.44 %
120	19	0.5073	0.50	-1.46 %

The results shown in Table 7.4 give the error percentages for each of the three HRs, with a percent error of less than 2 %. On average the system is accurate within  $\pm 0.1$  beats per minute for rates up to 120, and  $\pm 3.0$  beats per minute for rates greater than 120.

### 7.3.5.2 PPG

The MQP group used Masimo SET monitor as a one standard to verify the reliability of our software algorithm for the PPG signal. The MQP group obtained PR simultaneously from our prototype and the commercial monitor. Figure 7.20 (a) shows a typical 2 minute recordings. Initially, we determined that PR values obtained from the prototype deviated significantly from that of the gold standard with a standard error of estimate (SEE)  $\pm 5$ bpm.

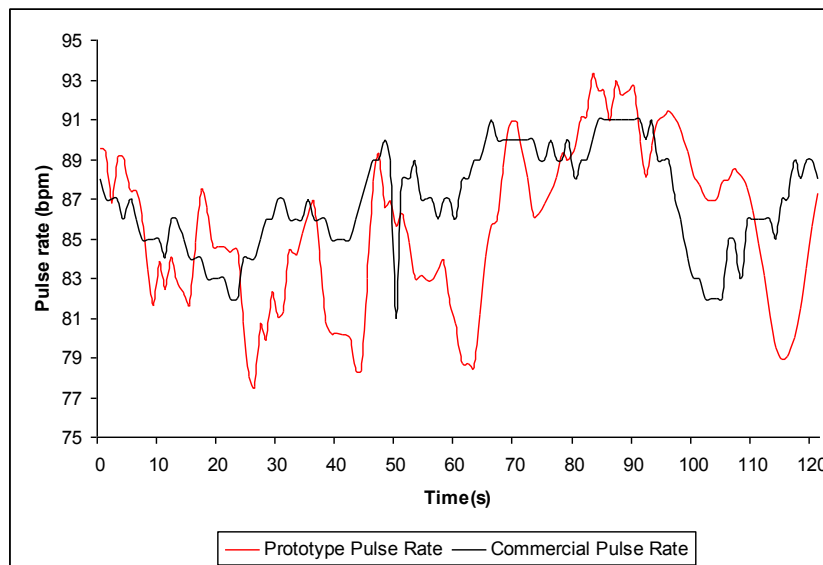


**Figure 7.20: PR comparison between prototype and commercial PPG devices**

The MQP group was unable to obtain the algorithms used to compute that PR in the commercial sensor due to trade secrets. Most monitoring device use different algorithms to compute PR and this might be a possible reason for the observed difference. However, because we observed an improvement in device accuracy after optimizing our software, this demonstrated that we solved some of the problems created by the difficulty of processing the PPG signal by using the derivative method of peak detection.

### 7.3.6 Manual Software Validation

The MQP group was able to validate device software against an ECG simulator and a commercial PPG device. However, for proper validation, it was determined that comparison between manual calculations and our software calculations of PR and HR, would better demonstrate the effectiveness of our algorithms. This was due to the uncertainty in guaranteeing the exact signal frequency in the ECG simulator, as well as unknown algorithms for the Masimo SET monitor. ECG signals were recorded for about 30s during rest. R-R intervals obtained from our software as well as those that were manually calculated were compared. This analysis revealed that those obtained from our software didn't exhibit a normal physiological pattern (see Figure 7.21).

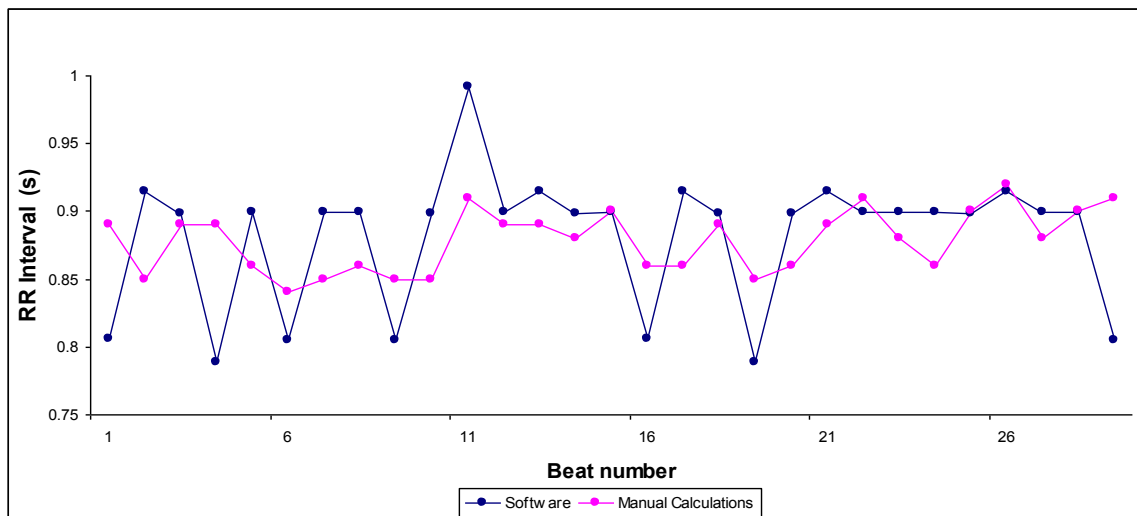


**Figure 7.21: R-R Interval comparison between manual and software calculations revealing inaccuracies in software algorithm**

During rest, the ECG of healthy individuals exhibits rhythmic variation in R-R intervals, a phenomenon known as respiratory sinus arrhythmia (RSA). RSA fluctuates at the phase of respiration; cardio-acceleration during inspiration, and cardio-deceleration during expiration [4]. This is observed in the manual R-R interval plot above, where the R-R intervals gradually rise and fall and R-R intervals do not typically differ over 20% from adjacent values during rest. However, the pattern observed from R-R intervals determined by our software did not exhibit this RSA, with a more or less jerky R-R interval pattern.

The MQP group determined that this was due to resolution errors in the timer method we implemented to calculate R-R time interval. This time interval detection method was later replaced with a method that used the number of data points between peaks to calculate R-R interval. A significant improvement was obtained with this new algorithm as almost exact correlation was observed between R-R intervals that were manually calculated as well as that obtained from our software (see Figure 7.22 ). An SEE of 0.13bpm or  $\approx$  0bpm of inter-beat interval was obtained using this method.

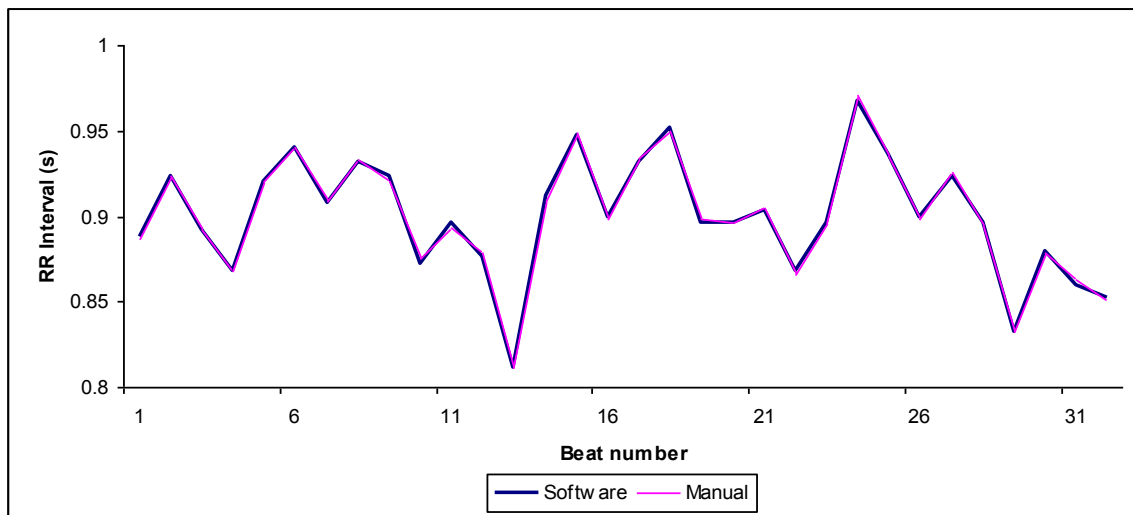


**Figure 7.22: R-R Interval comparison between manual and updated software calculations for ECG**

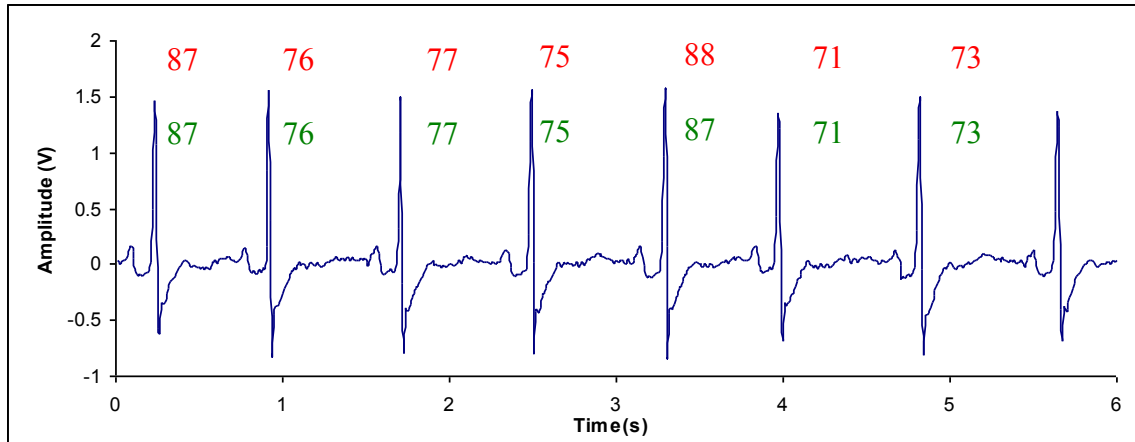
Results from SDNN and rMSSD indices obtained from ECG signals recorded for about 30s from three individuals are summarized in Table 7.5. These results demonstrate a

good correlation between SDNN and rMSSD indices of our software with respect to manual calculations. The average percentage errors obtained from these recordings were  $0.45 \pm 0.27\%$  for SDNN and  $0.77 \pm 0.80\%$  for rMSSD (ms units).

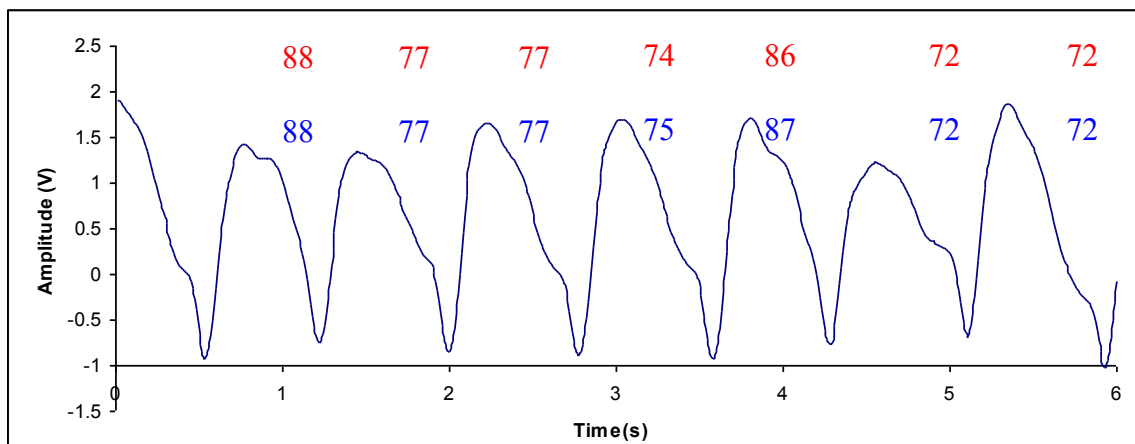
**Table 7.5: HRV Measures from 3 subjects**

Suresh			
	Software	Manual	% error
<b>Average HR (bpm)</b>	67	67	
<b>SDNN (bpm)</b>	2.6	2.6	0
<b>rMSSD (bpm)</b>	3.1	3.1	0
<b>SDNN (ms)</b>	34.8	34.7	0.28
<b>rMMSD (ms)</b>	40.8	40.7	0.24
Thomas			
	Software	Manual	% error
<b>Average HR (bpm)</b>	94	94	
<b>SDNN (bpm)</b>	3.9	3.9	0
<b>rMSSD (bpm)</b>	2.5	2.6	3.84
<b>SDNN (ms)</b>	26.1	26.3	0.76
<b>rMMSD (ms)</b>	17.4	17.7	1.69
Boyla			
	Software	Manual	% error
<b>Average HR (bpm)</b>	77	77	
<b>SDNN (bpm)</b>	6.2	6.2	0
<b>rMSSD (bpm)</b>	7	7	0
<b>SDNN (ms)</b>	65.2	65	0.31
<b>rMSSD (ms)</b>	78	77.7	0.38

Using the new algorithms, IHR and IPR from simultaneously recorded signals were re-evaluated and compared. Figure 7.23 shows IHR/IPR from software and manual calculations, against their respective beats, with an even better correlation between ECG and PPG derived instantaneous rates. Using MS Excel, we plotted a scatterplot of IHR and IPR with the new algorithm and obtained an  $R$  of  $= \sqrt{0.9841} = 0.99$ , an 11.2% increase from the previously calculated coefficients of 0.89. Based on this improvement, we inferred a likely improvement in SDNN and rMSSD correlation between ECG and PPG signals.



Red: Manual calculation of IHR (bpm)  
 Green: Software calculation of IHR (bpm)



Red: Manual calculation of IPR (bpm)  
 Blue: Software calculation of IPR (bpm)

Figure 7.23: Manual and Software IHR (top) and IPR (bottom) Correlation

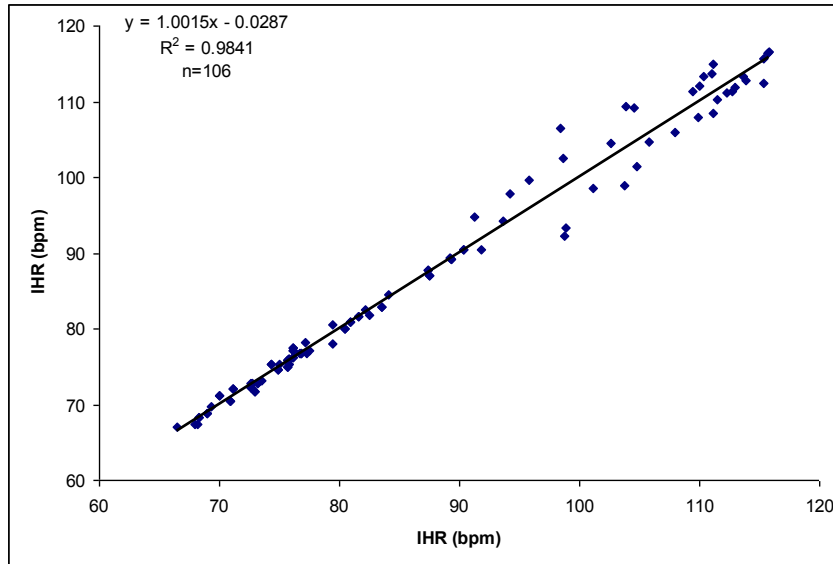


**Figure 7.24 Comparison of between IHR and IPR with updated software**

### 7.3.7 Valsalva Maneuvers

To better test the capacity of our device to measure dynamic HRV, as opposed to steady state conditions such as during rest, subjects were asked to perform a Valsalva maneuver. The Valsalva maneuver is a common test of sympathetic nervous system function which involves forcibly exhaling against a closed mouth and nose. This causes a temporary decrease in blood output from the heart, and people with fully functioning sympathetic system compensate for this decrease by increasing HR [55]. This exercise produces a characteristic feature with an up rise-and-decline in HR or a decrease-and-increase in R-R intervals, upon release. After obtaining a baseline HR for 1 minute, subjects were asked to perform a Valsalva maneuver and release at their convenience. Figure 7.25 (a) and (b) shows comparison between manual and software calculations of IHR and R-R intervals during one Valsalva maneuver. From the figures, our software was able to pick up the changes in HR during the Valsalva exercise, demonstrating its effectiveness in being able to detect other forms of physiological HRV.

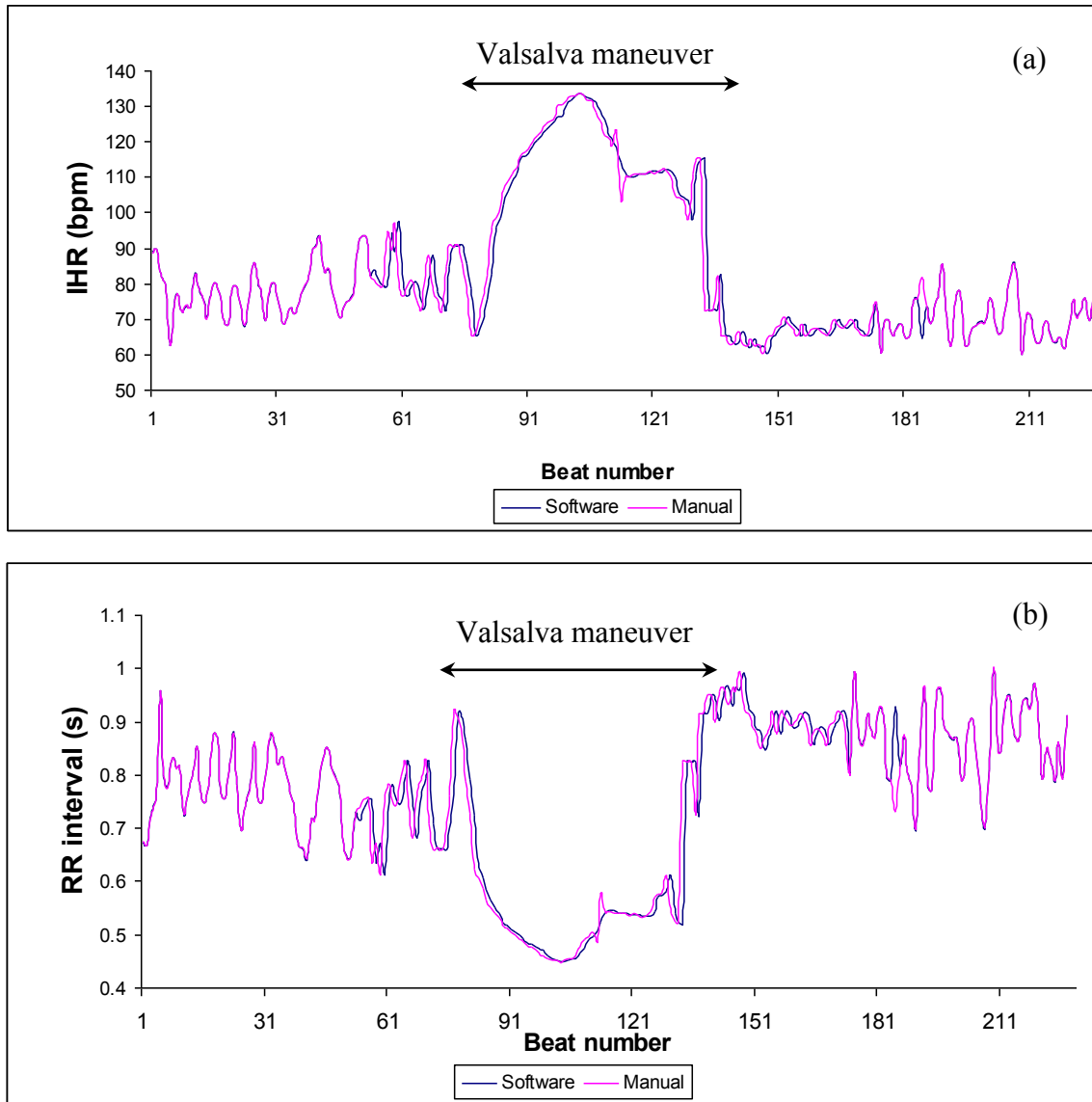


Figure 7.25: IHR (a) and R-R Intervals (b) changes during a Valsalva maneuver

#### 7.4 FDA Regulations

Prior to marketing any medical device, manufacturers have to fulfill specific standards and regulations of the US Food and Drug Administration (FDA), under the Federal Food Drug & Cosmetic (FD&C) Act, Title 21 Code of Federal Regulations (CFR). This includes protocol for proper testing of the device prior to FDA approval as well as labeling, marketing, and post-market monitoring procedures. Other regulatory requirements also follow depending on the device class, which evaluates the risk of using the device. Devices are classified Class I for (low risk, general controls), Class II (special

controls) and Class III (high risk, premarket approval) depending on the risk of the device user.

Based on an FDA database search of HRV monitors, our device would be likely be classified as a Class II device. For FDA approval, this would require a submission of a 510(k), with clinical data to demonstrate that our device is comparable to others already available in the market, in terms of safety and effectiveness. Our various tests were performed on a small group of individuals, with presumably normal heart conditions. Hence, further device testing needs to be carried out on a more significant population, especially that representative of those who are going to using the device i.e. cardiac patients. Also, although our device hardware is battery operated and contained within an insulated container, we could not demonstrate if the device was waterproof to assess the risk of electric shock as this would involve destructive testing. The device was labeled not to be used around any fluids.

## **8. Analysis and Discussion**

### **8.1 PPG**

One of the challenges in designing wearable biomedical sensors is guaranteeing signal integrity during acquisition. Placement location of sensors plays an important role as it can affect signal quality. For the PPG, while signals obtained from forehead and finger sensors are obtained via different detection modes, the considerable increase in signal amplitude with the forehead sensor demonstrates its superior characteristics (see Figure 7.1). Signals obtained via reflectance mode from the forehead are generally strong due to the combination of thin skin tissue layer as well as high bone density that facilitate light reflection. The high signal amplitude allowed for significant reduction in LED drive current to improve on device battery life. In addition, it is also important to design a proper sensor package to guarantee good surface contact, especially for long term recordings. While signals obtained from adhesive and headband sensor probes were similar, the adhesive probe was more susceptible to dislocation as a result of wear of the glue adhesive. A headband forehead sensor is thus preferred due to its greater stability.

Optimizing power consumption is also important due to the major power requirement of the PPG device LED, as it is directly related to the amount of LED drive current. Although drive current can be reduced, this has a diminishing effect on signal amplitude, due to the effective reduction of light intensity detected by the photodiode (see Figure 7.2). Low signal amplitudes can adversely affect accuracy during signal processing. Thus there has to be a balance between reducing current and obtaining a signal of adequate amplitude for signal analysis. From Figure 7.2, the positive linear relationship confirms that current values indeed have an effect on signal amplitude. Current values below 5mA resulted in signals with high SNR. The MQP group determined that a current of about 8mA achieved the right compromise between minimizing current and attaining adequate signal quality. It is also important to note that this value is specific for our selected LED and photodiode characteristics, and might change when different supplier LED's are used. Savage et al were able to observe adequate PPG signals with as low current as 1.9mA in multi photodiode forehead reflectance sensor [23]. The MQP group

hypothesizes that if the photodetection area of the photodiode is increased, this current requirement can further be reduced.

Alternatively, LED drive current can be reduced by reducing the duty cycle of the LED drive current i.e. the time between which the LED is turned on and off during signal acquisition. Nyquist sampling theorem dictates that a sampled signal can be reconstructed to its original waveform as long as the sampling frequency is at least twice the maximum frequency content of the signal. For the PPG waveform, a sampling rate of at least 20 Hz can satisfy this requirement. Switching the LED on and off thus “samples” the PPG signal at a rate equal to the duty cycle of the current. The signal is “reconstructed” with the sample hold circuit. A pulsatile current reduces the effective current of the LED, with a root mean square value of  $0.01 * \delta * \text{current}$ , where  $\delta$  is the current duty cycle. Battery life of the device is thus inversely proportional to the LED drive current. Estimated battery life calculated from a typical battery of 500mAh for various current modes is compared in Table 8.1.

**Table 8.1: Comparison of estimated battery life for different LED currents**

Current	Duty Cycle	Battery Life Estimate
40mA	DC	12.5 hours
8mA	DC	62.5 hours
8mA	20%	312.5 hours

However, this does not take into account the power requirement of the other device components. Nonetheless, since the PPG circuit consumes a significant amount of power in the device, it can be assumed that battery life estimated from its power requirement can give a fair estimate as to the expected battery life. The battery life estimate improved by a factor of 25, using a lower current and reduced duty cycle current source.

## **8.2 ECG**

Tests for the ECG section of this project involved determining the functionality of the circuits, and their abilities to acquire a clean signal from the given sources. Original tests

with the ECG section focused on acquiring the signal through the hardware based sensors. As discussed in Section 5.2.3, the two possible design alternatives were to completely filter the ECG signal through hardware, or for limited hardware filtering only as necessary with software filtering. Tests were accomplished using both circuit design types. The original results obtained were through using the limited hardware filtering. This design was to limit the number of hardware components to the minimum necessary to acquire the signal. As this portion is necessary for all other designs of the circuit, it is the basis for both the expanded and limited versions of the hardware. The limited circuit design can be seen in Figure B.1 as Revision A. This circuit design consisted simply of an instrumentation amplifier to acquire the signal and a single high-pass filter to remove baseline drift from the signal. Results obtained using this design can be seen in Figure 7.4. With this design, it is important to note that there is significant high frequency noise within the system. Without further filtering this may prevent the location and analysis of the smaller features of the ECG signal. From the signal, the P and T waves can both be identified due to the displacement of the baseline noise. This however is not an effective method for analysis, since specific features of the waves are not readily visible. An additional problem may arise should the baseline noise and QRS peaks not be sufficiently different. Should this become true, it may not be possible to locate the peaks of the signal in order to perform signal analysis for determination of the HR and variability indices.

To account for the problems seen with Revision A, shown in Appendix B, a second ECG hardware design was developed to improve the acquired signal. This design was to include signal acquisition and complete filtering utilizing analog hardware filters. Initial tests for this were conducted using the second circuit design revision, shown in Figure 8.1. This circuit design implemented both a HPF and LPF. Use of this design was to attenuate any problems associated with baseline drift with the HPF and eliminate high frequency noise through the LPF. Results however did not show a significant difference from the previous tests conducted with Revision A (Refer to Figure 7.4 for example results).

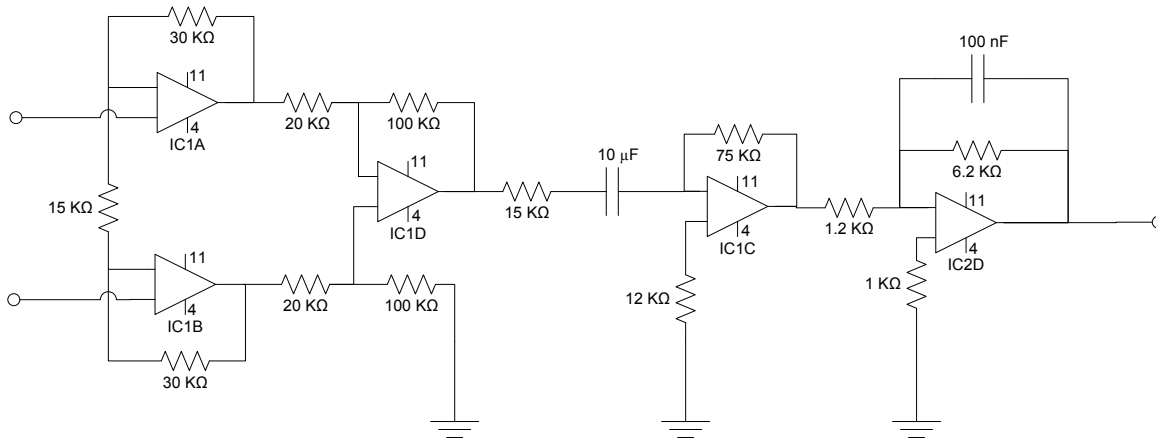


**Figure 8.1: ECG circuit Revision B**

The final circuit revision was to attenuate noise due to 60 Hz corruption. This was accomplished by utilizing a HPF to eliminate possible baseline drift of the signal, a low-pass filter to remove high frequency noise, and a band-stop filter to eliminate 60 Hz noise from within the signal. The band-stop filter had a stop frequency of 60 Hz and a bandwidth of 20 Hz. The schematic for this design alternative can be seen in Figure B.3. The results of implementing this design can be seen in Figure 7.5. Using this design, the problems within the signal associated with the 60 Hz noise were significantly reduced. As can be seen within the figure, there continues to be a minor form of baseline noise. However, this noise is significantly reduced from the prior tests, as the noise component of the signal is of lower amplitude than the P and T waves. This in itself allowed for a greater ability for signal analysis both from the software to determine rates and with graphical analysis of the raw waveform by a clinician.

Of the design alternatives, analyzed in Section 5.2.3, the final design choice was to use the minimum number of hardware filters. The rationale for this is that by reducing hardware components, there is a reduced possibility of component failure and lower device costs. Additional filtering necessary to analyze the signal can be accomplished through digital software filters. The final design choice was to use the Revision A circuit design, output results shown previously in Figure 7.4. Using this implementation, the signal was primarily processed through software filtering algorithms. By utilizing this

method, the overall design of the hardware was simplified by removing unnecessary components, thus reducing the possibility for component failure. As an example, final results of filtering can be seen in Appendix F, where the overall benefits of the final filter design are shown. This overall design, utilizing only minimal filtering within the hardware, provided for the majority of the filtering to be done by the software component of the project. Filtering within the software allowed for a more precise signal filtering, thus allowing for additional signal artifacts to be removed from the signal. As can be seen Figure 7.6, the baseline noise of the signal has been further reduced. This implementation of the design was better equipped to adhere to the design objects, set forth in Section 4.3. Minimal hardware components complimented the reliability objects by reducing the possibilities for device failure, thus increasing durability, and reducing the overall device costs.

For this project, dry electrodes were developed and tested. The purpose of this was to create electrodes for general use that would not be affected by problems such as skin irritation and electrode gel drying [11]. The different design alternatives for the electrodes that were tested are further described in Section 5.2.1. Following the analysis and selection of the design alternatives, the experimental electrode was tested in comparison with standard industry electrodes. Three tests were run to compare the results obtained using a Lead I setup; (i) using the experimental dry electrodes, (ii) using standard gel-based electrodes, and (iii) commercially available dry electrode suite. These two final tests were run to determine the effectiveness of the experimental electrodes with regards to current industry products. The test results, seen in Figure 7.6, showed the gel-based electrodes and the experimental dry electrodes to be comparable in signal content. Within each signal the P wave, QRS complex, and T waves are clearly visible. Major differences between the gel and experimental dry electrodes are that the experimental dry electrodes have a slightly lower peak value in comparison. This is due to the higher skin resistance between the skin and electrode metal contacts, normally attenuated through the electrode gel. Comparison between the experimental dry electrodes and a commercially available electrode suite, shown in Figure 8.2, revealed significant differences between the two signals amplitudes. The commercial electrode suite, being placed closer to the

heart, provided a signal of greater intensity. However, also within the signal there is a greater degree of baseline noise when using the commercial electrode suite. This may be due to problems associated with physical movement of the electrodes, which can cause baseline drift and additional noise within the signal due to capacitive coupling [11]. A specific example of this can be seen at approximately the midpoint of the commercially available signal test. At this point there is a significant increase in the amount of baseline noise due to movement of the electrode suite, due to movement of the patient. This problem is eliminated with the use of the experimental dry electrodes as each electrode is isolated on the body, with the perimeter of the contact surrounded by vinyl adhesive to secure the electrode in place. The experimental signal shown within the test results is the most robust of the tested electrodes for abilities to maintain a stable baseline value, and reduce the amount of baseline noise within the signal.



**Figure 8.2: Industry dry electrode suite**

Of the electrode tests, the experimental electrodes chosen in Section 5.2.1 provided an inexpensive option for attaining the project objectives. The experimental electrodes selected do not contain any electrode gel used for conduction. For this reason, there is no possibility for the electrode properties to alter over time. Furthermore, there is no gel for there to cause skin irritation with the user. Lastly, the user friendly object for the electrodes was met by simplifying the placement of the electrodes. Using easy to locate areas on the body, users of the device require no specialized training to locate the appropriate electrode locations, instructions for which are given in Appendix E.

### ***8.3 Software***

HRV data has been used to assess cardiovascular irregularities in patients with SCD. This data is traditionally obtained from ECG signal analysis. However, problems associated with ECG gel-based electrodes limit the utility of the signal for long term monitoring. Alternatively, since changes in blood volume during the heart cycle are reflected in as pulsations in arterial blood flow, PPG signals can be used to derive the same physiological data for HRV analysis. PPG systems offer the various advantages, as discussed in Section 2.4, of more compact sensor packages, fewer sensor wires, no electric interference, as well as more user comfort. A correlation coefficient close to 1 is thus desired between calculated values obtained from both signals, to demonstrate their close relationship.

The MQP group implemented software algorithms to determine and calculate IHR/IPR through signal peak detection. The threshold peak detection was made adaptable to account of physiological differences in signal amplitudes, as well as variations between individuals. The close agreement between manually calculated values and those obtained from our software revealed that our algorithms were robust and accurate in determining beat-to-beat interval with a lesser degree of error after software optimization. Statistical analysis of data from three individuals during rest revealed a SEE of 0.13bpm for IHR and an average percent error of  $0.45 \pm 0.27\%$  for SDNN and  $0.77 \pm 0.80\%$  for rMSSD indices (ms units). The ability of our software algorithms to track dynamic HRV was best demonstrated during the Valsalva's maneuvers, where the characteristics time series plots for R-R or IHR were observed during the exercise.

Correlation coefficient of 0.99 was calculated between IHR and IPR from simultaneously recorded ECG and PPG signals during rest. By inference, a more improved correlation of their SDNN and rMSSD indices, from the previously calculated values of 0.88 and 0.94. This indicates the strong relationship between these two signals, thus PPG signals can be used as an alternative to the ECG signal. Johnston et al identified the difference in the geometry of PPG signals as a potential reason for not being able to perfectly achieve a correlation coefficient of 1 [22]. Unlike the ECG signal, which has a distinct QRS

complex, the lack of a distinguishable peak makes it difficult to process PPG signals. By using a differential peak detection method, signal correlation was greatly improved. However, missed beats was observed due to the lack of routinely adjusting peak detection window during signal processing. A better alternative will be to create a variable self adjustable window that updates itself based on signal peak-to-peak time interval duration.

Motion artifacts are a considerable limitation in signal processing. The application of this device necessitates the stability of signals as well as accuracy of calculated measures during continuous patient monitoring. In ECG, muscle activity poses a great problem due to the overlapping bandwidths of ECG and EMG signals. In PPG, sensor movement and severity of motion artifacts, (usually dependent on sensor location) poses a significant problem in system accuracy. There was good signal correlation during moderate motion activity, although the ECG waveform demonstrated greater stability during movement exercises. As expected, increased signal noise was observed in the ECG especially during limb activities. The noise intensity was more severe during upper limb movements, significantly masking the P and T waves of the signal. This is due to the relatively close positions of active muscles of the upper limbs to the ECG electrode system leads. However, it was still possible to obtain good HR values due to the stability of the high amplitude QRS complex. Poor signal correlation was obtained from the PPG waveform, especially during head movements, causing a greater variance in PR.

## **9. Conclusion**

The dual channel HRV monitor developed has the potential to impact the global society by providing a new tool for physicians and scientists. Given the large number of people affected by SCD, the data provided can aid their inquiries on noninvasive methods of risk stratifying patients susceptible to SCD.

The dual channel HRV monitor is capable of acquiring and processing ECG and PPG signals to obtain HR, PR, and their respective variability indices. Manual calculations confirmed the robustness and accuracy of our algorithms, with lesser degree of error in computing interbeat intervals, SDNN and rMSSD indices. Correlation coefficient obtained from the analysis of the system outputs for the IHR and IPR of 0.99, revealed that similar data measures could be obtained from both signals. The ability of the device to track dynamic changes in HRV was also demonstrated via Valsalva maneuver, where the characteristic time series plot of IHR and R-R intervals, during this exercise was observed.

By reducing power requirements of the PPG through reducing current amplitude and duty cycle, device battery life was optimized by an estimated factor of 25. Dry electrodes were shown to function as effectively as gel-based electrodes in providing adequate signal amplitude while reducing the effects of skin irritation. The software was shown to perform adequately under moderate motion artifacts situations and produced results showing good correlations between the HR and PR, as well as their respective variability indices. However, further developments for the software analysis and sensor suites should focus on allowing the system to perform reliably under situations of greater motion artifacts.

## **10. Recommendations**

### ***10.1 PPG***

#### **10.1.1 PPG Circuit**

The MQP group recommends that the total number of components in the PPG circuit be reduced, to decrease large scale device costs as well as minimize the possibility of component failure. This might include a shift to entirely software filtering, using more robust filters.

#### **10.1.2 Device Battery life**

Battery life can also be improved by increasing the effective photodetection area through multiple diode usage or a diode with increased area. This allows for a decrease in the overall light output for the light emitting diode, hence lesser current, due to the increase probability of diffused light detection. The MQP group recommends a using a PPG sensor architecture with the photodiodes arranged concentrically around the LED source. Another desirable feature for this device would be a low battery indicator to alert the user that a change is required, in order to avoid system failure during monitoring. The MQP group utilized two 9V batteries for the device design, with the option of using rechargeable type batteries to reduce device cost. However, smaller sized batteries like coin cell batteries can be used to further reduce device hardware size, and maintain it within a PDA size range.

#### **10.1.3 Motion Artifact Reduction**

Given the importance of signal integrity in wearable monitoring sensors, it is critical to remove noise components especially due to motion artifacts. The MQP group implemented a frequency based signal filtering methods to remove high frequency noise. However, this method was not effective in completely eliminating motion artifacts, resulting in signal distortion and possibility of system accuracy errors during measurements. In this design, the MQP group minimized the effect of motion artifacts by rejecting abnormally high peak amplitudes or short R-R interval times introduced by multiple peaks. Further reduction motion artifacts will provide the system better clinical acceptability to ensure accurate measurements.

The MQP group recommends adaptive filtering for motion artifacts reduction as it has been demonstrated to be a more effective method of noise cancellation in PPG signals. This is based on the fact that since noise signal is not removed as a result of bandwidth overlap, its frequency content can be “subtracted” from the signal of interest to obtain a better signal (see Figure 10.1). A reference signal is usually used to simulate the noise component since actual noise signal is usually unknown. The characteristics or tap weight of the adaptive filter changes in an effort to minimize the error resulting from this subtraction.

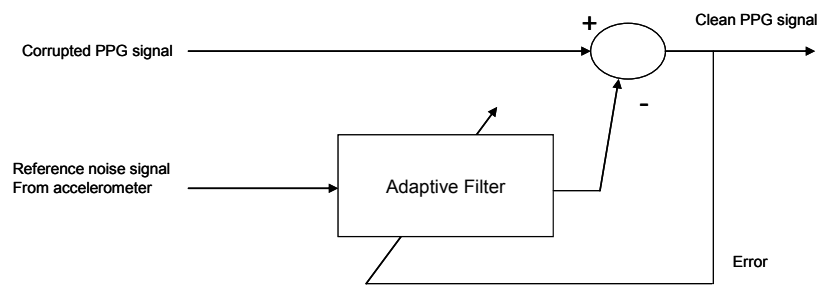


**Figure 10.1: Adaptive noise cancellation for motion artifacts reduction in PPG signal**

A signal from an accelerometer can be used as a reference signal for reduction in motion artifacts in PPG signal analysis. An accelerometer generates an electrical signal proportional to body acceleration. Relente et al. utilized a Recursive Least Square adaptive filter, using signals from a single axis accelerometer as a reference signal [57]. They determined that a filter with coefficients  $\lambda=0.999$  and  $N=32$  was effective in reducing motion artifacts with a HR to within a  $\pm 5\%$  error.

The MQP group also proposes the exploration of removing motion artifacts by signal correlation. Weng et al proposed cross-correlation to minimize motion artifacts in the PPG waveform. This is based on the fact that if waveforms from one cycle do not match those of previous or an average reference waveform, most likely it is due to artifact. Following cross correlation detection, this section is either truncated or extrapolated depending on the severity of the motion artifacts. By comparing signal quality before and after signal algorithm implementation, they were able to demonstrate that their proposed

cross-correlation detection was effective in enhancing signal to noise ratio of the PPG waveform.

#### **10.1.4 Sensor Platform**

One limitation of the sensor platform designed by the MQP group is the introduction of additional artifacts due to the wire motion. There is also the possibility of wire entanglement, which is undesirable in ambulatory conditions. Modern wireless communication technology have proved a significant medical innovation, as it has allowed for better health care management through rapid communication of data between physicians and patients. The MQP group suggests using an integrated cordless sensor and microprocessor technology to assimilate sensor components into a single small unit and signals obtained wirelessly transmitted to a processing unit. This further reduces the burden on the user of carrying the device at all times. In a pilot study, Lindberg et al were able to demonstrate the possibility of using the area above the radial artery as a PPG sensor location site by using a wireless PPG sensor [58]. Mendelson et al. have developed a PDA-based wireless reflectance forehead sensor for monitoring HRV and other physiological conditions of soldiers in the battlefield, for better care management of especially injured soldiers [21].

Sometimes it was necessary to adjust the PPG headband sensor a couple of times in order to obtain a proper signal. To alleviate this problem, sometimes the band had to be tightly fastened for good skin contact. This often led to a reduction in signal amplitude due to compression of the blood vessels beneath the skin. This also resulted in sensor demarcations on the forehead, suggesting that the device was not properly shielded, with the possibility of patient skin inflammation and injury. The MQP groups suggest softer and pliable plastic materials for shielding to minimize patient injury.

The materials used for the sensor also have to be improved to make it more durable to guarantee sensor integrity during multiple uses. The sensor designed by the MQP group utilizes a sports band as an attachment method, which may not be clinically acceptable in terms of biocompatibility, as some people can develop skin reactions. Proper textiles,

which are clinically acceptable, will have to be used. The aesthetic appearance of the sensor can also improved by making it smaller, to improve on patient comfort.

## ***10.2 Device Testing***

Although the MQP group was able to demonstrate the correlation of HR and HRV indices in a small group of individuals with assumingly good heart conditions, it is necessary to demonstrate the effectiveness of our device and reproducibility of our results on heart patients requiring monitoring. Extensive clinical testing on a significant population is thus necessary to validate and qualify our device for clinical use especially for FDA device approval. Although the device hardware was portable, the additional bulk from the PC severely limited the nature of our motion tests. These motions studies are indeed vital since it plays a significant limitation of PPG sensor usage. As noted above, elimination of the PC will render our device more portable for better motion exercise testing or better yet, longer monitoring times.

The MQP group also determined that the rMSSD and SDNN indices were not effective in obtaining valid measurements during motion. The MQP suggests the possibility of exploring geometrical based frequency domain methods, as recommended for long term studies such as the Poincaré plot. This is because abnormal heart beats will usually be observed as outliers in the plot.

## ***10.3 ECG***

The following recommendations are focused on improving the sensor interface of the ECG. These improvements are intended to provide for a better interface with regards to acquisition of the ECG signals. Utilizing a better acquisition of the signals allows for an overall better quality of the signals to be analyzed. Overall, the better quality signals will provide for better signal analysis, and more reliable data.

### **10.3.1 Adaptive Filtering (Active EMG)**

The ECG sensors did not perform well enough to perform exercise while monitoring the electrical signals of the heart. This is primarily due to the overlapping of EMG

frequencies with ECG frequencies. Tests with this type of noise have shown that it is isolated primarily to the upper body movement, which correlated well with the placement of the electrodes and the areas of muscle activity. Potential problems with this may arise when utilizing the system while performing an exercise. This may be especially true when performing a cardio related exercise where the entire body is in motion. Such an event would cause widespread EMG artifacts within the ECG sensors, causing a poor quality signal.

A possible improvement for this would be through active noise filtering. For this to be accomplished, a second set of sensors would need to be placed to obtain the EMG. This signal would need to be acquired in such a fashion that only the EMG signals are acquired, isolating other possible signal artifacts from possibly entering the system. Theoretically, the attempt is to remove the EMG artifact from a signal containing an ECG and EMG signal, thus providing a clean ECG signal with no artifacts. The theory behind this is that the EMG artifacts present in the ECG signal are equal to the EMG signals acquired from elsewhere in the body, thus by subtraction, the EMG portions can be eliminated. As this may not be entirely true, further conditioning of the EMG signal may be required to provide for a more robust system capable of isolating the ECG signal.

## ***10.4 Software***

The following recommendations detail further improvements that could be implemented within the software section of this project. Furthermore, the recommendations contained within this section do not have an overall affect towards the actual functionality of the device. The improvements will improve either the user interface or functionality of the device. The lack of implementation of any of the given improvements will not prevent the software portion of the project from operating.

### **10.4.1 Signal Discrimination**

The assumptions made with regards to this project were that all physiological signals received by the system were not irregular rhythms. This is due to the fact that the HRV indices are specified as being the variations between normal to normal heart beats.

Depending on the type of irregular heart beat, the system is incapable of detecting and compensating for the anomaly.

A further improvement should enable the program to detect whether the system is or is not receiving a normal sinus rhythm. When it has been detected that the heart rhythm is irregular, the program will then have to be further designed to disregard any peak-to-peak times. Therefore the system should be designed to be sufficiently robust that any anomalous rhythms and time intervals would be eliminated from the variability indices buffers, ensuring that no irregular time values are computed. As the normal-to-normal requirement for HRV calculations is true for both the ECG and PPG signals, the device should have the ability to determine whether this is true from either the ECG or PPG signals, such that the signals could reliably function independently.

#### **10.4.2 Threshold Reset Control**

The current design of the software program is to allow for the program to automatically reset itself should a fault be detected due to the timers running too long between peaks. This was implemented by using a simple comparison between the elapsed times of the timers and a constant set value. Should the elapsed times increase above 3 seconds, the system determines that a fault has occurred and attempts to correct for this by resetting the peak detection threshold. This is done due to the possibility that the system may not be capable of detecting peaks due to the threshold setting being set higher than the actual signal peaks. This may occur should there be a significant amount of signal artifact either from sensor movement or acquisition of anomalous signals. Should a significantly higher peak value enter the automatic threshold adjuster, shown in Section 6.3.3.1, the calibrated threshold may become sufficiently high to prevent the detection of further peaks.

The current design of the automatic reset controls are that they are dependent on the elapsed timers going above a constant value of 3 seconds. As such, after having reset the threshold, once a peak has been detected, the reset function is disabled. Should this occur when the anomalous signal peak is still contained within the threshold adjuster buffer, shown in Figure 6.17 and Figure 6.18, the system will continue to be unable to detect

signal peaks unless the threshold is reset. Utilizing a buffer size of 5 points, and a fault detection of 3 seconds, should an anomalous signal peak enter the buffer, it will take a minimum of 15 seconds for the system to recover. Future improvements should work to determine which of the two signals are faulting, and to create a more robust system for resetting the thresholds. Possible methods for improvement involve resetting all points within the buffer to the threshold reset value, eliminating any problematic values. A second method of improvement involves a system to hold the reset value once activated, allowing new signal peaks to replace the anomalous signal peak contained within the adjustment buffer.

### **10.4.3 Microcontroller Development**

A final development for the software portion of this project would be to implement the LabVIEW software into a self-contained unit. This would involve the use of an embedded microcontroller to perform the necessary functions of the software analysis and the eventual display of the signals and calculated indices. For use with this section, the current designs for the PPG and ECG hardware sensor suites could be retained, necessitating a replacement of the software portions of the project.

## References

- [1] *HRV*. American Heart Association. 1996
- [2] Kara, Tomas, Jiri Nykodym, and Virend K. Somers. "HRV: Back to the Beginning." Journal of Cardiovascular Electrophysiology 14 (2003): 800-802. 16 June 2007.
- [3] *HRV Analysis Scientific Background*. Oct. 9, 2007. <<http://www.biocomtech.com/hrvscientific>>
- [4] Javorka, Michal, Ivan Zila, Tomas Balharek, and Kamil Javorka. "On- and Off-Responses of HR to Exercise - Relations to HRV." Clinical Physiology and Functional Imaging 23 (2003): 1-8. 15 June 2007.
- [5] Bilchick, Kenneth C., and Ronald D. Berger. "HRV." Journal of Cardiovascular Electrophysiology 17 (2006): 691-694.
- [6] Evrengul, Harun, Halil Tanriverdi, Sedat Kose, Basri Amasyali, Ayhan Kilic, Turgay Celik, and Hasan Turhan. "The Relationship Between HR Recovery and HRV in Coronary Artery Disease." Annals of Noninvasive Electrocardiology 11 (2006): 154-162.
- [7] Task Force Of The Europea. "HRV: Standards of Measurement, Physiological Interpretation, and Clinical Use." Circulation 93 (1996): 1043-1065.
- [8] Dubin, Dale. *Rapid Interpretation of EKG's*. COVER Publishing Company. 1974.
- [9] "The Electrocardiogram: Looking at the Heart of Electricity." Nobelprize.org <[http://nobelprize.org/educational\\_games/medicine/ecg/ecg-readmore.html](http://nobelprize.org/educational_games/medicine/ecg/ecg-readmore.html)>
- [10] Bruce, Nancie P., and Flynn, Janet-Beth M. Introduction to Critical Care Skills. Mosby-Year Book, Inc. 1993.
- [11] Tam, Hak W and Webster, John G. "Minimizing Electrode Motion Artifact by Skin Abrasion." IEEE Transactions on Biomedical Engineering 24 (1977): 134-139.
- [12] Webster, John G. Medical Instrumentation: Application and Design. Wiley and Sons, Inc, 1998
- [13] Leach, R M., and D F. Treacher. "ABC of Oxygen Transport---1. Basic Principles." BMJ 317 (1998): 1302-1306. 10 Aug. 2007 <<http://www.bmj.com/cgi/content/full/317/7168/1302>>.
- [14] Webster, John G. Design of Pulse Oximeters. CRC Press, 1997.
- [15] Elwell, Clare, and Jem Hebden. "Near-Infrared Spectroscopy." UCL Department of Medical Physics and Biomedical Engineering. 6 Jan. 1999. University College London. 9 Oct. 2007 <[http://www.medphys.ucl.ac.uk/research/borg/research/NIR\\_topics/nirs.htm](http://www.medphys.ucl.ac.uk/research/borg/research/NIR_topics/nirs.htm)>.
- [16] Sherwood, Lauralee. Human Physiology: From Cells to Systems. 4th ed. Pacific Grove: Brooks/Cole, 2001.
- [17] Deni, Hassan, Diane M. Muratore, and Robert A. Malkin. "Development of a Pulse Oximeter Analyzer for the Developing World." Bioengineering Conference, 2005. Proceedings of the IEEE 31<sup>st</sup> Annual Northeast (2005): 227-228.
- [18] Pujary, Chirag J. Investigation of Photodetector Optimization in Reducing Power Consumption by a Noninvasive Pulse Oximeter Sensor. Diss. Worcester Polytechnic Institute, 2004.
- [19] Wouda, Jan C., Petra M. Hartman, Riksta M. Bakker, Jan O. Bakker, Harry B. Van De Wiel, and Willibrord M. Weijmar Schultz. "Vaginal Plethysmography in Women with Dyspareunia." The Journal of Sex Research 35 (1998): 141-147. 9 Aug. 2007.
- [20] Kyriacou, P A., S Powell, R M. Langford, and D P. Jones. "Esophageal Pulse Oximetry Utilizing Reflectance Photoplethysmography." IEEE Transactions on Biomedical Engineering 49 (2002): 1360-1368. IEEE Xplore. Worcester Polytechnic Institute. 9 Aug. 2007
- [21] Johnston, W S., P C. Branche, C J. Pujary, and Y Mendelson. "Effects of Motion Artifacts on Helmet-Mounted Pulse Oximeter Sensors." Bioengineering Conference, 2004. Proceedings of the IEEE 30th Annual Northeast (2004): 214-215.
- [22] Such, O, and J Muehlsteff. "The Challenge of Motion Artifact Suppression in Wearable Monitoring Solutions." 3rd IEEE/EMBS International Summer School on Medical Devices and Biosensors (2006): 49-52.
- [23] Savage, M, C Pujary, and Y Mendelson. "Optimizing Power Consumption in the Design of a Wearable Wireless Telesensor: Comparison of Pulse Oximeter Modes." Bioengineering Conference, 2003 IEEE 29th Annual. Proceedings Of (2003): 150-151.
- [24] Atapattu, S A., R D. Mitrani., H V. Huikuri, and P P. Tarjan. "A Computer Program to Acquire, Analyze and Track the HRV of Patients in a Clinical Research Environment." Engineering in

- Medicine and Biology Society, 2000. Proceedings of the 22nd Annual International Conference of the IEEE 4 (2000): 2590-2593.
- [25] Bolanos, M, H Nazaren, and E Haltiwanger. "Comparison of HRV Signal Features Derived From Electrocardiography and Photoplethysmography in Healthy Individuals." 28th Annual International Conference of the IEEE (2006): 4289-4294.
- [26] Srinivas, K, R Srinivas, and L Reddy. "Estimation of HRV From Peripheral Pulse Wave Using PPG Sensor." 3<sup>rd</sup> Kuala Lumpur International Conference on Biomedical Engineering 2006 (2007): 325-328.
- [27] Johnston, W, and Y Mendelson. "Extracting HRV From a Wearable Reflectance Pulse Oximeter." Bioengineering Conference, 2005. Proceedings of the IEEE 31<sup>st</sup> Annual Northeast 2 (2005): 157-158.
- [28] Kim, Jaywoo, Mi-Hee Lee, Hyoung-Ki Lee, Kiwan Choi, Seokwon Bang, and Sangryong Kim. "HR Monitor for Portable MP3 Player." 27th Annual International Conference of the Engineering in Medicine and Biology Society, 2005 (2007): 5207-5210.
- [29] Malik, Marek. "Time-Domain Measurement of HRV." Cardiac Electrophysiology Review 1 (1997): 329-334.
- [30] Bilchick, Kenneth C., Barry Fetics, Ronnie Djoukeng, Susan G. Fische, Ross D. Fletcher, Steven N. Singh, Erez Nevo, and Ronald D. Berger. "Prognostic Value of Heart Rate Variability in Chronic Congestive Heart Failure (Veterans Affairs' Survival Trial of Antiarrhythmic Therapy in Congestive Heart Failure)." The American Journal of Cardiology 90 (2002): 24-28.
- [31] Nolan, James, Phillip D. Batin, Richard Andrews, Steven J. Lindsay, Paul Brooksby, Michael Mullen, Wazir Baig, Andrew D. Flapan, Alan Cowley, Robin J. Prescott, James M. Neilson, and Keith A. Fox. "Prospective Study of HRV and Mortality in Chronic Heart Failure." Circulation 98 (1998): 1510-1516.
- [32] Kleiger, R E., J P. Miller, J T. Bigger Jr, and A J. Moss. "Decreased HRV and Its Association with Increased Mortality After Acute Myocardial Infarction." The American Journal of Cardiology 59 (1987): 256-262.
- [33] "Interbeat Interval Monitor." Mini Mitter. 9 Oct. 2007  
<<http://www.minimitter.com/Products/MiniLogger/Interbeat.html>>.
- [34] Micco, Gianluca D., J P. Bourke, R Saharia, S S. Furniss, A Iacono, and R W. Campbell. "HRV Following Myocardial Infarction: Prognostic Panacea or Enigma?" Heart Views 1 (2000): 291-300.
- [35] Odemuyiwa, O, M Malik, T Farrell, Y Bashir, J Polonieki, and A J. Camm. ". Comparison of the Predictive Characteristics of HRV Index and Left Ventricular Ejection Fraction for All Cause Mortality, Arrhythmic Events and Sudden Death After Acute Myocardial Infarction." The American Journal of Cardiology 68 (1991): 434-439.
- [36] Brennan, M, M Palaniswami, and P Kamen. "Do Existing Measures of Poincaré Plot Geometry Reflect Nonlinear Features of HRV." IEEE Transactions on Biomedical Engineering 48 (2001): 1342-1347.
- [37] Varoneckas, Giedrius, and Danguolė Žemaitytė. "HR Analysis During Sleep Stages Using Poincare Plots." Institute Psychophysiology and Rehabilitation. 9 Oct. 2007  
<[http://www.pri.kmu.lt/Publication\\_HRV/Heart%20rate%20analysis%20during%20sleep%20stages\\_Presentation.pdf](http://www.pri.kmu.lt/Publication_HRV/Heart%20rate%20analysis%20during%20sleep%20stages_Presentation.pdf)>.
- [38] Paškevičiūtė, R, D Žemaitytė, and G Varoneckas, comps. HRV in Diagnostics of Atrial Fibrillation or Atrial Flutter. Kaunas University of Medicine, Klaipėda Hospital, Lithuania. 12 Oct. 2007  
<[http://www.pri.kmu.lt/Publication\\_HRV/Heart%20rate%20variability\\_Full\\_text.pdf](http://www.pri.kmu.lt/Publication_HRV/Heart%20rate%20variability_Full_text.pdf)>.
- [39] Contreras, Paola, Rafael Canetti, and Eduardo R. Migliaro. "Correlations Between Frequency-Domain HRV Indices and Lagged Poincaré Plot Width in Healthy and Diabetic Subjects." Physiological Measurement 28 (2007): 85-94.
- [40] Akselrod, Solange, Itzik Pinhas, Linda R. Davrath, Zvika Shinar, and Eran Toledo. "HRV (HRV)." Wiley Encyclopedia of Biomedical Engineering (2006): 1-12.
- [41] Hoffmann, Klaus-Peter, and Roman Ruff. *Flexible dry surface-electrodes for ECG long-term monitoring*. Proceedings of the 29<sup>th</sup> Annual IEEE EMBS Conference. August 26, 2007.
- [42] Cester, Ivan and Dunne, Stephen and Farres, Esteve and Fuentemilla, Lluís and Grau, Carles and Marco-Pallares, Josep and Ruffini, Giulio and Silva, S. Ravi and Vandecasteele, Bjorn and

- Watts, Paul. *ENOBIO Dry Electrophysiology Electrode: First Human Trial plus Wireless Electrode System*. Proceedings of the 29<sup>th</sup> Annual IEEE EMBS Conference. August 26, 2007.
- [43] Bigger Jr, J T., J L. Fleiss, R C. Steinman, L M. Rolnitzky, R E. Kleiger, and J N. Rottman. "Frequency Domain Measures of Heart Period Variability and Mortality After Myocardial Infarction." Circulation 85 (1992): 164-171.
- [44] Lin, Kang-Ping, Gen-Hong Lin and Bor-Iuan Jan (2005). U.S. Patent No. 20060287605. Washington, DC: U.S. Patent and Trademark Office.
- [45] Karlsson, M, R Forsgren, E Eriksson, U Edstrom, T Backlund, J. S. Karlsson, and U Wiklund. "Wireless System for Real-Time Recording of HRV for Home Nursing." 27th Annual International Conference of the Engineering in Medicine and Biology Society (2005): 3717-3719.
- [46] "Photoplethysmography Measurements." Medis. 04 Aug. 2006. Medizinische Messtechnik GmbH. 18 Oct. 2007 <<http://www.medis-de.com/en/ppg.html>>.
- [47] "Pulse Oximeter Sensors." AeromedixRx. 18 Oct. 2007 <[http://www.aeromedixrx.com/category-exec/parent\\_id/31/category\\_id/33/nm/Pulse\\_Oximeter\\_Sensors](http://www.aeromedixrx.com/category-exec/parent_id/31/category_id/33/nm/Pulse_Oximeter_Sensors)>.
- [48] Hummler, Helmut D., Anja Engelmann, Frank Pohlandt, Josef Högel, and Axel R. Franz. "Decreased Accuracy of Pulse Oximetry Measurements During Low Perfusion Caused by Sepsis: Is the Perfusion Index of Any Value?" Intensive Care Medicine 32 (2006): 1428-1431.
- [49] Pälve, Heikki. "Reflection and Transmission Pulse Oximetry During Compromised Peripheral Perfusion." Journal of Clinical Monitoring and Computing 8 (1992): 12-15. 12 June 2007 <<http://www.springerlink.com/content/pj5714057jv82578/>>.
- [50] Ogino, Hirokazu, Haruyuki Minamitani, and Takeshi Souma. "Reflectance pulse oximeter measuring central SpO<sub>2</sub> from Mouth." Proceedings of the 16th Annual International Conference of the IEEE 2 (1994): 914-915. 12 Aug. 2007 <<http://ieeexplore.ieee.org/iel4/3230/9234/00415210.pdf?arnumber=415210>>.
- [51] Wang, Lei, B. Lo, and G. Z. Yang. "Reflective Photoplethysmograph Earpiece Sensor for Ubiquitous HR Monitoring." 4th International Workshop on Wearable and Implantable Body Sensor Networks (2007): 179-183. SpringerLink. Worcester Polytechnic Institute. 12 Aug. 2007.
- [52] Branche, P, and Y Mendelson. "Signal Quality and Power Consumption of a New Prototype Reflectance Pulse Oximeter Sensor." Bioengineering Conference, 2005. Proceedings of the IEEE 31st Annual Northeast (2005): 42-43.
- [53] Dresher, Russell. Wearable Forehead Pulse Oximetry: Minimization of Motion and Pressure Artifacts. M.Sc. Thesis. Worcester Polytechnic Institute, 2006.
- [54] "PM-7000 Patient Monitor." Mindray. 9 Oct. 2007 <<http://www.mindray.com/main/products/show.jsp?catalogID=99&id=110>>.
- [55] Frazin, Natalie. "Study Finds Widespread Sympathetic Nerve Damage in Parkinson's Disease." The National Institute of Neurological Disorders and Stroke. 19 Oct. 2007. 25 Oct. 2007 <[http://www.ninds.nih.gov/news\\_and\\_events/press\\_releases/pressrelease\\_nerve\\_damage\\_pd.htm](http://www.ninds.nih.gov/news_and_events/press_releases/pressrelease_nerve_damage_pd.htm)>.
- [56] Webster, John G. Bioinstrumentation. Wiley and Sons, Inc, 2004. 6-7.
- [57] Relente, A R., and L G. Sison. "Characterization and Adaptive Filtering of Motion Artifacts in Pulse Oximetry Using Accelerometers." Proceedings of the Second Joint EMBS/BMES Conference 2 (2002): 1769-1770.
- [58] Lindberg, L G., and J Petterson. "A Wireless PPG Sensor Applied Over the Radial Artery – a Pilot Study." Med-E-Tel 2006 Proceedings (2006): 199-202.
- [59] E. Tur, M. Tur, H. Maibach, and R. Guy, "Basal Perfusion of the Cutaneous Microcirculation: Measurements as as Function of Anatomic Position," The Journal of Investigative Dermatology, vol. 81, pp. 442-446, 1983.

## Glossary

Glossary terms courtesy of Merriam-Webster OnLine

**Cardiac Arrest (CA):** Abrupt temporary or permanent cessation of the heartbeat (as from ventricular fibrillation or asystole) -- called also *sudden cardiac arrest*

**Congestive Heart Failure (CHF):** Heart failure in which the heart is unable to maintain adequate circulation of blood in the tissues of the body or to pump out the venous blood returned to it by the venous circulation

**Coronary Artery Disease (CAD):** A condition and especially one caused by atherosclerosis that reduces the blood flow through the coronary arteries to the heart muscle and typically results in chest pain or heart damage -- called also *coronary disease, coronary heart disease*

**Diastole:** The passive rhythmical expansion or dilation of the cavities of the heart during which they fill with blood

**Dicrotic Notch:** A secondary upstroke in the descending part of a pulse tracing corresponding to the transient increase in aortic pressure upon closure of the aortic valve -- called also *dicrotic wave*

**Dyspareunia:** Difficult or painful sexual intercourse

**Elastin:** A protein that is the chief constituent of elastic fibers

**Esophagus:** A muscular tube that in adult humans is about nine inches (23 centimeters) long and passes from the pharynx down the neck between the trachea and the spinal column and behind the left bronchus where it pierces the diaphragm slightly to the left of the middle line and joins the cardiac end of the stomach

**Hemoglobin (Hb):** An iron-containing respiratory pigment of vertebrate red blood cells that functions primarily in the transport of oxygen from the lungs to the tissues of the body

**HRV (HRV):** Variability of inter-beat intervals of the HR

**NI:** National Instruments; developer of the LabVIEW software suite.

**Parasympathetic Nervous System (PNS):** The part of the autonomic nervous system that contains chiefly cholinergic fibers, that tends to induce secretion, to increase the tone and contractility of smooth muscle, and to slow the HR

**Premature Ventricular Contraction (PVC):** Contraction of the left and right ventricles prior to depolarization of the atria

**Saturation Pressure of Oxygen (SpO<sub>2</sub>):** Partial pressure of oxygen present in arterial blood

**subVI:** Instance of a LabVIEW Virtual Instrument contained within a higher level Virtual Instrument

**Stroke Volume:** The volume of blood pumped from a ventricle of the heart in one beat

**Sympathetic Nervous System (SNS):** The part of the autonomic nervous system that is concerned especially with preparing the body to react to situations of stress or emergency, that contains chiefly adrenergic fibers and tends to depress secretion, decrease the tone and contractility of smooth muscle, increase HR

**Systole:** The contraction of the heart by which the blood is forced onward and the circulation kept up

**P Wave:** A deflection in an electrocardiographic tracing that represents atrial depolarization of the heart

**QRS Complex:** A deflection in an electrocardiographic tracing that represents ventricle depolarization of the heart

**T Wave:** A deflection in an electrocardiographic tracing that represents ventricle repolarization of the heart

**VI:** Virtual Instrument; a LabVIEW program consisting of a front panel control and a functional block diagram

## **Appendix A. LabVIEW Files**

# HRV Monitor

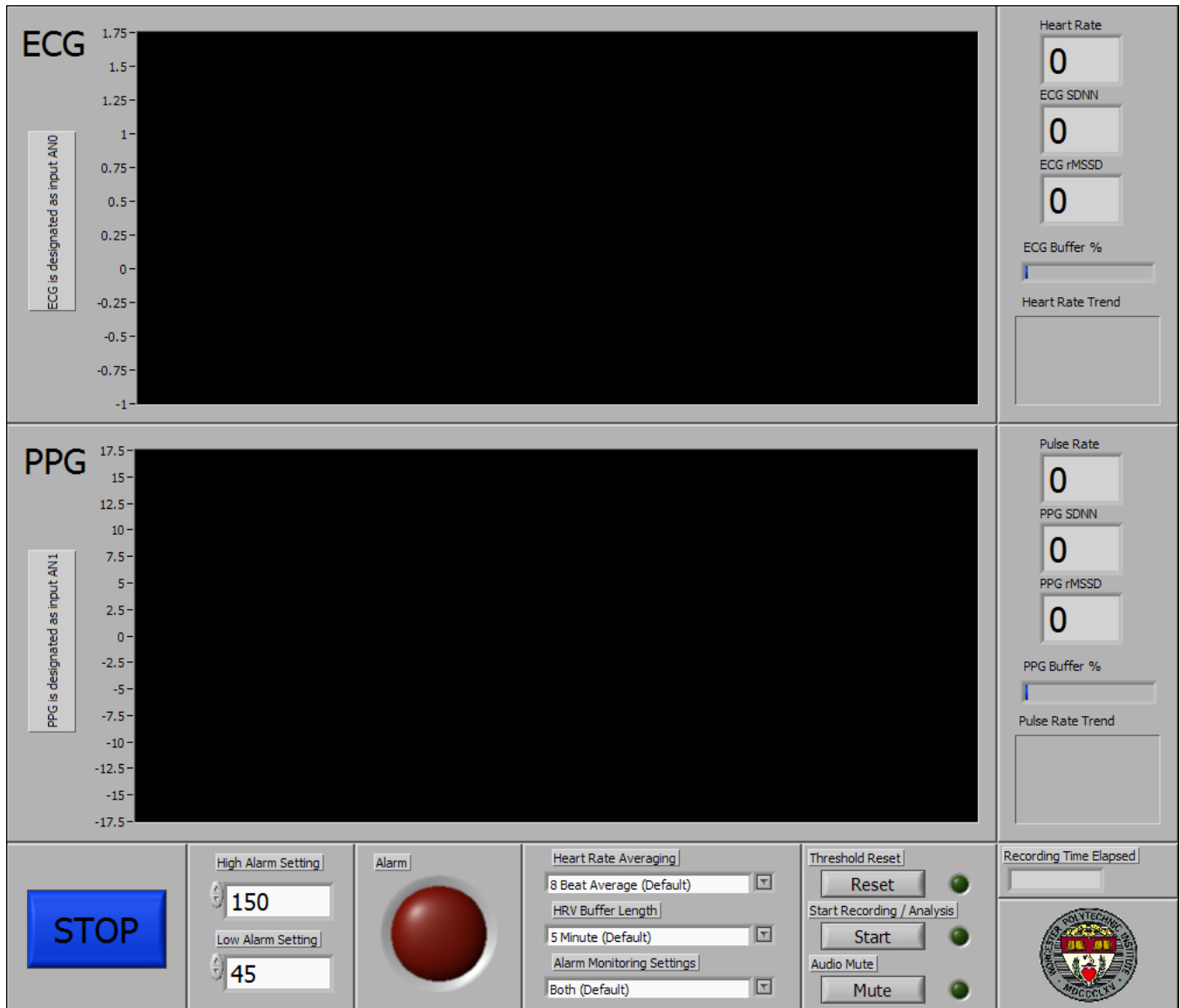


Figure A.1: LabVIEW front panel

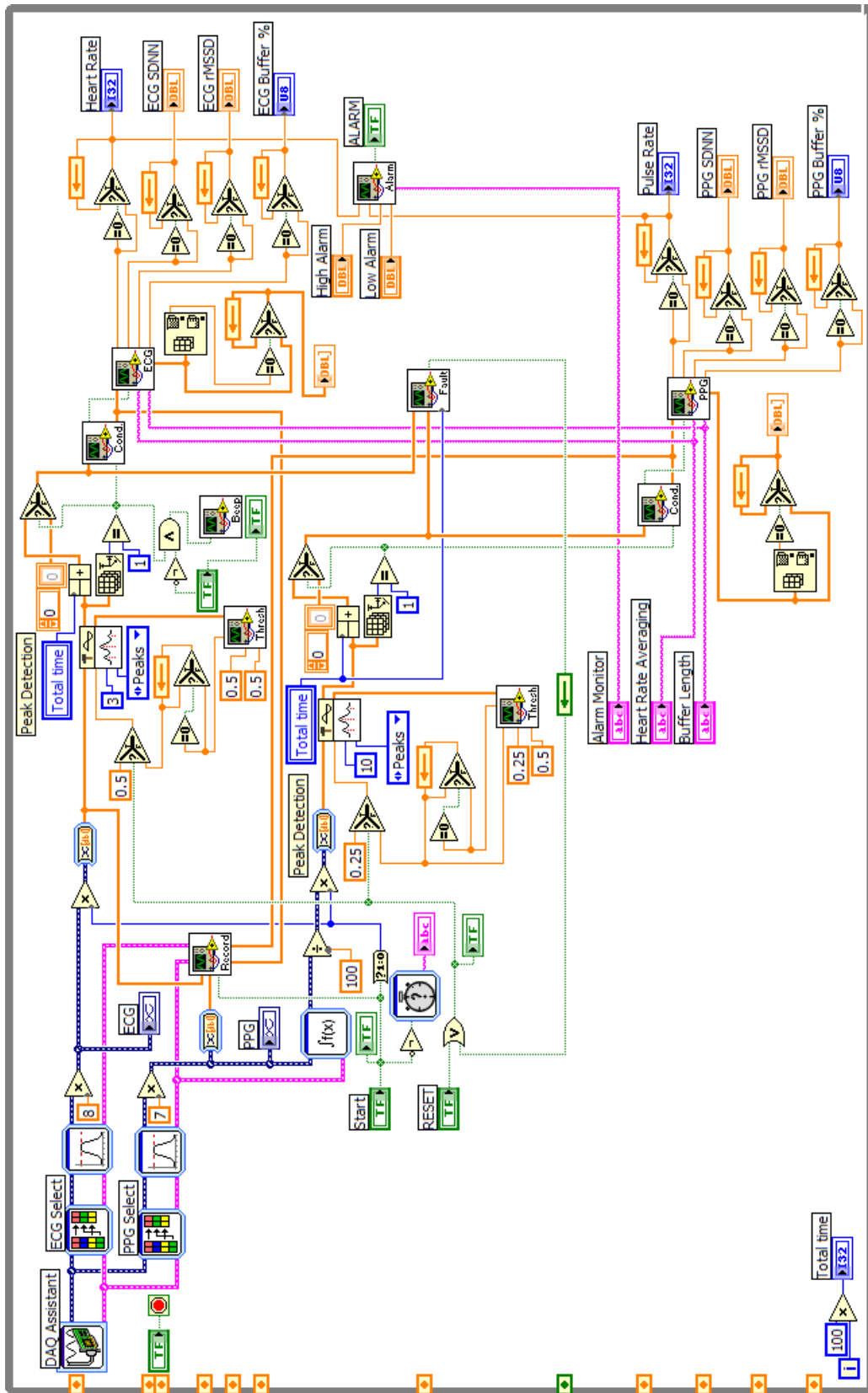


Figure A.2: LabVIEW block diagram



## ***DAQ Assistant***

DAQ Assistant

Creates, edits, and runs tasks using NI-DAQmx. Refer to the DAQ Quick Start Guide for information on devices supported by NI-DAQmx.

When you place this Express VI on the block diagram, the DAQ Assistant launches to create a new task. After you create a task, you can double-click the DAQ Assistant Express VI in order to edit that task. For continuous measurement or generation, place a loop around the DAQ Assistant Express VI.

For continuous single-point input or output, the DAQ Assistant Express VI might not provide satisfactory performance. Refer to examples\DAQmx\Analog In\Measure Voltage.llb\Cont Acq&Graph Voltage-Single Point Optimization for techniques to create higher-performance, single-point I/O applications.



## ***PPG Select***

Select Signals

Accepts multiple signals as inputs and returns only the signals you select. You can specify which signals to include in the output and change the order of the input signals.

-----  
This Express VI is configured as follows:

Selected Signals: 1,



## ***PPG Filter***

Filter

Processes signals through filters and windows.

-----  
This Express VI is configured as follows:

Filter Type: Band-pass  
Upper Cut-Off: 6  
Lower Cut-Off: 0.8  
IIR/FIR: Infinite Impulse Response (IIR) Filter  
Topology: Butterworth  
Order: 4



## ***ECG Select***

Select Signals

Accepts multiple signals as inputs and returns only the signals you select. You can specify which signals to include in the output and change the order of the input signals.

-----  
This Express VI is configured as follows:

Selected Signals: 0,



## ***ECG Filter***

Filter

Processes signals through filters and windows.

This Express VI is configured as follows:

Filter Type: Band-pass  
Upper Cut-Off: 35  
Lower Cut-Off: 1  
IIR/FIR: Infinite Impulse Response (IIR) Filter  
Topology: Butterworth  
Order: 3



### ***Convert from Dynamic Data***

Convert from Dynamic Data

Converts the dynamic data type to numeric, Boolean, waveform, and array data types for use with other VIs and functions.



### ***Differential***

Time Domain Math

Performs one of several math functions on time domain signals.

-----

This Express VI is configured as follows:

Math Operation: Differential  
Calculation Mode: Continuous Calculation



### ***Timer***

Elapsed Time

Indicates the amount of time that has elapsed since the specified start time.

-----

This Express VI is configured as follows:

Time Target: 1 s  
Auto Reset: Off

## Threshold Adjust ECG

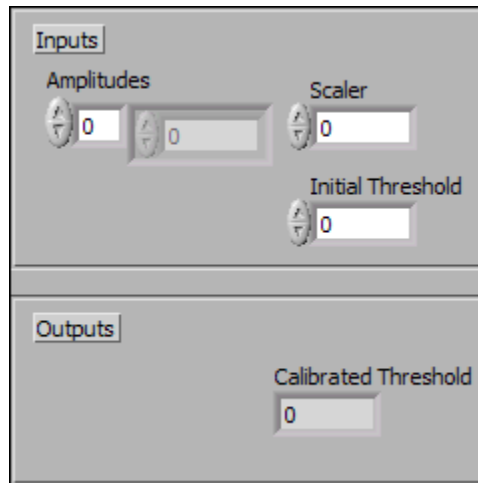


Figure A.3: ECG threshold adjust control front panel

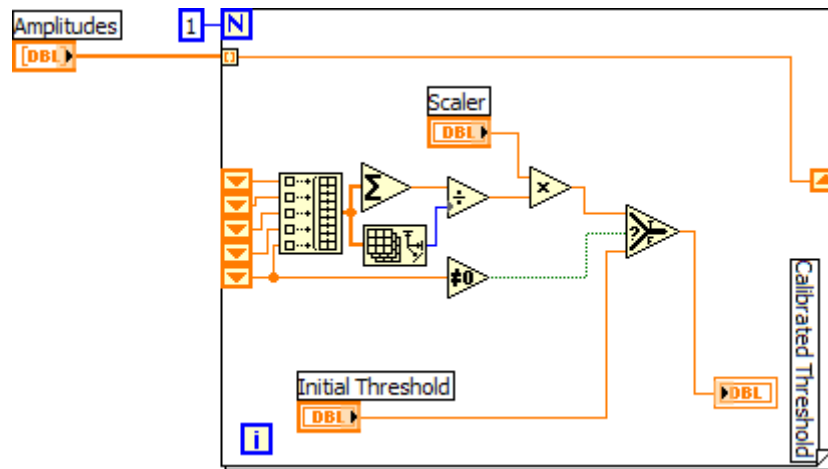


Figure A.4: ECG threshold adjust control block diagram

## Threshold Adjust PPG

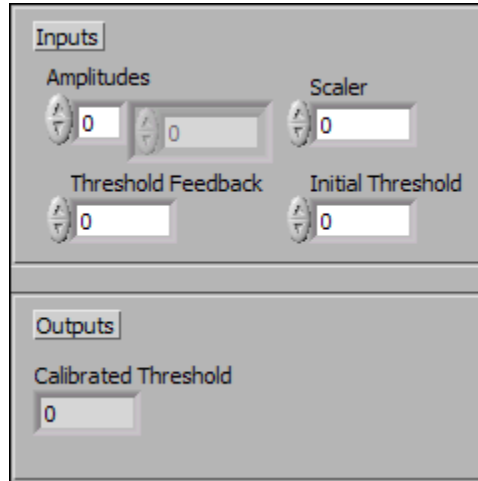


Figure A.5: PPG threshold adjust control front panel

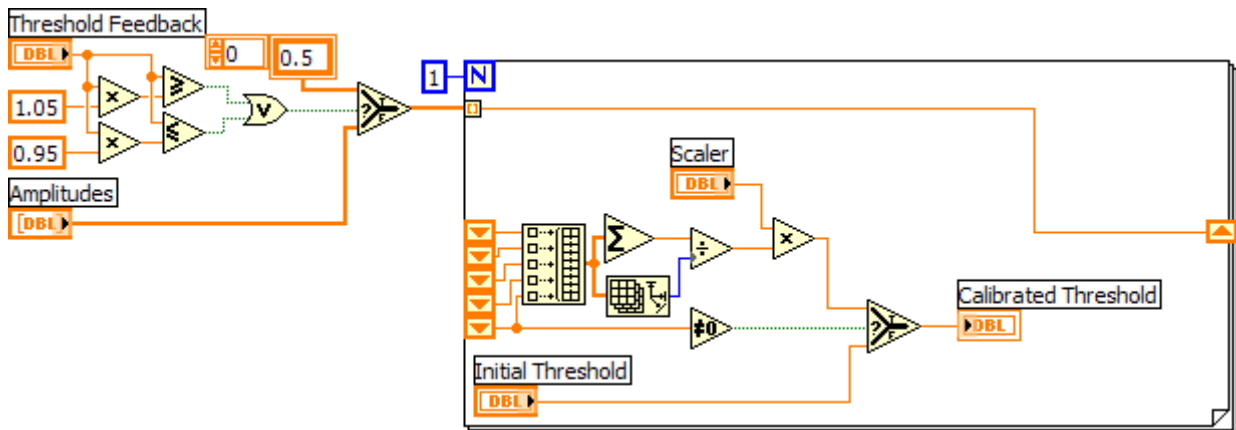


Figure A.6: PPG threshold adjust control block diagram

## Signal Conditioning ECG

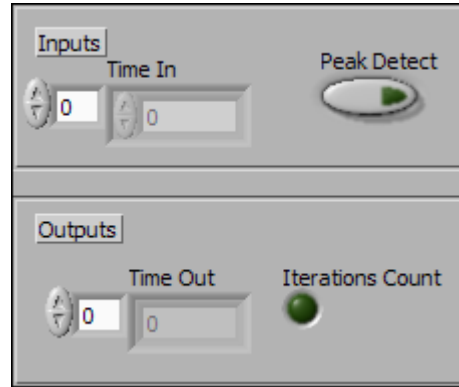


Figure A.7: ECG signal conditioning front panel

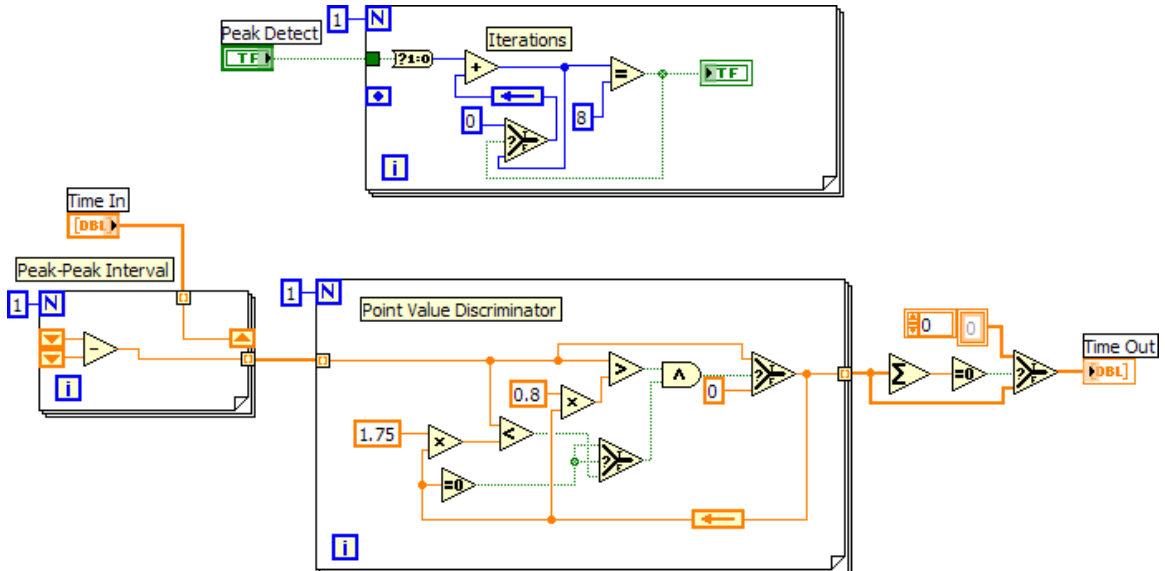


Figure A.8: ECG signal conditioning block diagram



## Analyze ECG

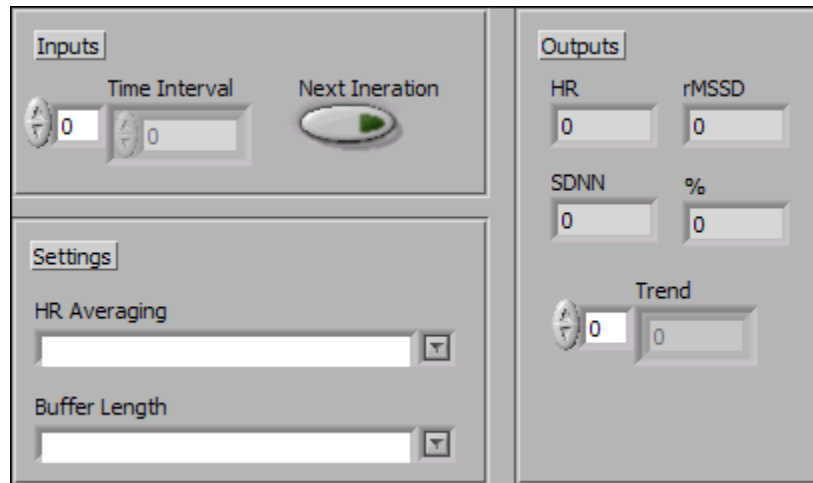


Figure A.11: ECG signal analysis front panel

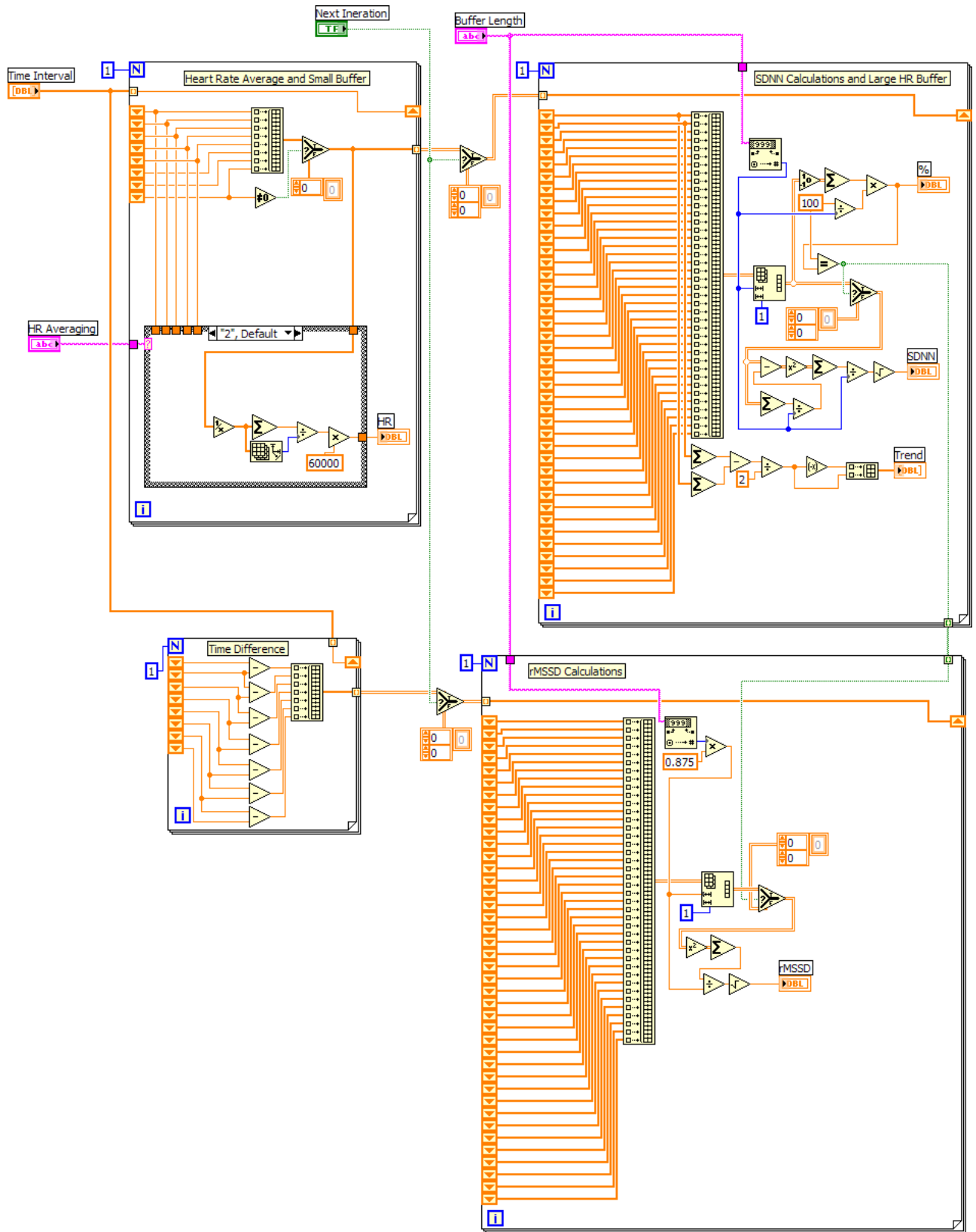


Figure A.12: ECG signal analysis block diagram with 8-beat HR average

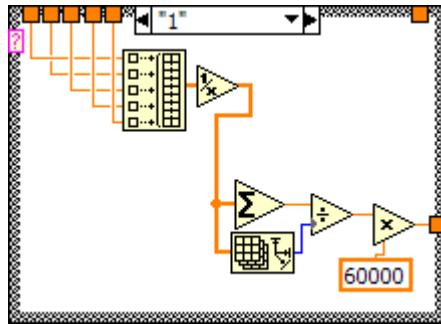


Figure A.13: ECG 5-beat HR average

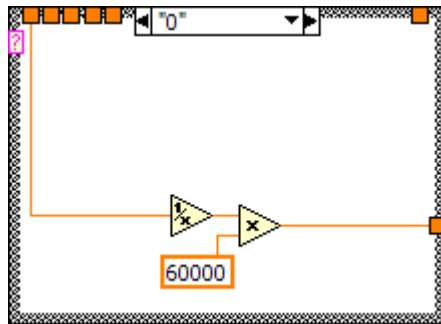
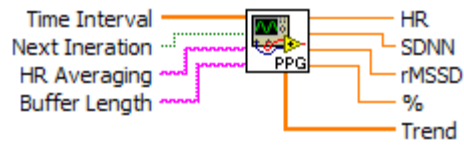


Figure A.14: ECG instantaneous HR

*Analyze PPG*



Inputs		Outputs	
Time Interval	Next Iteration	HR	rMSSD
0	<input type="button" value="Next"/>	0	0
HR Averaging	Buffer Length	SDNN	%
		0	0
		Trend	
		0	0

Figure A.15: PPG signal analysis front panel

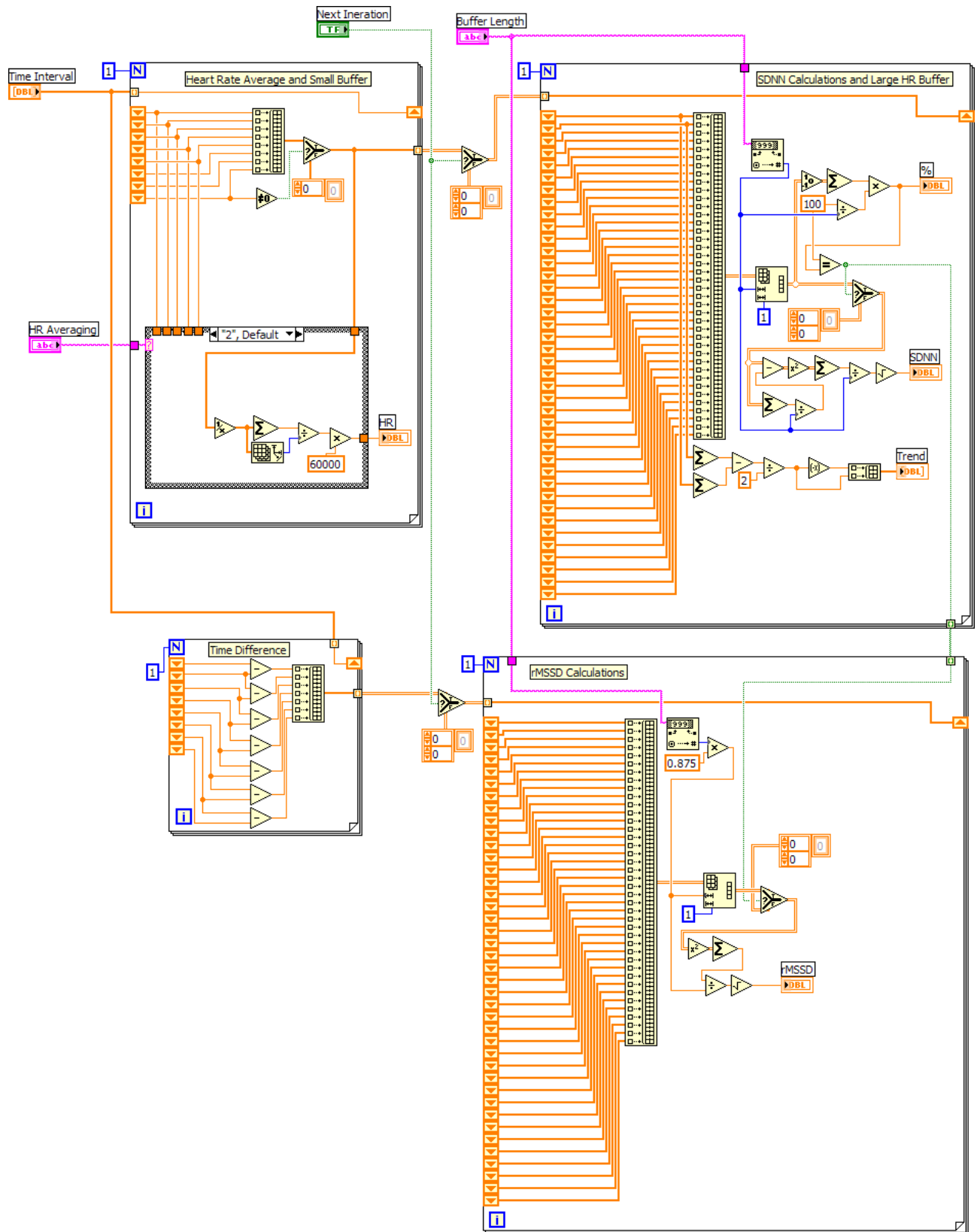


Figure A.16: PPG signal analysis with 8-beat PR average

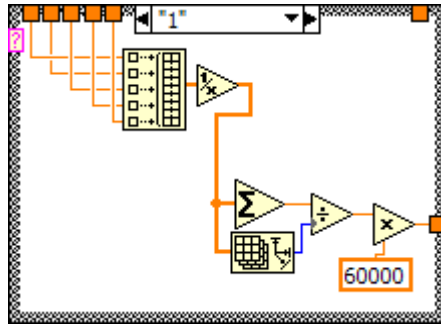


Figure A.17: PPG with 5-beat PR average

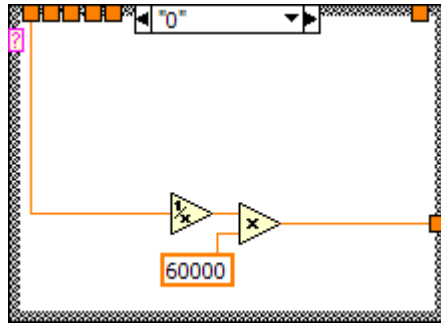


Figure A.18: PPG instantaneous PR

### *ECG Beep*

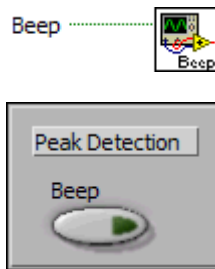


Figure A.19: ECG audible beep front panel

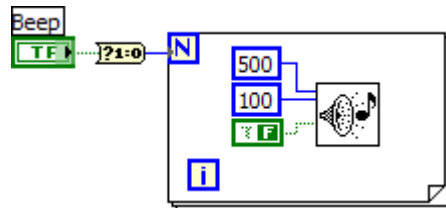


Figure A.20: ECG audible beep block diagram



## Record

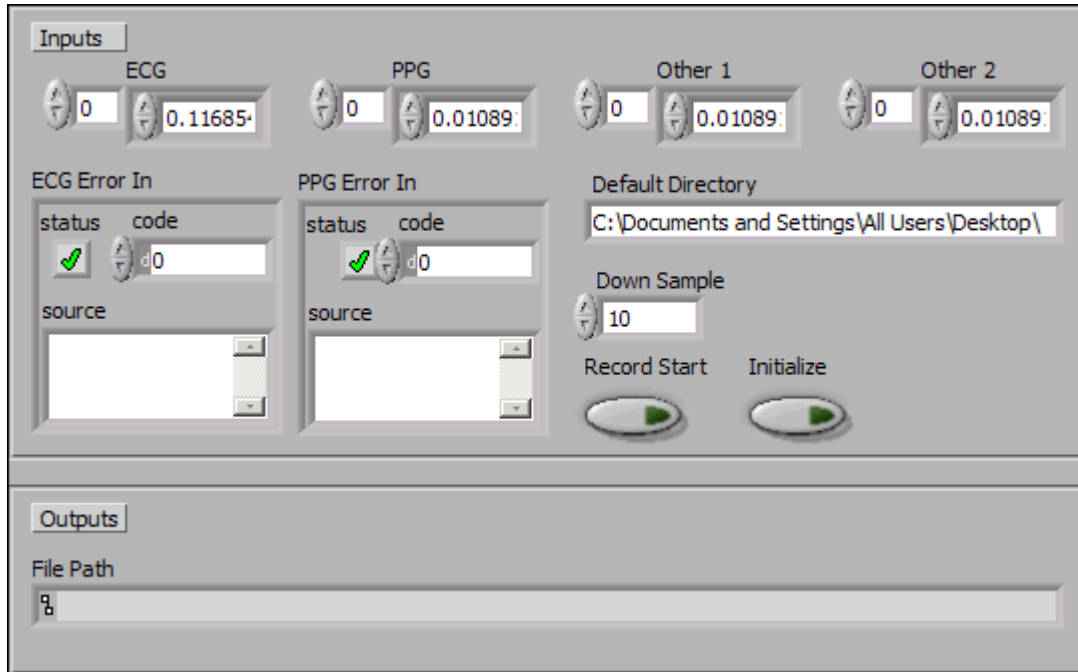
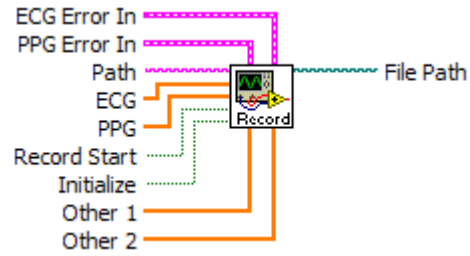


Figure A.23: Signal recording front panel

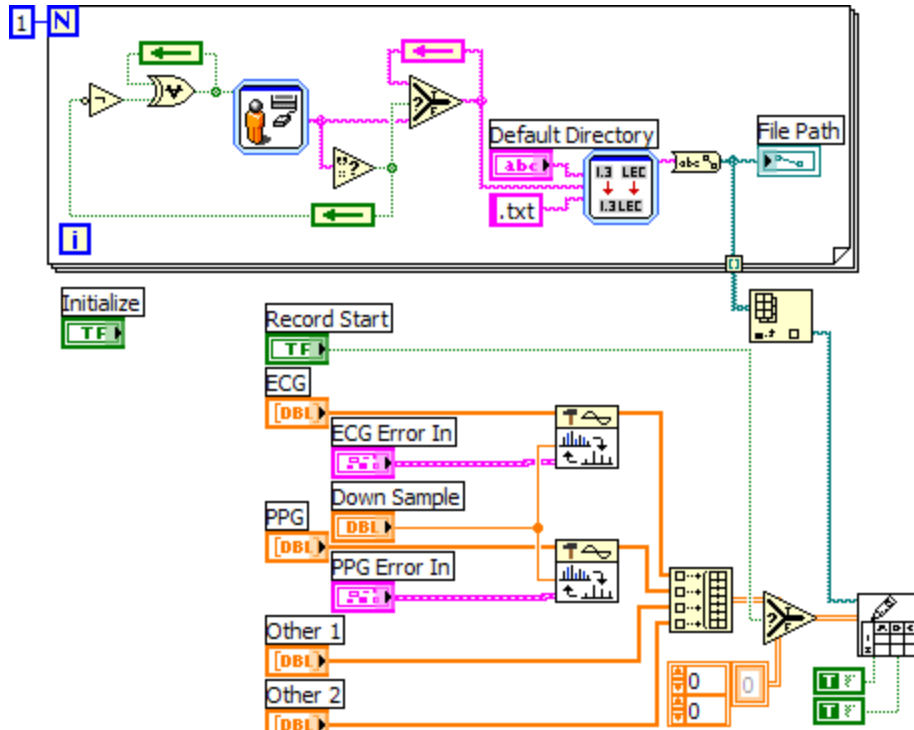


Figure A.24: Signal recording block diagram



**Waveform File Name**

Prompt User for Input

Displays a standard dialog box that prompts users to enter information, such as a user name and password.

-----

This Express VI is configured as follows:

Message to Display to the User: Please specify file name for recorded waveform data

The inputs are:

Text Entry Box: Name



**Build Text**

Build Text

Creates an output string from a combination of text and parameterized inputs. If the input is not a string, this Express VI converts the input into a string based on the configuration of the Express VI.

-----

This Express VI is configured as follows:

Text with parameters: %Path%%Name%%Type%

# Alarm

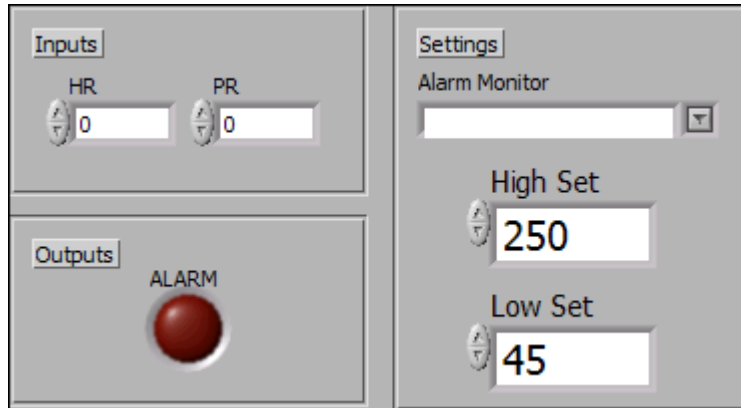
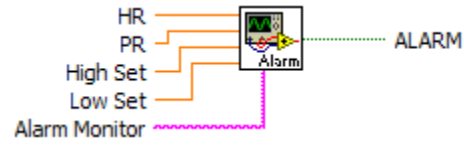


Figure A.25: Alarm control front panel

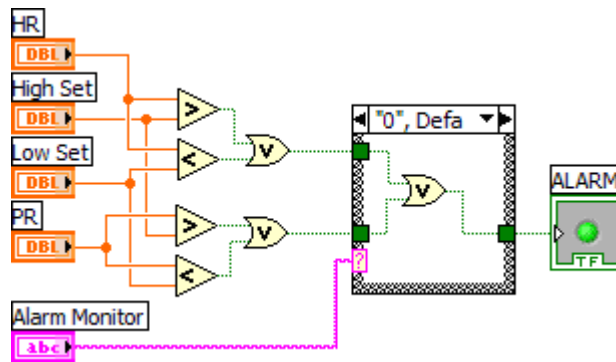


Figure A.26: Alarm control block diagram showing dual analysis

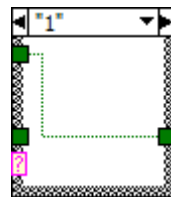


Figure A.27: Alarm control for HR analysis

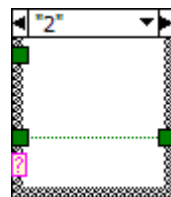


Figure A.28: Alarm control for PR analysis

## **Appendix B. Device Drawings**

## ECG Circuit Design

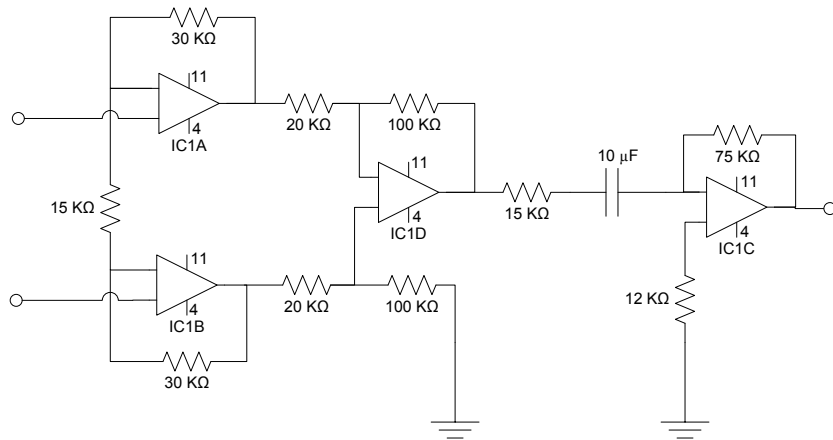


Figure B.1: ECG Circuit Revision A

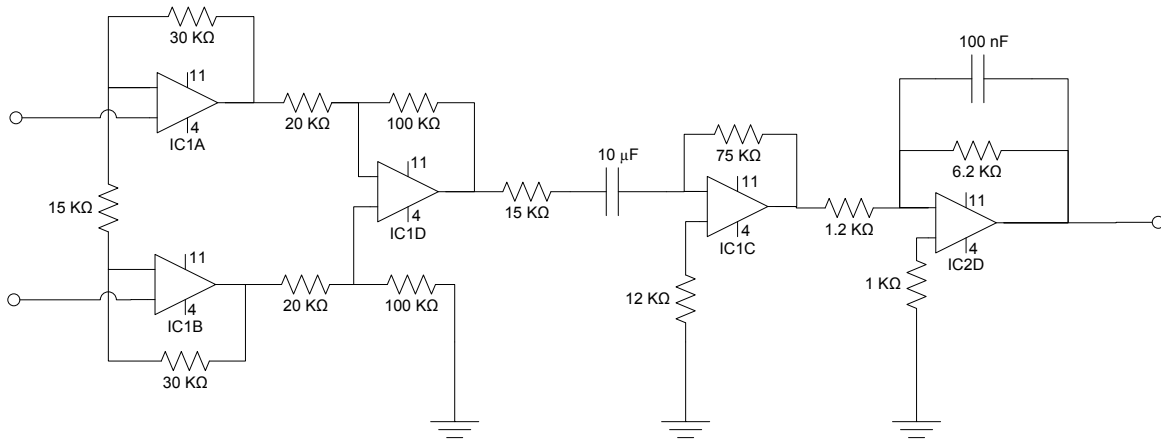


Figure B.2: ECG Circuit Revision B

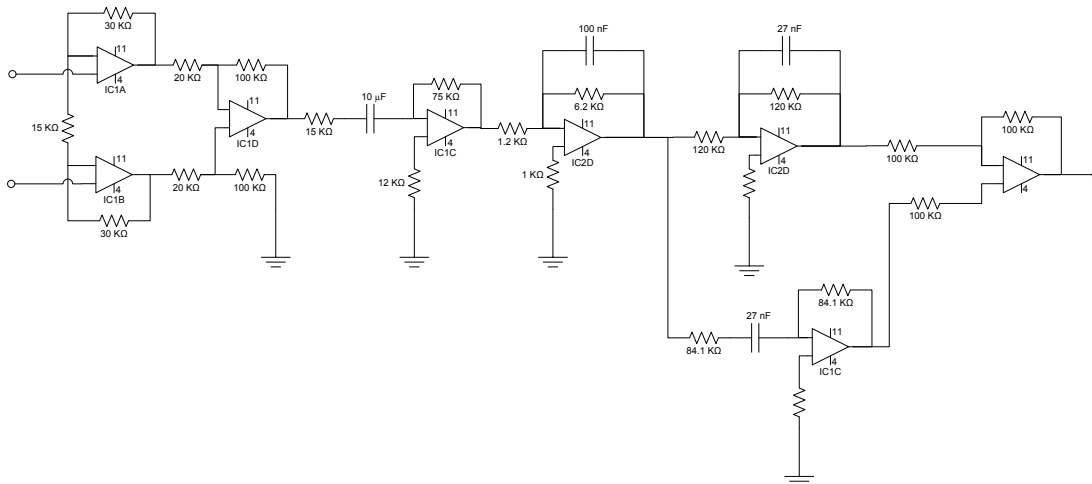


Figure B.3: ECG Circuit Revision C

## PPG Transimpedance Amplifier Circuit

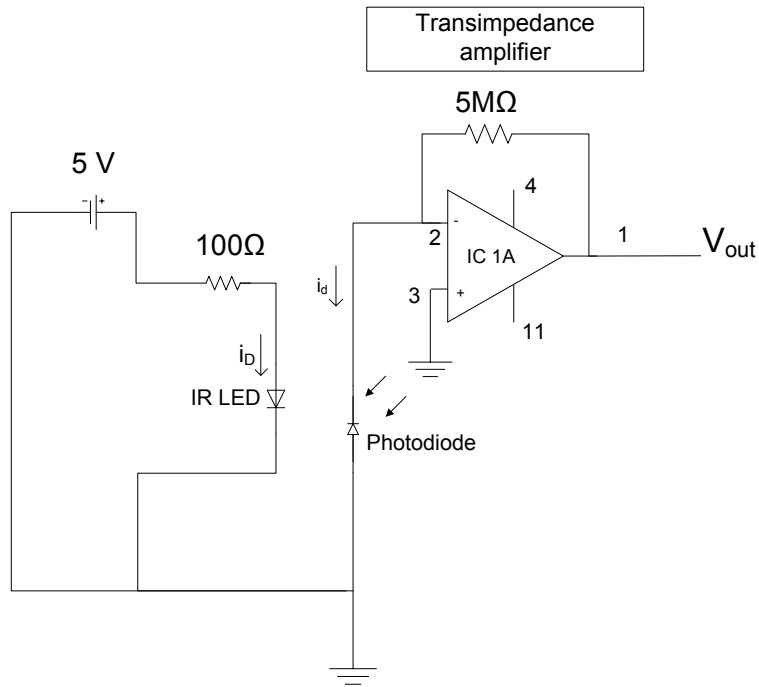


Figure B.4: Simple transimpedance amplifier

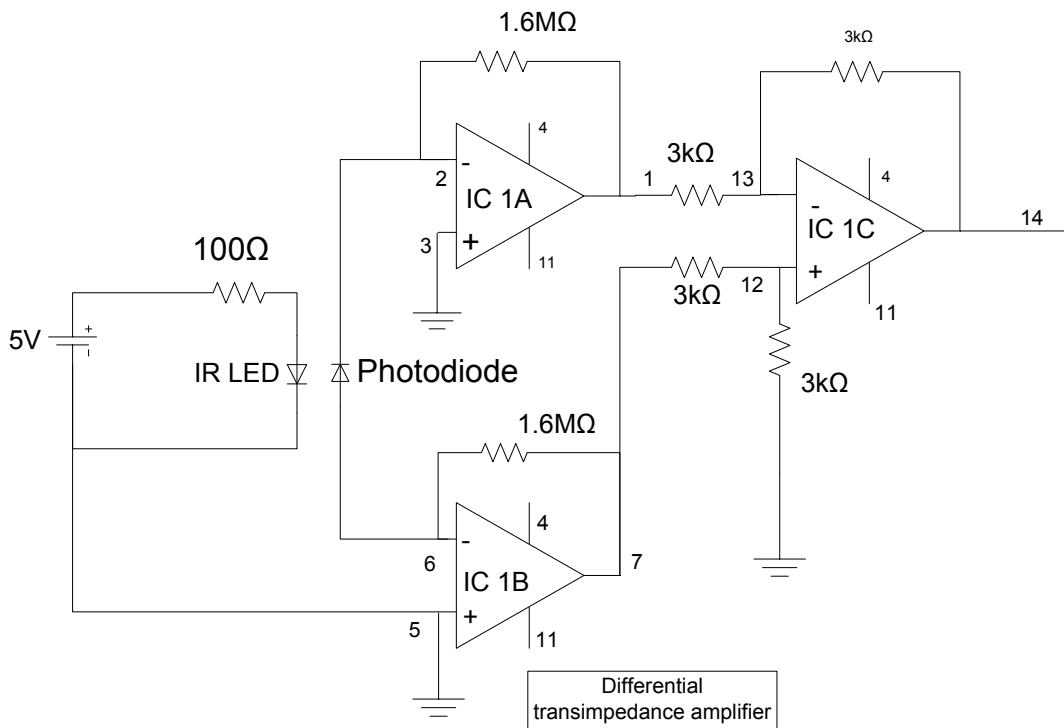


Figure B.5: Differential transimpedance amplifier

# PPG Circuit Design

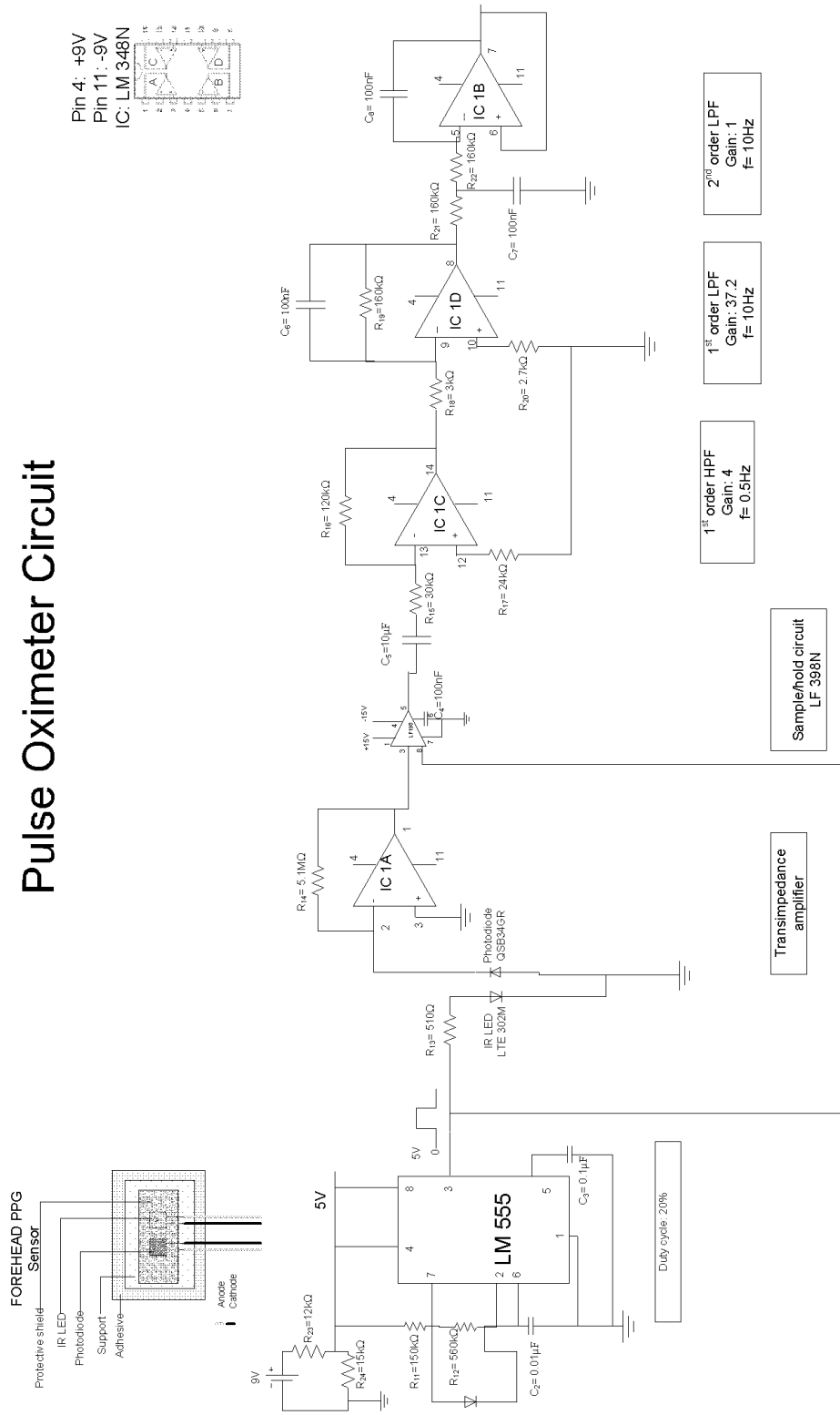


Figure B.6: PPG circuit schematic

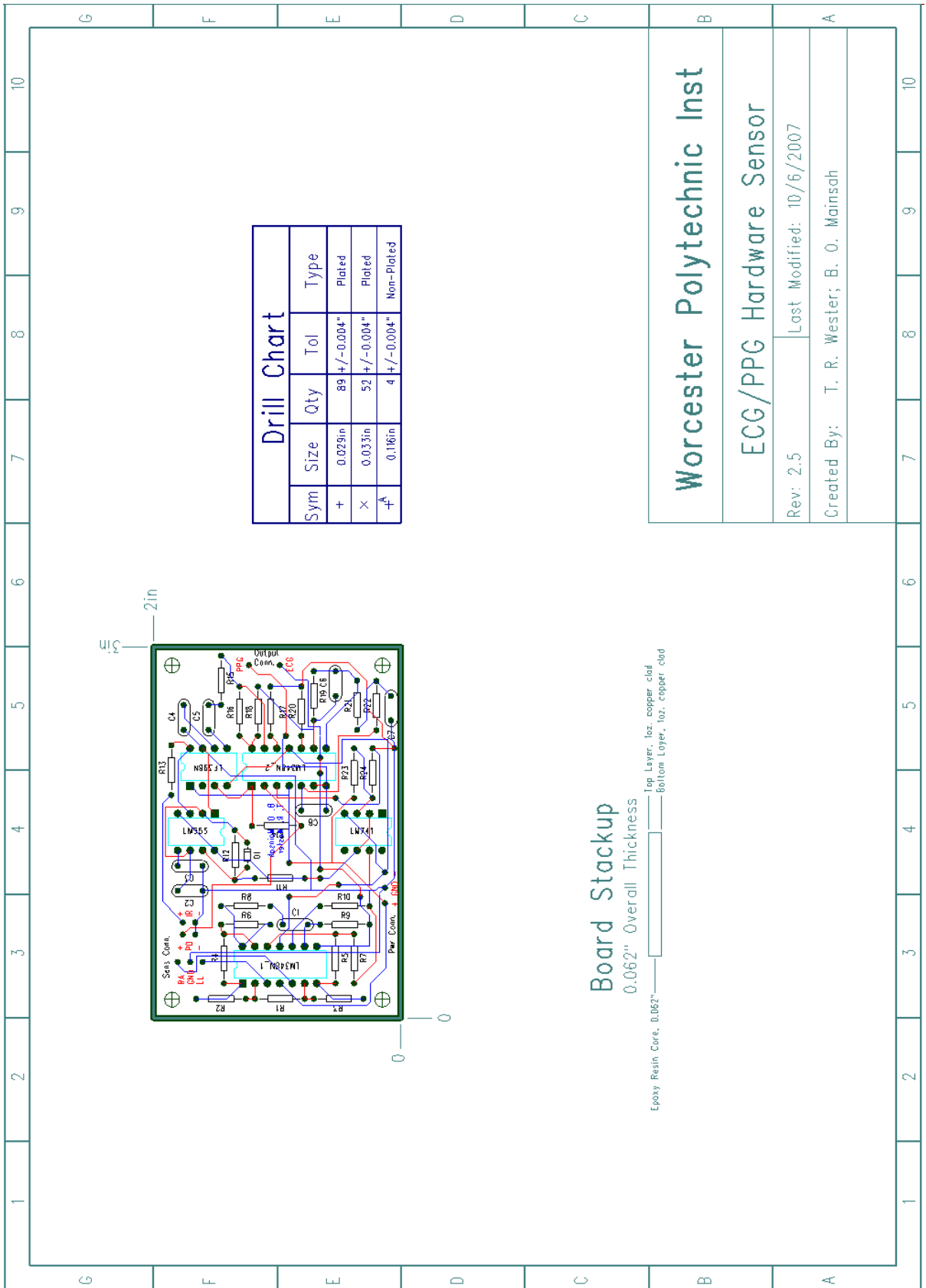
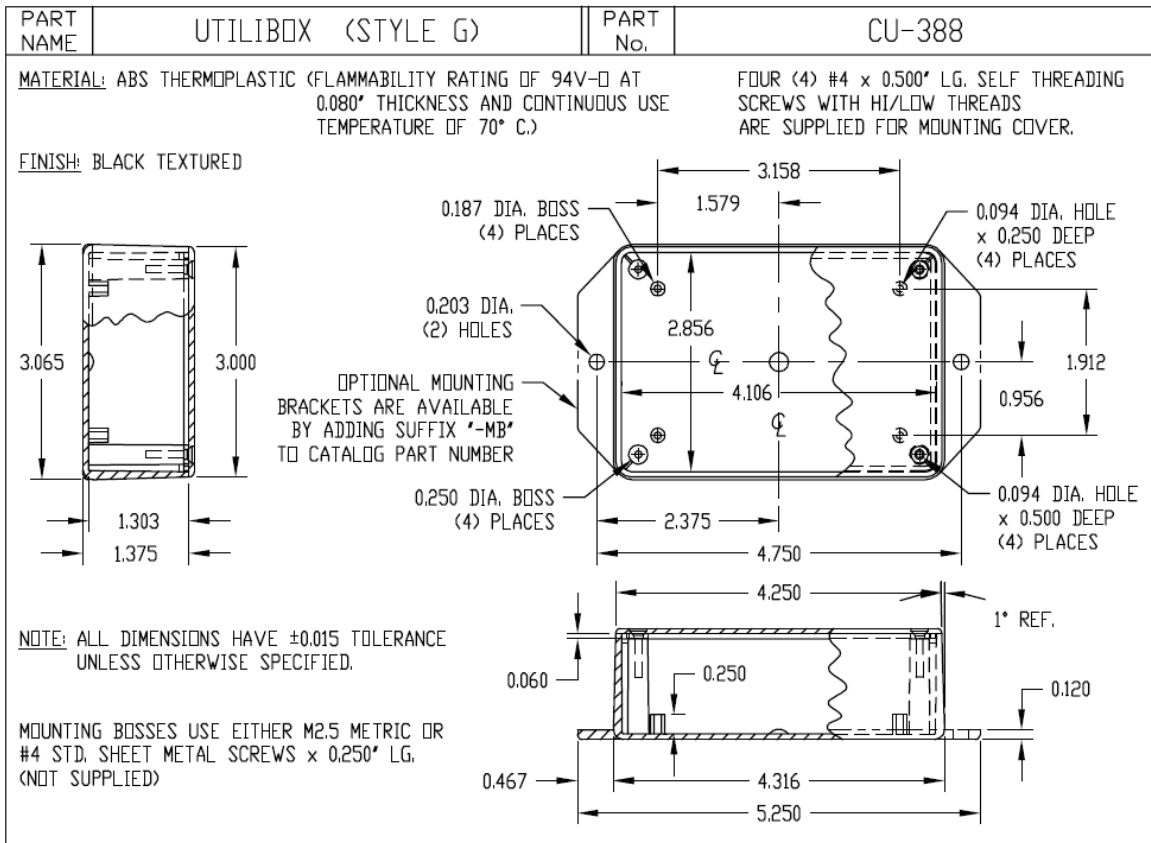
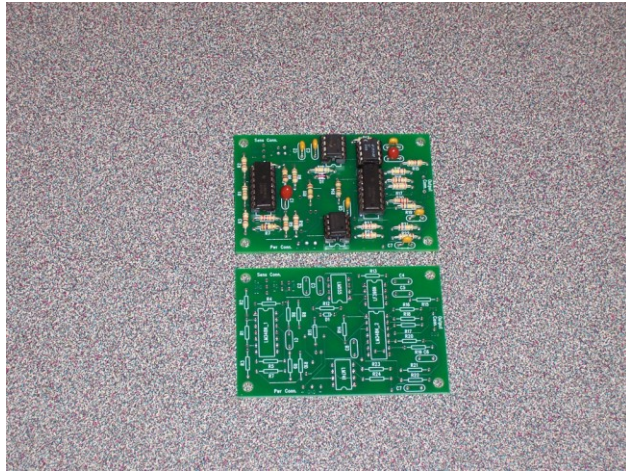


Figure B.7: Printed circuit board schematic



**Figure B.8: Hardware case specifications**

*Printed Circuit Board*



**Figure B.9: Printed circuit board images**

*Visual Assembly*

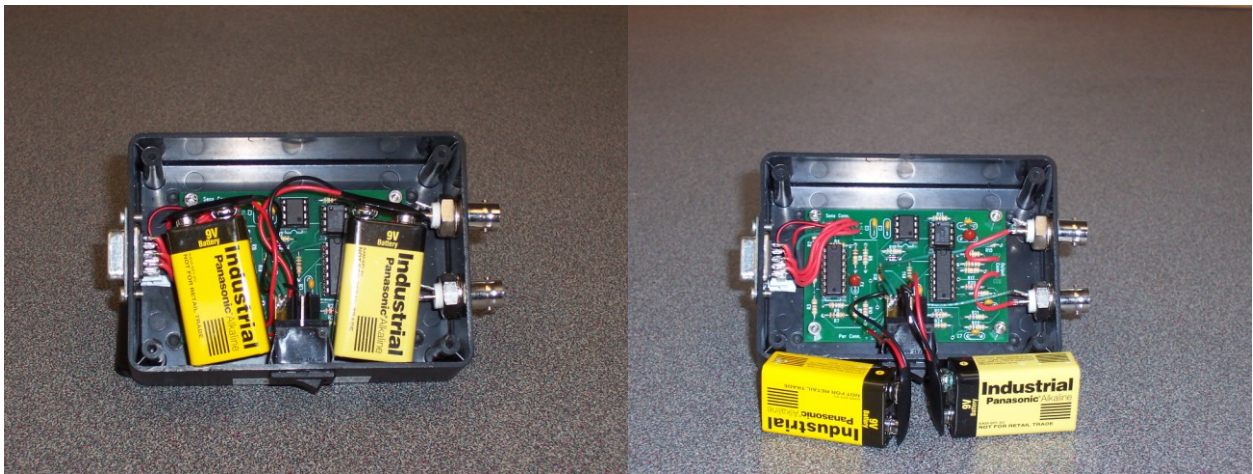


**Figure B.10: Hardware assembly images**

*External Hardware Views*

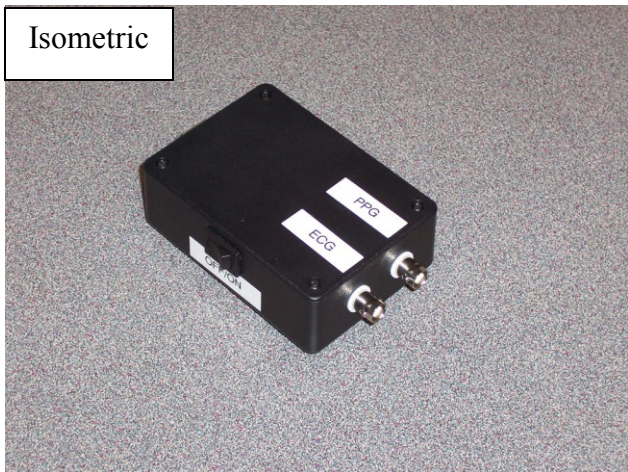
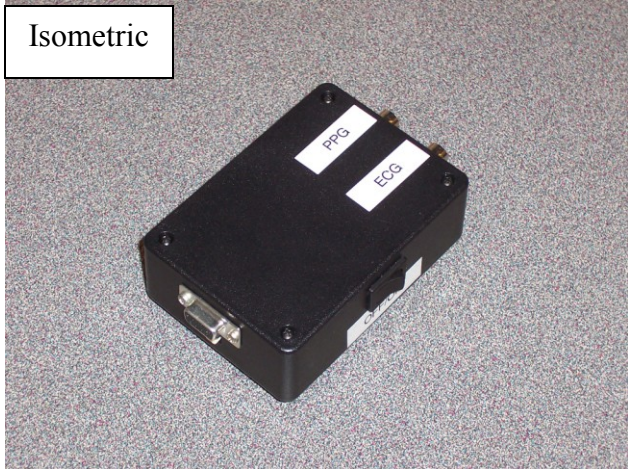


**Figure B.11: Exterior hardware views**

## **Appendix C. Bill of Materials**

**Table C.1: Bill of Materials**

<b>Component</b>	<b>Quantity</b>	<b>Cost per Unit</b>	<b>Total Cost</b>
Resistor – 15 K	3	0.1	0.3
Resistor – 30 K	3	0.1	0.3
Resistor – 20 K	2	0.1	0.2
Resistor – 100 K	2	0.1	0.2
Resistor – 75 K	1	0.1	0.1
Resistor – 12 K	2	0.1	0.2
Resistor – 150 K	1	0.1	0.1
Resistor – 560 K	1	0.1	0.1
Resistor – 510	1	0.1	0.1
Resistor – 5.1 M	1	0.1	0.1
Resistor – 120 K	1	0.1	0.1
Resistor – 24 K	1	0.1	0.1
Resistor – 3K	1	0.1	0.1
Resistor – 160 K	3	0.1	0.3
Resistor – 2.7 K	1	0.1	0.1
Capacitor – 0.1 $\mu$ F	5	0.25	1.25
Capacitor – 0.01 $\mu$ F	1	0.25	0.25
Capacitor – 10 $\mu$ F	2	0.25	0.5
Diode	1	0.1	0.1
PPG LED	1	0.3	0.3
PPG Photodiode	1	0.74	0.74
IC Socket – 8 Pin	3	0.29	0.87
IC Socket – 14 Pin	2	0.29	0.58
LM348N	2	0.5	1
LM741	1	0.5	0.5
LM555	1	0.5	0.5
LF398	1	0.5	0.5
Printed Circuit Board	1	35.83	35.83
DB9 Connector	1	1.99	1.99
ECG Connector Block	1	1.45	1.45
Forehead Sensor	1	5	5
ECG Electrodes/leads	1	N/A	
Device Case	1	5.8	5.8
Rubber Support Feet	4	2.49	9.96
Switch	1	2.34	2.34
BNC Connectors	2	1.99	3.98
Battery – 9V	2	3.99	7.98
<b>Total Device Cost</b>			<b>83.82</b>

## **Appendix D. Component Specifications**

**Table D.1: Component Value Listing**

Component	Value
R1	15 K $\Omega$
R2	30 K $\Omega$
R3	30 K $\Omega$
R4	20 K $\Omega$
R5	20 K $\Omega$
R6	100 K $\Omega$
R7	100 K $\Omega$
R8	15 K $\Omega$
R9	75 K $\Omega$
R10	12 K $\Omega$
R11	150 K $\Omega$
R12	560 K $\Omega$
R13	510 $\Omega$
R14	5.1 M $\Omega$
R15	30 K $\Omega$
R16	120 K $\Omega$
R17	24 K $\Omega$
R18	3 K $\Omega$
R19	160 K $\Omega$
R20	2.7 K $\Omega$
R21	160 K $\Omega$
R22	160 K $\Omega$
R23	12 K $\Omega$
R24	15 K $\Omega$
C1	10 $\mu$ F
C2	0.01 $\mu$ F
C3	0.1 $\mu$ F
C4	0.1 $\mu$ F
C5	10 $\mu$ F
C6	0.1 $\mu$ F
C7	0.1 $\mu$ F
C8	0.1 $\mu$ F

## **Appendix E. User's Manual**

### ***Device Description***

- PC-Based Dual Channel HRV/PRV Monitor

### ***Hardware Suite***

- Dimensions: 4.31x3.06x1.37 inches
- Weight: 8.1 oz (not including sensor probe and electrode leads)
- Color: Black
- Power: Two 9V batteries

### ***Accessories***

- 3-lead electrodes
- Forehead PPG sensor
- CD: HRV Assist
- User manual

### ***System Requirements***

- NI Data Acquisition Board
- LabVIEW 8 or higher

### ***Patient Range***

- Adult

### ***Performance Specifications***

- Waveform Displays
- Alarm indicator
- High and Low Alarm controls
- QRS beep and alarm sound
- HR/PR Averaging: Instantaneous, 5-beat, 8-beat averaging
- HRV/PRV Averaging buffer: 30 seconds, 1 minute, 5 minutes

### **ECG**

- Input: 3-lead: RA; LA; LL or R; L; F
- Lead selection: Lead IIECG waveform: 1 channel
- Bandwidth: 0.05-35Hz
- HR range: Adult: 15-240bpm
- Accuracy:  $\pm 1$ bpm or  $\pm 1\%$ , whichever is greater
- Alarm range: Adult: 15-240bpm
- QRS indicator: Audible

### **PPG**

- Input: Forehead sensor
- Sensor mode: Reflectance (IR wavelength only)
- PPG waveform: 1 channel
- Bandwidth: 0.05-10Hz
- PR range: Adult: 30-240bpm
- Accuracy:  $\pm 1$ bpm, @ 30 - 120 bpm during rest
- Alarm range: Adult: 15-240bpm

### **Software**

- Adjustable Threshold Peak detection
- Abnormal R-R Interval Rejection

### *PPG Sensor Suite*

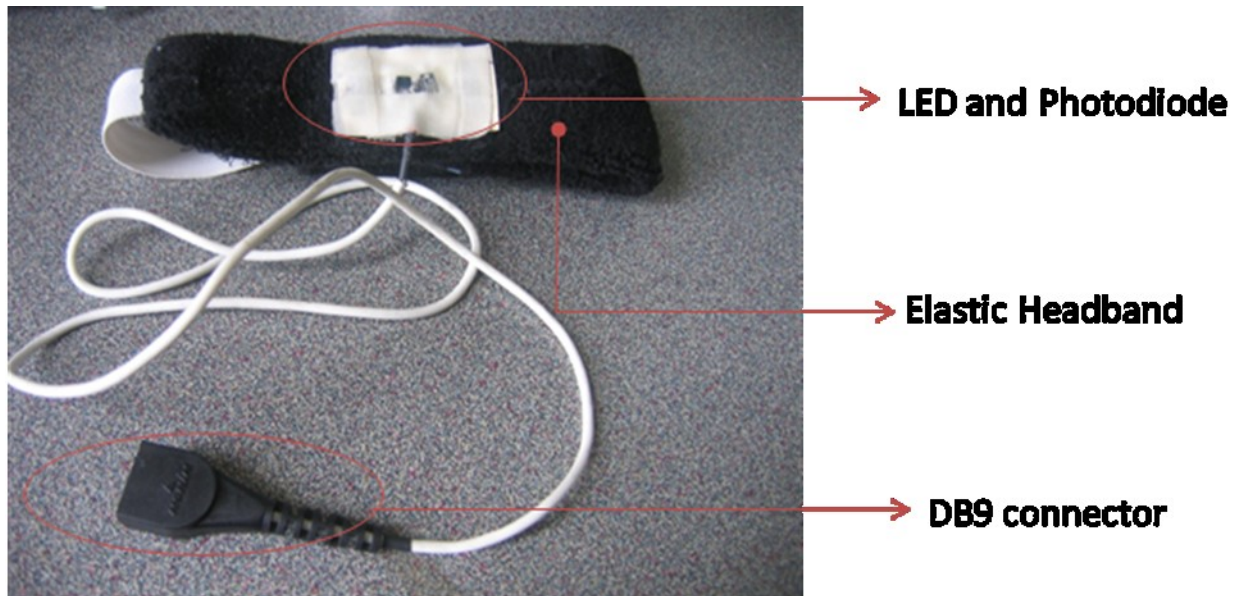


Figure E.1: PPG sensor suite

### *ECG Electrode Leads*

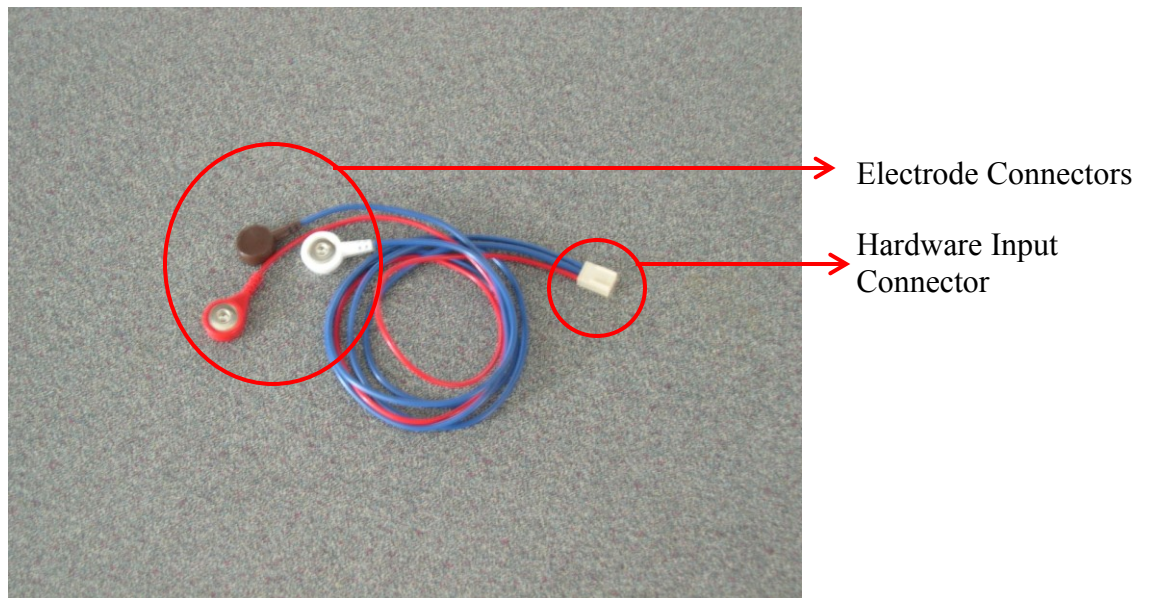


Figure E.2: ECG electrode leads

## Hardware Suite

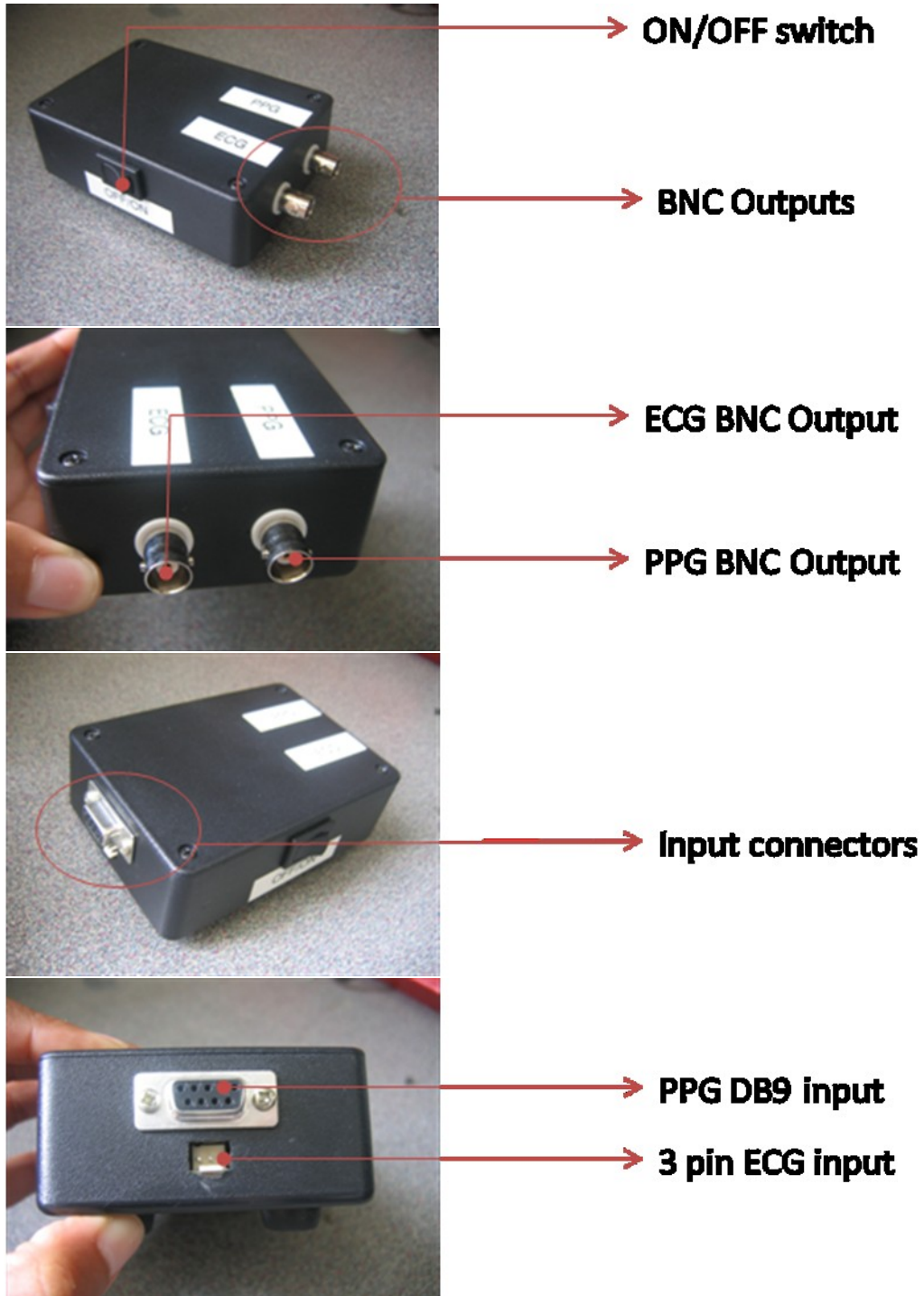
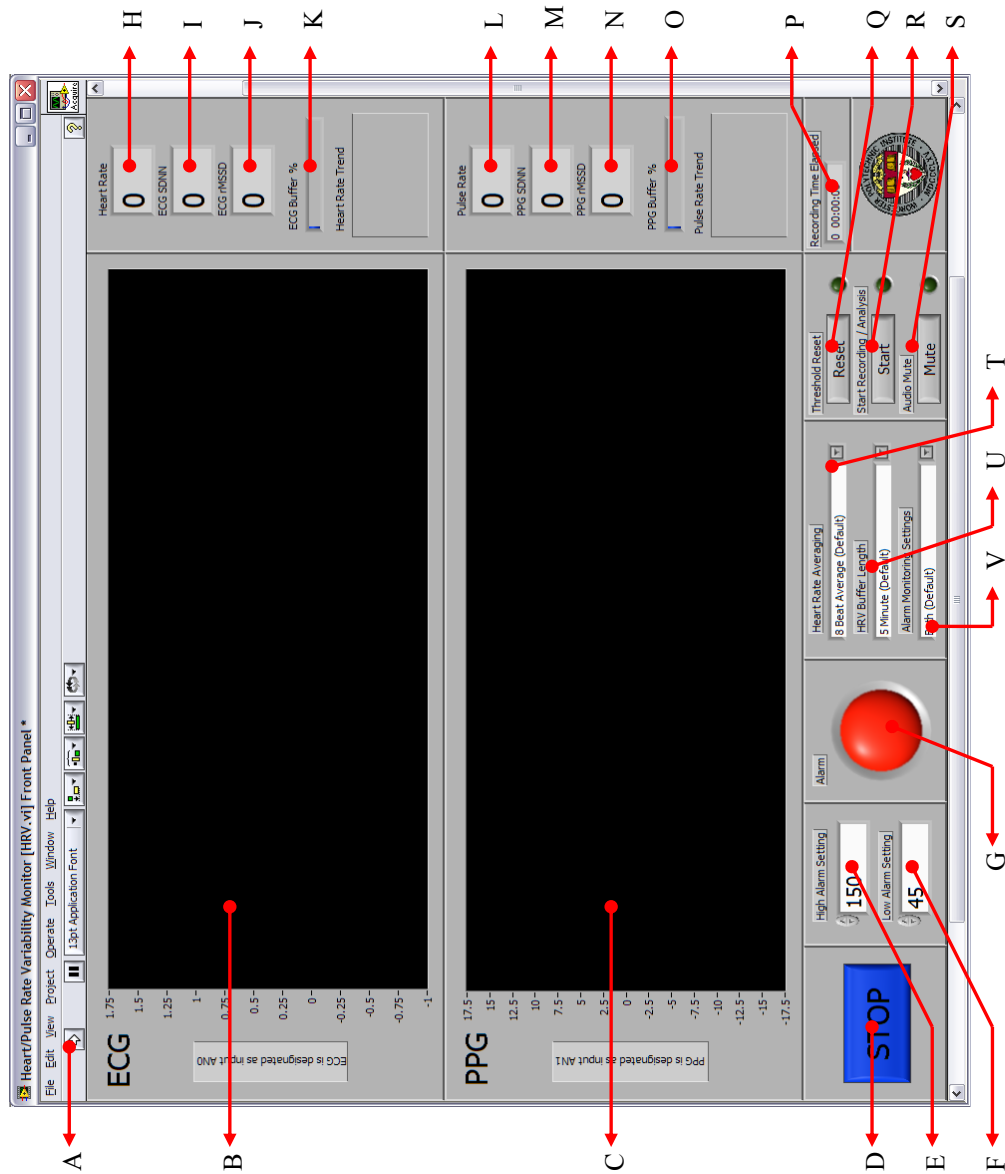


Figure E.3: Hardware suite with labels

**Software: HRV Assist**

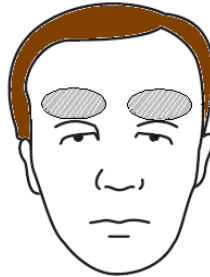


**Figure E.4: Software front panel with labels**

- |                          |                                            |
|--------------------------|--------------------------------------------|
| A Start Data Acquisition | L PR display                               |
| B ECG Signal display     | M PPG SDNN display                         |
| C PPG Signal display     | N PPG rMSSD display                        |
| D Stop button            | O PRV Buffer Indicator                     |
| E High alarm control     | P Recording Time Elapsed                   |
| F Low alarm control      | Q Manual Threshold Reset and LED indicator |
| G Alarm LED              | R Start Data Analysis and LED indicator    |
| H HR display             | S Beep Mute Switch and indicator           |
| I ECG SDNN display       | T HR/PR averaging control                  |
| J ECG rMSSD display      | U HRV/PRV Buffer Size control              |
| K HRV Buffer Indicator   | V Alarm setting control                    |

### ***PPG Sensor Application***

1. Clean the PPG sensor site with alcohol to remove any skin oils. See shaded illustration below for the recommended site.



2. Fasten elastic band around head, placing LED /Photodiode arrangement being placed directly over cleaned area. Avoid hair covering the diode unit. Fasten to ensure close contacts between sensor and skin.
3. Plug in the PPG sensor into the DB9 connector of the hardware unit.



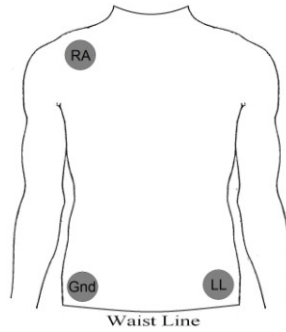
**PPG DB9 connector**

4. Plug in BNC connector labeled PPG to AN1 of the DAQ Assist



### ***ECG Sensor Application***

1. Clean the ECG electrode site with alcohol to remove any skin oils. See shaded illustration below for the recommended site.
2. Place adhesive electrode over cleaned area
3. Snap electrode lead connectors unto electrode with the following
  - a. Red: Ground (Gnd)
  - b. Brown contact with blue wire: Right Arm (RA)
  - c. White contact with blue wire: Left torso (LL)



4. Plug in the tri-electrode lead wire to the electrode connector of the hardware unit.

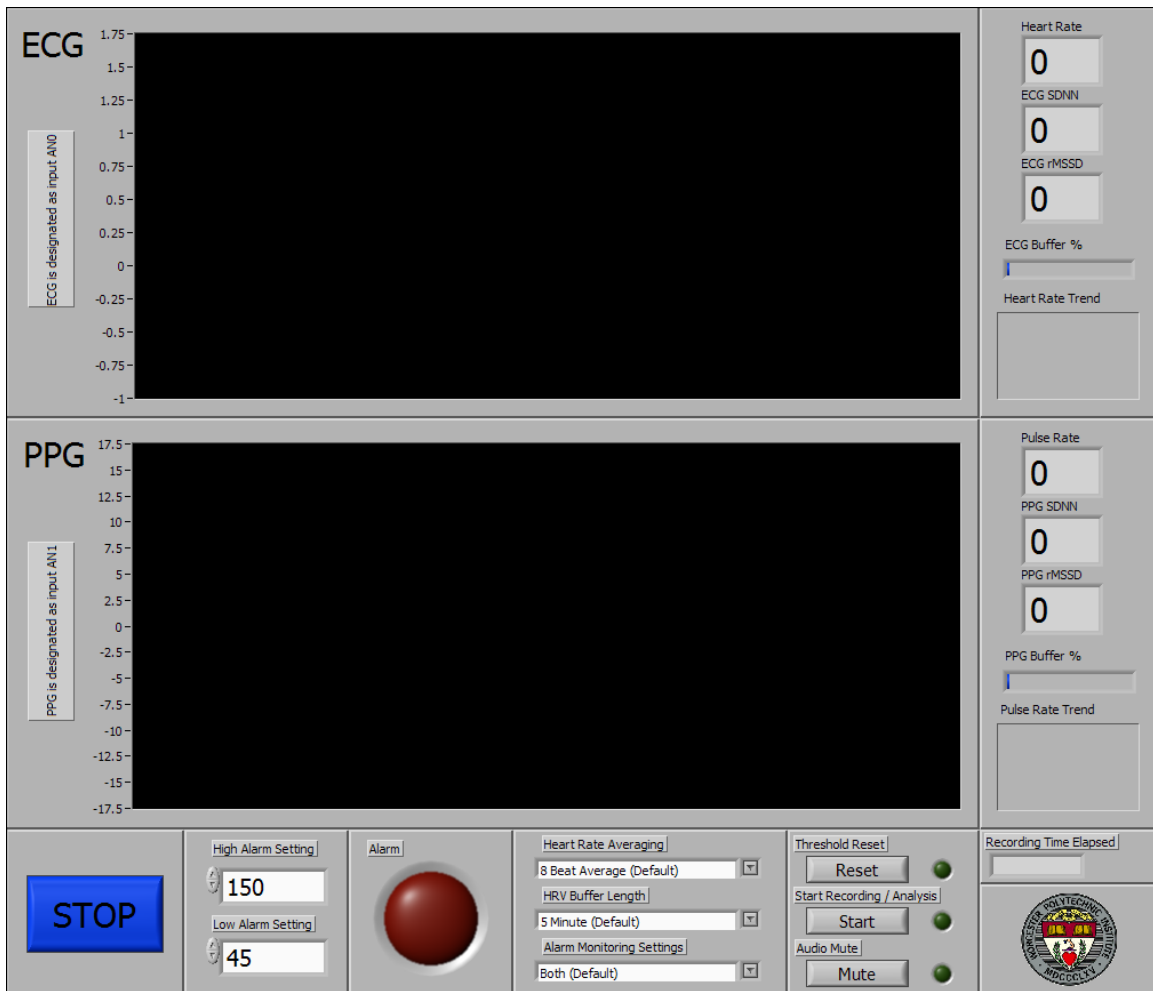


5. Plug in BNC connector labeled ECG to AN0 of the DAQ Assist.



### ***To start signal acquisition***

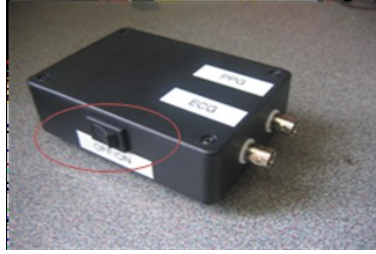
1. Adjust patient properly in front of computer.
2. Open LabVIEW VI labeled "HRV.exe"



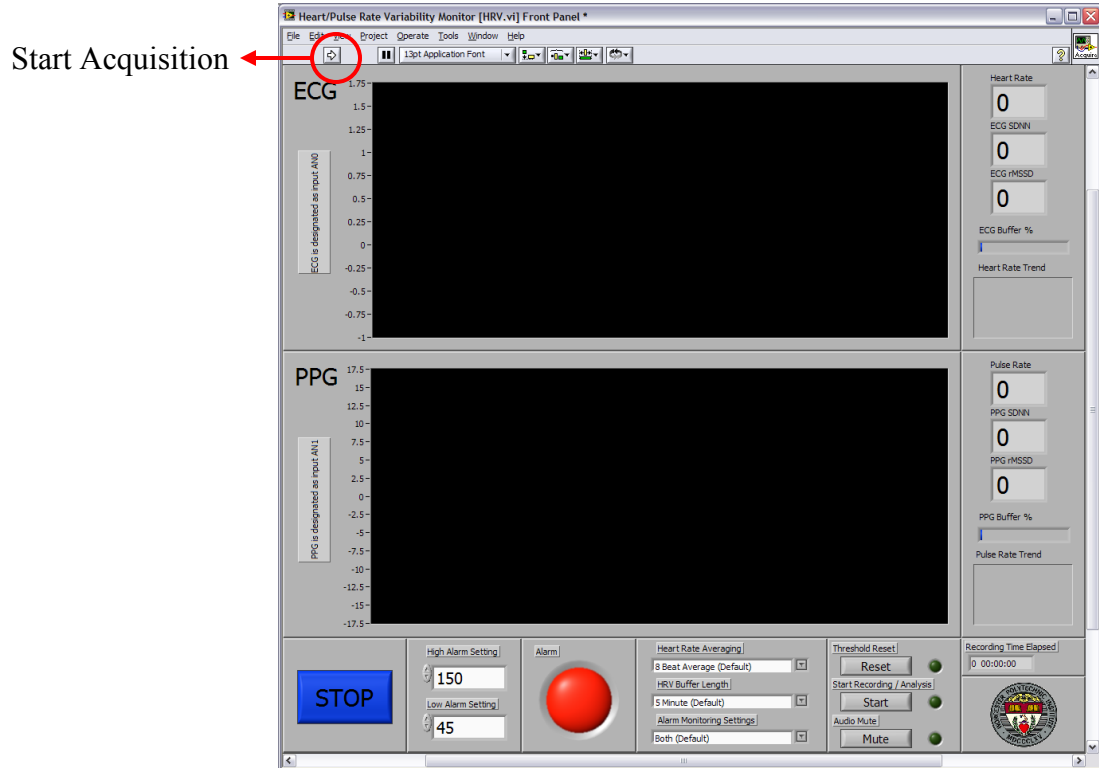
3. Enter HR alarm range in the controls labeled HIGH AND LOW ALARMS. Default values are 150 and 45 BPM respectively.
4. Configure the following parameters from the following options as desired:

Control	Description	Options
HR Averaging	Controls the number of beats used to compute the HR/PR.	Instantaneous HR 5-beat Average 8-beat Average (Default)
HRV Buffer Size	Controls window size to compute HRV and PRV indices	30 seconds 1 minute 5 minutes (Default)
Alarm Monitor Setting	Controls which signals to trigger alarm off its high or low values	ECG Signal PPG Signal Both (Default)

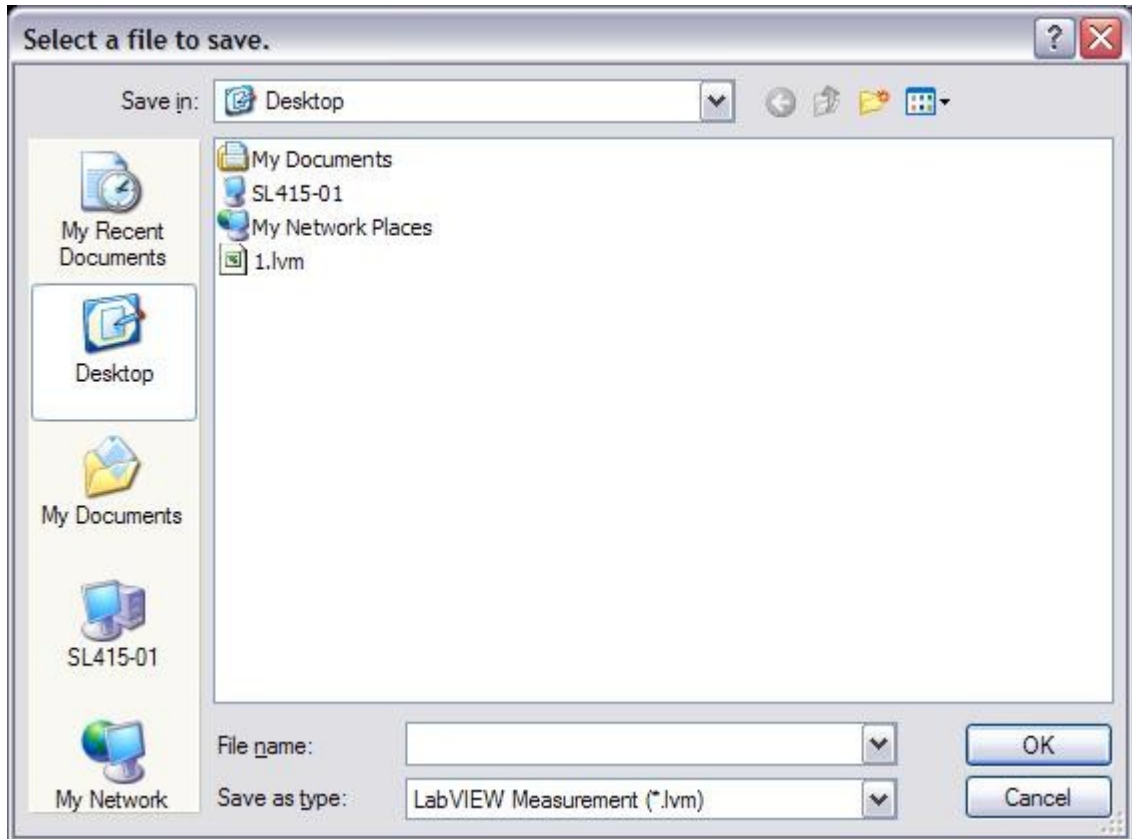
5. When patient is ready, turn on the switch on the hardware.



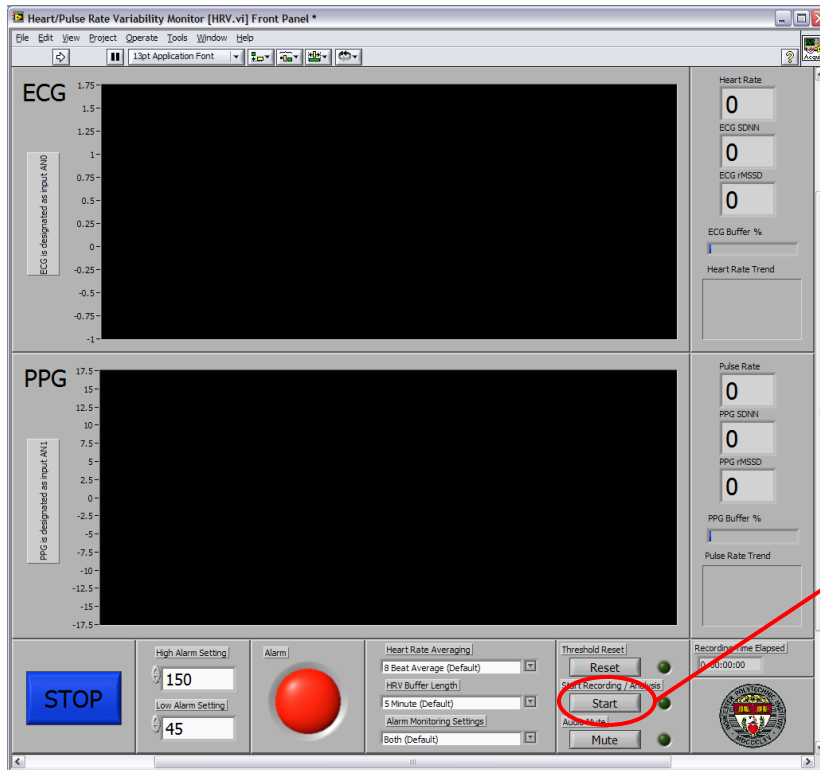
- To start data acquisition, click on the arrow key () labeled below.



- This will prompt a dialog box named SELECT A FILE TO SAVE. Enter desired file name and save location, then click OK.



8. You should ECG and PPG signals on the monitor, and hear heart beep sound. Beep sound can be turned off with the MUTE button.  
Note: If signals do not display:
  - check that ECG and PPG are connected to inputs 0 and 1 respectively
  - check that ECG leads are properly attached using the specified colour codeIf an unusual PPG waveform is observed, adjust PPG sensor till a proper signal is observed.  
If no signals displayed after the above adjustments, replace device battery
  
9. To start signal analysis recording analysis, click the START button. The Start LED should turn ON.  
Note: HRV and PRV indices will not display till respective buffers (blue) are full.



Start Data Analysis

10. If an abnormally high PR or HR is observed, click on the RESET button to reset threshold value. Deactivate, clicking on button when adjusted HR is observed.
11. To stop data recording analysis, click the start button. The Start LED should turn OFF. Signals will still be observed.
12. To stop data acquisition, click on the blue STOP button.

## **Appendix F. Test Results**

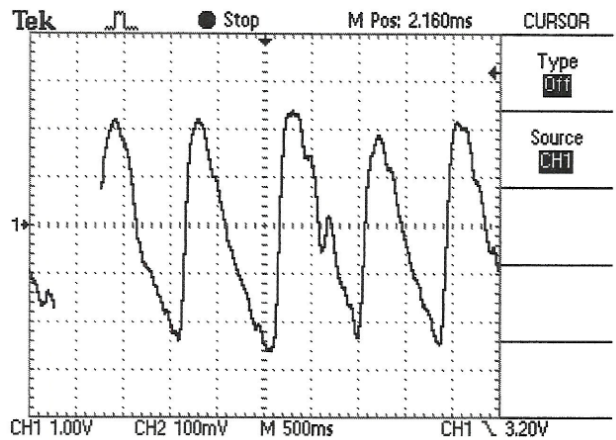
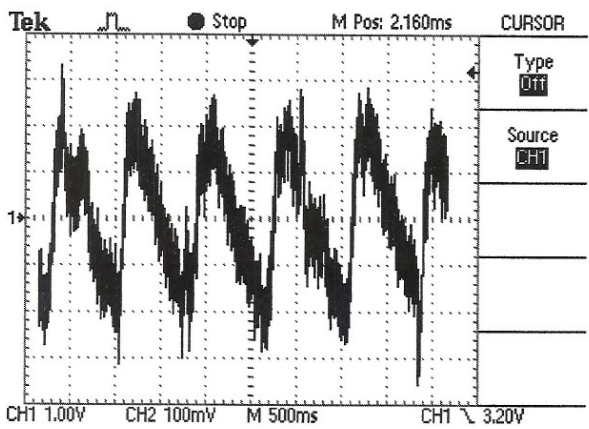
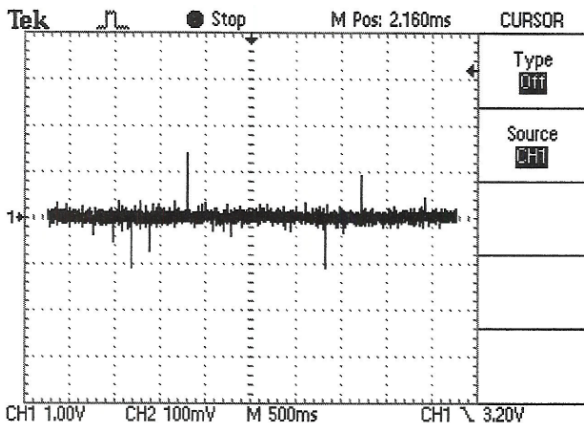
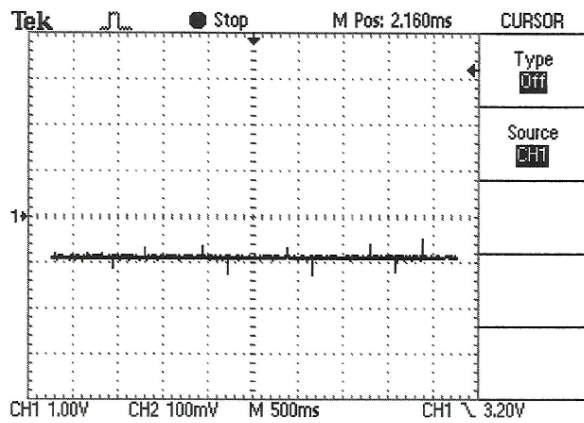
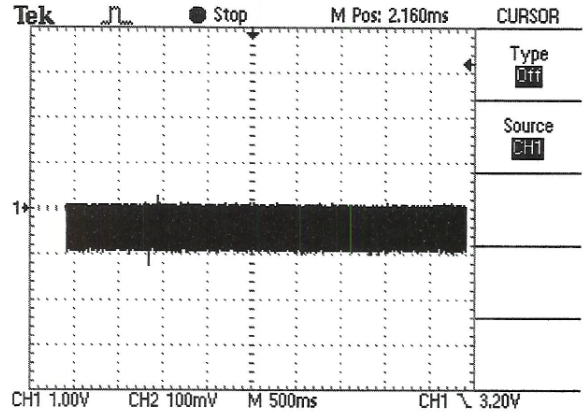
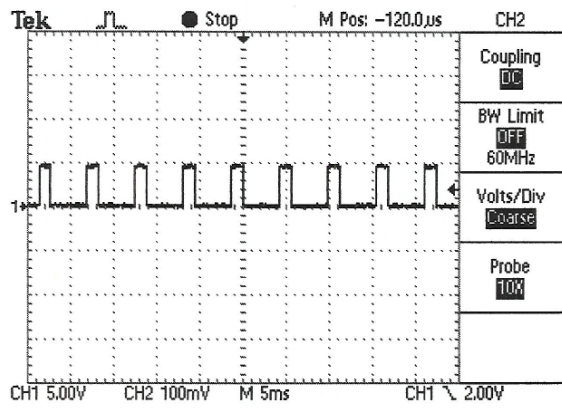


Figure F.1: PPG circuit test points

**Table F.1: ECG elapsed time error analysis**

30 BPM	60 BPM	120 BPM	240 BPM
1.891	0.906	0.391	0.109
1.906	0.906	0.406	0.203
1.891	0.891	0.406	0.109
1.907	0.891	0.391	0.203
1.891	0.891	0.406	0.109
1.891	0.906	0.406	0.203
1.907	0.906	0.406	0.109
1.907	0.906	0.406	0.203
Expected (Seconds)			
2	1	0.5	0.25
Averaged Error (Seconds)			
0.101125	0.099625	0.09775	0.094

**Table F.2: PPG elapsed time error analysis**

30 BPM	60 BPM	120 BPM	240 BPM
1.89	0.89	0.407	0.203
1.89	0.89	0.407	0.109
1.89	0.906	0.407	0.203
1.906	0.89	0.407	0.109
1.797	0.89	0.407	0.203
1.906	0.89	0.407	0.109
1.906	0.906	0.407	0.203
1.703	0.89	0.407	0.109
Expected (Seconds)			
2	1	0.5	0.25
Averaged Error (Seconds)			
0.139	0.106	0.093	0.094

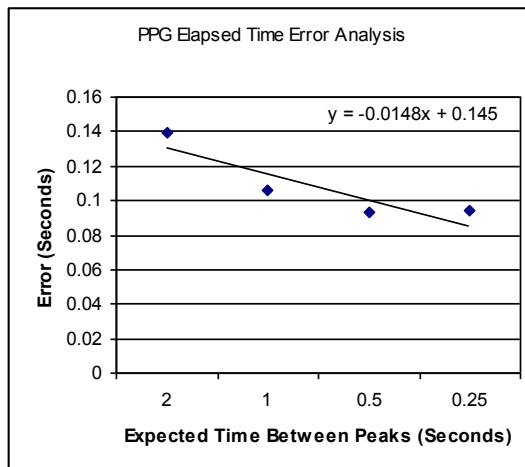
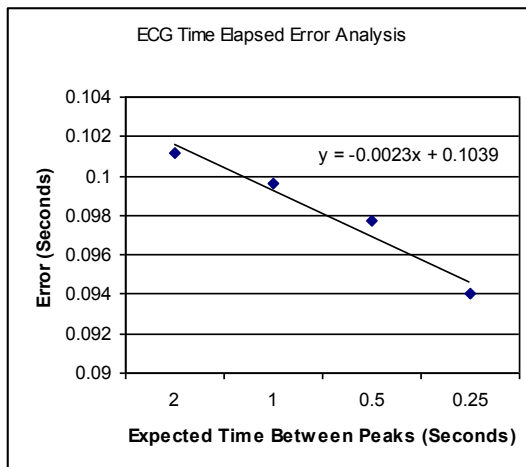


**Figure F.2: ECG/PPG elapsed time error analysis**

**Table F.3: Signal comparison with motion artifact**

	Moderate Intensity		High Intensity	
Rest	95.50	93.95	84.20	83.68
	7.41	7.74	4.15	4.77
Upper Body Motion	101.79	91.49	88.72	89.61
	18.12	21.14	7.24	8.02
Lower Body Motion	100.34	100.25	93.44	92.10
	8.82	10.89	7.56	35.45
Lateral Head Motion	91.97	91.35	95.61	93.20
	4.74	15.15	5.81	7.28
Up-Down Head Motion	89.37	85.97	90.43	91.09
	4.41	12.82	5.24	8.36
Fast Breathing	94.35	95.99	85.68	87.44
	4.04	12.04	7.77	7.00
Slow Breathing	100.72	102.19	90.81	89.75
	9.52	13.72	5.18	6.34

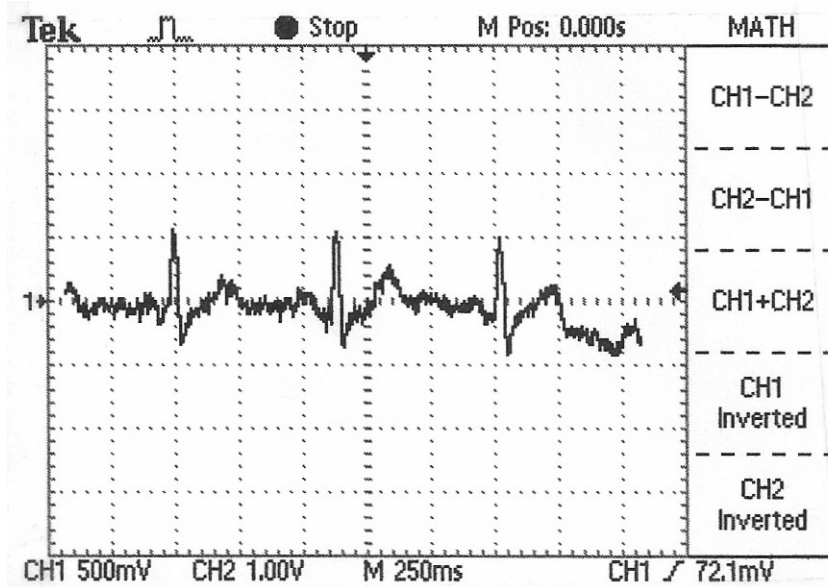


**Figure F.3: Stainless steel electrodes**

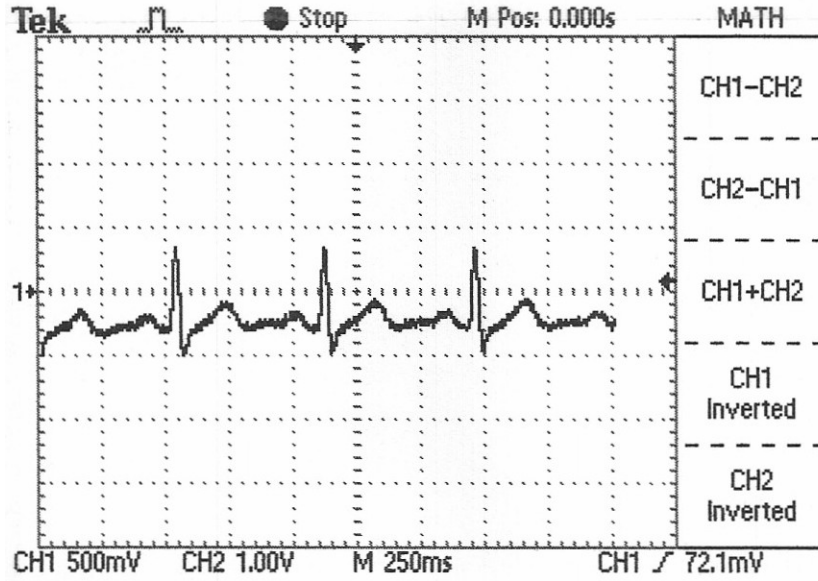


Figure F.4: Ag/AgCl electrode without adhesive

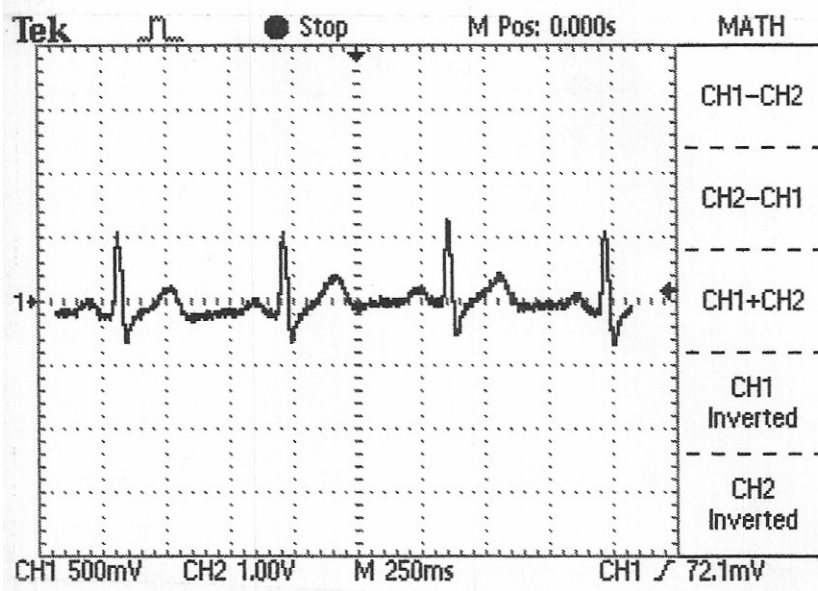


Figure F.5: Ag/AgCl electrode with adhesive

## **Appendix G. Industry Product Specifications**

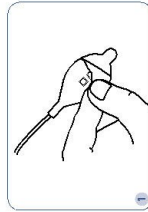
**Table G.1: Dual channel ECG/PPG monitor**

		<b>Mindray PM 7000</b>	<b>Vitalmax 4100CL</b>	<b>DINAMAP Pro 100</b>
Display type		Color	Color	Color
ECG	Input	5 lead 3 lead	3 lead	3 lead
	HR range	Adult: 15-300bpm Pediatric/neonatal: 15-350bpm	30-254bpm	30-300bpm
	Heart rage averaging		4 beat average	
	Accuracy	±1bpm or ±1%	±5bpm or 10%	±3bpm
	Bandwidth	0.05-100Hz	0.5-40Hz	0.5-40Hz
	Alarm	Yes	Yes	Yes
PPG	Sensor type	Mindray SpO <sub>2</sub> , Masimo SET SpO <sub>2</sub> , Nellcor SpO <sub>2</sub>	Finger, universal, earlobe clip, disposable and reusable wrap probe	Nellcor, Masimo SET SpO <sub>2</sub>
	PR range	0-254bpm	30-254bpm	25-250bpm
	PR averaging		8 second averaging	
	Accuracy	±2bpm	±2% at 30-100bpm	±3 digits

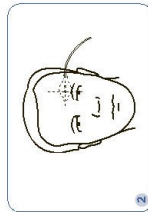
**Table G.2: Portable pulse oximeter sensor battery life**

<b>Model</b>	<b>Battery Life</b>
Nonin PalmSAT® 2500	100 hrs : 45 hours from rechargeable batteries
Nellcor OxiMax® N-65™	19 or 40 hours depending on battery type
Nellcor N-20PA	32 hours
Mindray PM-60	36 hours
Mindray VS-800	10 hours

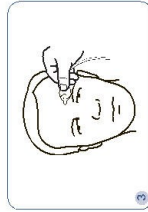
## OXIMAX<sup>®</sup> MAX-FAST<sup>®</sup> FOREHEAD SENSOR



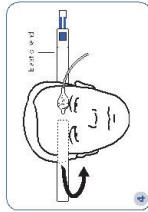
1 Before applying the sensor, clean the site with an alcohol wipe to remove skin oils. The Oximax<sup>®</sup> Max-Fast<sup>®</sup> sensor has three extra adhesive layers with different colored tabs. Peel off the white paper backing to expose the first adhesive layer.



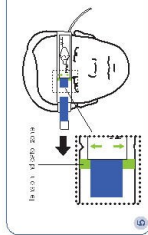
2 Place the sensor just above the left or right eyebrow, centering it with the iris. This position is key to obtaining optimal results, since pulse perfusion is stronger in the lower forehead area and is weaker higher up. Do not place the sensor on the temple.



3 Press the sensor firmly on the site for 10 seconds to ensure the entire surface adheres to the patient's skin. If desired, secure the sensor cable to the patient's clothing with the cable clip to prevent it from pulling on the sensor. Push the sides of the clip to open it and release to close.



4 To apply the optional Max-Fast Headband included in the sensor pouch, place the headband behind the patient's head with the printed elastic band facing out. Allow the headband to extend more on the side with the elastic band. Wrap the short end of the headband toward the patient's forehead. Bring the elastic band side across the patient's forehead, overlapping the sensor and other end of the headband.



5 Align the sensor outline on the elastic band over the Max-Fast sensor. Pull the Velcro<sup>®</sup> tab until the green arrows on the elastic band are within the tension indicator zone. Adjust within the tension indicator zone for optimum patient comfort and oximetry performance. To secure the headband, fasten with the Velcro tab. The headband is now properly placed. Periodically check headband. When the arrows are no longer aligned within the tension indicator zone, readjust the headband for proper fit.



Max-Fast Package

Read the instructions for use included in the Max-Fast<sup>®</sup> sensor pouch. For more information, visit [www.nellcor.com](http://www.nellcor.com).

## OXIMAX<sup>®</sup> MAX-FAST<sup>®</sup> FOREHEAD SENSOR



### WHY PROPER SENSOR PLACEMENT IS ESSENTIAL

As part of the Nellcor<sup>®</sup> Oximax Pulse Oximetry System, the Max-Fast Forehead Sensor offers an advancement in patient safety monitoring, because it detects changes in arterial oxygen saturation (SpO<sub>2</sub>) significantly sooner than distal sensors for patients with poor pulse perfusion. However, complexities of the anatomy make it essential to place the Max-Fast sensor on the proper area of the forehead to ensure reliable, accurate pulse oximetry readings.

### INTERNAL CAROTID ARTERY—THE KEY TO SENSOR PLACEMENT

Optimal placement of the Max-Fast Forehead Sensor is based on arterial circulation from the region of the skin in the forehead. The internal carotid artery is an artery that branches off from the aorta and carries oxygenated blood to the head and brain. This region has the following advantages for pulse signal detection:

- Little vasoconstriction compared with peripheral or ear sensor sites.
- Strong pulsatile signals without interference from large vessels.

### BENEFITS OF USING THE HEADBAND

The Max-Fast Headband helps hold the sensor in place and applies gentle pressure to expel any pulsing venous blood from the sensor site, if present. The headband is strongly recommended for optimal performance when patients are:

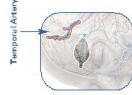
- Lying down and the head is near or below chest level.
- Subject to elevated venous pressure.
- Diaphoretic.
- Moving excessively, such as during exercise.

Note: Forehead sensors are contraindicated for patients in Trendelenburg's head-down position.

### SENSOR APPLICATION TIPS

Check the forehead sensor site every 12 hours for skin integrity and sensor adhesion. Move the Max-Fast Forehead Sensor to a new area as necessary.

When repositioning the sensor following a site check, remove the current adhesive ring to expose a fresh layer of adhesive, and clean the new site prior to application.



### AREAS TO AVOID

Large, pulsing blood vessels (e.g., arteries) can cause the sensor to give a false reading. Avoid placing the sensor directly on large, light-absorbing objects that move with the heartbeat. Therefore, do not place the Max-Fast sensor on the temple, or on the midline or upper areas of the forehead.

If you have any questions about the Max-Fast Forehead Sensor or would like to receive instructional copies of this Application Guide, contact your local Nellcor representative or call Customer Service at 1-800-NELLCOR.



4245 MacArthur Drive  
Parsippany, NJ 07054  
USA  
Tel: 908-252-3355  
Fax: 908-252-3356  
www.tyco.com



Figure G.1: Industry forehead PPG sensor

**Marquette Medical Systems 8500 Series Holter Monitor**

**Table G.3: Marquette Medical Systems Holter Monitor**

Length	Width	Height	Weight
6.0 inches	3.25 inches	1.125 inches	~10 oz



**Figure G.2: Marquette Medical Systems holter monitor**



**Figure G.3: Internal view of Marquette holter monitor**

## **Appendix H. Physiological Information**

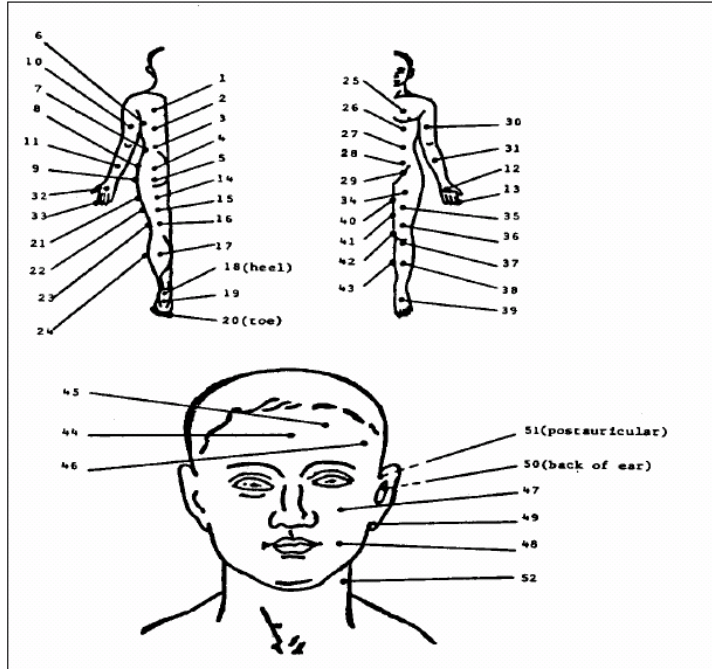


**Figure H.1: Anatomic references of perfusion measurements**  
 Figure courtesy of E. Tur *et al* [59]

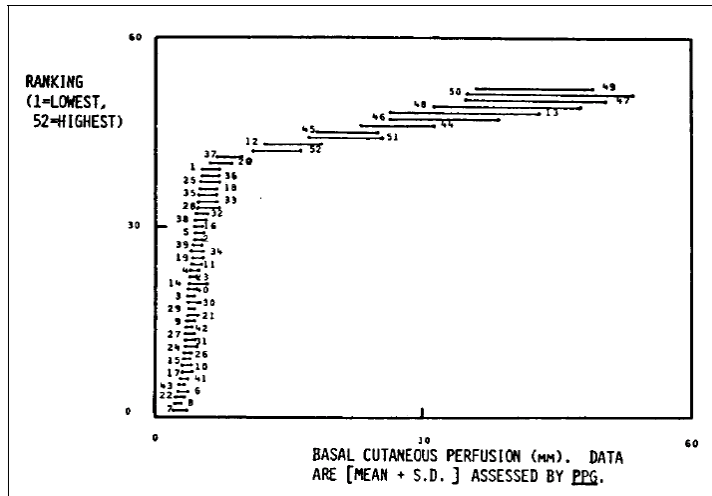


**Figure H.2: Ranking of perfusion measurements**  
 Figure courtesy of E. Tur *et al* [59]

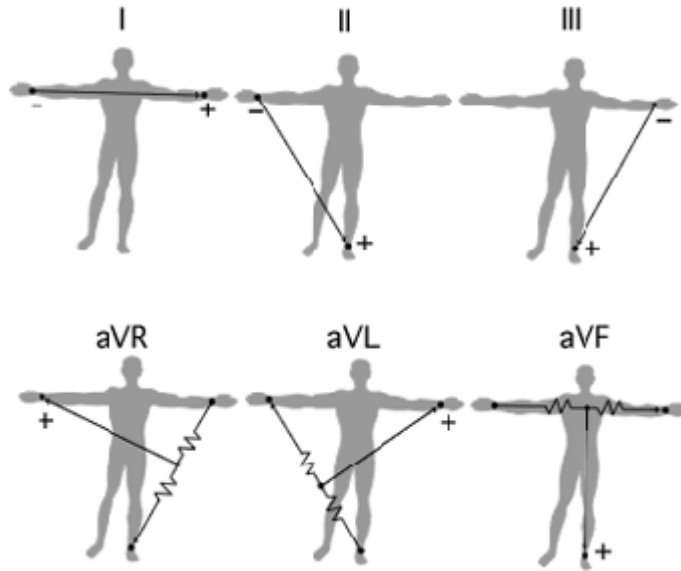


Figure H.3: Einthoven's triangle [9]

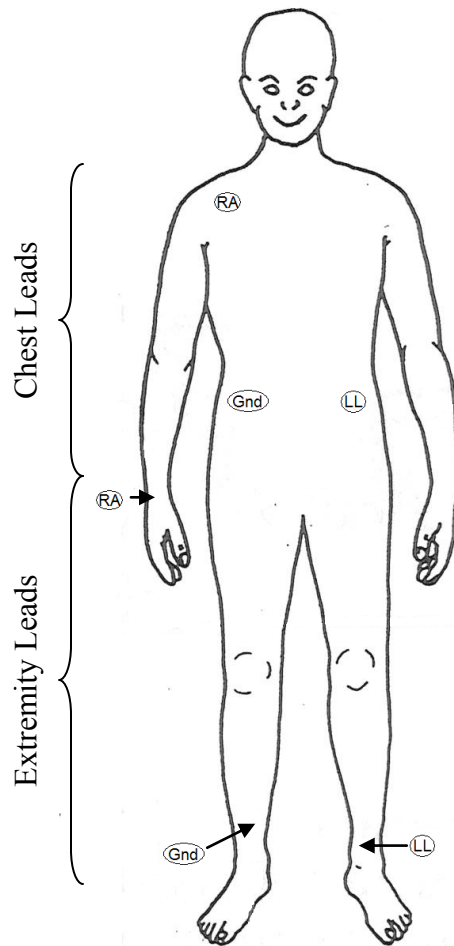


Figure H.4: ECG Electrode placements [12]